UNIVERSITY OF CAPE COAST

DETERMINATION OF STANDARD REFERENCE RENAL VOLUME MODEL AND DOSE OPTIMISATION PROCEDURES FOR CLINICAL APPLICATIONS

BY

ISSAHAKU SHIRAZU

Thesis submitted to the Department of Physics of the School of Physical Sciences, College of Agriculture and Natural Sciences, University of Cape Coast, in partial fulfilment of the requirements for the award of Doctor of Philosophy degree in Physics

JANUARY 2018

DECLARATION

Candidate's Declaration

I hereby declare that this thesis is the result of my own original research and that no part of it has been presented for another degree in this university or elsewhere.

Candidate's Signature: ……. Date:…….

Name: Issahaku Shirazu

Supervisors' Declaration

We hereby declare that the preparation and presentation of the thesis were supervised in accordance with the guidelines on supervision of thesis laid down by the University of Cape Coast.

Principal Supervisor's Signature: Date:…….....

Name: Professor Cyril Schandorf

Co-Supervisor's Signature: Date:.....

Name: Professor Samuel Yeboah Mensah

ABSTRACT

The study is based on measurements of renal dimensions and related body indices to establish standard reference body and renal parameters, renal volume model, renal and effective dose in relation to patients' dose optimization procedures. The materials used include: MDCT Machine, Weighing scale, BMI calculator and MVL workstation. Technical parameters were obtained from three groups of randomly selected patients undergoing abdominal CT examinations including: 175 patients of age 20-40 years, 258 patients of age 41-60 years and 227 patients of age 61-80 years. In addition, the models design were based on age and gender variations. Voxel count method was used as the measuring tools with an integrated MVL application software platform, together with Minitab 16 statistical tools. The average values of the measured parameters include: the renal volumes: 146.74 cm^3, 151.76 cm^3, 142.04 cm^3, 148.29 cm^3 for male and female, with each corresponding right and left kidneys, respectively: renal length: 103.35 cm, 105.13 cm, 101.43 cm and 102.98 cm for male and female with the corresponding right and left kidneys respectively, the estimated renal volumetric ellipsoid coefficient (K) and renal shape index for both gender were approximately 0.53±0.01 and 1.00±0.02 respectively. The mean BMI, BSI and BSA were: 25.19 kg/m^2, 39.81 kg/m^2 and 2.02 m^2 for male and 21.91 kg/m^2, 36.58 kg/m^2 and 1.69 m^2 for female respectively. In addition, the mean dose parameters were: 6.33 mGy, 936.25 mGy cm, 3.26 mSv and 14.09 mSv for CTDIV, DLP, RD and E respectively. Two Comprehensive Clinical Decision Support Application Software were designed to provide a user friendly platform for comfortable working process. Finally, the established reference parameters are recommended for clinical application.

KEY WORDS

Effective Dose

MeVisLab

Minitab

Optimization

Renal Dose

Voxel.

ACKNOWLEDGEMENTS

I take this opportunity to express my sincere and heartfelt appreciation to my supervisors: Professor Cyril Schandorf, School of Nuclear and Allied Science, University of Ghana, Atomic campus and Professor Samuel Yeboah Mensah of the Department of Physics, University of Cape Coast. They gave me excellent advice, thoughtful correction, research materials for reference and encouragement throughout this work.

In addition, my sincere gratitude goes to Prof. Mary Boadu of Ghana Atomic Energy Commission and School of Nuclear and Allied Sciences, University of Ghana, Atomic Campus and Dr. Aliu Aduna Mahama of Department of Agricultural Engineering, University of Ghana, Legon, for their guidance, both material and financial support.

Furthermore, my sincere thanks also goes to the entire staff of the Medical Radiation Physics Centre, Radiological and Medical Sciences Research Institute of Ghana Atomic Energy Commission, Department of Radiology, Korle-Bu Teaching Hospital, Tamale Teaching Hospital, Komfo Anokye Teaching Hospital, Cocoa clinic and 37 Military Hospital, for their support and cooperation during the data collection process.

Finally, I wish to thank my family, especially, my two daughters, Zuleiha and Raheema, Mr. Issahaku Tahidu of Ministry of Food and Agriculture, Alhaji Zachariah Attah and Mr. Kofi Opoku, both of Federal Express (FEDEX) Ghana, for their guidance and financial support.

DEDICATION

To my parents, Alhaji Issahaku Wumbei and Hajia Ayisha Mahama of blessed memory for their prayers, guidance, love and care.

TABLE OF CONTENTS

LIST OF TABLES

LIST OF FIGURES

LIST OF ABBREVIATIONS

A-P	Anterior-Posterior
AAPM	America Association of Physicist in Medicine
AFRA	African Regional cooperative Agreement for research
ANOM	Analysis of Mean
ANOVA	Analysis of Variance
BEIR	Biological Effect of Ionizing Radiation
BMIRV	Renal volume related body mass index
BSA	Body Surface Area
BSARV	Renal volume related body surface area
BSIRV	Renal volume related body surface index
BSI	Body Surface Index
BSS	Basic Safety Standard
CAD	Computer Assisted Design
CNR	Contrast to noise ratio
CT	Computed Tomography
CTDI	Computed Tomography dose index
CTDIVOL	Volume Computed Tomography dose index
CTDIW	Weighted Computed Tomography dose index
CV	Coefficient of variation
DICOM	Digital Communication in Medicine
DLP	Dose Length Product
DNA	Deoxyribonucleic acid
DRL	Diagnostic Reference Levels
DVD	Digital Versatile Disk

E	Effective Dose
EC	European Commission
EDLP	Effective dose-conversion coefficients
GE	General Electric
GUI	Graphic User Interface
IAEA	International Atomic Energy Agency
ICRP	International Commission on Radiation Protection
IMACS	Image Management and communication systems
IVP	Intravenous Pyelogram
K	Standard Volumetric Ellipsoid Coefficient
K*	Model Volumetric Ellipsoid Coefficient
LAR	Lifetime attributable risk
LGN	Longitudinal Diameter
LNT	Linear Non-Threshold
LT	Lateral Diameter
MANOVA	Multivariate Analysis of Variance
MDCT	Multidetector Computed Tomography
MIRD	Medical internal radiation dose
MRI	Magnetic Resonance Images
MSAD	Multislice Average Dose
MVL	MeVisLab
NCRPM	National Council on Radiation Protection and Measurements
NRA	Nuclear Regulatory Authority
NRC	National Research Council
NURBS	Non-uniform rational B-spline

ORNL	Oak Ridge National Laboratory
P	Pitch factor
Pt	Normalized renal dose factor
PACS	Picture Archiving and Communication Systems
PET	Positron Emission Tomography
RD	Renal Dose
Re	Renal ellipsoid Product
RIS	Radiology Information System
RL	Renal length
ROI	Region of Interest
RRL	Relative Renal Length
RRV	Relative Renal Volume
RSA	Renal Surface Area
RSI	Renal Shape Index
RV	Renal Volume
SPECT	Single Photon Computed Tomography
SNR	Signal to Noise Ratio
VB	Visual Basic programming language
Ve	Volumetric Ellipsoid Equation
VeC	Volumetric Ellipsoid Coefficient
VTK	Visualization Toolkit
VOI	Volume of Interest
US	Ultrasound
WHO	World Health Organisation

CHAPTER ONE

INTRODUCTION

The study is a local based representative of renal volume model that has been developed to significantly and better understand the anatomical structure of the human kidney using abdominal CT images. Anatomical features of the model of the kidney has been designed to include shape and volumes and the relationship between these parameters with the Body Surface Area (BSA), Body Surface Index (BSI), Body Mass Index (BMI), the height and the weight of a normal average Ghanaian within a specific age group. GUI and CAD models has also been designed to adequately reflect the comfortable working process of all the mathematical model equations. The basic fundamental principles, theories methodology and available literature on these parameters has been discussed under a broad area of medical imaging in terms of organ measurement and dose optimization procedure.

Background to the Study

Medical imaging is described as the method for non-invasive assessment of physiological and anatomical information about human tissues or organ (Hendee, 1999). For this reason medical imaging is used to accurately and timely diagnose health problems, allowing for a more efficacious treatment. It can therefore be applied to examine the effective remedies and evaluate the effects of treatments for specific diseases (Löfstedt, Ahnlund, Peolsson & Trygg, 2012). As a result of its effective use, it is gradually replacing most laboratory chemical assessments of human body for clinical pathological condition. Therefore, over the past two decades, a great number of medical imaging modalities have emerged, and more technological advance systems

like, Fluoroscopy, Mammography, Magnetic Resonance Imaging (MRI), Computed Tomography (CT), Single Photon Computed Tomography (SPECT) and Positron Emission Tomography (PET) continue to improve clinical diagnoses of complex pathological conditions, based on basic physics principles for patient care (Löfstedt, Ahnlund, Peolsson & Trygg, 2012; Mattsson & Söderberg 2011; Hendee, 1999).

Furthermore, medical imaging facilities have become more dependable, accessible and to a large extend more affordable, due to increased availability of technological advance systems (National Council on Radiation Protection and Measurements (NCRPM), 2009). The evolution of these modalities is remarkable, from Roentgen to CT, single detector with very few slices for anatomical or physiological pathological condition to multidetector systems with as many as 640 slices (; ICRP Publication 89, 2002; Tsapaki, Kottou & Papadimitriou, 2001), which has changed the global view of medical imaging. In addition, these developments have made medical image acquisition, analysis and interpretation much easier and faster, with the use of appropriate diagnostic tools (Hendee, 1999). Unfortunately, however, as a result of these developments, two outstanding issues emerged; the first was the technical know-how of imaging staff, in addition to set of challenges with how to analyze images with appropriate and available technological advance tools. The other was the fact that almost all these imaging modalities are major sources of exposure to ionizing radiation with direct and indirect prognostic health consequences (NCRPM, 2009; ICRP Publication 89, 2002; Tsapaki, Kottou & Papadimitriou, .2001; ICRP Publication 73, 1996). Additionally, even though due to continuing collaborative efforts between the clinical practitioners and

researchers, these two challenges have been addressed in the developed world, however it still remains a challenge in the developing world including Ghana.

Furthermore, apart from the mainly diagnostic use, medical imaging also plays crucial role in therapeutic procedure, especially in cancer control and management processes. In fact, these modalities comprehensively support the implementation of cancer control programs, which goes a long way to meet the standard of practice of clinical oncology. These are essential for successful cancer treatment which require medical images like CT, in order to determine organ position, location and size in relation to the treatment area for comprehensive design of the treatment planning protocol. Additionally, however, the design of treatment protocols depends on diagnostic assessments of these organs, which are founded on several factors, including race, gender and age, hence reference organ models are best designed based on these stated variation.

Admittedly, the standard of practice of clinical oncology required the availability of comprehensive clinical reference organ models and dose parameters, which currently is unavailable in most developing countries including Ghana. Therefore, there is an urgent need to design an organ model that best represent the local population for appropriate diagnosis, in addition to CT Dose Reference Levels (DRLs) in order to comprehensively address clinical diagnostic challenges in relation to radiation protection issues caused by the increasing use of CT in Ghana.

Even though the beneficiaries of these increased use of CT are mainly patients, there is the need for a tradeoff between these benefits and the high potential biological effects due to exposure to ionizing radiation with high

possible prognostic health challenges (ICRP Publication 89, 2002; Tsapaki, Kottou & Papadimitriou, 2001, ICRP Publication 73, 1996). Indeed, for this reason there is also the need to create awareness and provide enough information to clinicians and patients for all forms of ionizing radiation imaging procedures, including CT. This is essential in order to address the high possible stochastic effect of cancer development from exposure to low dose radiation regardless of the etiological process, which has a latent period of 10-20 years or more (NRC, 2006). Additionally, there is the need to improve dose optimization procedures of exposed individual and exposure parameters in relation to recommended exposure and DRLs set up by the recognized regulatory institutions (Tsapaki, Kottou & Papadimitriou, 2001; ICRP Publication 73, 1996). This is achieved through a comprehensive process called the Radiology Information System (RIS), for electronic data management within the imaging department. The major functions of the RIS is to manage patient scheduling, examination performance tracking, examination reporting, results distribution, procedure billing, archiving and storage systems, above all appropriate protocols for protection of patients, clinicians and the general public. Generally, the RIS is an application software that helps to improve the health care delivery to patients by fast-tracking the various procedures involve in the imaging process, in order to increase accessibility to the general public.

Comparatively, the RIS system is indispensable because due to the high level of accuracy in the outcome of anatomical investigations with CT procedures, quite a high proportion of people are opting for these procedures on a daily basis. This seemly satisfactory outcome is being challenged by delays in

getting accurate examination reports, performance tracking, and results distribution. This has accordingly led to the development of more and more advanced systems for archiving and data transfer of images in digital format as part of the integrated RIS system using various networks. Undoubtedly, the RIS system is a software platform within the imaging department, which enables integration with digital networks where other application software, including; Picture Archiving and Communication Systems (PACS) are embedded for data management, archiving and storage systems.

The PACS systems is the most commonly used archiving and storage systems in clinical settings, because it is fast and easy to integrate into the RIS system (Bryan, Weatherburn, Watkins & Buxton, 1999).

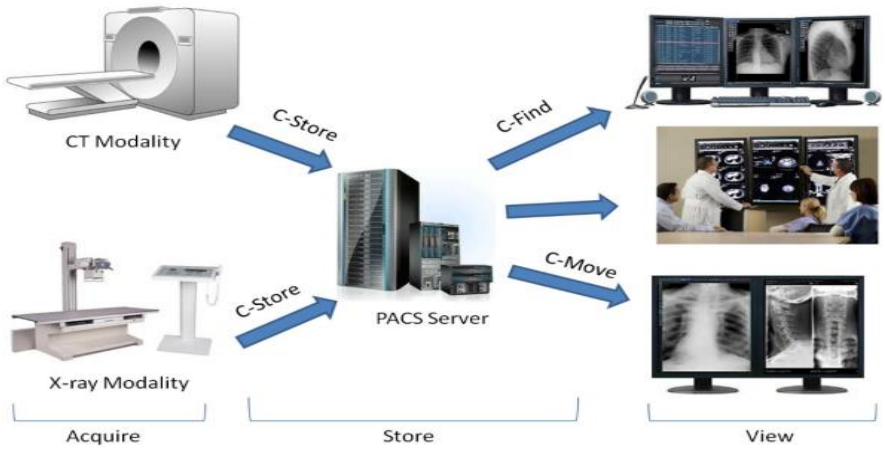

Figure 1: A typical RIS at a medical imaging department.

(Source: Safa IT Systems)

The development of the PACS has enabled medical images to be acquired and transfer from the imaging equipment to more technologically advanced viewing systems for processing and analysis. A pictorial display of an integrated RIS network in a typical imaging department is summarised in Figure 1, where processes such as acquisition, storage, processing, viewing, reporting and decision making are interconnected for comfortable working process.

The existence of these archiving and storage systems led to the development of a more advanced DICOM application software, like MeVisLab (MVL) application software for viewing, analyzing, and reporting writing at a convenient time, long after it has been taken and stored by the PACS systems. Accordingly, this helps to improve the accuracy in medical image analysis and interpretation of diagnostic and therapeutic results in clinical and scientific research environments. In addition, it also enable large volumes of images to be captured and stored to be analysed and reported at a convenient times.

Furthermore, medical image analysis using the RIS system has become an excellent possibility for research and clinical application irrespective of the numbers and original source of the images (Rexilius *et al*., 2005; Bryan, Weatherburn, Watkins & Buxton, 1999). Additionally, together with the technologically advanced software, MeVisLab application software, has made the analysis and interpretation of medical images for diagnosis and or therapeutic decisions easier and faster. Ordinarily, based on its ability to analyze, displayed patterns of observable parameters, which enables a trained clinician to determine whether the tissues are repaired or impaired, malignant or benign. Additionally, it also enabled organ size and exact location in relation to the surrounding tissues to be determined because these are influenced by the pattern of observable parameters which manifest as morphological and functional changes.

Moreover, the interpretation of medical images based on comprehensive analysis for diagnosis and/or therapeutic decisions enables differentiation between abnormal and normal tissues by the differential radiation dose distribution based on their morphological variations (NCRPM, 2009). In

addition, the availability of a standard reference organ volume model, which is affected by the tissue pattern, increases the accuracy in differentiating normal and abnormal organ size. This principle has been used to model standard reference renal volumes and the radiological prognostic effects using abdominal CT images based on clinical research application by researchers including this study.

Indeed, in clinical research and the applications of medical image analysis, organ models have gradually gained sufficient prominence (Löfstedt, Ahnlund, Peolsson & Trygg, 2012; Hendee, 1999). This is because the research based design models aid radiologists, nuclear medicine experts and oncologists make important diagnostic and therapeutic decisions by comparing the patient's organ parameters to the existing established standard reference values (Löfstedt, Ahnlund, Peolsson & Trygg, 2012). In addition, standard reference organ parameters provide more important and accurate assessments of the organ size using qualitative and quantitative analysis than the traditional methods of qualitative (appearance) assessment only without available baseline reference values for quantitative assessment (Löfstedt, Ahnlund, Peolsson & Trygg, 2012). For example, establishment of basic radiological baseline reference linear renal dimensions, like the Anterior-Posterior (A-P), longitudinal and lateral diameters are important for the evaluation of renal volume and therefore aid in the renal morphological analysis to assist in the diagnosis of kidney disease. Above all, the reference information from the designed models are used as standard baseline information to test future research data as well as to explain anatomic variations between individuals of the same population and across other populations.

Comparatively, models are mentally visual way of linking experiment with theory, it is a simplified representation of an imagined reality that enable predictions to be developed and tested by experiment in research and for scientific applications. Additionally, models are used to provide explanation of complex data, which are presented to test hypotheses and predict information. Therefore, in clinical application of radiation for medical imaging, well-developed human organ systems are modelled with mathematical expressions based on basic physics and mathematics principles (Hendee, 1999). Indeed, to enable a user friendly approach, modelled expressions in the form of equations are converted to computer aided design (CAD) models for analysis and reporting, in terms of GUI and visual indicators for clinical application (Hendee, 1999). These two forms of display enable its implementation in surgery, organ studies, treatment planning and radiological analysis using CAD models.

Currently, image assisted construction of organ models is done with a voxel model of various reconstructed images, based on the differential gray level values. It is of interest to note that with the CT scan, Hounsfield numbers are used to represent the gray level values, which are represented as the organ identification numbers in the voxel container (Link *et al*., 2004). The voxels in these container are described by a single data point, in three-dimensional grid in a regularly spaced. This may present a single piece of datum, such as an opacity or multiple pieces of data such as opacity and colour. Several voxels are reconstructed through interpolation to form the volume of an entire tissue or organ, depending on the type of data and the intended use of the dataset (Xu & Chen, 2009). In view of this, voxels are used in medical image analysis to represent the smallest three-dimensional (3D) unit of various organs volumes,

which represent the pixel size in addition to the slice thickness (Link *et al.*, 2004). Hence, measurements of voxel volumes enable the determination of the entire organ volume regardless of the shape and form.

Comparatively, there are two common ways by which voxel representation of the structures of human organs models can be represented; these are; the statistical shape and the statistical appearance models (Xu & Chen, 2009). The statistical shape model represents the shape information, such as renal volume, renal surface area and linear renal dimensions (NRC, 2006; Xu Chen, 2009). These are regarded as the most useful tools for studying variations in anatomical shape of organs and has been widely used in medical image analysis, such as, medical image segmentation, shape registration and interpretation (NRC, 2006). The statistical appearance model focuses on texture information and accounts for both shape and volume element description. This helps to differentiate the appearance of normal organs morphology from abnormal organs morphology. It is important to note that diseases change the texture or volume element values of the affected organ, thereupon making it possible to assess both shape and texture (voxel value) variations in diagnostic decision. Hence, clinical research scientists uses this basic voxel value principle to establish volume models of organs for clinical applications.

Admittedly, this study is based on the inspiration of a number of studies that measured and established reference renal dimensions and volume models with dose estimates in several countries, including: India, China, Germany, UK, Austria, Netherlands, Japan, Korea, Pakistan, Turkey, Canada and the United State of America (Garland, 2014; Breau *et al.*, 2013; Egberongbe *et al.*, 2013; Saeed *et al.*, 2012; Sahni, Jit, Sodhi, 2012; Scholbach & Weitzel, 2012; Ozbek

et al., 2012; Moorthy & Venugopal, 2011; Muto *et al*., 2011; Glodny *et al*., 2009; Shin *et al*., 2009; Wong *et al*., 2009; Kang *et al*., 2007; Geraghty, Boone, McGahan, Jain, 2004; Janoff *et al*., 2004; Bakker *et al*., 1999; Lee *et al*., 1999; Lerner, Henriquez, and Harris, 1999; Ferrer, McKenna, Bauer & Miller, 1997; Emamian, Nielsen & Pedersen, 1995; Emamian, Nielsen, Pedersen and Ytte, 1993; Ninan *et al*., 1990; Troell, Berg, Johansson & Wikstad, 1984; Brandt *et al*., 1982; Wald, 1937). This is because, all the established models varied significantly from country to country. The standards set by these measurements and design of the models in those countries were the motivation and fundamental basis for this study, which was to measure and design the established race specific renal volume model for Ghana using abdominal CT images, associated patient dosimetry and the optimization of patient radiation protection protocols for dose optimization. In addition, dose estimates based on age and gender variations have been modelled for purposes of radiation protection of workers, patients and the general public.

Furthermore, it should be noted that, dose estimates are not used for the exact determination of radiation dose to patients during image studies, but for issues of risk assessment using DRLs. The dose reference levels are mainly used by medical equipment manufacturers, radiation regulatory authority and the various institutions involved with radiation, whose main objective is to safeguard the peaceful use of ionizing radiation through appropriate planning, regulation and to formulate laws to specifically provide general patient health care. The purpose of this is to propagate a three-point initiative to ensure radiation protection of patients. These include: Promote the safe use of medical imaging devices to both clinicians and patients; Support and informed clinical

decision-making that is, the benefit verses the effects; Increase patient awareness of exposure and its prognostic health consequences. Therefore, availability of information on institutional dose levels, determined based on population specific research, to the regulatory authority will go a long way to help their operations and regulate the imaging center serving those populations appropriately. Thereupon, determination of radiation dose to human tissues is important as it contributes significantly to health care delivery.

Similarly, the estimation of radiation dose, to a human body from low-dose radiation sources, requires information about the anatomical and physiological characteristics of both the exposed individual and the exposure parameters. In recent times, the need for this information is particularly important due to a compelling case for the reduction of radiation exposure from CT imaging, which is considered to contribute significantly to the radiation dose to patients (Mattsson & Söderberg, 2011; NCRPM, 2009). Additionally, in order to have consistent and reproducible radiation protection guidelines for CT exposure, it is important to have a consistent set of reference values, to describe prospectively, various anatomical and physiological characteristics of an exposed individual and the corresponding exposure parameters. An important attribute is that these reference values for tissues and organs, when summed, define a reference organ. Consideration of an entire reference organ helps to ensure that there will be an internal organ consistency about how the volume or functional characteristics of various organs or tissues are specified and the possible effects of radiation exposure.

Indeed, it is also important to have detailed information on age- and gender-related morphological variations of reference renal organ volume model

based on specific values in African just as what is available in Europe, the America and Asia. Whereupon, these reference values provide necessary input to prospective dosimetry estimates from low-dose radiation sources, mainly for the protection and safety of patients, workers and the general public. In diagnostic imaging, it is important to recognize the potential biological effects from radiation, not only on the radiation dose to a tissue or organ, but also on the biological sensitivity of the tissue or organ irradiated. Consequently, the concept of effective dose has been designed for clinicians and the general public who patronizes the services of a machine with ionizing radiation background. It reflects radiation detriment averaged over age and gender variations and can also be applied to medical populations with specific limitations. Consistently, it also facilitates the comparison of biological effect between various diagnostic examinations and modalities.

Comparatively, effective dose answered the question of communication as to the potential harm of ionizing radiation during medical imaging to patients. As the consequences must be explained to patients in clearer and simple language, of the possible harm of ionizing radiation. For example, answers to questions as to the harm should be in language that are understandable to patients not just in units of fundamental quantities, but characterizing the radiation dose in terms of effective dose and compare the expected values to other radiation risks. For instance comparing effective dose with one year of naturally occurring background radiation, better conveys to the patient the relative potential harm from the medical examination (ICRP Publication 73, 1996). It is also important to point to the patients the consequences of not undertaking the procedure and to weigh that as against the obvious danger

involved in the procedure. This is an important information to patients, especially for those in developing nations (including Ghana) requiring the services of recent emerging imaging modalities such as CT. In summary, effective dose is to provide a means in order to demonstrate dose limit compliance.

Conversely, another important parameter of interest is the patient organ dose management during clinical CT examinations using reference organ dose. This is important because, the reference organ dose is used to predict the possible damage to human tissue by photon energy. Reference organ dose related to radiation exposure from CT is especially critical in paediatric and young adult female patients (Mattsson & Söderberg, 2011; NCRPM, 2009; ICRP Publication 89, 2002). Therefore, the increased use of radiation exposure from CT examinations has been of concern to radiologists, medical physicists, regulatory authorities and CT equipment manufacturers. Accordingly, manufacturers and users of CT equipment are encouraged to design and implement their own techniques to appropriately manage or reduce organ radiation doses. In addition too, ensured high quality images are produced for dose optimisation procedure to enabled appropriate diagnostic decisions.

Furthermore, the CT scanning procedure has many image quality components and this is influenced and affected by many technical parameters in clinical application. These include noise, slice thickness, low/high contrast resolution, and high/low signal intensity, as well as photon energy. It is important to assess how image quality may be affected by the selection of these technical parameters. These assessments determined the tradeoff between the input exposure parameters and the corresponding output dose parameters with

adequate image quality to answer all the clinical questions. It is, therefore, important to bear in mind the reference organ dose when making the assessment of the radiation dose that will produce adequate image quality. In a clinical environments image quality is properly appreciated by estimating the signal to noise ratio (SNR) of the image. This is, achieved by, first establishing the difference between the signal intensity of the region of interest and that of the background, in relation to the noise, then the difference is divided by the standard deviation of the signal intensity from the background, an indication of the variability of the background noise.

Indeed, the introduction of 3D imaging where voxels of the images are determined, accordingly enabled SNR to be estimated quantitatively as the mean signal strength in a given volume to the standard deviation of the average value in that volume. Conversely, this allowed the relationship between the quality of images (SNR) and the safety of patients due to radiation dose to be established, this process is referred to as dose optimization. Interestingly, this has become an important issue within radiology today, as how to reduce the radiation dose during CT examinations without compromising the image quality has become a challenge. This is because the higher radiation doses result in higher image resolution, while lower doses lead to increased image noise and unsharp images. Consequently, increased dose may increase the possible adverse side effects, including the risk of radiation induced cancer. This is because, improving the quality of medical images always means increasing the radiation dose to the patient, which in turn increases the radiation risks. For this reason, it is of interest to note that the objective of medical imaging is not to deliver the perfect image but rather an image that is diagnostically adequate for

the specific health problem. This is, however, the essence of optimization, which requires balancing image quality with radiation dose. Furthermore, it is of interest to note that application of the optimization principle of exposure due to medical imaging requires a tradeoff approach, because too high a dose is as bad as low a dosage. This may lead to unnecessary dose or unsuitable diagnostic images and a resulting bad diagnostic decision.

In conclusion, abdominal CT images are the most accurate imaging modality used to estimate various organ sizes, texture information, masses, benign, malignant and exact organ location which aid treatment planning processes. The assessment of all this information is better placed by the use of various reference chart based on data collected over a period of time. Furthermore, physical, physiological and metabolic parameters of the human body are the very basic data for internal dosimetry (Löfstedt, Ahnlund, Peolsson. & Trygg, 2012; Hendee, 1999). For example, renal volume and other renal parameter estimates are best measured by standard reference renal volume model, this enable the calculation of dose to various internal organs. Additionally, CT scanners, is a major source of relatively high ionizing radiation, which uses relatively high photon energy to produce images, and thereupon affect patients and clinicians with radiation dose. Unfortunately, this gives rise to higher patient's dose; hence dose optimization is essential to avoid the risk of patients' tissue damage. As a results, clinical research scientist identifies this as challenge and efforts are currently ongoing through collaborative high level scientific research programs between clinician and physicist for solution. Consequently, some of the problems associated with the use of CT scanners for clinical oncology are elaborated below.

Statement of the Problem

The study identified and answered five major challenges with the use of contiguous multidetector CT slices to evaluate renal parameters, related body indices and dose optimization procedures in clinical oncology; these include:

Firstly, undoubtedly, there has been a tremendous increased use of CT scanners in Ghana, which called for an appropriate action plan to facilitate accurate CT image reporting based on appropriate protocols. The objective of this is to answer all the clinical questions within the shortest possible time, in order to improve health care delivery in Ghana. Therefore, standardizing the use of CT scanners for reliable, fast and accurate analysis will enable excellent results.

Secondly, admittedly, even though available literature have shown that CT images are the most authentic, objective and reproducible method of assessing renal volume, which is the best precise indicator of normal renal size than any other renal measurements (Ozbek *et al*., 2012; Muto *et al*., 2011; Glodny *et al*., 2009; Shin *et al*., 2009; Geraghty, Boone, McGahan & Jain, 2004; Janoff *et al*. 2004; Lerner, Henriquez & Harris, 1999), it is still to be fully implemented clinically due to the difficulty in assessing renal volume. Consequently, clinical assessment of renal volume using CT images are not widely used partly due to the complex renal shape, hence the difficulty in its measurements. Therefore, establishment of a standard unified renal volume measuring protocol with appropriate procedure will bring a great relief to clinicians.

Thirdly, the availability of standard reference renal volume model for accurate diagnoses, in order to avoid poor intra-observer and inter-observer variations and poor reproducibility as a result of the level of individual skill and

technical know-how is a challenge in clinical practice. Therefore, the best detailed assessment of renal volume measurements is performed with the help of a reference chart and appropriate measuring protocol (Bakker *et al*., 1999; Emamian, Nielsen & Pedersen, 1995). This is because standard reference values provide a powerful framework to ease the comparison of anatomical structures over time, between patients and within and across populations. Alas, this is lacking in the developing world, including Ghana, which has a negative influence on health care delivery. Hence the availability of standard renal volume models will allow new datasets collected to be mapped onto these established standard reference values for appropriate prognostic diagnostic decisions.

Fourthly, currently, due to lack of resources and the availability of research materials, very few information on renal volume and volumetric ellipsoid coefficient publications data are reported in Africa. As a result, African clinicians and researchers have relied on existing American, European and Asian based models for clinical assessment and references of renal dimensions. It is of interest to note that review of various models from a number of publications of different geographical locations yielded different specific reference values. These were strongly correlated with the variations in the physical characteristics of the various studied populations (Sahni, Jit & Sodhi, 2012; Scholbach & Weitzel, 2012; Glodny *et al*., 2009; Emamian, Nielsen, Pedersen & Ytte, 1993; Troell, Berg, Johansson & Wikstad, 1984). Hence, this called for an urgent need to provide local based reference values which will be used to provide information in validation and accuracy in dosimetry calculations in medical imaging, radiotherapy and radiation protection applications.

Finally, in Ghana, comparatively, comprehensive patient's dose optimization protocol does not exist to alleviate patients' safety concern and avoid prognostic health consequences. As a result, in clinical practice, the establishment of improved accuracy in radiation dose estimates with low ionizing radiation has been identified as a major concern to clinicians for implementation in dose optimization protocols. These called for setting up of standard reference renal and effective dose values, in relation to image quality. This will effectively deal with dose optimization challenges for radiation protection of patients during abdominal CT examinations which will be consistent with acceptable image quality for prognostic referencing. Therefore a tradeoff between dose and image quality to address the balance between abdominal effective and renal dose on one hand and image quality based on SNR on the other using abdominal CT images for the optimization process required an urgent action.

In conclusion, with these problems in mind this study was designed with the objective stated below to minimize, if not, completely do away with the undesirable effects indicated.

Objectives

The aim of the study was to establish Ghanaian based standard reference values of renal and body parameters and the associated dose optimization procedure.

This specifically led to the:

Determination of standard reference body Weight, Height, Body mass index (BMI), Body surface index (BSI) and Body surface area (BSA) for clinical application.

Determination of standard reference longitudinal diameter, transverse diameter and anterior-posterior diameter for clinical application.

Determination of a unified local based standard reference renal volumetric ellipsoid coefficient and to establish a renal volume model in Ghana for clinical application.

Prediction of renal volume of an average Ghanaian adult with standard reference body parameters like BMI, BSI and BSA using a GUI for clinical application.

Determination of the standard reference renal organ dose and effective dose values of an average adult Ghanaian undergoing abdominal CT examinations for clinical application.

Establish patient dose optimization procedures without loss of acceptable image quality during abdominal CT scan.

Review and compare measured parameters with international reference values.

In conclusion, the above seven point action plan led to the design of appropriate scope as stated below to achieve the desire study objectives.

Scope

The scope of the work was confined to:

Measurements of weight and height of an average Ghanaian to determine BMI, BSI and BSA values and to establish the relationship between these body parameters with renal parameters in a clinical environment.

Measurement of A-P diameter, lateral diameter and renal length of an average adult Ghanaian kidney using 660 abdominal CT images.

Measurements of the total number of voxel in each slice of all the 660 images that contain the renal organ to determine renal organ volume and renal

volumetric ellipsoid coefficient of renal volume model using MVL for various age groups and gender variations in the clinical environment.

Determination of the relationship between renal organ dose and effective dose using weighted-Computed Tomography dose index ($CTDI_W$) and Dose Length Product (DLP) respectively.

Estimate SNR together with dose parameters for dose optimization.

Modelling the relationship between the various established parameters with mathematical expressions and Computer Assisted Design (CAD) as GUI using VB with MVL application software.

Relevance and Justification

In the clinical practice, it is important to provide normative data that allow radiologists and other clinicians to evaluate the normal scope of values for a particular organ size through measurements of its dimensions for clinical diagnostic determination. For example, knowledge of renal parameters and the relationship with body indices is significant for clinical assessment of kidney diseases (Garland, 2014; Glodny, *et al*., 2009; Emamian, Nielsen, Pedersen & Ytte, 1993; Troell, Berg, Johansson & Wikstad, 1984; Wald, 1937). This is because, renal volume changes throughout human development from fetus through to maturity and to elderly, therefore, the evaluation of the renal volume model as compare with human body parameters is crucial. This enables the hypothesis that the function of the renal volume meets the metabolic requirements of the whole organism, which are best described by other factors including body parameters (height, weight, BMI, BSA and BSI).

The growth in chronic dialysis due to renal diseases has doubled in Ghana for the past few years. According to a report by the Ghana Kidney Foundation,

currently, over 3000 Ghanaians annually develop chronic renal disease. A majority of these cases was observed among the youth, specifically between the ages 20 and 50 years (Osafo, 2012). Unfortunately, early detection is quite elusive due to poor and difficult renal assessment, which has become a challenge to clinicians and the general public.

However, renal volume assessment has been found to be a very accurate predictor of renal size. The knowledge of locally determined standard renal size, through the use of renal volume measurement, will allow new datasets collected to be mapped onto established standard reference values. This will provide enough clue for taking an early diagnostic decision on renal diseases, which will ensure effective cure or treatment and prevent the progression to end stages of renal diseases. Furthermore, from available data, the renal volumetric ellipsoid coefficient that is used in renal volume estimates varied based on several factors, including geographical location (Sahni, Jit, Sodhi, 2012; Glodny et al., 2009; Emamian, Nielsen, Pedersen & Ytte, 1993). As a result, various radiologist uses variable renal volumetric ellipsoid coefficient to estimate renal volume. Therefore standardizing volumetric ellipsoid coefficient based on population specific study information will unify the accurate calculation of renal volume in the Ghanaian.

Comparatively, low-dose radiation based medical procedures have been determined by a number of research organizations to be potentially carcinogenic which is affecting millions of people all over the world (Mattsson, Söderberg, 2011). A major concern is that the total exposure to ionizing radiation in the world has nearly doubled over the past 20 years (Mattsson & Söderberg, 2011; NCRPM, 2009) based on a recent report by International

Commission on Radiation Protection (ICRP). Unfortunately, however, this is predicted to continue exponentially due to increased incidence of low-dose radiation exposure from medical imaging procedures. This is because more patients are opting for CT, SPECT and PET, which account for more than two thirds of all medical imaging procedures (NCRPM, 2009). Hence, adequate information on abdominal CT images that will enable easy and accurate assessment in single a scan will reduce the likely tissue damage that might cause by ionizing radiation that may result from multiple scan.

Furthermore, the designed renal volume model will be used as a standard reference model, in addition to setting a standard reference renal dose and effective dose values as DRLs that will yield an adequate image quality for diagnosis and interventional decision. This is based on the ICRP recommendation of the Linear Non-Threshold (LNT) model (ICRP Publication 102, 2007; ICRP Publication 103, 2007). Accordingly, this will provide the most reasonable description of the link between low-dose exposures and cancer incidence. In addition, the study also makes available protocol, processes and procedures that will improve radiation protection through effective use of exposure parameters (kVp, mAs) and the resultant dose parameters ($CTDI_{VOL}$ and DLP) for dose optimization of patient in a clinical environments during abdominal CT examination.

Finally, in conjunction with the experimental work, the mathematical and CAD models will help to test, confirm, refute, or suggest a number of hypotheses that relate the morphological and physiological description of the kidney in relation to body indices. This will therefore provide significant contribution to the challenges facing measurements and documentation of

standard reference chart of Ghanaian renal and other body parameters. In addition, this will also provide enough documentation to issues of radiation protection of patient dosimetry during the abdominal CT examination, which will be consistent with acceptable image quality for prognostic referencing.

Organization of the Study

This write-up is presented in five chapters.

It began with Chapter One which gives a vivid background information about the study, problem statement and objectives. It also described the scope in relation to its relevance and justification its clinical application in Ghana and ends with the summary of the study organization.

Chapter Two reviews the literature on existing publications on exposure and patients dose optimization procedures, organ measurements and modelling. It also includes further discussions on the quantity that relates dose to the risk associated with radiation exposure and thus the correlation with stochastic effects, as a results of various dose estimates. Furthermore, the review also includes basic practical and clinical reference information from EC and ICRP recommendations. The final review are based on estimates of renal and other related body parameters, including BMI, BSI and BSA related renal volume.

Chapter Three provides relevant information about the materials and the methodology used to achieve the desired goal of the study. The chapter also described the various measuring procedures that were used to measure and process the primary data in order to successfully design the modelled equations and the various tools such as: Minitab application software and statistical models that were used to analysed the data.

Chapter Four describes the pictorial view of the relationship between the various parameters in tables and graphical representation. It provides a space platform to answer all the questions by presenting the data that are necessary to facilitate the implementation process in a pictorial format. It describes the relationship between the various measurable quantities that were used to calculate the derived quantities in order to draw reasonable conclusions. Finally, the analysis of the presented data using various practical and theoretical tools based on the study objectives is also captured in this chapter.

Chapter Five presents a comprehensive summary of the major findings in relation to the measured renal parameters, body indices, exposure and effective dose optimization procedures during the Abdominal CT examinations. The development of mathematical and computed aided design models of the measured parameters for clinical application are also presented. This chapter provides the concluding summary of this work and recommendations to relevant stakeholders.

Chapter Summary

In summary a comprehensive discussion of the background information was done in relation to the various scientific bases of the study. In addition, it also discusses the identified problem statement and a clearly setout objectives to achieved the desired goal. Furthermore, it explained the scope in relation to its relevance and justification for use clinically in Ghana and ends with the summary of the study organization.

CHAPTER TWO

LITERATURE REVIEW

Introduction

This chapter presents a review of publications on measurements of body parameters, renal parameters and patients exposure and dose optimization procedures. It is based on the review of methodology and techniques of clinical research materials of the processes, spanning the period from 1937 to 2014 with various imaging modalities using the theoretical principles of physics and mathematics in medicine. The techniques of Biological Effects of Ionizing Radiation (BEIR) VII model and four other exposure and dose models (LNT, threshold, hormesis and hypersensitivity) were used to discuss risk associated with low-dose radiation (ICRP Publication 103, 2007; ICRP Publication 102, 2007; Khan, 1984). This section also includes further discussions on mAs, kVp, CTDI and DLP that tries to relate radiation dose to the risks associated with radiation exposure and thus the correlation with stochastic effects, as a result of the radiation dose estimates (Mattsson & Söderberg, 2011; NCRPM, 2009; ICRP Publication 102, 2007; ICRP Publication 103, 2007; Hendee, 1999; Khan, 1984). The review includes basic practical applications of reference data from AAMP, IAEA, EC and ICRP recommendations.

Review of Existing Publications

Latest publications on measurements of renal dimensions using various imaging modalities together with its effects on dose to patients were reviewed. This section discusses; established renal dimension, the effects of low dose radiation and computed tomography as an imaging modality.

Existing Renal Dimensions

Several authors have reported estimates of normal renal dimensions using radiological and non-radiological methods. Currently, three imaging modalities are commonly used for measurements of renal dimensions for clinical application; this includes ultrasound (US), Magnetic resonance imaging (MRI) and multidetector computer tomography (MDCT) (Garland, 2014; Breau *et al*., 2013; Egberongbe *et al*., 2013; Saeed *et al*., 2012; Sahni, Jit, Sodhi, 2012; Scholbach & Weitzel, 2012;; Ozbek *et al*. 2012; Moorthy & Venugopal, 2011; Muto *et al*., 2011; Glodny *et al*., 2009; Janoff *et al*., 2004; Lerner, Henriquez & Harris, 1999; Shin *et al*., 2009; Wong *et al*., 2009; Kang *et al*., 2007; Geraghty, Boone, McGahan, Jain, 2004; Bakker *et al*., 1999; Lee *et al*., 1999; Ferrer, McKenna, Bauer & Miller, 1997; Emamian, Nielsen and Pedersen, 1995; Emamian, Nielsen, Pedersen & Ytte, 1993; Ninan *et al*., 1990; Troell, Berg, Johansson, Wikstad, 1984; Brandt *et al*., 1982; Wald, 1937). Despite several challenges facing US as a measuring tool, it is still the most widely used imaging modality to measure renal dimensions as reported in literature (Egberongbe *et al*., 2013; Saeed *et al*., 2012; Wong *et al*., 2009; Lee *et al*., 1999; Ferrer, McKenna, Bauer & Miller, 1997; Emamian, Nielsen & Pedersen, 1995; Emamian, Nielsen, Pedersen & Ytte, 1993; Ninan *et al*., 1990; Troell, Berg, Johansson & Wikstad, 1984; Brandt *et al*., 1982). This is because of its availability, affordability and possible apparent safety considerations as compared to MRI and MDCT, which are quite expensive. MRI on the other hand is associated with a lot more discomfort of having to stay for quite a long time during scanning and the healthy use of strong magnetic field is uncertain, especially in young and pregnant patients.

Furthermore, MDCT imaging on the other hand, are constantly and continuously been associated with high risk of ionizing radiation and its possible potential prognostic carcinogenic attributes and consequences (NCRPM, 2009). However, all these three radiological methods are associated with some amount of prediction errors (Ozbek *et al*., 2012; Glodny *et al*. 2009; Bakker *et al*., 1999). Despite all these, the abdominal coronal MDCT examination is considered to be more accepted and can predict renal dimensions more accurately than all other radiological methods, due to clearer anatomical boundaries. MDCT system with a well-structured image analyzing applications software provides superior and interactive images at substantially lower cost with minimal patient time, discomfort and morbidity (Breau *et al*., 2013; Ozbek *et al*., 2012; Muto *et al*., 2011; Glodny *et al*., 2009; Shin *et al*., 2009; Kang *et al*., 2007; Janoff *et al*., 2004; Geraghty, Boone, McGahan & Jain, 2004; Lerner, Henriquez & Harris, 1999). In addition, 3D CT images can be used to compute renal volumes accurately for clinical application, Hence, it has become one of the most widely used medical imaging modalities in the world in recent past (Ozbek *et al*., 2012; Muto *et al*., 2011; Geraghty, Boone, McGahan & Jain, 2004; Ninan *et al*., 1990). Additionally, because of this high level of accuracy, it is currently being used together with a number of software applications and the ellipsoid equation method to estimate renal volume and other renal parameters for clinical applications (Breau *et al*., 2013; Glodny *et al*., 2009; Janoff *et al*., 2004; Bakker *et al*., 1999; Emamian, Nielsen & Pedersen, 1995; Ninan *et al*., 1990). Indeed, in clinical application, renal size is predicted accurately using renal volume, which has been found to correlate very well with and influence by BMI, BSA, height and weight (Garland, 2014; Glodny *et al*., 2009; Emamian, Nielsen,

Pedersen & Ytte, 1993; Wald, 1937). As a result, these body parameters are used to estimate renal volume, since it is easier and quicker to measure them.

Furthermore, a number of studies estimated renal volume by using the voxel count method with known pixel size and the slice thickness for computation (Ozbek *et al*., 2012; Muto *et al*., 2011; Glodny *et al*., 2009; Shin *et al*., 2009; Kang *et al*., 2007; Geraghty, Boone, McGahan & Jain, 2004; Janoff *et al*., 2004; Lerner, Henriquez & Harris, 1999; Ninan *et al*., 1990). The results of these studies predicted kidney size with the following dimensions: longitudinal diameter was found to vary between 10.2±1.8 cm to 11.8 cm±2. 3cm on the left side of the spine and 9.8±2.0 cm to 10.9 cm ±2. 1 cm on the right side of the spine. Transverse diameter was found to vary between 5.80±0.3 cm to 6.25 ± 0.67 cm on the right and from 6.01±1.3 cm to 6.43±1.7 cm on the left and A-P diameter varied between 4.06±0.60 cm to 4.73± 0.65 cm on the right and 4.15±0.73 cm to 4.88 ± 0.95 cm on the left kidney. The findings have also put renal volumes to be between 132±25.8 cm^3 to 204± 35.05 cm^3 for the left kidney and 128.4±24.3 cm^3 to 198±28.17 cm^3 for the right kidney. Most of the variation was based on age and gender, with the male kidneys slightly larger than the corresponding female estimates (Garland, 2014; Breau *et al*., 2013; Egberongbe *et al*., 2013; Saeed *et al*., 2012; Sahni, Jit, Sodhi, 2012; Scholbach & Weitzel, 2012; Ozbek *et al*., 2012; Moorthy & Venugopal, 2011; Muto *et al*., 2011; Glodny *et al*., 2009; Shin *et al*., 2009; Wong *et al*., 2009; Kang *et al*., 2007; Geraghty, Boone, McGahan, Jain, 2004; Janoff *et al*., 2004; Bakker *et al*., 1999; Lee *et al*., 1999; Lerner, Henriquez, and Harris, 1999; Ferrer, McKenna, Bauer & Miller, 1997; Emamian, Nielsen & Pedersen, 1995; Emamian, Nielsen, Pedersen and Ytte, 1993; Ninan *et al*., 1990; Troell, Berg, Johansson &

Wikstad, 1984; Brandt *et al*., 1982; Wald, 1937). A number of these organ measurements show that normal adult renal weight varies between 153.0±27.3 g to 196.3 ± 41.0 g for the left and 146.7±29 g to 193.5±33 g for the right (Breau *et al*., 2013; Saeed *et al*. 2012; Moorthy & Venugopal, 2011; Bakker *et al*., 1999; Emamian, Nielsen & Pedersen, 1995). Most of the study concluded, by predicting, that kidney sizes diminish with advancing age (fully matured at age 20 years and begins to shrink after 60 years), due to a parenchymal reduction of the kidney (Sahni, Jit & Sodhi, 2012; Emamian, Nielsen, Pedersen & Ytte, 1993; Wald, 1937).

Finally, it has also been observed that, despite decades of experimental efforts, some aspects of the fundamental kidney structure are currently being studied in more advanced clinical and scientific environments (Garland, 2014; Breau *et al*. 2013; Egberongbe *et al*., 2013; Ozbek *et al*. 2012; Moorthy & Venugopal, 2011; Muto *et al*., 2011; Wong *et al*., 2009; Geraghty, Boone, McGahan, Jain, 2004; Lee *et al*., 1999; Ferrer, McKenna, Bauer & Miller, 1997; Emamian, Nielsen and Pedersen, 1995; Ninan *et al*., 1990; Troell, Berg, Johansson, Wikstad, 1984; Wald, 1937). However, in Africa, including Ghana, very few studies regarding renal dimensions and related body parameters have been reported in literature. Additionally, there is an urgent need to improve on the issues of appropriate methods of image analysis and radiation protection of patients and clinicians through the establishment of appropriate dose optimization protocols, to deal with the effects of low dose radiation in the developing world including Ghana.

The Effect of Low-Dose Radiation

A significant number of publications have discussed the causes of solid cancer due to high dose radiation for therapeutic purposes (Ozasa *et al*., 2012; Faletra *et al*., 2010; Sanders, 2010; Mullenders *et al*., 2009; Smith-Bindman, Lipson & Marcus, 2009; Berrington de Gonzalez *et al*., 2007; Einstein *et al*., 2007; Einstein, Henzlova & Rajagopalan, 2007; Feinendegen, 2005; Young & Kerr, 2005; Preston *et al*. 2003). As a result, it is generally an accepted fact that ionizing radiation exposure to high-dose radiation increases the risk of solid cancers and leukemia. This assertion is based on evidence from epidemiological studies of radiation workers and atomic bomb survivors (Ozasa *et al*., 2012; Young & Kerr, 2005; Preston *et al*., 2003). In addition, for the past two decades, awareness has been created and accurately predicted issues of radiation in the high dose therapeutic environments (Khan, 1984). Unfortunately, however, not enough has been done with regard to the potential effect of diagnostic medical imaging (low-dose radiation) on human body organs. This is partly due to the stochastic nature of the latter and the deterministic nature of the former. In addition, the relationship between medical imaging and the effect of radiation dose to clinicians, patients and the general public is yet to be fully agreed on by experts in the field of health physics.

Furthermore, most of these reported literature, have argued that radiation exposure from photon based medical imaging procedures is a potential carcinogen, affecting hundreds of millions of people all over the world, a major concern is that the world total exposure to low dose ionizing radiation has doubled over the past 20 years (Mattsson & Söderberg, 2011; NCRPM, 2009), as stated by ICRP in its latest publications (Khan, 1984). In

the next decade, this is projected to quadruple (Mattsson & Söderberg, 2011). These challenges seem to be affecting more people in the developing world, partly due to lack of proper regulation and other factors.

Medical imaging procedures like Fluoroscopy, CT, SPECT and PET account for major sources of ionizing radiation in recent times (Mattsson & Söderberg, 2011, ICRP Publication 103, 2007; ICRP Publication 102, 2007). The procedures have also become increasingly available and affordable, but poorly handled in the developing world. Furthermore, a report from the Swedish Radiation Safety Authority showed that CT and nuclear medicine constituted 16% of all radiological investigations and contributed to 64% of the collective radiation dose in Sweden in 2005 (Mattsson & Söderberg, 2011). In addition, the National Council on Radiation Protection and measurements of the USA reports that CT and nuclear medicine procedures constituted 22% of all radiological investigations, but account for 75% of the collective US radiation dose in 2006 (NCRPM, 2009). However, the precise data from annual mean effective dose for direct and indirect medical imaging procedures to patients and radiation workers is not readily available in Ghana.

Conversely, despite the growing concern based on these statistics made available by the clinical professionals, regulatory authorities and the public, it remains unclear whether low-dose radiation leads to an increased risk of cancer. A number of these publications suggest that the risk of cancer from high-dose radiation is proportional to the dose, and can be extrapolated to low dose, following the design of the LNT model (Sanders, 2010; Mullenders *et al*. 2009; Feinendegen, 2005). The LNT model is built on the assumption that any

radiation dose greater than zero poses a potential risk of cancer in a simple proportionate manner (Mullenders *et al*. 2009).

To address these concerns and to improve the skill of experts in the field of radiation field workers, the International Atomic Energy Agency (IAEA), International Commission on Radiological Protection (ICRP) and other international and national bodies continue to provide training and other services by supporting several activities in diagnostic radiology and radiotherapy in the developing world. The IAEA in particular, has developed an initiative to partner African countries in the African Regional Cooperative Agreement for Research, Development and Training Related to Nuclear Science and Technology (AFRA) programs to train radiation health workers and practitioners in nuclear medicine and diagnostic radiology. These are meant for experts specialized in medical imaging with low-dose radiation for diagnosis and for research programs to promote awareness and increase patients' safety. In collaboration with other bodies they issue requirements for manufacturers and users to include safeguards in their machines and its usage to minimize radiation risk and to provide appropriate training to support safe use by practitioners. They also encourage and empower radiological health service providers to develop diagnostic radiation DRLs and to establish registries for radiation dose optimization procedures in their countries. Furthermore, ICRP and other agencies have made available procedures and processes for radiation dose optimizations in order to estimate the effect of radiation dose to human body organs and tissues (ICRP Publication 103, 2007; ICRP Publication 102, 2007; Khan, 1984)

In conclusion, exposure to low-dose radiation due to medical imaging

like MDCT scan according to the various publications poses a potential risk to the DNA of human cells (Ozasa *et al*. 2012; Faletra *et al*., 2010; Mullenders *et al*., 2009; Smith-Bindman, Lipson & Marcus, 2009; Ojima, Ban & Kai, 2008; Berrington de Gonzalez *et al*., 2007; Einstein, Henzlova, Rajagopalan, 2007; Feinendegen, 2005; Young, Kerr, 2005; Preston *et al*., 2003). All factors and techniques must be considered to reduce the effect of radiation exposure to human body cells due to medical imaging, in order to reduce the possible prognostic health consequences of solid cancer. This is because, the application of low dose radiation equipment such as CT scanners has come to stay and its usage will continue to see exponential growth especially in the developing world including Ghana. In addition, there is the need to understand the basic application principles in the use of this equipment by the clinician and the associated allied professionals.

Basic Application of Computed Tomography

Computed Tomography (CT) was clinically introduced in 1971 (A in Figure 2) and limited to axial imaging of the brain in Neuroradiology. This has been developed into a versatile 3D whole body imaging modality for a wide range of applications. The basic operation is based on the background that; the structural formation of an object can be reconstructed from multiple projections of the object by using computer algorithms developed from mathematics equations and physics principle of attenuation based on the variation of tissue radiodensity and sensitivity (Bydder**,** Harry**,** Lucyna-Bassan **&** Kreel, 1981**;** Duncan & Panahipour, 2014).

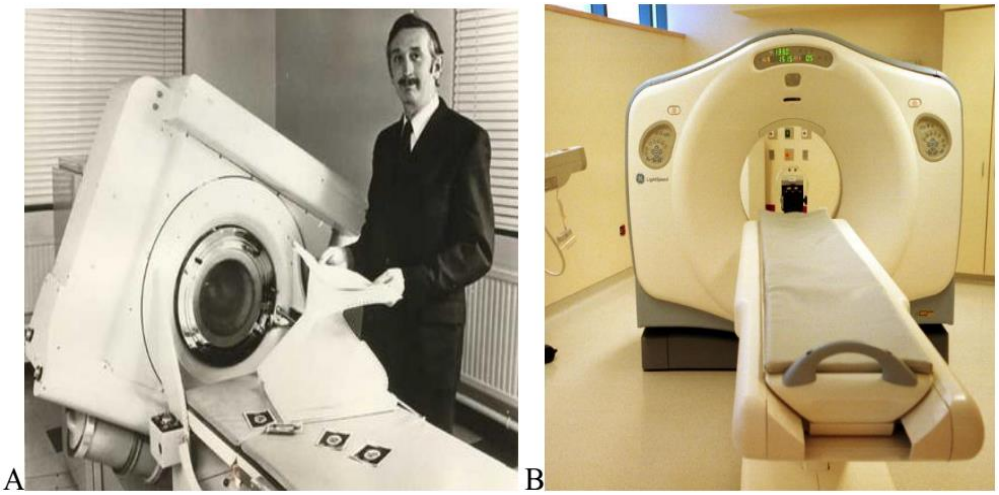

Figure 2: Old (A) and Latest (B) CT scanner systems.

Source: Emaze.org

This principle was initially postulated by Radon in 1917, he was able to obtain an image of an object with an infinite number of projections through the object (Stanley, 2007). In addition, clinical applications of this principle, require the physics principle of radiation attenuation, based on attenuation coefficient, which describes the extent to which the radiant flux of a beam is reduced as it passes through a specific tissue. Clinically, attenuation coefficient is used in the context of X-rays or Gamma rays, where it is denoted μ and measured in cm^{-1}. The attenuation of X-ray through human body enables the tissue attenuation map of the human body to be estimated when a photon passes through the human body, where attenuation (absorbed or scattered) of the photons by the tissues occur (Duncan & Panahipour, 2014). The attenuation depends on photon energy and the tissue radiodensity as it passes through human tissue. It is of interest to note that, the primary causes of this form of attenuation in human tissue are based on the photoelectric effect and Compton scattering (Aabha & Dixit, 2016).

This principle has been applied in the photon based imaging procedure like conventional X-ray and CT scanners, resulting in accurate and effective imaging procedures for clinical applications. After it was introduced in the early 1970s, CT scanning gained rapid acceptance in clinics and hospitals. A physicist, Allan Cormack and an engineer, Godfrey Hounsfield, shared the Nobel Prize in Physiology or Medicine in 1979 for their contributions to its development.

As shown in the Table 1, the technology of CT scanners has improved dramatically since the first scanner was introduced in the 70s.

Table 1- *Old and Latest Technology of CT Scanners*

Specifications	First CT Scanner (1970) (Figure 2.1A)	Latest CT Scanner (2014) (Figure 2.1B)
Acquisition Time of an image	5 minutes	0.25 seconds
Pixel size	3 mm x 3 mm	0.25 mm x 0.25 mm
Number of pixels in an image	6,400	640,000

Source: imagewisely.org

Today's CT scanners (B in Figure 2) can image the entire abdomen and pelvis of most adults, for example, making a total of 640 CT images, in less than 30 seconds. The amount of detail in the image has increased over hundredfold since 1970. In recent years CT image study has become popular, this is partly because the use of CT scanners have increased tremendously, with a little available in the 90s, to over hundreds of thousands CT units in the world today including Africa. Additionally, a CT imaging procedures increase from a little over 2% of all radiological examinations in most developing countries a decade ago to over 15 % now (Mattsson & Söderberg, 2011). In contrast, even though

CT examinations constituted only 5% of procedures worldwide in the 90s, yet it contributes 34% of the world total radiation dose in the same period and doubled in the first decade of the 21st century and this is expected to quadruple in the next decade (NCRPM, 2009). CT imaging procedures together with nuclear imaging techniques (SPECT and PET) account for more than one-third of all diagnostic imaging modality studies (Mattsson & Söderberg, 2011), in the world today.

After the introduction of multi-slice CT in 1997, the number of slices acquired per rotation has until recently doubled every 18 months, resulting in improved temporal and spatial resolution and shorter scan times (Mattsson & Söderberg, 2011). Modern, dual energy, 64-slices spiral CT can scan a whole body in 25s using a gantry rotation time of 0.33 s. Multislice CTs records up to 640 slices per revolution (Mattsson & Söderberg, 2011). The significant increase in the use of CT, from single techniques to 'hybrid imaging' using SPECT-CT and PET-CT for many applications have raised concerns about patient radiation exposure and the possible consequent increased risk of malignancy later in life (Mullenders *et al*., 2009; Smith-Bindman, Lipson & Marcus, 2009; Einstein, Henzlova & Rajagopalan, 2007; Berrington-Gonzalez & Darby, 2004; Khan, 1984).

The continuous increase in CT imaging is partly due to the fact that it produces accurate, detailed visualized anatomical description of human organs. It has the best image resolution that produced close to the real anatomical structure of an organ. Current CT scanners can produce 3D images of organs in 640 slices within a few seconds (Mattsson & Söderberg, 2011; NCRPM, 2009). These and many more features justify the selection of CT scanner

system for a study of an organ when the anatomical details and boundaries of the organ are of paramount interest.

In the geometric design of the CT scans, the X-ray tube and detectors rotate (Figure 3), with the axis of rotation running from the patient's head to toe.

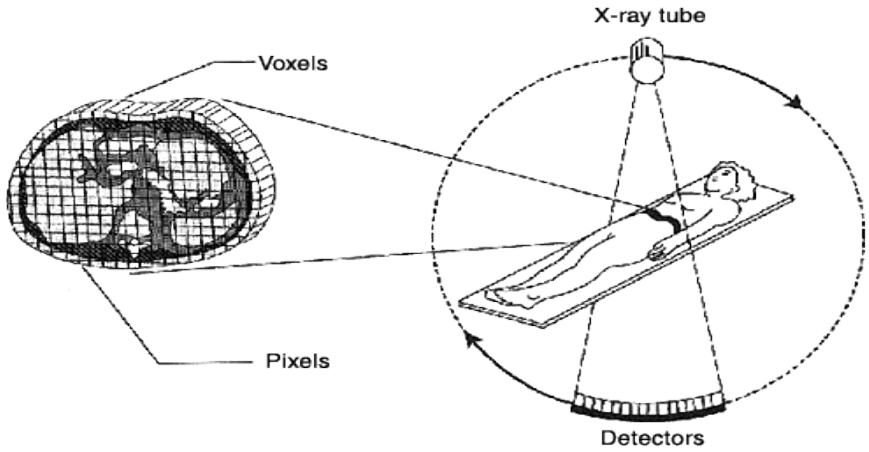

Figure 3: CT geometry of voxel and pixel.

Source: physicscentral.com

This works with the fundamental principle that the density of the tissue through which the X-ray beam passes can be measured from the calculation of the attenuation coefficient of the scanned slice. These scanned slices are composed of matrix of small boxes (Figure 4) of tissue called voxels. Additionally, the total number of voxels in a tissue is the sum of the voxels in each slice that contain the tissue as shown in figure 3. CT scan image matrix consists of voxels (Figure 4) within a specific region of interest. Interestingly, the matrix may be drawn to represent an organ and the total volume of the organ calculated with a known pixel size in 2D, together with the slice thickness forming the 3D component of the image (Xu & Chen, 2009).

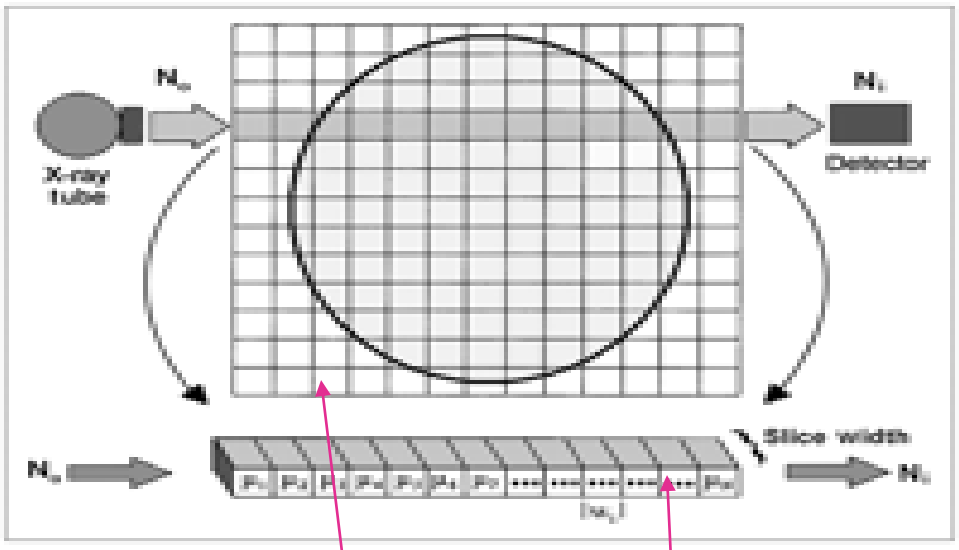

Figure 4: Pixel and voxel representation with CT scanner system

(Source: Sprawls.org) Pixel Voxel

The summation of all these voxels in each slice multiplied by the slice thickness determines the volume of the organ (Figure 5). That is, a slice organ volume is determined by calculating the volume of each voxel and multiplying this by the total number of voxels in a slice. The total organ volume is estimated as a product of the single slice volume and the number of slices. In other words the entire organ volume is estimated as slice thickness * row * column * total number of voxels representing the organ. For instance, assuming an organ has a total voxel of 47449, a slice thickness of 5 mm and a pixel size (row * column) of 0.740 x 0.740 mm, then the organ volume is calculated as 5 x 0.740 x 0.740 x 47449 = 129.915 cm^3 (Bakker, et al., 1999). This is the fundamental bases of this study, as the volume of the kidney is estimated based on this principle (Breau, et al. 2013; Muto, et al. 2011; Emamian, Nielsen & Pedersen, 1995).

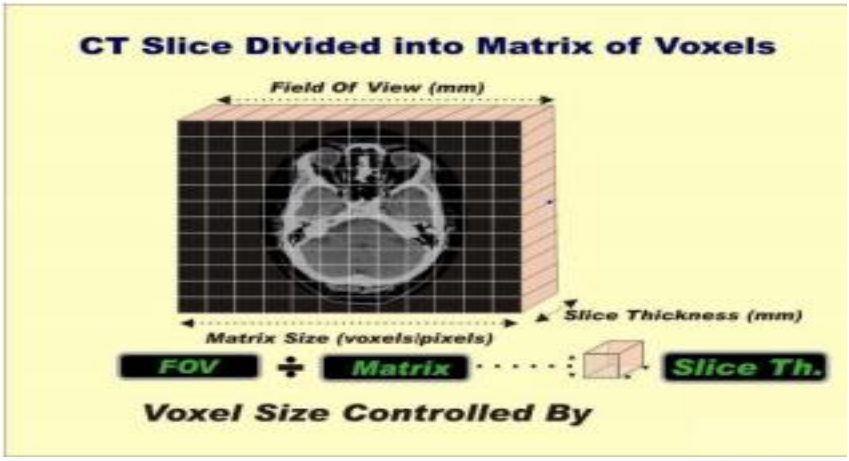

Figure 5: Pixel and voxel representation of CT image slice.

Source: Sprawls.org

Image Quality and Dose Optimization

In photon based medical imaging, diagnostic decision is primarily based on the quality of images produced which are also based on the intensity of the photon energy delivered. Unfortunately, however, the higher the number of photons (mAs) and energy of a photon (kVp) intensity the higher the dose received, hence there is always the need for a tradeoff between image quality and radiation dose to patients and clinicians. These are needed to assure that adequate quality of images is produced for clinical decision and at the same time hold the minimum measure of radiation dose to patients to avoid prognostic challenges. In current CT images, the quality of images is discussed in terms of either signal to noise ratio or the contrast to noise ratio (CNR). However, according to an American Association of Physicists in Medicine (AAPM) publication, there is incoherent limitation regarding the use of CNR, mainly because it does not take into account background noise correlations (I Lu & Nishikawa, 2012). The signal-to-noise ratio (SNR) on the other hand, accounts for noise correlations, since it correlate well with the performance of human observers in the task of detecting low-contrast signals in uniform backgrounds.

Indeed, the framework of statistical decision theory is used as a method of measuring the image quality of medical imaging equipment. With this approach, image quality is defined in the context of the image information available for performing a specified detection or discrimination task. This approach offers a means of measuring image quality, as linked to the sleuthing of an image detail of interest, without reference to the actual physical mechanisms involved in image formation and without separate measurements of signal transfer characteristics or image noise. The detectability of an image detail can be conveyed in terms of the ideal observer's signal-to-noise ratio at the decision point. Thus, the use of individual observer judgment (Qualitative) in addition to quantitative analysis has been proposed by clinical research scientist and accepted and implemented by clinicians. Hence, image quality is measured using the relationship between the process signals in the noise described as SNR of the image.

Principles of Signal to Noise Ratio Estimate

Signal to Noise Ratio in terms of picture element value is the ratio of mean to the standard deviation of a signal or measurement taken into consideration the background distortion. It is also reported in the voxel format as a measure of the ratio of the mean of the standard deviation of voxel values expressed mathematically as:

$$\text{SNR} = \frac{\mu}{\sigma}, \tag{2.1}$$

where μ is the signal mean or expected value and σ is the standard deviation of the noise, or an approximate thereof. This is useful for photon counts in image processing, where the SNR of an image is commonly computed as the ratio of the mean pixel value of the standard deviation of the pixel values over a given

region or background. It can as well be defined as the second power of the signal mean value of the standard deviation.

$$\text{SNR} = \sqrt{\frac{\mu^2}{\sigma^2}} = \sqrt{\frac{r}{1-r}}, \tag{2.2}$$

where r is the correlation coefficient. Equation (2.2) is used in cases where r is known, however, Equation (2.1) is the standard definition for SNR.

It is also used to characterize the sensitivity of imaging systems. Optimization of patient protection is done by determining the tradeoffs between the minimum doses that matches with a clinically acceptable image quality for accurate diagnosis decision. For instance, the tradeoffs between dose reduction and image quality include: Reducing mAs where radiation dose is reduced in proportion to the reduction in mAs; this may however increase image noise in proportion to $\sqrt{\frac{(\text{mAs}_{\text{original}})}{(\text{mAs}_{\text{reduced}})}}$.

Thus, if the mAs is reduced to ½ of the original, then the noise is expected to increase by 1.41 (41% increase) (I Lu & Nishikawa, 2012). As illustrated above, this should degrade the low contrast resolution performance. In summation, an increase table speed or pitch, may also reduce radiation dose in proportion to the gain in pitch. Even so, this may increase the slice sensitivity profile, creating larger effective slice thickness and reducing z-axis resolution. Additionally, reducing kVp, may also reduce radiation dose, increase signal contrast for some tissues due to increased photoelectric effect and may significantly increase beam hardening artifact if the beam energy gets too low (e.g., 80 kVp). In conclusion, both the exposed and the exposure parameters must be taken into consideration through appropriate dose optimization protocol to achieve effective radiation optimisation program. Accordingly, radiographer,

radiologist and medical physicist must standardize issues of exposure and dose parameters for successful clinical diagnostic pathological condition.

Principles of Exposure and Dose Parameters Estimate

It is important to note that high energetic photons can overcome the binding energy of orbiting electrons in atoms. Therefore, an energetic photon with sufficient energy can knock away an electron from its orbital shell, thereby creating an ion. In the human body, this knock off of electrons following exposure to photons, results in the creation of hydroxyl radicals (Mullenders *et al*., 2009; Rothkamm, Lobrich, 2003). These radicals are formed due to the interactions of photons of the X-ray with water molecules, which constitute approximately 70% of a human cell. The action of these high energy photons may directly cause damage to bases in DNA or indirectly through the reactions of the hydroxyl radicals with the bases in DNA. It should be noted that, various systems within the cell may rapidly repair most of these radiation-induced damage, this, withal, is based on a number of factors, including photon energy and the tissue. Comparatively, it is less easy to repair double-strand DNA breaks, an accumulation of which may lead to permanent tissue damage and the initiation of cancer (Rothkamm & Lobrich, 2003).

These biological responses to photon energy absorption gives rise to the determination of various fundamental dosimetric quantities in radiological imaging. In medical imaging where low-dose radiation is used, risk-related criteria can be obtained from practical dosimetric quantities. These dosimetric quantities are expressed from $CTDI_W$ and DLP, using the dose-conversion coefficients (E_{DLP}) shown in Table 2 for specific organ dose and regional effective dose respectively. These measures are obtained as part of the image

data and on the console. In addition, specific organ dose and regional effective dose are generally estimated for referencing and as an advisory note to clinicians.

Table 2- *Region Specific Normalized effective Doses for CT scan*

CT Examination	Effective Dose	DLP mGy	$CTDI_W$ mGy	$CTDI_{VOL}$ mGy	E_{DLP} (coefficients) mSv mGy cm^{-1}
Head	1-2	1050	60	73.80	0.0023
Chest	5-7	650	30	36.90	0.0170
Pelvis	3-4	570	35	43.05	0.0190
Abdomen	5-7	780	35	43.05	0.0153
Abdomen-Pelvis	8-14	780	35	43.05	0.0150
Kidney	1-3				0.0086 (normal renal dose factor)

Source: ICRP

Computed Tomography Dose Index

An acceptable radiation doses descriptor known as the CT Dose Index (CTDI), is an integral of all radiation dose delivered both within and beyond the scan volume. Comparatively, across the field of view, the average dose descriptor, which takes into account variations in absorbed dose across a body is described as the weighted-CT dose index CTDIw (weighted average of center and peripheral to arrive at a single descriptor). Additionally, $CTDI_W$ represents the average dose in the scan volume for contiguous CT scans. However, in the case where there is either a gap or an overlap between sequential scans, the dose descriptor volume-CTDI (CTDIvol) is used. In other words CTDIvol represents

the average dose within a scan volume and this can be assessed on the user interface of the CT scanner. In addition, CTDIvol is an indicator that measures the intensity of the CT radiation X-ray beam.

$CTDI_{Vol}$ is derived directly with the volumetric multidetector row system and estimated by dividing $CTDI_W$ with the pitch factor (P), in order to get the total CTDI volume (I Lu & Nishikawa, 2012). This is because, the pitch factor (P) is delineated as the ratio of the table speed per rotation and the total collimation. Mathematically, it is interpreted as the slice separation (Δd) divided by a product of the number of slices (N) and the slice thickness (T), expressed as:

$$\text{pitch factor (P)} = \frac{\Delta d}{N.T} \tag{2.3}$$

Hence, $\frac{1}{P} = \frac{N.T}{\Delta d}$

$$CTDI_{VOL} = CTDI_W . \frac{N.T}{\Delta d} = \frac{CTDI_W}{P}.$$

$$CTDI_{VOL} = \frac{CTDI_W}{P}. \tag{2.4}$$

Many modern CT systems calculate and display the ($CTDI_{VOL}$). Additionally, $CTDI_{VOL}$ is a useful indicator of scanner radiation output for a specific kVp and mAs. Values of $CTDI_{VOL}$ can vary with nominal slice thickness, particularly in the narrowest settings (Perisinakis et al. 2007). Hence, it was introduced to account for fluctuations in radiation exposure in the z direction when the pitch is not equal to 1. So, $CTDI_{VOL}$ takes into account the helical pitch or axial scan spacing (Perisinakis *et al*. 2007; AAPM Report No. 39, 1993). Furthermore, doses to organs (e.g., kidney) are determined using the $CTDI_{VOL}$ and a conversion factor for renal tissues as recommended by ICRP publication 103 (ICRP Publication 103, 2007; Perisinakis *et al*. 2007).

Therefore, because of the significant of $CTDI_{VOL}$ parameter in the determination of dose to patients during CT scan, it is part of the image data recorded by the DICOM MVL application software as demanded by EC and ICRP. This is to provide clear an ambiguous detailed information to the exposed individual for prognostic monitoring in order not to exceed the recommended annual dose level.

In addition, CTDIvol represents the average absorbed radiation dose over the x, y, and z directions, so it is applied to estimate organ dose to represent the 3D description of the organ and defined mathematically as:

$$CTDI_{VOL} = \frac{1}{N.T} \int_{-\infty}^{\infty} D(Z)\, dz, \quad (2.5)$$

where; D (z) is the radiation dose profile along the z-axis,

N is the number of slices in a single axial scans

T is the width/slice thickness of the tomographic section along the z-axis.

The international standard (S.I) unit for CTDI is the mGy.

Similarly, another important parameter of interest that is associated with CTDI is the Multislice Average Dose (MSAD) (ICRP Publication 103, 2007; AAPM Report No. 39, 1993; AAPM Report No. 96, 2008).

MSAD is defined as the product of $CTDI_{vol}$ and the ratio of the slice thickness and the increment between successive slices (AAPM Report No. 96, 2008). The formula is expressed mathematically as follows;

$$MSAD = \frac{T}{I} CTDI_{vol}, \quad (2.6)$$

where T is the slice thickness and I the increment between successive slices. This parameter account for the slice thickness and the increment between

successive slices and has been recommended for specification and acceptance testing of CT scanners using $CTDI_{vol}$ as the input factors. The S.I unit is mGy.

Dose Length Product

Another important dose parameter of interest is the dose length product (DLP) which is associated with the $CTDI_{VOL}$. DLP accounts for the irradiated volume and represents the overall exposure for an examination, expressed mathematically as:

$$DLP = CTDI_{VOL} * L, \quad (2.7)$$

where L is the scan length of an examination.

DLP is obtained by multiplying the Computed Tomography dose Index, CTDI by the length of the body section covered by the scanning procedure. To compute the DLP, the absorbed dose can be integrated along the scan length. This better represents the overall energy delivered by a given scan protocol (Origgi *et al*., 2006). Hence, the DLP is a dose quantity that describes the dose to the patient for a complete examination, thereby the potential biological effect described as effective dose is estimated using this parameter. Consequently, it is employed to calculate the effective dose to a body part. It is mandatory for manufacturers of CT equipment to factor this parameter as part of the image data (AAPM Report No.23, 2008). The SI unit is the mGy cm.

Organ Dose

Recommendation by International Commission on Radiation Protection (ICRP) provides an appropriate dosimetric indicators for the probability of stochastic radiation effect, by employing the average absorbed dose in a tissue or organ (ICRP Publication 102, 2007; ICRP Publication 103, 2007). The absorbed dose is defined as the mean of the stochastic distribution of energy

deposited in a volume element (Voxel). The mean absorbed dose in a specified organ or tissue is farther simply referred to as organ dose (AAPM Report No. 96, 2008).

In this study, the renal organ dose was estimated using ICRP publication 103 recommendations, defined as the normalized renal dose factor, P_t:

$$P_t = \frac{\text{organ dose } (D_T)}{\text{measured or calculated quantity}} \quad (2.8)$$

For CT examination, where stochastic effects are of interest, the specified dosimetric quantity is the organ dose, D_T, and the weighted Computed Tomography Dose Index ($CTDI_W$), is used as normalization quantity (AAPM Report No. 96, 2008). Thus,

$$C_{T\,Ca}(P_t) = \frac{(D_T)}{CTDI}$$

That is,

$$\text{organ dose } (D_T) = P_t \text{ CTDI (measured or calculated quantity)}$$

$$D_T = P_t \, CTDI_W, \quad (2.9)$$

where the normalized renal dose factor, P_t is 0.0086 and D_T represent the dose to kidney tissues hence equation 2.9 becomes:

$$D_{kidney} = 0.0086 CTDI_W, \quad (2.10)$$

where 0.0086 is the normalized renal dose factor from ICRP publication 103 and $CTDI_W$ is the weighted Computed Tomography dose index.

The SI unit of D_{kidney} is the mSv.

Effective Dose

Effective dose, E, is a dose descriptor that shows the difference in biological sensitivity of various human body tissues. It is a single dose parameter that present a clear understanding of the risk of a non-uniform exposure in terms of an equivalent whole-body exposure. The effective dose is defined as the sum of the weighted equivalent doses in all the tissues and organs of the body. A broad estimate of effective dose (E) may be derived from values of DLP for an examination using appropriately normalized coefficients (E_{DLP}) (Table 2) designed by ICRP and the European Commission (Huda, Ogden & Khorasani, 2008). The effective dose is defined as the product of the region-specific normalizing constant and the dose length product (Jones & Shrimpton PC., 1993). The effective dose is defined mathematically as:

$$E = E_{DLP} * DLP \quad (2.11)$$

In the case of the abdomen, E_{DLP} is 0.0153, hence, Equation (2.11) becomes:

$$E = 0.0153 * DLP, \quad (2.12)$$

where E_{DLP} (0.0153) is the conversion factor ($mSv \cdot mGy^{-1}cm^{-1}$) that depends on patient age and scanning regions (Brandt et al. 1982). The S.I unit of E is the mSv. This definition by ICRP was used in this work to calculate the effective dose with known DLP and EDLP (Huda, Ogden & Khorasani, 2008; Jones & Shrimpton, 1993). Thus, these values are purely for purposes of comparison, but not for estimating the dose to individual patients. The international S.I unit is the mSv. Furthermore, individual countries have developed a reference chart for comprehensive DRLs to guide them in the use of various modalities. For instance, Table 3 shows the effective radiation dose in adults for various CT scan of the abdomen, Pelvis and Trunks regions in

Europe (Table 3) (Tsapaki, Kottou & Papadimitriou, 2001; Leitz, Axelsson & Szendro, 1995), unfortunately, none exist in Ghana.

Table 3- *Typical effective dose in various European countries.*

EU COUNTRIES	ABDOMINAL E. Dose (mSv)	PELVIS E. Dose (mSv)	TRUNK E. Dose (mSv)
Austria	14.7	8	4
Belgium	8.6	NA	NA
Bulgaria	11.2	11.2	14
Croatia	11.3	8	10.5
Cyprus	10.4	6.3	8
Czech	6.7	5	NA
Denmark	12.2	6.1	17.8
Estonia	10	7.8	15.8
Finland	6.7	14.5	8.8
France	9.4	0.8	33
Hungary	12.1	7	12
Iceland	14.1	9.3	NA
Ireland	8.4	NA	8.1
Italy	8.6	7.8	NA
Liechtenstein	28.7	6.5	NA
Luxembourg	10.5	NA	10.9
Macedonia	17.2	4.2	2.4
Malta	12.4	6.7	7.1
Monaco	13.5	8.8	24.4
Montenegro	20.1	7.1	NA
Netherland	10.6	7.4	NA
Norway	10	7.3	NA
Poland	17	NA	NA
Portugal	6.7	4.1	7.7
Romania	2.6	2.1	NA
Russia	8.2	7.3	17
Serbia	9.7	8.7	17
Slovakia	12.6	12.7	5.5
Slovenia	15.3	9.8	17
Ukraine	13.5	8.8	24.4
UK	5.5	6	8
Mean	11.3	7.3	14.8
Maximum	28.7	14.5	50.5
Minimum	2.8	0.8	2.4
Max/Min	11	18.1	21.5

Source: EC

Renal Anatomy

Renal anatomy refers to the description of the kidney in terms of the basic shape and volume morphology. Here two basic terminology has been discussed, including renal morphology and renal shape and volume model.

Basic Renal Morphology

The kidneys (renal), the urethra, bladder and the ureter are collectively described as the urinary system (B in Figure 6). The kidneys are the central point of operation of the urinary system, as a result it is sometimes described as the renal system and contains millions of nephrons as the functional units. In vertebrate, the kidneys, plays several regulatory roles, and serve an essential function in the body while running several and constant biological and cellular activities, resulting in constant wear, tear and repair. In addition, the kidneys are also described as variably ellipsoid or bean-shaped organs (A in Figure 6), due to their morphological formation.

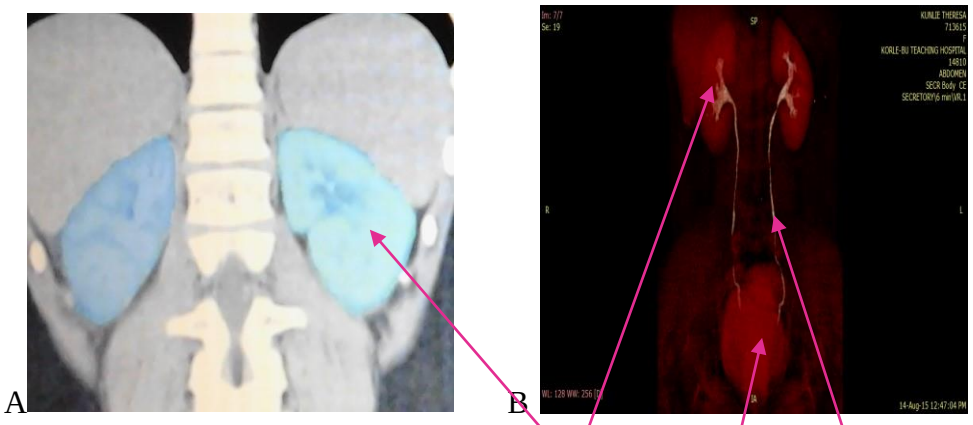

A B

Figure 6: The kidney radiograph (kidneys Bladder ureter)

A is a radiograph showing the kidney as beans shape

B is a radiograph showing the urinary system

Furthermore, human kidneys are located behind the peritoneum at an oblique angle in the abdominal cavity. On each side of the spine lies each of the two kidneys, and are described as left and right kidneys. The position and shape

of the liver cause the abdominal cavity to be asymmetrical and this results in the right kidney being slightly lower than the left. The left kidney is located between T12 (twelfth thoracic vertebra) to L3 (third lumbar vertebra) and slightly more medial than the right. Both the right and left kidneys sit just under the diaphragm and are stern to the liver and the spleen respectively. The eleventh and twelfth ribs partially protect the upper parts of the kidneys where two layers of fat surround the adrenal glands on top of each kidney; this fat is described as the perirenal and pararenal fat. Both kidneys have a concave (renal hilum) and convex surface, where the arteries supply oxygenated blood to the kidney and the vein takes deoxygenated blood away from the kidneys.

Renal Shape and Volume Model

The renal shape is described as a kind of an ellipsoid, which is a type of quadric surface that is a 3D analogue of an ellipse. Mathematically, the equation of a standard axis-aligned ellipsoid body in xyz-Cartesian coordinate system is expressed as:

$$(\frac{x^2}{a^2}) + \frac{(y^2)}{b^2} + (\frac{z^2}{c^2}) = 1, \quad (2.13)$$

where a and b are the transverse, equatorial radii along the x and y axes respectively, and c is the conjugate, polar radius along the z-axis; all of these are fixed positive real numbers which represent the shape of the ellipsoid. Hence, with known a, b and c radii along x, y and z axes, the shape index of the ellipsoid is estimated to be less than or equal to one (1) as shown by Oak Ridge National Laboratory (ORNL), in Equation (2.14).

In a publication by ORNL, the volumetric shape of the kidney is defined as a uniform ellipsoid model cut by a plane perpendicular to the x-axis (McAfee, Cloutier, Edwards & Snyder, 1969). These are generally positioned

symmetrically in relation to the z and y planes. According to ORNL report (McAfee, Cloutier, Edwards & Snyder, 1969), the human renal volume model can be represented mathematically by the ellipsoid equation representing the external envelope of the kidney.

Mathematically, the ORNL publication defines the position and shape of each kidney as:

$$\left(\frac{(x \pm x_{ki-0})}{a_{ki}}\right)^2 + \left(\frac{(y \pm y_{ki-0})}{b_{ki}}\right)^2 + \left(\frac{(z \pm z_{ki-0})}{c_{ki}}\right)^2 \leq 1, \qquad lxl \geq x_{ki-1} \qquad (2.14)$$

where the ± sign is used to indicate the right (+) or left (-) kidney, respectively:

a_{ki}---- Half X-axis of each kidney, b_{ki}--- Half Y-axis of each kidney

c_{ki}--- Half Z-axis of each kidney, x_{ki-0}--- X-position of center of each kidney, y_{ki-0}--- Y-position of center of each kidney, z_{ki-0}--- Z-position of each kidney

x_{ki-1}--- X-limit for each kidney

Generally, models are described as either visual indicators or text-based GUI design with mathematical expression. Visual indicators represent an object using a collection of points in space, connected by various geometric entities such as triangles, lines and curved surfaces, for instance visual indicator for kidney is shown by A of Figure 7, while text based are represented by text descriptors in words or numbers as shown by B of Figure 7.

A  B 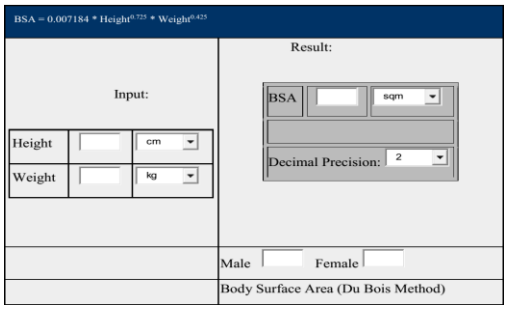

Figure 7: Kidney visual indicators (A) and text-based interface (B).

Source: faqs.org

After collection of points and other information, models can be created by three processes; these include, by hand, algorithmically (procedural modeling), or scanned. In most scientific processes the combination of all the procedures is essential just as in the case of this study. This is because it allowed direct conversion of object into images through scanning, extraction of the data through measurements and algorithmically using procedure modeling. Most current studies adopt the use of data extraction. This is key in designing the organ volume model which is described as a semi-automated modeling technique, mostly with direct measurements and assisted with computer application software.

Application Software

One important visual programming and application software language is the MeVisLab (MVL). MeVis Medical Solutions AG in collaboration with the research institute Fraunhofer MEVIS developed MeVisLab application software. It is a special tool focus on medical imaging for processing and analysing images and image data for research and clinical application. It is an excellent clinical software for fast integration and development of new algorithms including testing of new clinical application prototypes.

MeVisLab application software has advance modules features for volume analysis, registration, segmentation as well as quantitative functional and morphological analysis. MeVisLab enable clinical prototypes, including software assistants for dynamic image analysis, Neuro-imaging, surgical planning and other image analysis (MeVis Medical Solutions, 2015).

Comparatively, well-known third-party libraries and technologies are best implemented using MeVisLab application software, most importantly in

the application of visualization and interaction tools, Python scripting language and for graphical standard analysis. Significantly, part of the modules incorporated in the MeVisLab distribution are directly led by Fraunhofer MEVIS.

In addition, MeVisLab contribute significantly to DICOM as a standard software protocol for distributing as well as viewing all kinds of medical images, regardless of the origin of the images; these include CT and other tomographic images (MeVis Medical Solutions, 2015). MeVisLab and Python standard software are identified to carry out the current study requirements. These are used to accurately carry out the measurement of the various organ dimensions. In lieu of this it is currently used to measure radiological and other non-radiological organ parameters like renal parameters and the implementation of the CAD modeling during image analysis and visual indicators in clinical reporting and research. The MeVisLab application software has application features that are used to extract basic data from the real, raw Tomographic images to fulfil research study requirements. The application software features help users to identify and define the complex organ shape and extra the dimensions of organs with all the needed information on the images. MeVisLab application software is distinguished as a rapid prototype and development program for medical image processing and visualization (MeVis Medical Solutions, 2015).

MeVisLab software is capable to manage large volume of data and can process all dimensional images (x, y, z, color, time or user-delimited), included those in this study. MVL offers easy and fast-breaking ways to customize any application on medical images by developing novel algorithms or improve

existing ones in a modular C++ or VB interface, which is the fundamental bases of this study for the development of GUI. MVL offers easy ways of combining algorithms to algorithm pipelines and networks which is required in this study.

MVL platform enables integration with digital networks such as PACS and IMACS. It is quick and easy to incorporate into clinical environments due to standard interfaces with other DICOMs used by the imaging equipment. MVL has a fair performance for clinical routine due to a page-based, demand-driven approach in the image processing.

In a clinical environment, the working process is made easier and comfortable using a GUI design. This enables an adequate graphical display of a design model, in parliamentary procedure to produce a final product of user interactions. For instance the GUI of a modeled BSA equation, shown in Figure 7B; where in clinical environment only the input parameters are measured and the BSA are generated by the user interface as shown.

Mathematical Modelling

This section discuss the basic principle in modelling; including the procedure and protocols in developing rotational renal volume model.

Basic Modelling Techniques

In scientific applications relationships among various variables and parameters are best described using mathematical formulae to clearly establish a parametric relationship refers to as models to express correlation or causation. Generally speaking, variable in data are developed in a form of models and used to develop in order to evaluate a particular unknown variable or variables in the data, with some residual error depending on model accuracy. Mathematically (Charles & Gary, 1989), data are expressed as:

Data = Model + Error. (2.15)

In addition, models derived from data are best described by inferential statistics mode, which includes techniques to measure relationships between particular variables. For example, regression analysis is applied to model a relationship between independent variable X and a dependent variable Y and are described mathematically as Y is a function of X and stated as:

Y = aX + b + error, (2.16)

where the model is designed such that 'a' and 'b' minimize the error when the model predicts Y for a given range of values of X (O'Neil & Schutt, 2014). Equation (2.16) demonstrates a simple, modeled linear relationship between Y and X, whilst Figure 8 shows a graphical representation of a linear relationship between two parameters Y and X, where an increase in X results in a corresponding increase in Y.

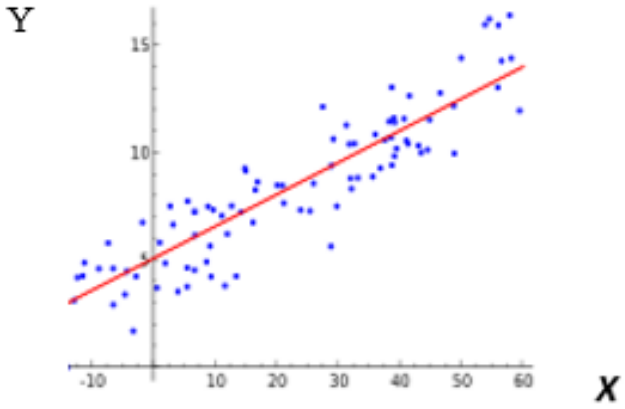

Figure 8: Linear relationship between X and Y.

Modelling Procedure

A mathematical model is a set of mathematical statements, mostly with two or three variables, say S, Q and M where S is a system, Q is a question relating to the system S, and M is a set of mathematical statements, where M = {1, 2,…,

n} which can be used to answer the Q. For instance, to an observer B, an image A^* is a model of an object A to the extent that B can use A^* to answer questions that interest him about A (Velten, 2009).

In recent times mathematical modeling is used to design an interface for an interactive relationship between various elements in a system. It typically depends on a number of input parameters, which when processed through mathematical formulae, results in one or two outputs. Figure 9, shows a schematic diagram of the process of mathematical modelling (Feeman, 2010).

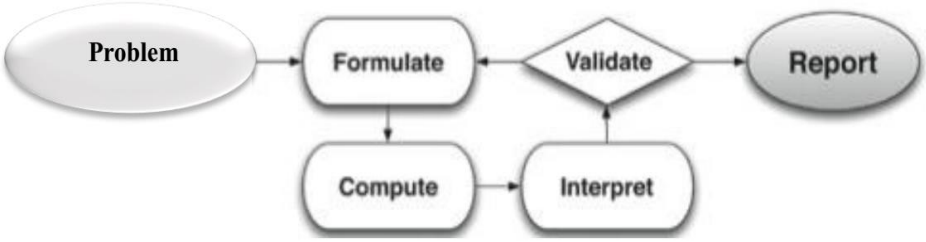

Figure 9: Schematic diagram of mathematical modelling process.

Mathematical models together with a suitable computer algorithm are used in a variety of fields. For example, organ models and its application in medical image analysis is employed to identify the patterns of human organs by combinations of mathematical equations which describe planes, cylindrical, conical, elliptical and spherical surfaces (Feeman, 2010; Velten, 2009; Sargent, 1963). These are answered by developing equations of human body organs using CT imaging or induce current density and electric field from applying low frequency of electric and magnetic field in MRI imaging. This provides standard reference data to aid image analysis and enable clinicians to provide accurate data for clinical decision.

In conclusion, mathematical models are easy to work out and standardize by changing variables and factors in the designed expression. However, mathematical expressions are too simplified when compared with real human

anatomy, which is in the form of a three dimensional object. To overcome this challenge a 3D diagram are applied to represent human organs. In the case of the kidney, the ellipsoid instead of an ellipse is best fitted for kidney 3D description in terms of its volume and external envelope representation. More importantly, these are done with the use of a specially designed software during the modeling processes and procedure in order to overcome the obvious challenge of user interaction capabilities.

Rotational Ellipsoid Equation

Generally, kidneys are described as rotational ellipsoid, which is a 3D analogue of an ellipse, it represents and describes the volume and its associated dimensions of an object. Mathematically, the volume of an ellipsoid is calculated by estimating the product of the length, width, thickness and the ellipsoid constant. This can be stated mathematically as:

$$V = \frac{4\pi}{3} abc, \tag{2.17}$$

where 'a' is the longitudinal (length), 'b' is the transverse (width), 'c' is the A-P (thickness) diameter of the ellipsoid and $\frac{4\pi}{3}$ is the ellipsoid constant (A in Figure 10). From Equation (2.17), unknown ellipsoid coefficient, K^* (ellipsoid like shape, e.g. kidney) can be estimated as:

$V \times K = \frac{4\pi}{3} abc \times K = K^* abc$

If $V \times K = V^*$ and $\frac{4\pi}{3} K = K^*$

Then,

$$K^* = \frac{V*}{abc}, \tag{2.18}$$

where K^*, a, b and c are the renal volumetric ellipsoid coefficients, renal length (longitudinal diameter), renal width (transverse diameter) and renal thickness (A-P diameter) respectively. Thus, renal volume (V*) can be estimated with known longitudinal diameter, transverse diameter, renal thickness and renal volumetric ellipsoid coefficient K^*. However, in regular clinical practice the K* is determined as a reference standard value and usually multiplied by the three estimated dimensions (the length, width and thickness) to determine the renal volume (Equation (2.19)).

With known K^*, the RV is determined from the expression:

$$RV = K^* * \text{renal length (a)} * \text{renal width (b)} * \text{renal thickness (c)} \quad (2.19)$$

NB. This K^* is a unique factor that determines the variation of all race-specific renal volume models.

Basics of Renal and Body Parameters

This section discuss various theories and principles that correlate renal and body parameters in clinical applications. It also established the mathematical relationship between kidney and rotational ellipsoid.

Basic Principles of Renal Parameters

In addition to ORNL (Oak Ridge National Laboratory) (McAfee, Cloutier, Edwards & Snyder, 1969) description, renal organ volume has been classified and defined as rotational ellipsoid volume, as shown in Figure 10, by a number publications (Breau *et al.*, 2013; Shin *et al.*, 2009; Glodny *et al.*, 2009; Geraghty, Boone, McGahan & Jain, 2004; Emamian, Nielsen & Pedersen, 1995; Brandt *et al.*, 1982). The shaded portion (B in Figure 10) represents real human kidney, forming a solid ellipsoid. In clinical application, renal volume is determined by either the voxel count method or by the rotational ellipsoid

equation with standard reference volumetric ellipsoid coefficient (K^*) as explained. However, the voxel count method cannot be easily used on a daily base due to the complex procedures involved, hence the ellipsoid method is preferred. However, this method requires the use of renal volumetric ellipsoid coefficient as a reference standard value together with the measured renal parameters to estimate renal volume.

Accordingly, to determine the standard renal volumetric ellipsoid coefficient, the voxel count method is used with an advanced DICOM application software. One such software is the MeVisLab application software, which is an innovative image analysis DICOM application software. Together with CT images the MeVisLab is used to measure the linear renal dimensions (A-P (major axis), transverse (b) and longitudinal diameters (minor axis)) as shown by A in Figure 10. Mathematically, diagram A in Figure 10 represents rotational ellipsoid, whose volume can be calculated using Equation 2.17.

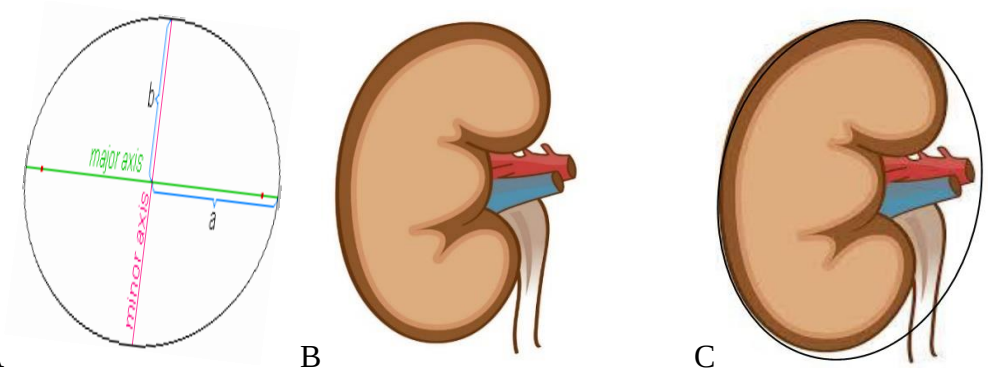

A B C

Figure 10: Kidney as rotational ellipsoid. (A represent Rotational ellipsoid, B represent Kidney and C represent kidney as rotational ellipsoid).

Source: www.nhs.uk

Additionally, B in Figure 10 represents the human kidney, which can be compare with A in Figure 10. Combining the two diagrams shows that Figure B is fitted exactly into A as shown by C of Figure 10, this demonstrate that the

kidney can mathematically be described as a rotational ellipsoid, and its volume can be estimated by using Equation (2.17).

In addition, clinically, renal volume is best measured with the MVL application software by the voxel count method using the snake technique with the region of interest drawn around the shaded portion to determine the total voxels. This method enables complex renal shape challenges to be overcome as the anatomy of the kidney is irrelevant during voxel count measurements.

In other words, the voxel count method is used to determine the exact voxels in the kidney and with a known pixel size (row * column) and the slice thickness, the renal volume is estimated. Additionally, with known renal volume (RV) and renal linear parameters (a, b, c) as in (Equation 2.19), then K^*, the renal volumetric ellipsoid coefficient is determined. Finally, in clinical practice, renal length, renal width and renal thickness are also determined by DICOM linear measurements and multiply by K^* to estimate RV (Breau *et al*., 2013; Ozbek *et al*., 2012; Muto *et al*., 2011; Glodny *et al*., 2009; Janoff *et al*., 2004; Ninan *et al*., 1990). Furthermore, a number of publications have reported varied K^* value, depending on several factors including race and geographical location. Nevertheless, the general universally accepted value has been estimated to be $\frac{\pi}{6}$ or 0.52 in standard rotational ellipsoid formulae of renal volume model. Currently, most countries have moved away from this value and have adopted local based varied K^* value and these have ranged between 0.51-0.55 (Emamian, Nielsen & Pedersen, 1995; Breau *et al*., 2013; Sahni, Jit & Sodhi, 2012; Ozbek *et al*., 2012; Moorthy & Venugopal, 2011; Muto *et al*., 2011; Ferrer, McKenna, Bauer & Miller, 1997). Broadly speaking, the international

renal ellipsoid equation is determined as the product on length, width and thickness, which is equal to the volume shown as:

$$RV = length * width * thickness * (\frac{\pi}{6}). \quad (2.20)$$

Two other renal parameters are discussed in relation to renal volume in literature, this includes; renal shape index (RSI) and renal surface area (RSA). Renal shape index describes the ratio of longitudinal diameter to the sum of the transverse diameter and the anterior-posterior diameter. Renal surface area is determined as the total surface area of the kidney. It is accurately estimated by drawing a region of interest around the kidney surface using the boundary of interest method. This is a pixel summation method, where all the pixels are summed together and multiplied by the size of the picture element. It is expressed as:

$$RSA = Pixel\ Size * Total\ number\ of\ pixels, \quad (2.21)$$

where the total number of pixels is the sum of the number of pixels in the slice that contains the complete renal surface.

Basic Principles of Body Parameters

This section discuss the relationship between various body parameters, including; height, weight, BMI, BSI and BSA. It also include discussions that relate this parameters with renal volume of individuals, in addition to various publications regarding the use of these parameters in clinical applications.

Body Height and Weight

The relationship between body height and body weight has been described by using various terms. Notable among them is the body mass index, body surface area, body shape index and body surface index. In addition, there is a positive correlation between body height and weight as published by

Dorothy W. Sargent (Sargent, 1963). She devised a relationship between weight and height in the American population, which she stated as:

$W = 12.1e^{0.01H}$ For men (2.22)

$W = 9.5e^{0.0108H}$ For women (2.23)

where W is the weight in kg and H is the height in cm.

Body Mass Index

A BMI scale provides information about whether an individual body weight is appropriate for the individual body height. This was first estimated by a Belgian Polymath Adolphe Quetelet (1796-1874) who formulated a method to evaluate the body index during the path of developing social physics (Eknoyan, 2008). It was known as the Quetelet Index until it was termed the Body Mass Index (BMI) in 1972 by Ancel Keys (Du Bois & Du Bois, 1916). The universal unit for BMI is the kg/m^2. Basically, it represents the human body fat between ages 18 and 65 years. Available publications show that, the average Ghanaian adult BMI is 25.7 kg/m^2 for male and 21.65 kg/m^2 for female (Frempong, 2013).

The relationship between renal volume and BMI is used to study the progressive development of the human body in relation to renal development. The relationship between BMI and renal volume can be analysed using major axis regression analysis with Minitab statistical application tools as applied to any two or more unknown relationship.

Body Surface Area and Body Surface Index

Since the development of BMI, two other body parameters have been developed in an attempt to determine the relationship between body height and weight. These are the body surface area (BSA) and body surface index (BSI). To evaluate the surface region of a human body in relation to height and weight, the term body surface area was invented. It is specified as an estimated value that shows the relationship between the average body sizes to the height and normally increases with increasing age. The estimated body surface area of a human body is a measured total surface area of human body (Du Bois & Du Bois, 1916). Several scientists and authors have designed formulas to determine the body parameters and the relationship with the organ dimensions, this has contributed significantly to the understanding and solution to human health (Ferreira & Duarte, 2014; Sardinha, Silva, Minderico & Teixeira, 2006; Verbraecken, Van de Heyning, De Backer & Van Gaal, 2006; Shuter, 2000; Current, 1997; Mosteller, 1987; Haycock, Schwartz & Wisotsky, 1978; Gehan & George, 1970; Fujimoto, Watanabe, Sakamoto, Yukawa & Morimoto, 1968; Boyd, 1935).

All of these are broadly stated in the frame:

$$BSA = \alpha_0 \, H^{\alpha_1} + M^{\alpha_2}, \tag{2.24}$$

where, M is mass (kg), H is height (cm). All parameter values derived from various studies gave reasonably similar results. The mean body surface area varied based on age and gender. Generally, the average BSA estimated value of an adult male is 1.9 m^2, while the average body surface area for an adult female is approximately 1.6 m^2. Furthermore, the average body surface area for

younger children largely varied with age in the range of 1.07 m^2 and 1.14 m^2 between ages 10 to 16 years (IAEA, 1989).

Furthermore, BSA in relation to the body weight describes a new parameter called body surface index (BSI) which is a more precise indicator than both the BMI and the BSA. It is estimated by dividing the body weight by the calculated square root of its BSA, mathematically expressed as:

$$\text{BSI} = \frac{\text{WEIGHT}}{\sqrt{\text{BSA}}} \tag{2.25}$$

Indeed, BSA and BSI, which is significantly used to perform the following clinical services; for instance BSA and BSI is used to estimate the renal clearance (RC), as RC usually divided by either BSA or BSI to gain an appreciation of the true glomerular filtration rate (GFR). In addition the cardiac index is a measure of cardiac output divided by the BSA, giving a better approximation of the effective cardiac output. BSI on the other hand, is used to estimate weight in relation to BSA. The BMI, BSA and BSI define and show the relationship between the average body size to the height and normal increases with increasing age (Ferreira & Duarte, 2014).

Renal Volume Related Body Parameters

Determination of the correlation between the BMI and BSA in relation to kidney dimensions and other measurable parameters has been developed by various researchers (Ferreira & Duarte, 2014; Frempong, 2013; Verbraecken, Van de Heyning, De Backer & Van Gaal, 2006; Sardinha, Silva, Minderico & Teixeira, 2006; Shuter, 2000; Current, 1997; Mosteller, 1987; Haycock, Schwartz & Wisotsky, 1978; Gehan, George, 1970; Fujimoto *et al.*, 1968; Boyd, 1935; Du Bois & Du Bois, 1916)

However, a much precise, measurable parameter has been developed in relation to body weight and body surface area and described as the body surface index (BSI) (Ferreira & Duarte, 2014).

This unique parameter is also related to other body and internal organ measurements and described as BSI-related body parameters without direct measurement. For instance, the determination of the correlation between the BSI in relation to kidney dimensions and other measurable parameters has been developed by various researchers to arrive at BSI related body parameters without direct measurement. The relationship between renal volume and BSI is described as the relative renal volume BSI and defined as the ratio of renal volume to the total body surface index (Frempong, 2013; Verbraecken, Van de Heyning, De Backer &, Van Gaal, 2006). The determination of the relationship between BSI and renal volume is similar to that of BMI and BSA related renal volume. These are done by dividing the renal volume by the BMI or the BSA.

These parameters are important during body organ development, especially for a progressive period of childhood to adulthood and to the aged, where most renal failures occur. In view of these, a number of institutions have designed and modeled organ and body parameters; among them are: AAMP, ICRP, IAEA and EC (IAEA-TECDOC-1005, 1998; IAEA, 1989).

The relationship between renal volume and body parameters (BMI, BSA and BSI) are determined using the following equations to model the standard reference equations: First, the relationship between renal volume and BMI is determined as the ratio of the renal volume to the body mass index, defined mathematically as:

$$\text{RVBMI} = \frac{\text{RV}\,(\text{cm}^3)}{\text{BMI}(\text{kg/m}^2)}$$

$$RV = K\,BMI, \tag{2.26}$$

where k is RVBMI

Secondly, the relationship between renal volume and BSA is determined as the ratio of the renal volume to the body surface area, defined mathematically as:

$$RVBSA = \frac{RV(mL)}{BSA\ (m^2)}$$

$$RV\ (mL^3) = \beta \text{ x } BSA\ (m^2), \tag{2.27}$$

while β is RVBSA

Finally, the relationship between renal volume and BSI is determined as the ratio of the renal volume to the body surface index, defined mathematically as:

$$RVBSI = \frac{RV(mL)}{BSI(kg/m^2)},$$

$$RV\ (mL^3) = \mu * BSI\ (kg/m^2), \tag{2.28}$$

where μ is RVBSI.

In conclusion, several reference organ models and body parameters are reported in literature, this has led to the understanding of human anatomy through medical imaging and therapeutic procedures. Notable among these reference organ models, which are commonly used are the kidney, heart, lungs, brains and the trunk. Table 4 represent a summary of the ICRP and Asian reference man designed from data taken over a period to support individual states in clinical practice (LES, 2006; WHO, 2004; IAEA-TECDOC-1005, 1998; IAEA, 1989).

Table 4- *Asian and ICRP Reference Male/Female Models*

Parameter	Asian (1998)	ICRP (1975)	ICRP (1995)	ICRP (2015)
Male				
Age	35 (20-50)	35(20-50)	35(20-50)	42(20-80)
Race	Mongoloid and South Caucasoid	Caucasoid	Caucasoid	Caucasoid
Sex	Male	Male	Male	Male
Body weight (kg)	60	70	73	76
Body Height (cm)	170	170	176	179
BMI (kg/m^2)	22	24	24	24.6
BSA (m^2)	1.78	1.8	1.9	2.05
BSI (kg/m^2)	33.71	38.25	38.42	38.95
Female				
Age	35(20-50)	20-30	35(20-50)	42(20-50)
Race	Mongoloid and South Caucasoid	Caucasoid	Caucasoid	Caucasoid
Body weight (kg)	51	60	60	63
Body height (cm)	160	161	163	165
BMI (kg/m^2)	22	22	23	24.1
BSA (m^2)	1.55	1.60	1.69	1.70

Source: ICRP

Chapter Summary

In summary, a comprehensive review of the literature on exposure and patients dose optimization procedures, organ measurements and modelling were done in this chapter. It also includes further discussions on dose risk associated with radiation exposure in relation to CTDI, DLP and effective and renal dose parameters as related to EC and ICRP recommendations. The final discussions were based on how estimates of body parameters (BMI, BSI and BSA) as relate to renal volume models and modelling methods are presented in literature.

CHAPTER THREE

MATERIALS AND METHODS

Introduction

This chapter provides relevant information on the materials and the methodology used to measure, analyse and model the relationship between body, renal and dose parameters using mathematical equations. It started by identifying the diverse materials and measuring procedures that were applied to measure body and renal dimensions together with SNR and dose optimization procedures during CT scan. In addition, it includes a discussion of the procedures and protocols for estimating effective abdominal and renal organ dose for dose optimization using SNR. Furthermore, it includes a comprehensive modeling technique using Minitab statistical tools and MVL application software used to model the various equations. It terminates with a discourse on various limitations before, during and after the measurements, modeling and its applications in clinical environment.

Materials

The measurements, design and modeling requirements were specifically customized with specific materials and the appropriate methodology for execution. The specifications of the machines used are presented in Table 5, in addition to the following materials, equipment and tools: Weighing Machines, Automatic BMI Machine, Philip Tomoscan MDCT Machine, Siemens Somatom plus MDCT Machine, GE Max 640 Machine and Toshiba e/CT Machine, Abdominal MDCT images, Input user interface, and MeVisLab (MVL) workstation and interface.

Table 5- *Specifications of CT Scanners*

Manufacturers	Scanner Model/Scan Mode
Philips	Brilliance 64, Multislice, Axial and Helical Modes
Siemens	Emotions 16, Multislice, Axial and Helical Modes
General Electric	Lightspeed VCT 64, Multislice, Axial and Helical Modes
Toshiba	Toshiba-Aquilion ONE, Multislice, Axial and Helical Modes

The BMI machine (Figure 11) was used to simultaneously measure the height and weight of the patients and automatically generate the body mass index with predetermined model equation of the weight divided by the height squared as applied in equation 3.7. In centers where the BMI machine was not available, an improvised height measuring system (Figure 12) and a weighing scale (Figure 13) were used. This enabled manual calculation of the BMI using a written code with VB based on equation 3.7. These two measuring instruments together with an input user interface (Figure 19) where the input data are captured, were used as pre-imaging tools as part of the clinical assessment of patients before imaging. Other materials used included four different models of MDCT Machines (Figure 14), with varied number between 16 and 640 slices (Spefications shown in Table 5) . The Abdominal MDCT images (Figure 15) that met the selection criteria were copied onto DVD and transferred onto the MVL application workstation (Figure 16). The MVL user interface (Figure 17) enabled various measurements in coronary and axial planes to be undertaken. Additionally, it shows MVL user interface for measurements of images

information and also for recording of image data. Furthermore, Figure 18 shows a recommended standard designed of a simple CT imaging center.

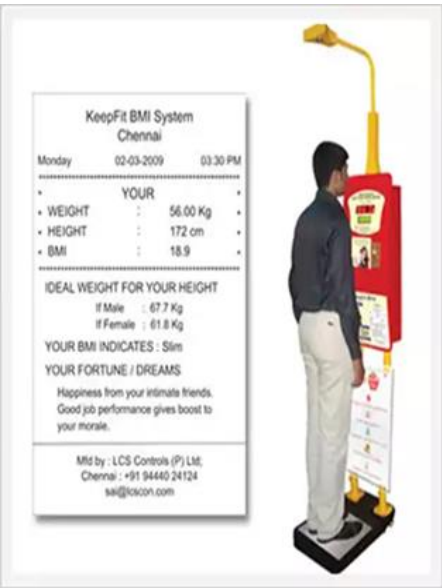

Figure 11: Measurements of BMI

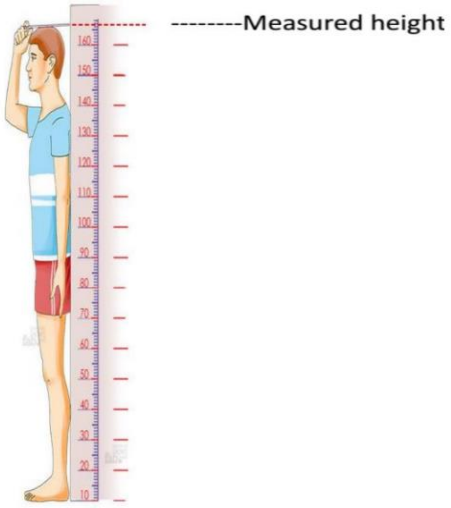

Figure 12: Measurements of height

Figure 13: Measurements of weight

Figure 14: 4 MDCT machine

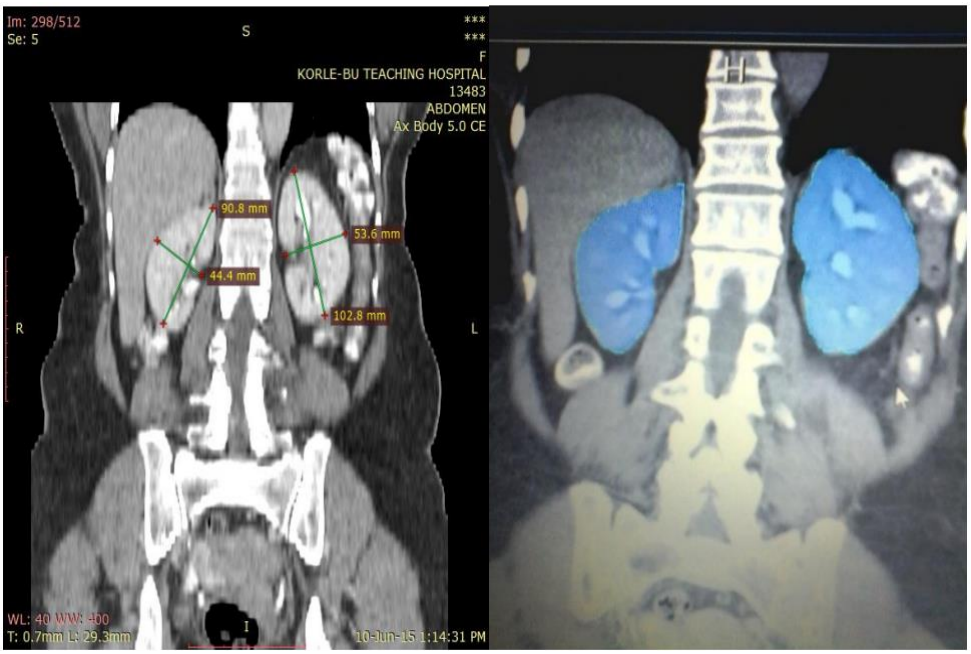

Figure 15: Abdominal CT images showing the kidney

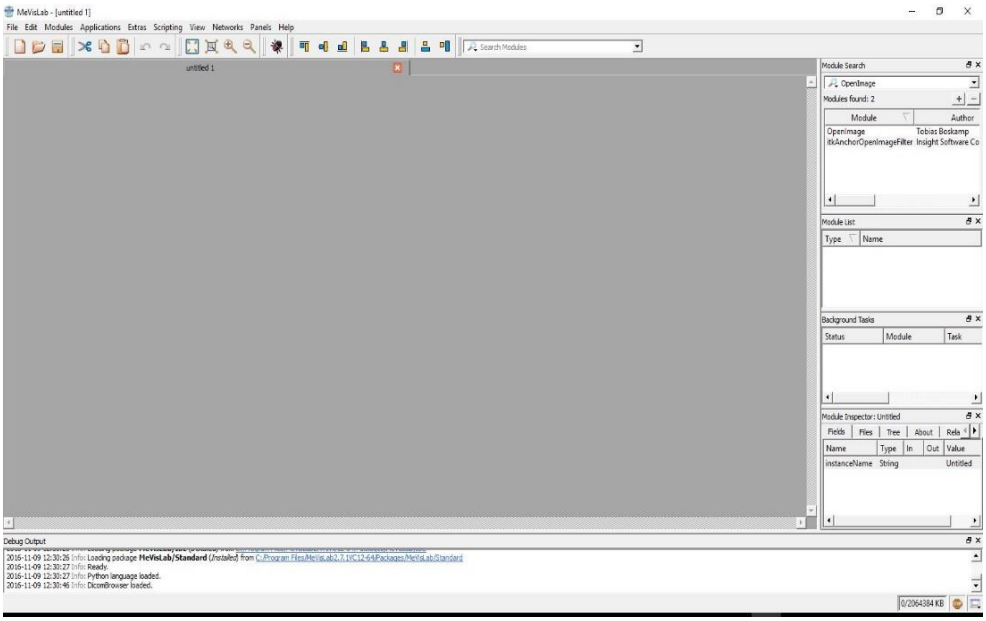

Figure 16: MeVisLab work station interface

Figure 17: MeVisLab interface with loaded with image data

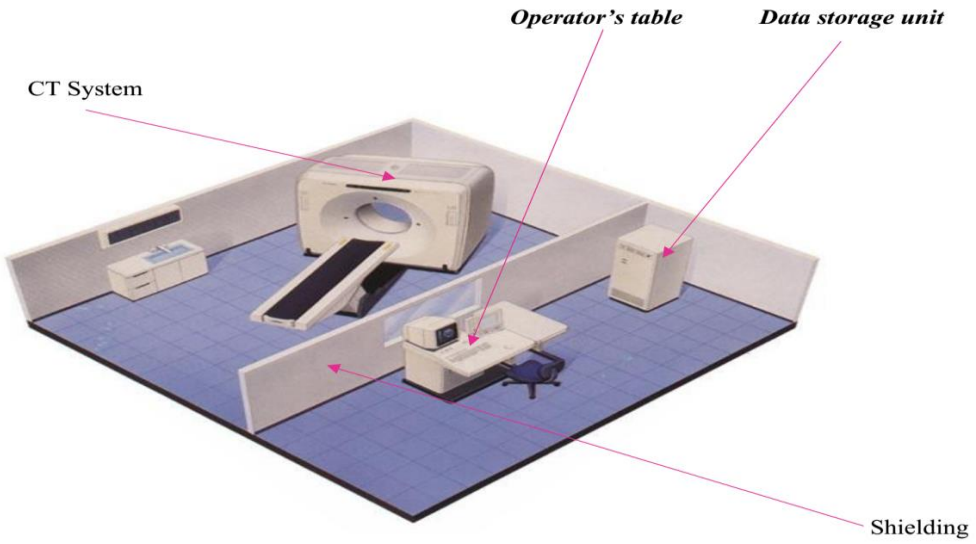

Figure 18: A designed CT room layout

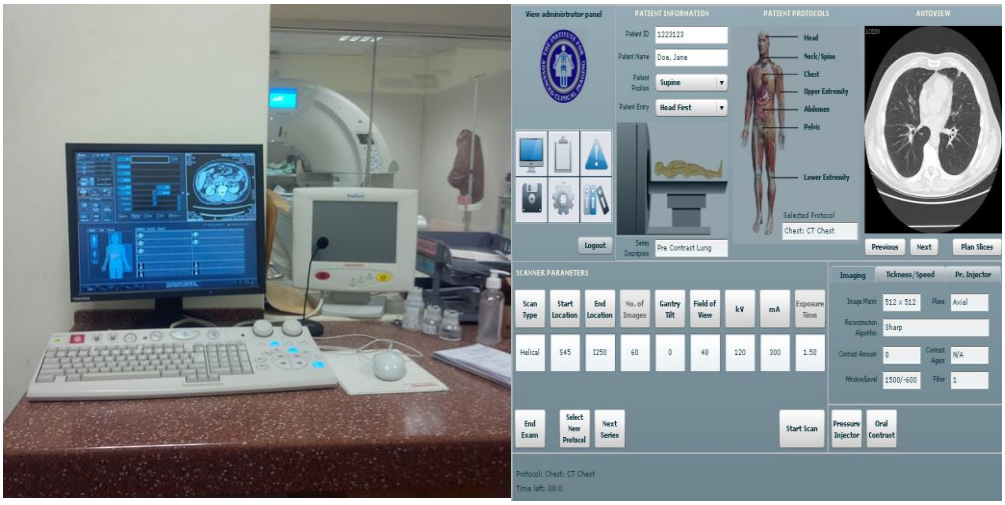

Figure 19: Input CT data user interface. Source: KTH

Methodology

To ensure the study represent the entire Ghanaian population, the data was collected all over Ghana. This was done by using two sampling techniques: Stratified random sampling and Simple random Sampling. The Stratified Sampling technique was used to select the five participating hospitals in Ghana. To do this the country was divided into three sectors; northern, middle and

southern sectors, consequently, one hospital each was selected from the three sectors whilst two other hospitals were selected from Greater Accra based on two factors; high density of CT units which increase the patients CT attendance in Accra and cosmopolitan nature of the region. In addition, the two hospitals selected were referral hospitals all over Ghana, hence can said to be representative of the country. The Simple random sampling technique was used to randomly select patients who came to the hospital for imaging, taken into consideration the selection criterion. Additionally, each individual patient was chosen entirely by chance and each person has an equal chance of being included in the sample.

To accomplish the study objectives, the data collection and application procedures involved two processes; these were pre-imaging data collection procedure and post imaging data collection procedure. The pre-imaging data collection process involved the collection of basic patients' information such as patient ID, gender, age, height, weight, patients' comments, BMI, BSI and BSI before imaging in all the hospitals (CT Centers). The post-imaging data collection process involved the selection of images that met the selection criteria after which the selected images are coded and transferred from the PACS onto DVD and then to the MVL platform for measurements of the renal parameter. In addition, the post-imaging data capturing also involved the recording of exposure and dose parameters including: $CTDI_{VOL}$, DLP, in addition to pixel size, pitch factor and slice thickness. Details of the image data interface are presented in Figure 20.

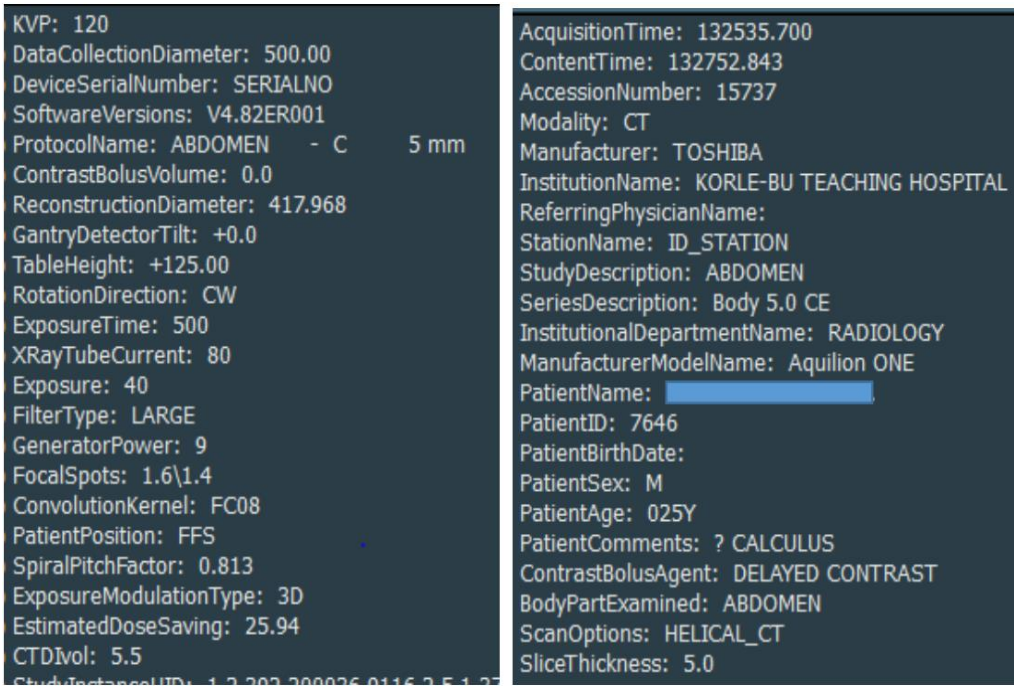

Figure 20: Acquisition dose parameters as displaced in image data

Pre-Imaging Procedure

The pre-imaging procedure were the first processes undertaken as part of the basic data collection protocol. It involved the collection of basic patients' information such as patient ID, gender, age, height, weight, patients' comments, BMI, BSI and BSI based on the standard protocol of the inclusion criteria in all the CT Centers, in addition to unified basic technical protocol.

Basic Data Collection Protocol

The first sets of the data collection process described as pre-imaging data collection process, included the collection of patients' basic information as part of the regular physical body check-up before imaging. The parameters captured include; patient ID, gender, age, height, weight, patients' comments, BMI and BSA using primary data form A (Appendix B). These were done as part of the basic imaging protocol as standard practice in all the five imaging centers.

Approximately 1000 abdominal MDCT examinations of patient data were collected between November 2014 and December 2015 from all the imaging Centers. This was reviewed based on both the patient comments and the radiologist's advice and approval. The sample population of 660 out of the 1000 patients took part in this study; this comprised outpatients who required CT examination for varied diagnostic requests other than those associated with renal pathology.

All the scanning processes were performed using similar standard abdominal scanning protocol, as shown in basic technical protocol to unify the data for analysis based on the selection criteria. Furthermore, all images used for the study were images of the simple abdominal X-rays MDCT examination which contain the kidneys. For clearer boundary demarcation, only images with adequately visualized renal boundaries as recommended by the radiologist were admitted as part of the inclusion criteria.

Since the study reviewed real patients' information, an application to the ethical review committee of the university of Cape Coast for ethical clearance was sought and duly approved (Appendix M).

The inclusion criteria for the sample selection were patients who had no account of renal disease, high blood pressure, or other vascular diseases, some of which include:

1-Inflammation of the intestines

2-Pre-surgery planning

3-Abdominal pain or swelling

4-Hernia

5-Masses and tumors of the intestines and

6-Infections or injury of the stomach

The exclusion criteria for sample selection were patients with renal diseases or conditions that affect renal function and anatomy some of which include:

Congenital, cystic and neoplastic abnormalities

Vesicoureteral reflux

After kidney transplants

Renal arterial stenosis

Presence of underlying diseases such as diabetes mellitus or high blood pressure, which are the two major sources of glomerular injury which affect renal function. Hypertension and diabetes mellitus are the most common causes of end stage renal disease.

The presence of any abnormal findings on CT examination that could affect kidney volume, include intrarenal diseases such as renal cysts, renal cancer, hydro nephrosis and single kidney

Patient with any abnormal interactive laboratory findings such as poor glomerular filtration rate and Albuminuria-to-creatinine ratio which indicate renal damage.

Lastly, images that were from patients whose weight exceeded 105 kg and below 45kg were not part of this survey.

Basic Technical Protocol

The CT scans were performed using the following technical parameters:

Collimation, 0.625-7.00 mm

Table Speed, 50.5-60.5 mm/rotation

Rotation Time, 0.5-0.8 seconds

Voltage, 120 kV (peak).

Body Part Examined: ABDOMEN

Scan Options: HELICAL_CT

Slice Thickness: 5.0mm

Exposure Time: 500s

X-Ray Tube Current: 80-253A

Exposure: 25-126

Filter Type: LARGE

Generator Power: 9

Focal Spots: 0.8-1.6

Estimated Dose Saving: 0-55.51

Spiral Pitch Factor: 0.813

Exposure Modulation Type: 3D

Pixel Spacing: 0.500 - 0.999

Window Center: 40

Window Width: 400

Post contrast scans of entire abdomens were performed with a 60-70-second delay after starting the infusion of 50-80 ml of nonionic contrast material. Coronary section data were reconstructed with a 5-mm thickness and a 5-mm increment and were then transmitted electronically to MVL application software for analysis.

Post-Image Data Collection

The second sets of data collection was the selection of images for renal measurements. The selection was done based on the inclusion criteria, from which six hundred and sixty (660) out of the one thousand (1000) images were

admitted for review and analysis. This was made up of one thousand three hundred and twenty (1320) kidneys, with 660 right kidneys and 660 left kidneys.

Post imaging data collection involved two processes: the measurements of various renal parameters using MVL application software and using appropriate formulae or equations to estimate other parameters.

The measured parameters include: measurements of longitudinal diameter, transverse and A-P diameters and renal volume on the MVL application platform, details of which are shown in primary data form B (Appendix C).

The estimated parameters include: renal volume, renal surface index, renal surface area and renal volumetric ellipsoid coefficient using the secondary data forms C (Appendix D), radiation exposure and dose parameters included: CTDI, DLP, renal and effective dose using secondary data form D (Appendix E).

Measurements of Linear Renal Dimensions

The first measured parameters include three linear dimensions, described as longitudinal diameter (renal length), transverse diameter or the lateral diameter (renal width) and the Anterior-Posterior (A-P) diameter (renal thickness). All these dimensions were measured at maximum values of strictly longitudinal, transverse and Anterior-Posterior sections through the center of the kidney. The renal lengths were evaluated using the coronary images while the axial images were applied to measure A-P and lateral diameters. The width and thickness were evaluated in the transverse plane perpendicular to the longitudinal axis of the kidney. The level of this transverse section was placed at the level of the hilum.

Two different methods were used to measure the longitudinal diameter (LNG) on the coronary images: the first method of measurements was done by drawing a single straight line from one edge of the renal parenchyma to another end with the linear measuring tool on the MeVisLab (MVL) platform as shown in Figure 21. This was repeated three times and the average of the three measured values calculated as the renal length.

Secondly, the renal length was calculated from axial slices by multiplying the slice thickness by the number of slices between the superior and inferior tips of the kidneys. This was also repeated three times and the average value estimated.

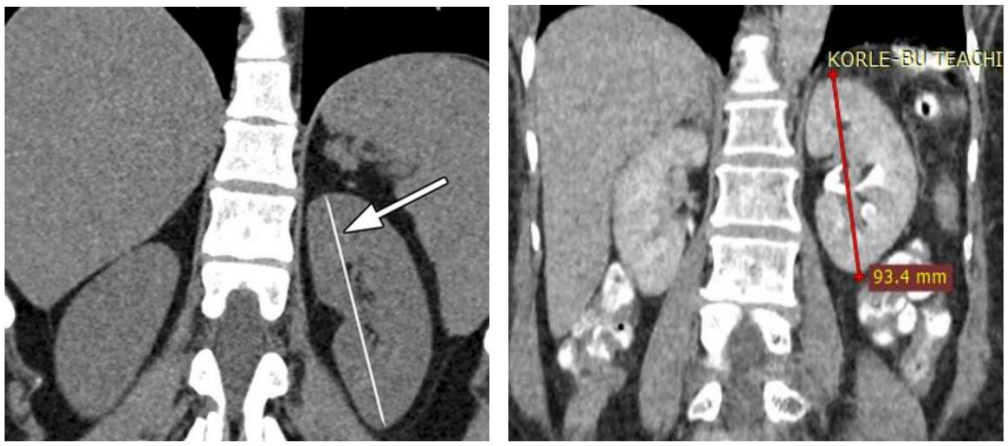

Figure. 21: Measurements of renal length

In addition, two other linear parameters were measured: the lateral diameter (LT), measured from the lateral extent of the kidney to the renal sinus and anterior-posterior (A-P) diameter measured perpendicular to the lateral diameter as shown in Figure 22. Altogether the two measurements were repeated three times and the mean values of both parameters, estimated to represent the average lateral and A-P diameters.

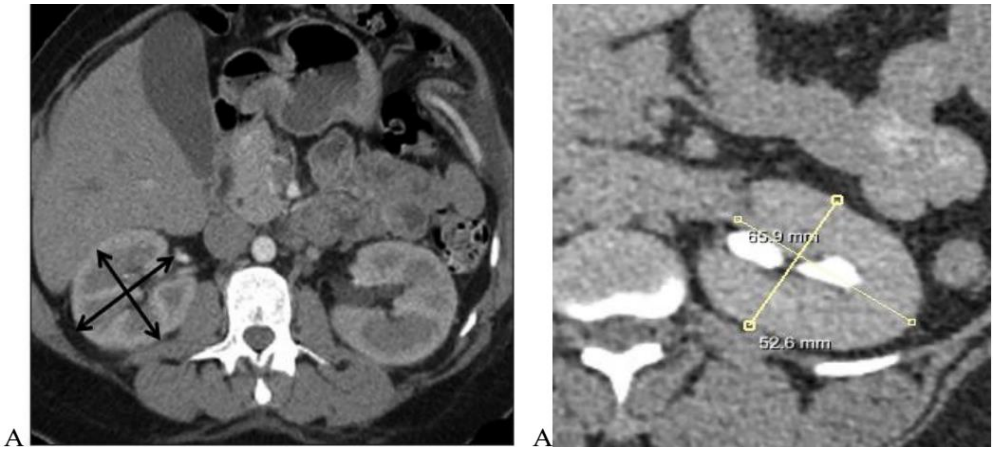

Figure 22: Measurements of lateral and A-P diameters

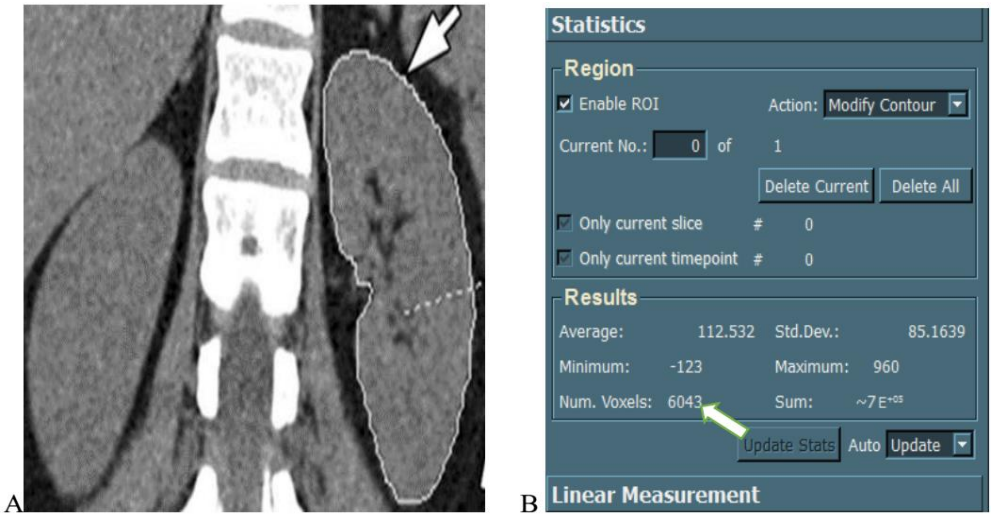

Figure 23: Measurements of RSA and RSI

Measurements of Renal Volume

The second component of this study was the measurements of renal volume from contiguous CT slices with voxel measuring tool on the MVL application software as shown in Figure 24B. These measurements were done using 3D volume-rendered image of the kidney shown in Figure 24A. The maximum length of the kidney was measured in the longitudinal plane and was visually estimated to represent the largest longitudinal section. Two different methods were also applied to estimate renal volumes.

The first method was the calculation of the total renal volume by using the voxel-count method of the MVL application software (block white arrow in Figure 23A), with a region of interest (ROI) drawn on each of the two kidneys on each slice to indicate the renal boundaries. The total voxel was automatically generated on each slice (block white arrow in figure 23B) by considering the amount of the voxel lying within the boundaries, including the central sinus fat but excluding perinephric fat as shown in figure 25, with yellow rectangle.

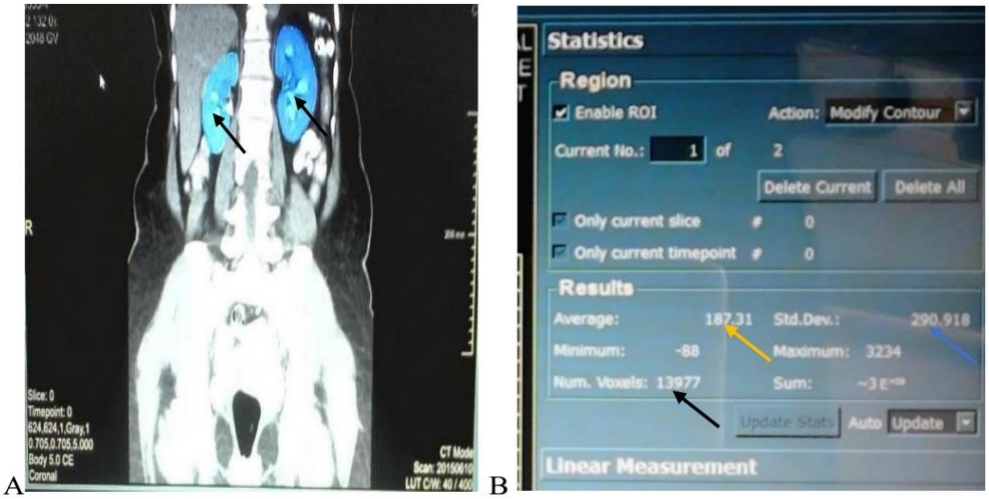

Figure 24: Measurements of renal volume by voxel count method.

Furthermore, with a known pixel size, slice thickness and the total number of voxels (black arrow in Figure 24B), in addition to computing for each average count and standard deviation of the voxels (yellow and blue arrows in Figure 24 respectively):

that is,

RV = Total number of voxels x slice thickness x pixel size (3.1)

Equation (3.1) was then used to compute for renal volume. The advantage of applying this method is that the anatomy of the kidney is irrelevant during measurements. An average of three voxel-count

measurements and three other repeated measurements were used as the reference-standard renal volume.

Indeed, this method of volume measurement may result in partial voluming, which occurs when voxels contain both kidney and surrounding tissue, could lead to an overestimation of the renal volume when all such voxels are included within the boundaries of the kidney (Bushberg, Seibert, Leidholdt & Boone, 2012; Krakauer & Krakauer, 2012; Huesman, 1984). To avoid this overestimation, the segmented line was drawn at the halfway point of the change in signal intensity, between the kidney and the surrounding tissue and, used as reference measuring point in all the slices (Bushberg, Seibert, Leidholdt, Boone, 2012). Figure 25A and 25B shows a reconstructed 3D volume-rendering renal images with clear boundary demarcation from the surrounding tissues.

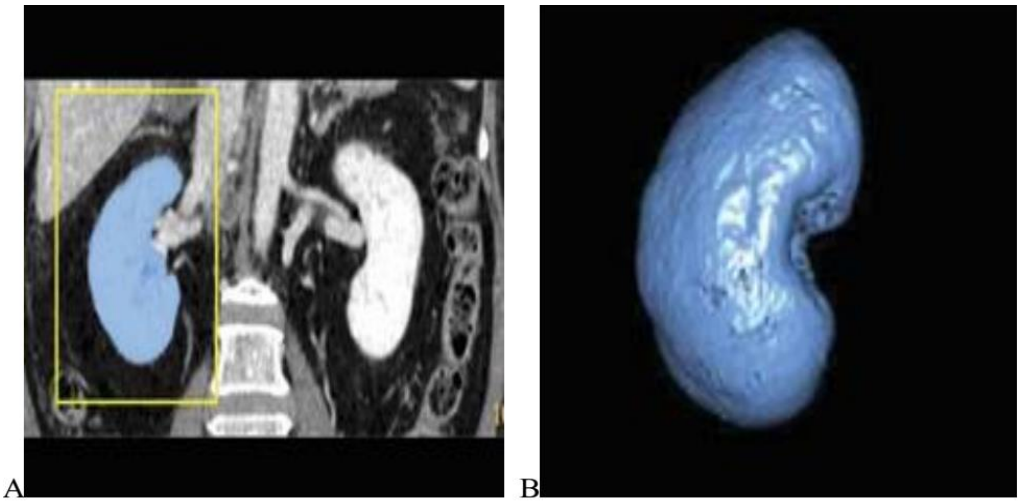

Figure 25: Mapped out renal volume and 3D volume-rendering

Measurements of Renal Volume Related-Renal Parameters

Four important parameters associated with the linear renal dimensions and volume measurements were also estimated. These include: Renal shape index (RSI), renal surface area (RSA), relative renal length (RRL) and relative renal volume (RRV). First, the renal shape index was estimated by finding the

ratio of the renal length to the sum of lateral and A-P diameters. That is, with known A-P diameter, renal length and the lateral diameter.

Mathematically, RSI is estimated as:

$$\text{RSI} = \frac{\text{renal length}}{\text{renal width} + \text{renal thickness}} \tag{3.2}$$

Equation (3.2) was used to estimate the renal shape index.

From Equation (3.2) relationship, renal length is proportional to the sum of renal width and renal thickness, expressed as:

$$\text{RSI} = \frac{R_L}{R_w + R_T},$$

therefore,

$$R_L = \text{RSI}(R_w + R_T)$$

$$R_L = (R_w + R_T). \tag{3.3}$$

Since RSI has constant value of one (1) by definition in Equation (2.13), it implied that renal length is equal to the aggregate of the renal width and renal thickness.

Secondly, the renal surface area was estimated by using the MVL application software tool to map out the kidney contour on a slice that contains the total surface area of the kidney as shown with a white arrow on Figure 23A. This was done by manually tracing the boundaries of the surface area of the kidney on the slice that contained the complete renal surface. The total number of pixels was automatically generated (block white arrow on Figure 23B) by MVL software based on the region of interest (ROI) lying within the surface boundaries of the kidney. The measurements were repeated three times and the average value calculated. With the known pixel size, and the total pixels on the surface, RSA was estimated.

Mathematically renal surface area is estimated as:

RSA = Pixel Size * number of pixels. (3.4)

Furthermore, two relative renal parameters were also calculated and reported as relative renal length and relative renal volume. This was performed to compare the relationship between the right and the left renal dimensions. The relative renal length was determined by dividing either the right or the left renal length by the total renal length (sum of the left and right renal length). In addition, the relative renal volume was also estimated by dividing either the right or the left renal volume by the total renal volume (sum of right and left renal volume). The relative renal volume enables volume capacity of the left and right kidneys, this is essential during renal transplant.

Estimate of Renal Volumetric Ellipsoid Coefficient

The renal volumetric ellipsoid coefficient K^*, was calculated by dividing the measured renal volume by the product of renal length, renal width and renal thickness. It symbolizes the constant of proportion in the ellipsoid equation. The K^*-values were determined by using the ellipsoid equation for estimating renal volume define as:

RV = K^* * renal length (RL) * renal thickness (RT) * renal width (RW),

This means that,

$$K^* = \frac{RV}{RL*RT*RW}. \quad (3.5)$$

Therefore, with a known renal volume by the voxel count method, renal length, renal width and renal thickness by linear measurements using MVL, then K^* was estimated and the standard reference ellipsoid equation with known K^* defined as:

$$RV = K^* * RL * RT * RW. \quad (3.6)$$

Estimate of Body Indices and Related-Renal Volume

The measurements of height and weight were part of the pre-image data collection process, where patients body weight and body height were measured as part of the regular physical check-up before imaging. Two different methods were used to estimate the BMI: By either direct registration with the BMI automatic measuring system (Figure 11) or by calculating from separated measurement of height (Figure 12) and weight (Figure 13) as defined by Equation (3.7). Whilst BSA was estimated indirectly using the Du Bois formula as presented in Equation (3.9), BSI was estimated by dividing measured body weight by BSA as shown in Equation (3.11).

Furthermore, the relationship between renal volume and BMI, BSA and BSI was established by applying two different methods: statistical analysis of Minitab statistical software and experimental analysis. The major regression analysis of the Minitab application software produced a statistical modeled relationship between the body parameters and the renal volume. In addition, the related renal volume-BMI, BSI and BSI hypotheses were estimated using experimental analysis by dividing the renal volume by BMI, BSA and BSI to get the renal volume related BMI, BSA and BSI (RV-BMI, RV-BSA and RV-BSI) respectively, for both left and right kidneys. The statistical results were compared with the results of the experiment analysis and presented.

Experimental analysis of the three renal and body parameters (RV-BMI, RV-BSA and RV-BSI) are expressed mathematically from the BMI relation:

$$\mathrm{BMI} = \frac{\mathrm{W}}{\mathrm{H}^2}. \tag{3.7}$$

The relationship between BMI and Renal Volume (RV) was determined

mathematically by dividing the renal volume by its corresponding BMI as in the expression:

$$\text{RVBMI} = \frac{\text{RV}(\text{Ml}^3)}{\text{BMI}(\text{kg/m}^2)},$$

$$\text{RV}(\text{Ml}^3) = \lambda\ \text{BMI}(\frac{\text{kg}}{\text{m}^2}), \quad (3.8)$$

where λ is equal to RVBMI ($\text{Ml}^3/(\frac{\text{kg}}{\text{m}^2})$)

The most widely used BSA calculated formulae are the DuBois formula expressed as:

$$\text{BSA}(\text{m}^2) = \text{weight}^{0.425}\ \text{kg} * \text{height}^{0.725}\ \text{cm} * 0.007184 \quad (3.9)$$

Mathematically, RV-related BSA was determined by dividing the renal volume by the BSA as in the expression:

$$\text{RVBSA} = \frac{\text{RV}(\text{Ml}^3)}{\text{BSA}(\text{m}^2)}$$

Hence, $\text{RV}(\text{Ml}^3) = \beta\ \text{BSA}\ (\text{m}^2)$ (3.10)

where β is equal to RVBSA ($\text{Ml}^3/(\text{m}^2)$),

Mathematically, BSI was calculated as:

$$\text{BSI} = \frac{\text{W}}{\sqrt{\text{BSA}}} \quad (3.11)$$

And, RV-related BSI was estimated by dividing the renal volume by the body surface index as in the relation:

$$\text{RVBSI} = \frac{\text{RV}(\text{Ml}^3)}{\text{BSI}(\text{kg/m}^2)}$$

Hence, the relationship between BSI and renal volume was estimated as

$$\text{RV}\ (\text{Ml}^3) = \mu * \text{BSI}\ (\text{kg/m}^2), \quad (3.12)$$

where μ is equal to RVBSI ($\text{Ml}^3/(\frac{\text{kg}}{\text{m}^2})$).

It implies from Equations (3.8), (3.10) and (3.12) that renal volume is proportional to the three measured parameters, BMI, BSA and BSI respectively.

Estimate of Renal and Effective Dose

MVL DICOM application software standard supplement was issued in 2007 for the reporting of dose parameters in CT (DICOM, 2007). This became mandatory for all manufacturers of CT equipment. It requires a report summary should be given for the whole patient examination and the accumulated dose applied after every CT scan. The patient bio data, study information and the general equipment information are stored within the general part of the structured report. This development enabled the obvious difficulties in measuring the distribution of dose within the body during CT imaging to be overcome since 2007 using image data. More practical dosimetric quantities captured as part of image data were applied to readily estimate dose parameters from closely related measurements. The risk-related quantities were obtained from the practical dosimetric quantities such as $CTDI_{VOL}$ and DLP, using the dose-conversion coefficients in Table 2.

On the image data, using MVL platform detail information of the $CTDI_{vol}$ and DLP were available for recording as shown in Figure 17 and 20. These parameters enabled renal organ and effective dose to be estimated using Equation (3.13) and (3.14) with the recommended ICRP region-specific normalized effective dose coefficient in Table 2. Hence, broad estimates of effective dose € and renal organ dose (RD) were derived from values of DLP and $CTDI_{VOL}$ respectively, for each examination using the appropriately normalized coefficients. For abdomen, E_{DLP} represent general values appropriate to abdomen to estimate effective dose as published by the ICRP

(ICRP publication 103, 2007; Hutton & Osiecki, 1998).

To estimate the abdominal effective dose, DLP and region-specific normalizing constant or DLP conversion factor (E_{DLP}) as developed by ICRP Publication 103 is defined as:

$$\text{Effective Dose} = 0.0153 * \text{DLP}, \quad (3.13)$$

where 0.0153 is the estimated abdominal conversion factor from ICRP publication 103 as stated in literature. This is because the effective dose is not measured, but it is a theoretically calculated dose based on the organs exposed to the applied radiation multiplied by tissue-weighting factors. The effective dose conversion factor estimates can change over time because the tissue-weighting factors can change with new data and continuing analysis of existing data with better analytical tools, the effective dose conversion factor estimates can change over time.

In addition, renal organ dose estimates were estimated as developed by ICRP 103 recommendations. This was calculated by using a converting factor known as weighted-CTDI (CTDIW). Once the $CTDI_W$ is known, it is straightforward to multiply it by the effective mAs value and the renal dose conversion coefficients to obtain the renal organ doses for all the examinations. For partial-body irradiation as in CT, effective dose is the weighted summation of the absorbed dose to each specified organ and tissue multiplied by the ICRP-defined tissue-weighting factor for that same organ or tissue (Deak, Smal & Kalender, 2010). Furthermore, the conversion factor for renal tissues as recommended by ICRP publication 103 was 0.0086 at 1 mAs. Hence, the renal organ dose was calculated as:

$$D_{kidney} = 0.0086 * CTDI_W * \text{eff(mAs)}, \quad (3.14)$$

where D_{kidney} is the renal dose, 0.0086 is the renal tissue conversion factor from ICRP publication 103, $CTDI_W$ is the weighted Computed Tomography dose Index and mAs is the effective millimeter per second, which were calculated by dividing the exposure (mAs) by the pitch factor. That's

$$\text{eff(mAs)} = \frac{\text{mAs}}{0.813}. \quad (3.15)$$

The estimated average exposure (mAs) for this study is 48.19mAs. Hence the eff(mAs) is 56.27mAs. The weighted CTDI ($CTDI_W$) was estimated by multiplying the volume CTDI ($CTDI_{VOL}$) by the pitch factor expressed mathematically as:

$$CTDI_W = 0.813 * CTDI_{VOL}, \quad (3.16)$$

where 0.813 is the average pitch factor of the scanning protocol.

In addition, with the above definitions organ and effective doses were estimated and a comprehensive standard reference renal organ dose (organ absorbed dose per unit Computed Tomography dose Index) was established. Details of this measured values are presented with form D in Appendix E. The mathematical model was produced to estimate effective and renal organ doses with specific input parameters and age and gender specific dose estimates. A graphic user interface was designed for user input of patient- and scan-specific parameters, and to calculate and display effective and renal organ doses. The dose parameters $CTDI_{VOL}$ and DLP could be estimated before imaging by using the relation as in Equations (3.17) and (3.18).

CTDIvol = 0.21mAs - 3.05 (3.17)

DLP = 27.60mAs - 240.06 (3.18)

The input mAs is test run with the Equations (3.17) and (3.18) at 120 kVp and the $CTDI_{VOL}$ and DLP are estimated. The organ and effective doses are

then estimated from $CTDI_W$ (which is a product of pitch factor and $CTDI_{VOL}$ Equation (3.16) and DLP Equation (3.13). The corresponding signal to noise ratios were also estimated to determine the dose optimization protocol.

Measurement of Signal to Noise Ratio

The homogeneous volume method was used to estimate signal to noise ratios of all the images by finding a homogeneous area within the image and to compute the process signal (mean) and the noise (standard deviation). That is, during the measurement of renal volume with the MVL, signal and noise were estimated by applying the natural variation of the end product of the process with the signal represented by the process standard deviation (blue arrow on B in Figure 24) of that output with the measured parameters average (yellow arrow on B in Figure 24) and the noise represented by the. The ratio of the mean of the standard deviation of the images is referred to as the signal to noise ratios of the images. Indeed, this was done as part of the voxel measurements for the calculation of renal volume with the ROI, the signal (process average) and noise (standard deviation) was measured simultaneously. The ratio of these two parameters was then evaluated using the relation: Process signal average minus background signal divided by standard deviation.

Mathematically the signal to noise ratio is expressed as:

$$\text{SNR} = \frac{\mu(\text{Signal on organ}) - \mu(\text{signal on background})}{\text{Noise or Standard deviation } (\sigma)} \quad (3.19)$$

The result of this will be described as large, if SNR has a magnitude of the signal or process average been large relative to the noise as measured standard deviation. In addition, if the SNR is large, then the signal is deemed to be significant and not just random variation.

To evaluate whether the image noise became more uniform, the coefficient of variation (C_V) (reciprocal of SNR) was calculated using the equation

$$C_v = \frac{\text{Noise or Standard deviation } (\sigma)}{\mu(\text{Signal on organ}) - \mu(\text{signal on background})} * 100\% \quad (3.20)$$

Summary of Measured and Calculated Parameters

The renal and body parameters were measured using the MVL application software to determine the basic renal dimensions. Other parameters were also calculated using various mathematical expressions as shown by the theories and principles in Chapter Two and in the methodology in Chapter Three.

Table 6- *Measured Parameters and Evaluating Methods*

Measured Parameters	Methodology
Body Height	Measuring tape
Body weight	Measuring scale
BMI	BMI Calculator
BSA	$BSA = Wt^{0.425} * Ht^{0.725} * 0.007184$
BSI	$BSI = \frac{W}{\sqrt{BSA}}$
RSI	$\frac{\text{renal length}}{\text{renal width}+\text{renal thickness}}$
Renal length	Linear MVL Platform
A-P Diameter	Linear MVL Platform
Lateral/Transverse Diameter	Linear MVL Platform
Renal Volume	Volumetric MVL Platform
Renal surface area	ROI MVL Platform
Volumetric ellipsoid coefficient (K*)	$K^* = \frac{RV}{RL*RT*RW}$
Renal dose	$RD_{kidney} = 0.0086CTDI_W * eff(mAs)$
Effective dose	$E = 0.0153DLP.$
SNR	ROI MVL Platform (Signal/noise)

These parameters were described as measured and or calculated depending upon the method used. Additionally, Table 6 represents a summary of the name and methodology used to obtain all the parameters that were used to design a comprehensive reference body, renal and dose parameters in this study. In conclusion, nineteen parameters were estimated, these include; five body parameters (height, weight, BMI, BSA and BSI), seven renal parameters (RSI, longitudinal diameter, A-P diameter, transverse diameter, renal volume, renal surface area and renal volumetric ellipsoid coefficient), in addition to three dose parameters (renal dose, effective dose and SNR) and four exposure parameter ($CTDI_{VOL}$, DLP, mAs and kVp)

Experimental Modelling Process

The experimental modeling process involved the use of mathematical modeling procedure, which reduces the data from empirical measurements to real clinical application process for implementation (Tzedakis, *et al*., 2005). This modeling process involved two procedures: the first modeling procedure is described as an experimental analytical modeling technique by using ellipsoid equation together with a voxel count method to determine the relationship between renal volume and linear renal dimensions. In this case, the voxel count method was used to measure the renal volume, which was divided by the product of the renal length, renal width and renal thickness to determine renal volumetric ellipsoid coefficient (VeC) presented as K^* in Equation (3.5). Hence, after the determination of the K^* values, the various age and gender variation models were developed.

Additionally, the experimental analytical modeling technique was also used to model the relationship between pre-set exposure parameters (mAs, kVp

and pitch factor) and the expected dose risk-related parameters including, CTDI, DLP, E and RD, so that with known exposure pre-set parameters (mAs, kVp), dose estimates (E, RD) were predicted before the imaging procedure starts.

In contrast, the second method involved the use of statistical analysis to determine the relationship between renal volumes, renal dimensions and other body parameters. The linear regression approach for modeling the relationship between a scalar dependent parameter and the explanatory or independent parameters. In addition, both simple linear regression (only one independent variable) and multiple linear regression (more than one independent variable) were used. Here, linear regression relationships were modeled using linear predictor functions whose unknown model parameters are estimated from the data. The results of the models with this method are presented in Chapter Four by using Normal Probability Plot (NPP) of all the various related parameters. Additionally, linear regression analysis models were used because in clinical applications, models represent real data of humans with linear body dimensions which with known depend linearly parameters allow for the unknown to be estimated, hence the statistical properties of the resulting estimators are easier to determine.

Furthermore, the linear regression analysis procedure involved the use of statistical regression analysis to determine the mathematical relationship between two or more variables. The idea of linear regression equation predictor which is used to estimate the relationship between two unknown variables in the form of the model equation predictor was used and expressed as:

$$Y = B_0 + B_1X \tag{3.21}$$

where Y is the unknown variable and X is the predictor with B_0 and B_1 as the intercept on the axis of the unknown variable and the slope of the relationship between the two variables respectively. In addition, each predictor in a regression equation has an estimated coefficient associated with the sample population regression coefficients; that is by using the estimated coefficients (B_1) with the predictors to calculate the fitted value of the response. Furthermore, the model equations were verified by estimating B_1 and B_0 and compared them with the modeled linear regression equation predictor above. In addition, the estimated coefficient (B_1) was also estimated using the formula of simple linear regression:

$$B_1 = \frac{\Sigma(X_1 - X)(Y_1 - Y)}{\Sigma(X_1 - X)^2} \tag{3.22}$$

whereas the formula for the intercept (B_0) was estimated using:

$$B_0 = y - B_1X \tag{3.23}$$

The second modeling technique was used to model equations that described the relationship between the renal volume and the body indexes (BSA, BSI and BMI). This enabled the prediction of renal volume when either BSA, BSI or BMI or both are known.

The regression analysis was also used to model the relationship between the pre-set parameters and the dose risk factors, with one dose factors, other dose factors were estimated. The relationship between renal dose and effective dose formed the final modeling process where a mathematical modeling procedure was used to establish the linear relationship between the two parameters. This enabled renal dose to be determined with known effective dose

by a prediction method for clinical application and vice versa. All the model equations are unique to the sample data and hence described the relationship between renal volume with a body and dose parameters for the Ghanaian CT scan-user population, which formed 45% of the medical imaging population in Ghana.

Statistical Modelling Process

This section discusses the various statistical tools that were used to perform the basic analysis of the experimental data. It also include decision and conclusion rule that were adapted to draw reasonable conclusion. Additionally, it also accounts for various modelling techniques that were applied to achieve the desire objectives.

Basic Statistical Analysis

Statistical analysis of the data were performed using Minitab 16 statistical analysis tools (Mazonakis, Tzedakis, Damilakis & Gourtsoyiannis, 2007). Additionally, it was also used to explain the excel plot of various relational analysis of the data. This involved the use of both Multivariate techniques for the distribution of a variable and Analysis of mean and variance technique for analyses of the data. The Multivariate Analysis of Variance (MANOVA) technique, suitable for large distribution of variable or sample population greater than 30 sample units or number of observations was applied, whilst the Analysis of Variance (ANOVA) which is a collection of statistical models was used to analyze the differences among the mean of the various age and gender variations and their associated procedures (Sullivan, 2010). Consequently, both ANOVA correlation and regression analyses were performed by comparing the mean and p-values. Whilst, the MANOVA technique was conducted so as to

compare both the body, the renal and the dose parameters across the different age groups (20-40 years, 41-60 years and 61-80 years) and gender (male and female) variations. Correlation and major regression analyses of MANOVA were also carried out to determine the relationship that exists among the three sets of parameters, including body, renal and dose parameters, with Minitab 16 statistical analysis tool.

These exploratory data analysis tools focused on the detailed description of the obtained data with respect to demographic factors such as age, sex, height and weight. All the parameters, were analyzed separately for male and female using the data from the various age groups. Additionally, renal length and the renal volume were correlated with gender, body surface index, body mass index and body surface area. The outcomes of all the compiled data were given as mean plus or minus standard deviation (± SD). The premises of the MANOVA model include multivariate normality, linearity and equality of variances of the dependent variables across the various groupings being compared. Finally, the decision and the conclusion rules were as described in the section below.

Decision and Conclusion Principle

In order to make a decision based on the analysis of the data for the various models, the decision rule and the conclusion hypothesis were used. That is the null hypothesis to accept a model must be rejected if the p-value was less than 5% significance level ($p < 0.05$) or fail to reject if otherwise. Based on the decision rule, comparative study on renal length, renal volume, body surface index, body mass index and body surface area across the various age groups were obtained. The output of the multiple comparison test conducted across the

various age groups and gender is presented in chapter four with respect to the underlying dependent variables.

In addition, SNR is similar to testing whether S_x is significantly different from zero. Hence, statistically by multiplying the SNR by$\sqrt{n}$, where n is the sample size, to test the hypothesis that the average value of X is significantly different from zero. For example, SNR is considered large, if SNR * $\sqrt{n}$ is greater than 5, for a confidence level of 99.5%. This implies an existence of a "signal" over and above the noise. If SNR * $\sqrt{n}$ is less than 5, this implies that the data could very well be simply Noise.

Statistically, various estimated parameters were presented as the average or mean values of the various parameters plus the standard deviation, written mathematically as:

$$\text{Mean, } \ddot{X} = \frac{X_i}{n-1} \tag{3.24}$$

$$\text{Standard Deviation, } SD = \sqrt{\frac{(\ddot{X}_i - X_a)^2}{n-1}} \tag{3.25}$$

$\ddot{X}$ represents an average or mean measured or estimated parameters of the sample population, with a standard deviation represented as ± SD. Hence, the standard reference renal, body and dose values will be presented as:

$$\ddot{X} = \text{mean} \pm SD = \frac{X_i}{n-1} \pm \sqrt{\frac{(X_i - \ddot{X})^2}{n-1}} \tag{3.26}$$

Computer Aided Design Model

The final component of the modeling process is the GUI applications. This was done in two different processes and procedures. The first was the coding process where a software was developed with a written code in VB and integrated on the DICOM application platform for clinical application. The second was the visual indicators where the shape and size were modeled to

represent the variation in age and gender that exist between the various model equations.

The codification process involved written codes with a VB and integrated the code on the DIMOM application platform. This was done by converting the mathematical representation into GUI in a text-based user interface which is applicable in a clinical environment. This served as an input interface for the radiology team (medical physicist for purposes of radiation protection, radiology for image analysis and radiographer for appropriate input parameters for control measure). The visual indicators were done on the MVL application platform to assist visualize the shape and size of the kidney. Both the mathematical model equations, designed as text based interface (GUI) and the visual indicators are presented under sub-title visual indicators and GUI models in chapter 4. These models allowed direct manipulation of the data by applying the standard reference values established to test run the system before imaging.

Limitations

The most important challenge with this study is the fact that, all measurements were based on individual judgment which were most likely to be affected by intraobserver and interobserver variability and poor reproducibility. This requires expert knowledge and experience for acceptable accuracy to be achieved and stand as a serious challenge for any data to be admitted from any source for analysis. In addition, for a clinical decision, it is important to independently and individually access renal volume, since many factors such as body mass index, height, gender, age, position of kidneys, sex, stenosis and number of renal arteries influence renal volume measurements. Thus, the thought of seeking to reduce time during image analysis, which the study aims

to accomplish, may result in determinants that may not apply in whole cases. Nevertheless, it is important to have an overview of general standard reference values for the shape and dimensions of various human organs, in order to simplify procedural analysis for clinical decision, all things being equal.

A number of limitations are associated with MDCT scans, which the study relied on; these include: breathing and other movement artifacts during in vivo abdominal MDCT examinations. Additionally, these affect specific organ measurements, as artifacts affect organ shape and size especially in kidney study due to its proximity to the lungs which is seriously affected by breathing and movement artifacts. Therefore, these made it difficult to overcome the challenge in renal volume measurement. Furthermore, during kidney study, the axis of the CT scan may not be parallel to the axis of the kidney. This mismatch may affect the accuracy and require advanced software for alignment, which were difficult to achieve. Furthermore, fat within the kidneys is difficult to exclude in MDCT estimates of various dimensions, resulting in underestimation or in some cases overestimation of various renal organ volumes, referred to as partial voluming and linear measurements. In addition, further investigation is required to quantify inter-observer and intra-observer variation in measurements of kidney size using MDCT scan. Additionally, exposure to X-rays is one potential limitation for the use of CT for this study, due to the radiation dose involved, therefore getting enough data for the study presents a serious challenge. There is also a risk of contrast media-induced nephropathy and this made the data acquisition a serious challenge which explains why very few of such studies exist despites its importance to clinicians. Various other imaging modalities have similar risk challenges.

In conclusion, images that were from patients whose weight exceeded 105 kg and below 45 kg were not part of this study. The study only accounts for a normal average size Ghanaian within the weight bracket of 45 kg to 105 kg and with ages between 20 to 80 years. Hence, it's limited in scope since it does not cover every Ghanaian including adolescents and the neonates, who are critical in the health care delivery chain in the developing world including Ghana. This study is limited in terms of establishing dose levels and comparing the estimated local values with published dose levels established in other countries since they may have potentially different CT practice and technology which may not be wholly relevant to a specific or particular circumstances, due to varied protocols that may be employed.

Finally, published dose values in terms of $CTDI_{vol}$ or DLP may not be expressed in relation to the same standard CT dosimetry method pertaining to a specific data. Furthermore, advances in technology, such as iterative reconstruction, will need to be taken into account when updating dose levels or benchmarking local dose levels as against doses relating to dissimilar technologies.

Chapter Summary

In summary this chapter discussed relevant information about the materials and the methodology used to achieve the study objectives. The chapter also gave a vivid information about the various measuring procedures that were used to measure and process the primary data in order to successfully design the modelled equations. It conclude with a description of the application software and statistical models that were used to analysed the data, in addition to the limitations encounter during the study.

CHAPTER FOUR

RESULTS, ANALYSIS AND DISCUSSION

Introduction

The basic framework of this chapter identifies the clear perspective of the relationship between the various parameters in tables, graphical representation and model equations in the configuration of GUI. This provides a platform to present the data in three convenient forms. First with tables that describe the mean, maximum and minimum values of all the parameters and the spread of data sets. This was followed with graphical presentations and visual description of the relationship between the various measured and the estimated parameters. Finally, the presented data was mathematically modeled using various practical and theoretical tools based on the study objectives. The chapter ends with description, trend analysis and discussions of the results based on the scope and study objectives.

Presentation of Results

All the measured primary data were in the unit of millimeters unless otherwise stated. Presentation of the summarized values of the entire experimental processes, including data analysis is presented in Table 7 to Table 12, while the details of the data are presented in Appendix B to E. The Tables are presented as the mean, maximum and minimum values in terms of age and gender variation of the body, renal and dose parameters.

Results of measured Body Parameters

Table 7 shows a presentation of five body parameters, including height, weight, body mass index, body surface area and body surface index in terms of the mean, maximum and minimum values based on age and gender variation.

Table 7- *Measured Height, Weight, BMI, BSA and BSI*

SEX/AGE	MEASURE	AGE years	W kg	H cm	BMI kg/m^2	BSA m^2	BSI kg/m^2
MALE							
20-40	Mean	33	81.1	177.9	25.48	2.02	39.93
	Max	40	105.3	189.0	33.99	2.25	47.65
	Min	20	56.5	162.0	18.97	1.75	27.16
41-60	Mean	52	83.4	181.0	25.36	2.06	40.21
	Max	60	110.0	195.0	31.47	2.40	46.23
	Min	41	55.8	167.0	18.64	1.78	26.20
61-80	Mean	68	68	63.9	22.23	1.77	36.15
	Max	80	80	73.8	24.1	2.01	39.05
	Min	62	62	55.7	21.26	1.56	33.88
20-80	Mean	45	80.83	178.6	25.19	2.02	39.81
	Max	80	110	195.0	33.99	2.4	47.65
	Min	20	52.1	156.0	18.64	1.5	26.20
FEMALE							
20-40	Mean	31	63.25	168.9	22.04	1.71	37.09
	Max	40	76.4	189.0	26.08	2.02	44.94
	Min	20	48.6	158.0	19.22	1.47	30.45
41-60	Mean	51	63.86	168.7	22.18	1.74	36.88
	Max	59	81.9	187.0	25.38	2.14	52.84
	Min	42	50.6	155.0	18.85	1.5	30.75
61-80	Mean	68	53.38	158.6	20.93	1.53	34.81
	Max	80	59	165.0	22.35	1.62	38.82
	Min	61	43.7	146.0	18.19	1.39	31.44
20-80	Mean	46	61.87	167.1	21.91	1.69	36.58
	Max	80	81.9	189.0	26.08	2.14	52.84
	Min	20	43.7	146.0	18.19	1.39	30.45

Results of measured Renal Parameters

Table 8 is a presentation of left and right A-P, LT and LNG diameters, in terms of the mean, maximum and minimum values based on age and gender variation.

Table 8- *Measured Renal Dimensions*

Sex/Age	MEASURE	AGE Yrs	$A\text{-}P_R$ mm	$A\text{-}P_L$ mm	LT_R mm	LT_L mm	LNG_R mm	LNG_L mm
MALE	MEAN	32	45.39	45.3	62.3	61.7	104.9	107.9
20-40	MAX	40	63.9	62.7	75.5	73	124.8	126.6
	MIN	20	39.3	39.1	51.5	48.1	85.9	88.5
41-60	MEAN	54	44.59	45.6	61.8	61.1	105.2	106.9
	MAX	60	58.3	59.5	71.3	76.8	118.3	121.6
	MIN	41	37.6	38.5	50.4	47.8	89	75.3
61-80	MEAN	73	42.0	43.6	57.7	57.9	98.9	99.6
	MAX	80	53.7	59.1	66.3	68.8	119.3	119.2
	MIN	61	31.9	26.7	49.3	47.9	84.2	83.6
20-80	MEAN	52	44.1	45.0	60.8	60.4	103.4	105.1
	MAX	80	63.9	62.7	75.5	76.8	124.8	126.6
	MIN	20	31.9	26.7	49.3	47.8	84.2	75.3
FEMALE	MEAN	34	43.46	45.2	60.2	59.2	105.4	107.6
20-40	MAX	40	52.6	54.8	68.4	66.0	124.1	126.6
	MIN	20	38.8	37.9	53.5	47.1	83.8	90.9
41-60	MEAN	51	44.0	45.3	60.1	60.5	103.9	105.3
	MAX	60	56.2	65.6	69.5	68.7	121.7	120.3
	MIN	41	38.8	39.1	47.4	47.1	86.4	87.4
61-80	MEAN	72	42.0	44.2	57.8	57.5	97.0	98.3
	MAX	80	56	59.8	68.8	71.7	124.3	134.8
	MIN	61	32.9	34.7	41.6	43.6	75.6	74.8
20-80	MEAN	56	43.1	44.8	59.2	59.0	101.4	103.0
	MAX	80	56.2	65.6	69.5	71.7	124.3	134.8
	MIN	20	32.9	34.7	41.6	43.6	75.6	74.8

Table 9 is a presentation of three measured renal parameters, including left and right RV, VeC and RSI parameters, in terms of their mean, maximum and minimum values based on age and gender variation.

Table 9- *Estimated Renal Parameters*

Sex/Age	STATISTICS	Age Yrs	RV_R mL^3	RV_L mL^3	VeC_R (K)	VeC_L (K)	RSI_R	RSI_L
MALE	MEAN	34	147.4	153.6	0.526	0.532	1.0	1.0
20-40	MAX	40	183.4	195.7	0.596	0.578	1.2	1.3
	MIN	20	97.52	116.1	0.493	0.500	0.8	0.9
41-60	MEAN	52	146.0	153.8	0.528	0.532	1.0	1.0
	MAX	60	229.8	254.4	0.606	0.620	1.3	1.2
	MIN	43	100.3	96.27	0.495	0.490	0.9	0.9
61-80	MEAN	72	124.5	132.3	0.529	0.530	1.0	1.0
	MAX	80	211.5	297.1	0.606	0.588	1.2	1.3
	MIN	61	74.41	66.89	0.491	0.495	0.8	0.7
20-80	MEAN	52	146.7	151.8	0.528	0.530	1.0	1.0
	MAX	80	312.0	272.9	0.595	0.595	1.3	1.3
	MIN	20	75.54	77.85	0.485	0.491	0.8	0.7
FEMALE	MEAN	32	155.5	159.5	0.529	0.529	1.0	1.0
20-40	MAX	40	311.9	272.9	0.586	0.595	1.2	1.2
	MIN	20	103.7	104.8	0.489	0.491	0.8	0.8
41-60	MEAN	53	152.6	158.0	0.528	0.530	1.0	1.0
	MAX	60	224.9	218.0	0.568	0.593	1.2	1.2
	MIN	41	108.5	108.8	0.485	0.491	0.9	0.7
61-80	MEAN	73	128.3	133.9	0.529	0.530	1.0	1.0
	MAX	80	205.7	190.3	0.595	0.588	1.3	1.3
	MIN	61	75.53	77.85	0.491	0.498	0.9	0.8
20-80	MEAN	54	142.0	148.3	0.528	0.530	1.0	1.0
	MAX	80	311.9	297.1	0.606	0.620	1.3	1.3
	MIN	20	74.41	66.89	0.485	0.490	0.8	0.7

Table 10 shows a relational description and comparison of the left and right kidneys in terms of the mean, maximum, minimum and the spread of data sets based on the relative renal length and renal volume.

Table 10- *Relative RL and RV Parameters*

Sex/Age	Statistics	Total RL mm	R-RRL	L-RRL	Total RV mL^3	R-RRV	L-RRV
MALE 20-40	Mean	212.8	0.492	0.507	317.6	0.495	0.505
	Max	251.1	0.519	0.5417	584.9	0.574	0.587
	Min	176.2	0.458	0.4807	209.2	0.414	0.427
41-60	Mean	212.11	0.497	0.504	310.7	0.493	0.508
	Max	236	0.611	0.539	416.7	0.615	0.566
	Min	182.3	0.461	0.389	217.3	0.435	0.385
61-80	Mean	198.21	0.4994	0.5007	259.7	0.488	0.512
	Max	229.4	0.5606	0.5481	361.6	0.569	0.620
	Min	172.5	0.452	0.4394	154.2	0.380	0.431
20-80	Mean	208.48	0.4959	0.5041	298.9	0.492	0.508
	Max	251.1	0.6111	0.5481	584.9	0.616	0.620
	Min	172.5	0.452	0.389	154.2	0.380	0.385
FEMALE 20-40	Mean	204.41	0.4963	0.5037	282.2	0.486	0.514
	Max	259.1	0.5563	0.5644	487.5	0.614	0.625
	Min	157	0.4356	0.4437	149.1	0.375	0.386
41-60	Mean	213.04	0.4947	0.5053	298.2	0.488	0.512
	Max	250.7	0.5184	0.5413	378.9	0.544	0.598
	Min	181.6	0.4587	0.4817	230.3	0.402	0.456
61-80	Mean	209.11	0.4966	0.5034	299.1	0.487	0.513
	Max	236.5	0.5268	0.5331	462.9	0.549	0.588
	Min	175.7	0.4669	0.4732	212.7	0.413	0.451
20-80	Mean	195.31	0.4968	0.5033	257.4	0.485	0.515
	Max	259.1	0.5563	0.5644	487.5	0.614	0.625
	Min	157	0.4356	0.4437	149.1	0.375	0.386

Results of measured Renal Volume Related Body Parameters

The relationship between the renal volume and the body parameters is presented in Table 11, in terms of the mean, maximum, minimum and the spread of data set values of all the sample population.

Table 11- *Renal Volume-BMI, BSA and BSI*

Sex/Age	Statistic	$RVBMI_R$ $mL^3/kg/m^2$	$RVBMI_L$ $mL^3/kg/m^2$	$RVBSA_R$ mL^3/m^2	$RVBSA_L$ mL^3/m^2	$RVBSI_R$ mL^3/m^2	$RVBSI_L$ mL^3/m^2
MALE	Mean	6.55	6.87	86.31	90.47	4.03	4.21
20-40	Max	8.48	8.89	111.04	120.82	5.42	5.57
	Min	4.12	4.76	57.70	56.35	2.59	3.14
41-60	Mean	6.69	7.06	86.82	91.68	4.00	4.22
	Max	10.96	11.71	150.19	158.23	6.63	8.27
	Min	4.55	3.98	57.37	55.65	2.45	2.53
61-80	Mean	5.76	6.13	74.53	79.18	3.42	3.64
	Max	8.85	13.63	121.27	189.24	5.51	8.36
	Min	3.59	2.95	40.09	38.01	2.18	1.80
20-80	Mean	5.95	6.12	72.97	75.12	3.75	3.87
	Max	12.36	10.81	144.44	126.36	7.55	6.61
	Min	2.98	2.68	35.53	36.21	1.88	1.81
FEMALE							
20-40	Mean	6.37	6.51	77.49	79.02	4.04	4.14
	Max	12.36	10.81	144.44	126.36	7.55	6.61
	Min	3.73	3.66	47.93	47.79	2.42	2.42
41-60	Mean	6.23	6.41	76.65	78.89	3.91	4.03
	Max	10.81	9.20	124.99	119.71	6.21	5.85
	Min	4.01	4.06	51.77	56.07	2.70	2.78
61-80	Mean	5.07	5.30	62.73	65.47	3.19	3.35
	Max	8.09	8.30	99.33	93.47	5.51	5.14
	Min	2.98	2.68	35.52	36.21	1.88	1.81
20-80	Mean	6.29	6.64	81.77	86.40	3.77	3.99
	Max	10.96	13.63	150.19	189.24	6.63	8.36
	Min	3.59	2.95	40.09	38.01	2.18	1.80

Results of measured Dose Parameters

Table 12 shows the variation of exposure and dose estimates, in terms of their mean, maximum, minimum and the spread of data sets.

Table 12- *Estimated $CTDI_{VOL}$, $CTDI_{W}$, DLP, E and RD*

Sex/Age	STATISTICS	AGE years	$CTDI_{VOL}$ mGy	$CTDI_{W}$ mGy	DLP mGy-cm	E mSv	RD mSv
MALE	MEAN	32	6.1	4.9	896.4	13.45	2.98
20-40	MAX	40	16.3	13.3	2127.2	31.91	4.94
	MIN	20	4.7	3.8	364.8	5.47	2.09
41-60	MEAN	51	6.37	5.2	964.8	14.47	3.27
	MAX	60	15.7	12.8	3200	48	8.08
	MIN	41	3.2	2.6	234.4	3.52	2.4
61-80	MEAN	68	5.75	4.7	903.4	13.56	2.75
	MAX	80	9	7.3	1590.9	23.86	3.11
	MIN	63	4.1	3.3	744.9	11.17	2.4
20-80	MEAN	48	6.17	5.0	921.53	13.83	3.12
	MAXIMUM	80	16.3	13.3	3496.4	52.45	8.11
	MINIMUM	20	3.2	2.6	234.4	3.52	2.09
FEMALE	MEAN	32	6.2	5.0	950	14.28	3.52
20-40	MAX	40	14.4	11.7	2568.3	38.53	8.16
	MIN	20	3.5	2.8455	244.6	3.67	1.53
41-60	MEAN	53	6.83	5.6	977.4	14.62	3.35
	MAX	60	16.3	13.0	3496.4	52.45	8.31
	MIN	45	3.0	2.4	213.6	3.2	1.53
61-80	MEAN	67	5.95	4.8	925.51	14.16	2.97
	MAX	75	11.3	9.2	1292	19.38	6.83
	MIN	61	4.7	3.8	234.4	3.52	1.63
20-80	MEAN	44	6.48	5.3	950.97	14.35	3.39
	MAXIMUM	75	16	13.0	2568.3	38.53	8.31
	MINIMUM	20	3	2.4	213.6	3.2	1.53

Graphical Representation of Body Parameters

Figure 26 shows a graphical representation of a variation of body weight, in terms of gender. Figure 26 shows that males has a larger body weight than females. This was supported by the analysis of mean in Appendix F-1.

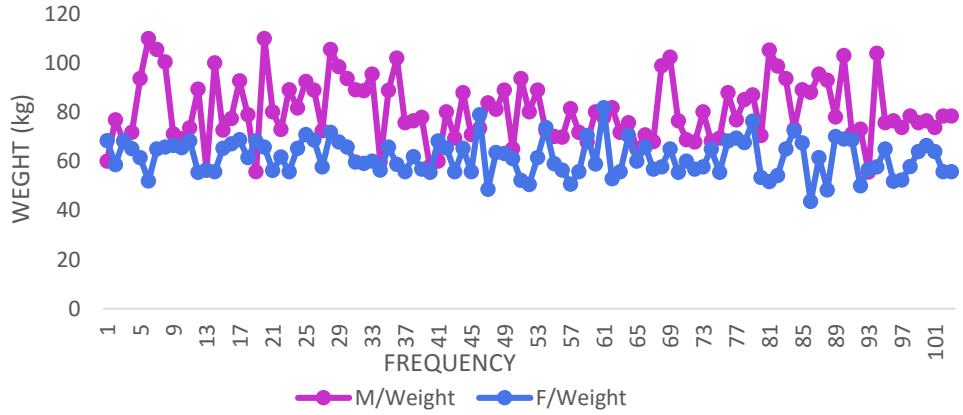

Figure 26: Variation of weight for male (M) and female (F).

Figure 27 represents a variation of body height in terms of male and female. The pictorial representation shows that males' height is slightly higher than their females' counterparts. This was collaborated by the analysis of mean in Appendix F-2.

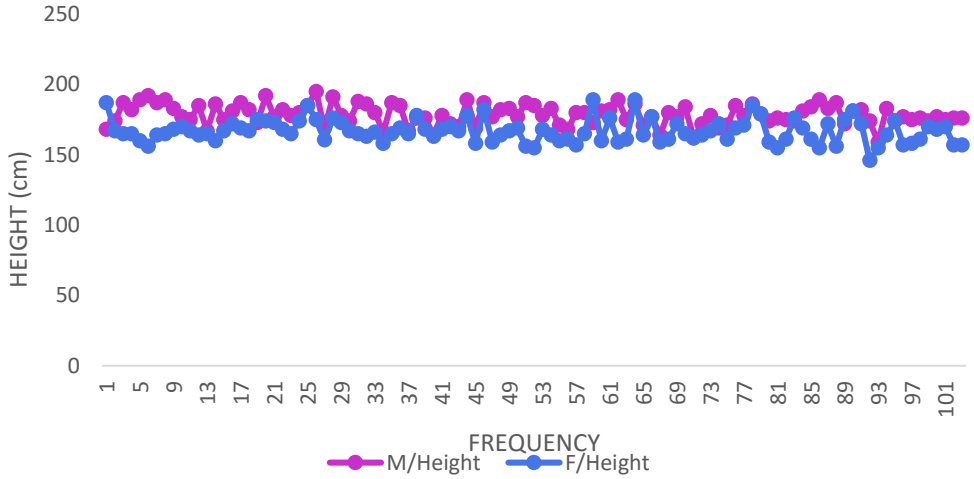

Figure 27: Variation of height for male (M) and female (F).

Figure 28 represents the relationship between male and female body surface index. This shows that males has a larger body surface index than females. This was supported by the analysis of mean in Appendix F-3.

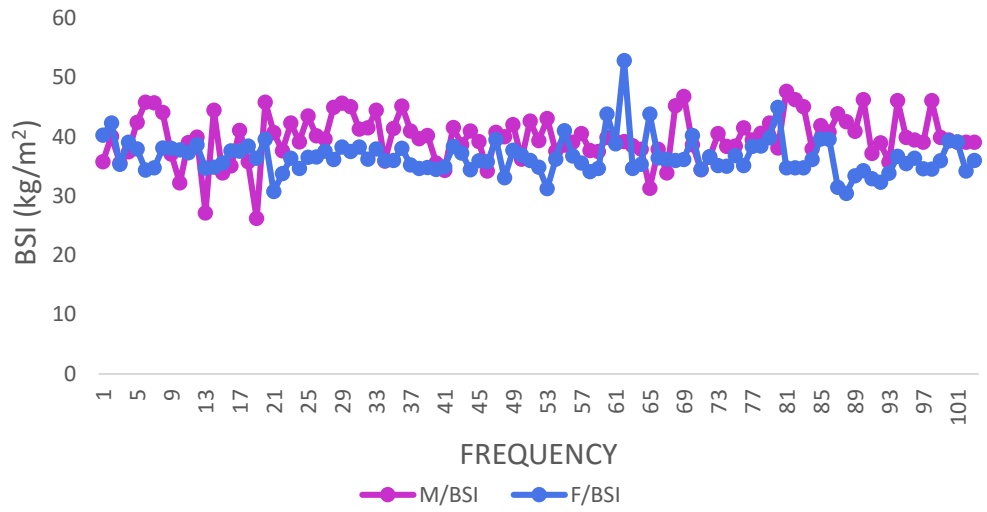

Figure 28: Variation of BSI for male (M) and female (F).

Figure 29 shows a relationship between male and female body mass index. The figure shows that the males has a larger BMI than their females' counterparts. This was supported by the analysis of mean in Appendix F-4.

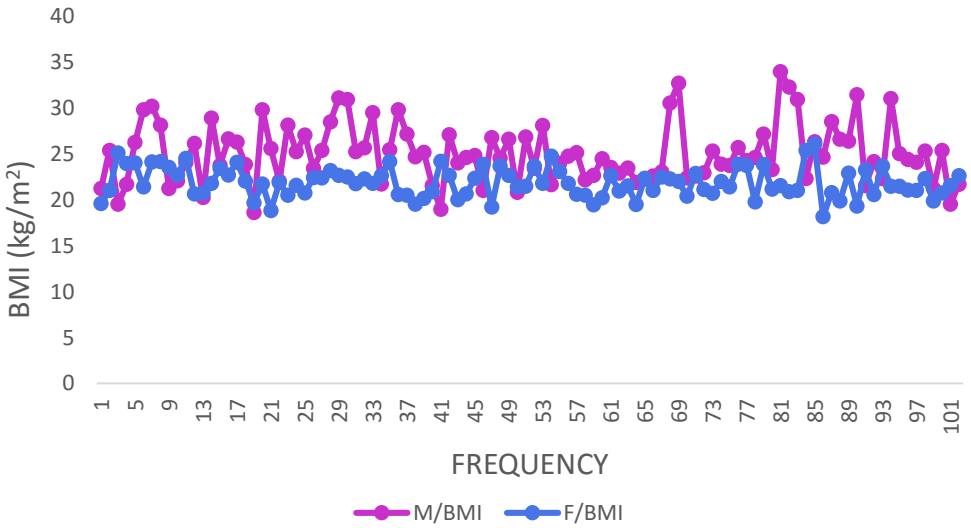

Figure 29: Variation of BMI for male (M) and female (F).

Figure 30 shows the relationship between male and female body surface area. It shows that males generally have a larger body surface area in relation to their females counterparts This was supported by the analysis of mean in Appendix F-5.

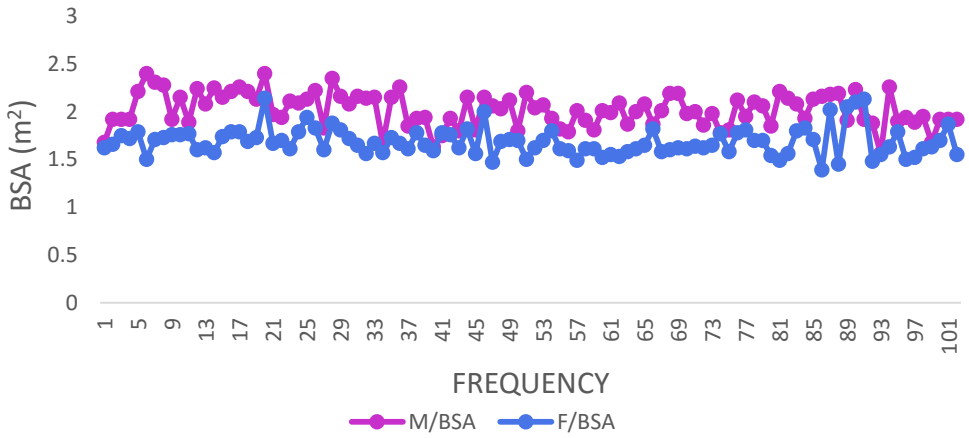

Figure 30: Variation of BSA for male (M) and female (F).

Graphical Representation of Renal Parameters

Figure 31 shows age and gender variation of renal length, with male having longer renal length than their female counterparts, which generally decreases with advancing age. This was supported with the Test of Variance of male and female renal length in Appendix G-1.

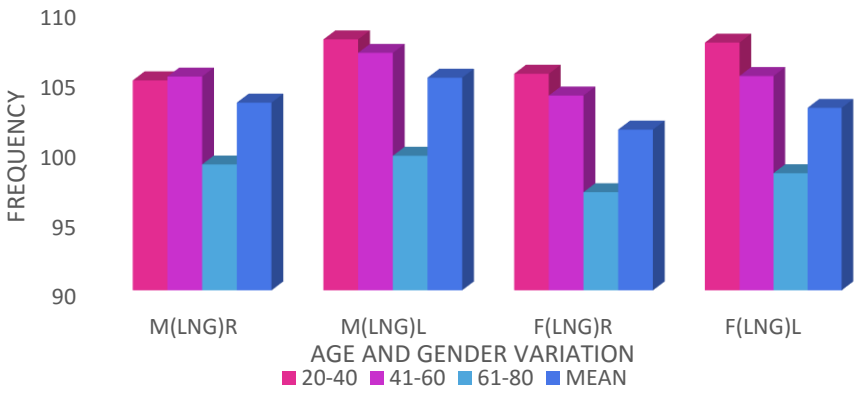

Figure 31: Variation of renal length for male (M) and female (F).

Figure 32 shows a pictorial representation of renal volume, in terms of age and gender, this shows that renal volume also decreases slightly with advancing age with the male having larger renal volume than the female counterparts. This was supported with the Test of Variance male and female renal volume in appendix G-2.

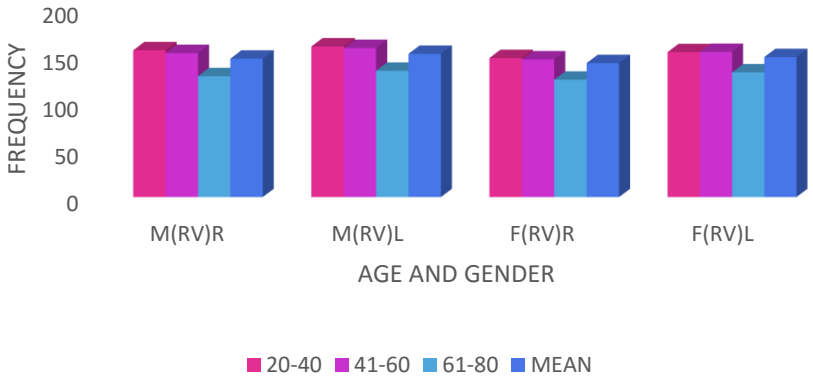

Figure 32: Variation of renal volume for male (M) and female (F).

Figure 33 shows a variation of male relative renal length in terms of right and left kidneys. It shows that the magnitudes of the kidney lengths is nearly evenly distributed, between the right (R) and left kidneys (L), with the right kidney slightly larger than the left. As collaborated by the normal distribution in Appendix H-1.

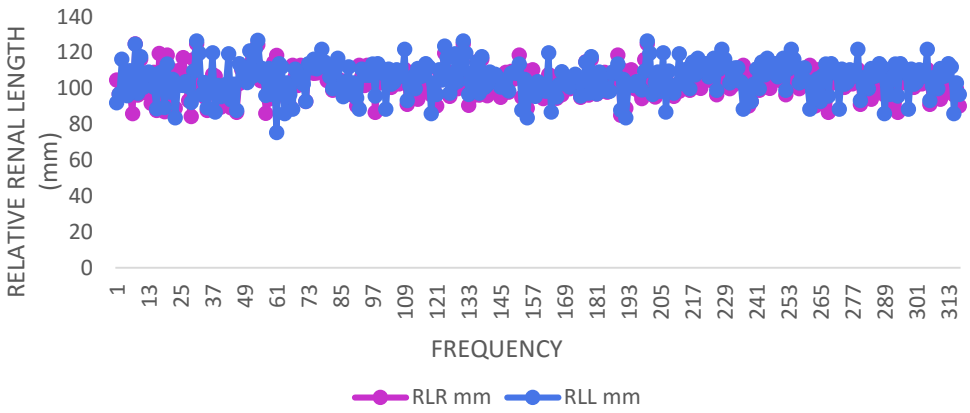

Figure 33: Variation of male relative renal length.

Figure 34 shows female relative renal length in terms of right and left kidneys. The plot shows that the left and right kidney lengths are near evenly distributed between the right (R) and left kidneys (L), with the right kidney slightly larger than the left. This was supported by the normal distribution in Appendix H-2.

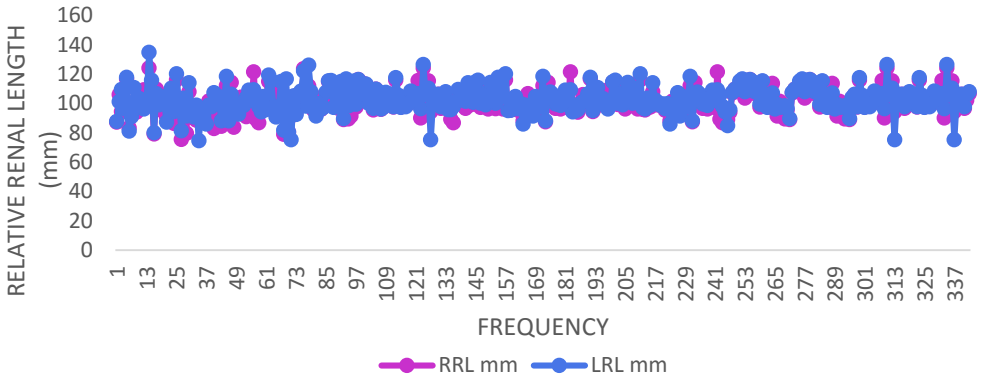

Figure 34: Variation of female relative renal length.

Figure 35 shows a variation of male relative renal volume in terms of right and left kidneys. It proves that the right (R) and left (L) kidney volumes are near evenly distributed, with the right kidney slightly larger than the left. This was supported with the normal distribution in Appendix H-3.

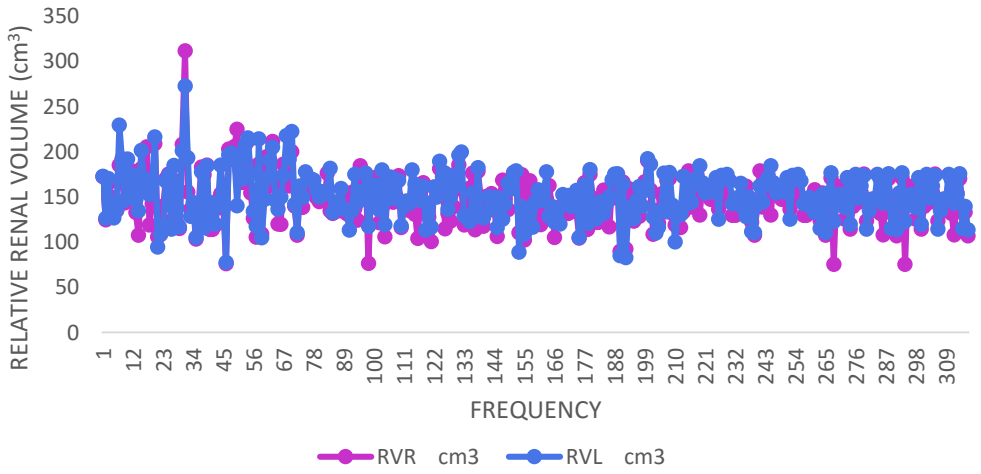

Figure 35: Variation of male relative renal volume.

Figure 36 shows a variation of female relative renal volume in terms of right and left kidneys. It expresses that the right and left kidney volumes are near evenly distributed, with the right kidney slightly larger than the left. This was supported with the normal distribution in Appendix H-4.

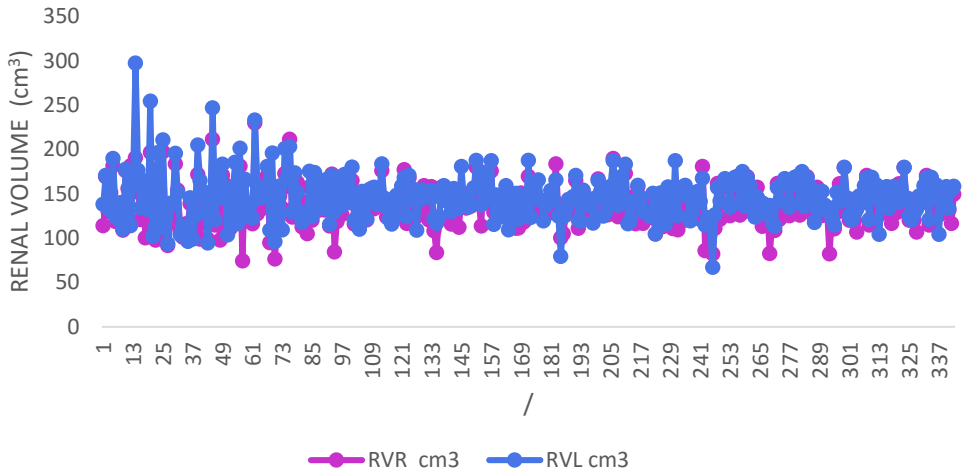

Figure 36: Variation of female relative renal volume.

Graphical Representation of Dose Parameters

Figure 37 shows age and gender variation of abdominal effective dose. It demonstrates that age related imaging protocols have not fully complied with, in addition to gender protocols as shown by age and gender related bars. This was collaborated by the analysis of mean in Appendix I-1.

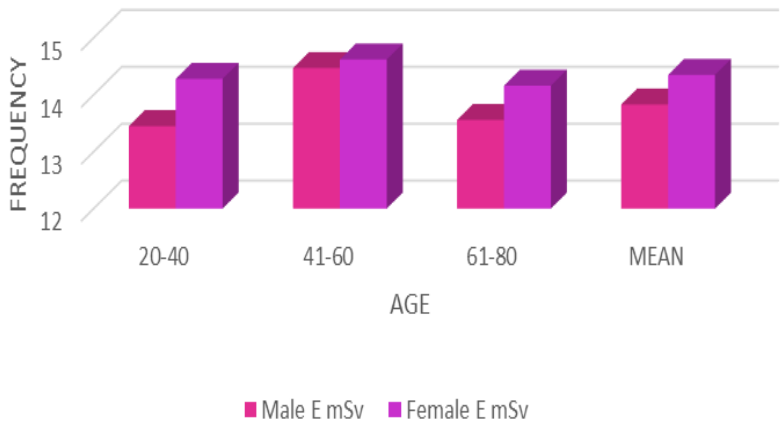

Figure 37: Variation of E in terms of age and gender.

Figure 38 shows age and gender variation of renal dose. This shows that the age and gender variation protocols were not followed as shown by age and gender related bars, where females received higher dose than their male counterparts against the protocol demand. This accession was supported by the analysis of mean in Appendix I-2.

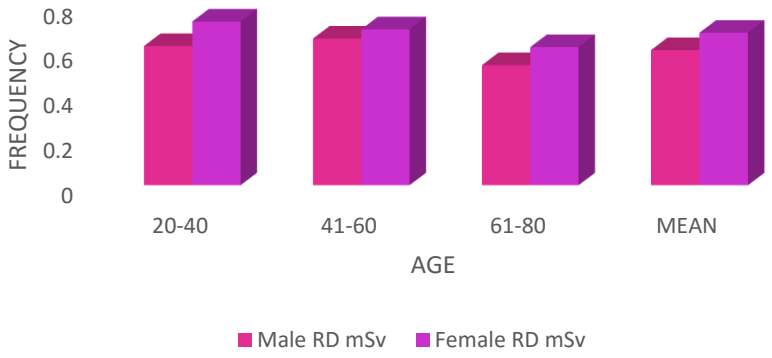

Figure 38: Variation of RD in terms of age and gender.

Figure 39 represents gender variation of effective and renal dose in male. It represents a quantitative description of the dose to the kidney (RD) and the abdominal tissues (E) during CT scan. Significantly, it shows that over 45 patients received an E of more than the mean value of 14.1 mGy. Additionally, similar patients had renal dose that exceeded the average dose of 3.3 mGy. This position was collaborated by the analysis of mean in Appendix I-3.

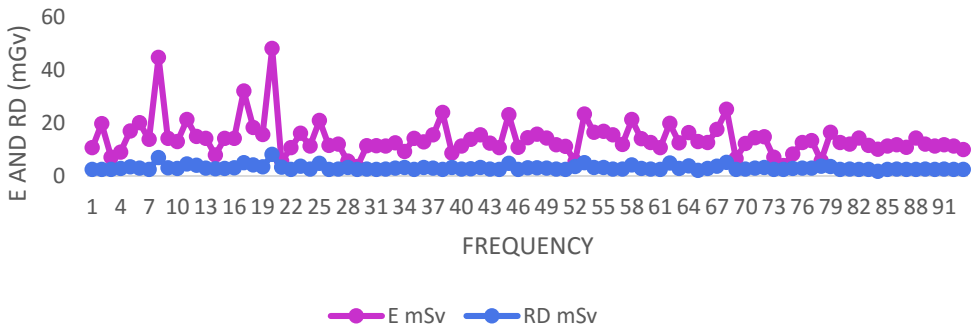

Figure 39: Variation of E and RD in male.

Figure 40 represents gender variation of effective and renal dose in female. It represents a quantitative description of the dose to the kidney and the abdominal tissue during CT scan. Incidentally, over 45% of patients had higher effective dose of more than 14.1 mGy. Additionally, similar patients received higher renal doses above the average values. This position was supported by the analysis of mean in Appendix I-4.

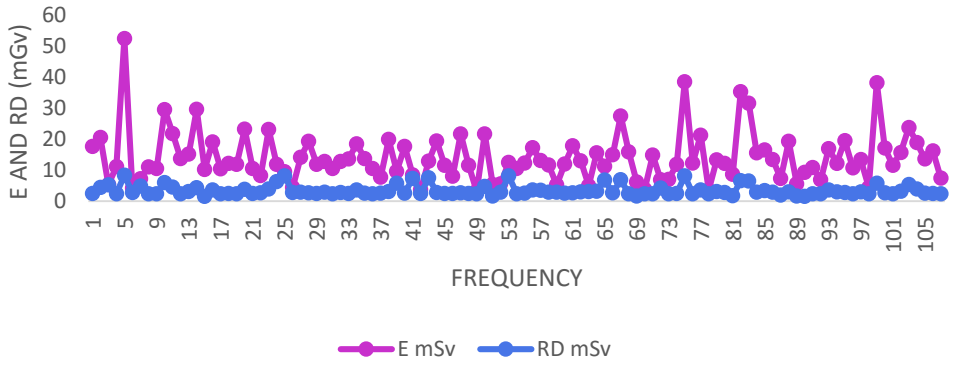

Figure 40: Variation of E and RD in female.

Figure 41 shows a relationship between image quality and dose to patients. It shows that image quality improves with increasing dose and a linear relationship exist between the two quantities.

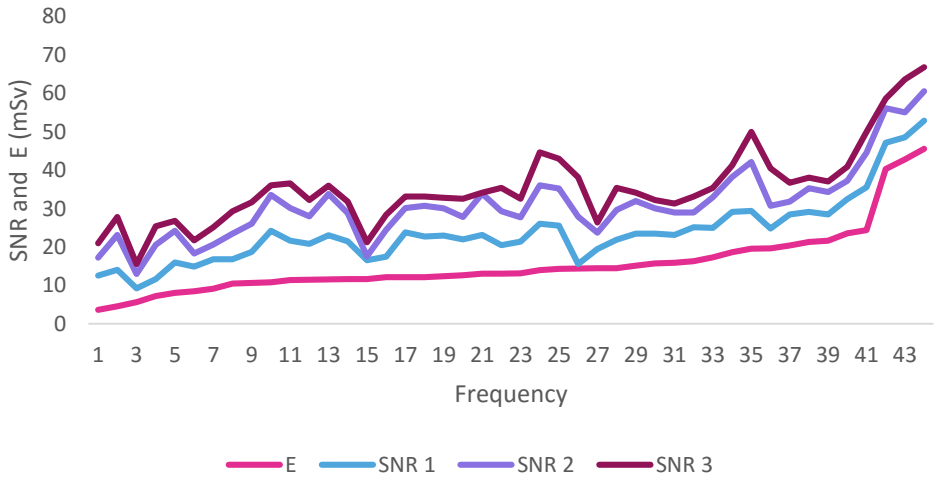

Figure 41: Variation of SNR against E.

Statistical Models

The statistical modeling process was based on linear approach for modeling the relationship between a scalar dependent variables and independent variables. The relationships between the parameters were modeled using linear predictor functions whose unknown model parameters were calculated from the data. Conversely, the linear regression were focused on the conditional probability distribution based on Normal Probability Plot (NPP) of a given variables.

The descriptive parameters of the modeled equations were obtained using the normal histogram, normal probability plot based on the statistical analysis by Chambers et al. (Chambers *et al*., 1983), Versus Fits and Versus Order. These were the four graphical techniques for assessing whether or not a data set is approximately normally distributed. In addition, the modeled equations of all the parameters were plotted against a theoretical normal distribution in such a way that the points formed an approximated straight line.

Additionally, the plots were based on the residual plots which formed graphs that were used to examine the goodness-of-fit in the linear regression analysis. This helps to find out whether the ordinary least squares assumptions were being played. The assumptions satisfactorily produced unbiased coefficient estimates with the minimal variance (≤ 0.05). The four techniques used were explained as follows:

Firstly, the histogram of residuals, which were used to ascertain whether the data are skewed or whether outliers exist in the data. Secondly the normal probability plot of residuals, which was used to verify the assumption that the residuals are normally distributed. Furthermore, the residuals versus fits were

also applied to verify the assumption that the residuals have a constant disagreement.

Finally the residuals versus order of data was employed to verify the assumption that the residuals are uncorrelated with each other.

The results of these model verification diagrams are given in Appendix I and J. Additionally, each model has four elements, comprising: the model equation, the standard deviation, the predictor and the p-value. A small p-value (typically ≤ 0.05) indicates strong evidence against the null hypothesis, resulting in rejecting the null hypothesis.

The model parameters are presented as body parameters, made up of; modeled height and weight; modelled BSI and BMI and modeled BSA and BMI. In addition, the renal parameters were presented as; renal volume model presentation. These were presented in relation to the modelled body parameters as; renal volume-related BMI presentation, renal volume-related BSA presentation and renal volume-related BSI presentation. Finally, the dose models were presented as; exposure and dose parameters presentation.

The models are presented as clinical application software for comfortable working process in two groups. The first group comprises the body and renal organ measurements software models and the second group made up of the dose parameter estimates software model, which has been designed for both exposure input and dose out data capturing mechanism. Both of these software models has been designed as GUI and CAD for use in clinical application.

The presentation of these models are discuss in terms of; Body parameters, renal parameters, renal volume related body parameters, dose parameters, exposure parameters in relation to dose and image quality:

Modelled representation of Body Parameters

This section present the graphical relationship between height and weight. It also shows the model equations for both male and female body parameters.

Modeled Height and Weight

Figure 42 represents a linear relationship between body weight and height. It is a linear approach for modeling the relationship between a scalar dependent variables weight and independent variables height. The graph shows that the weight linearly increases with increasing height, hence there is a linear relationship between weight and height as shown in Appendix J-1.

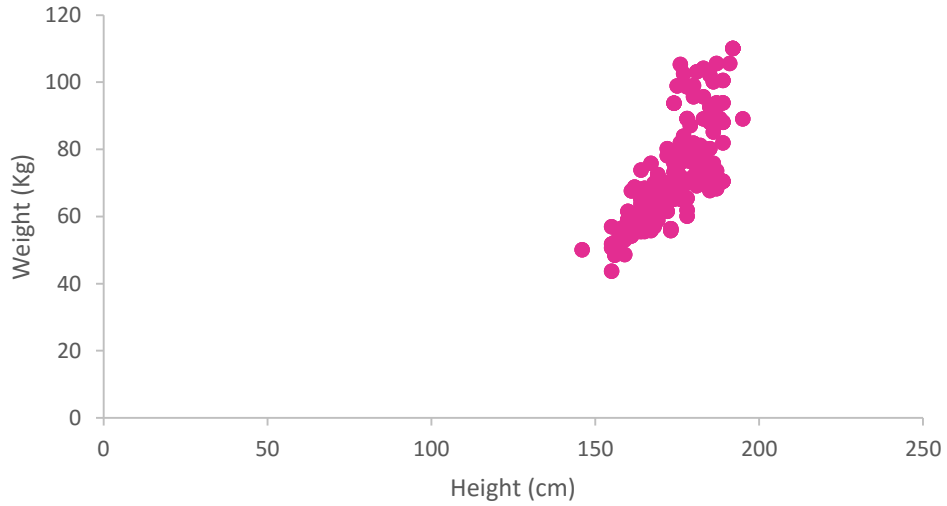

Figure 42: A plot of weight against height variations

Male Model

W = 1.14 H -123.09 (4.1)

SD = 10.1715. R-SQ (Predictor) = 98.75%, P-value (0.005)

Female Model

W = 0.66 H - 49.21 (4.2)

SD = 4.60123, R-SQ (Predictor) = 96.03%, P-value (0.005)

Modeled BSI and BMI

Figure 43 represents the relationship between BSI and BMI. It is a linear approach for modeling the relationship between a scalar dependent variables BSI and independent variables BMI. The graph shows that BSI linearly increases with increasing BMI, hence there is a linear relationship between BSI and BMI, as shown in Appendix J-2.

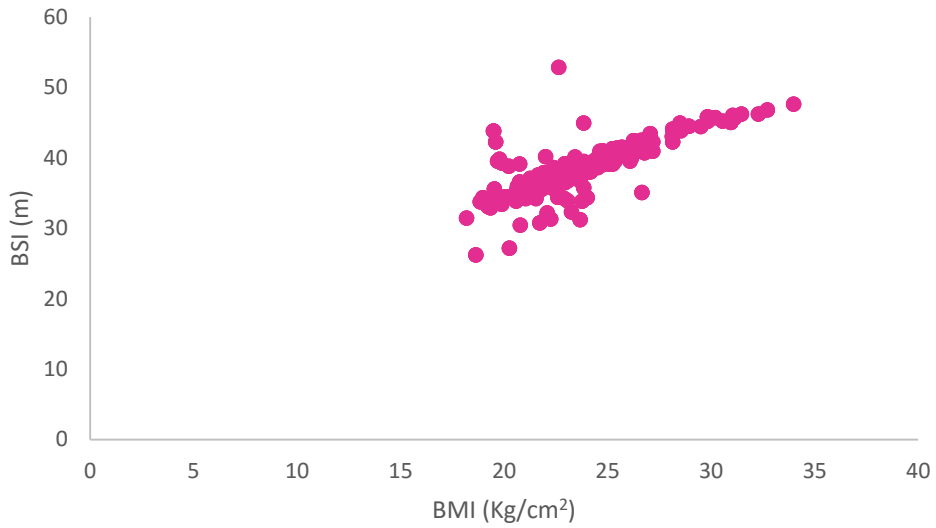

Figure 43: A plot of BMI against BSI variations

Male Model

BSI = 11.86 + 1.11BMI (4.3)

SD = 1.81259, R-Sq (predictor) = 98.68%, P-value (0.001)

Female Model

BSI = 23.9147 + 0.58BMI (4.4)

SD = 2.89, R-Sq (predictor) = 97.40%, P-value (0.005)

Modeled BSA and BMI

Figure 44 represents the relationship between BSA and BMI. It is a linear approach for modeling the relationship between scalar dependent variable BSA and independent variables BMI. The graph shows that BSA linearly increases with increasing BMI, hence there is a linear relationship between BSA and BMI as shown in Appendix J-3.

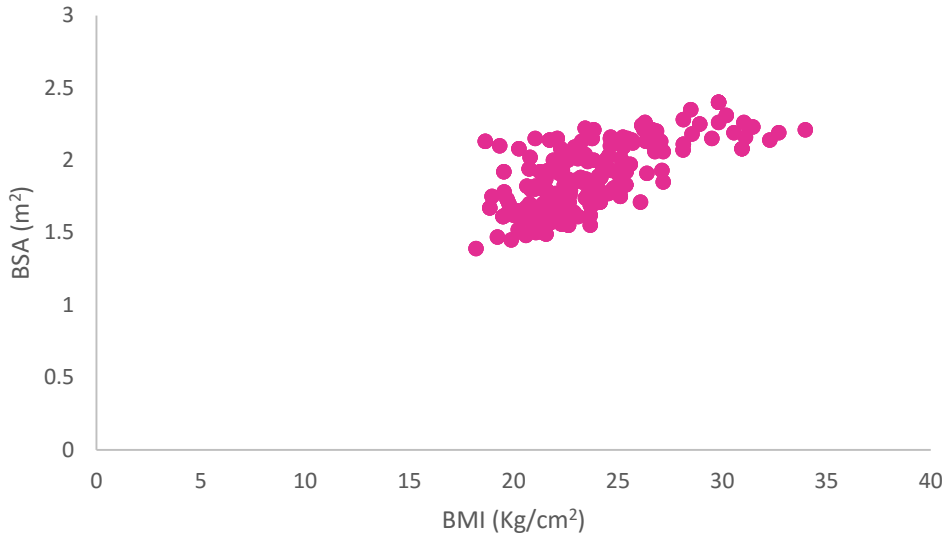

Figure 44: A plot of BSA against BMI variations

Male Model

BSA = 0.09BMI – 0.26 (4.5)

SD = 2.59, R-Sq (predictor) = 98.38%, P-value (0.007)

Female Model

BSA = 0.30BMI - 4.78 (4.6)

SD = 1.50, R-Sq (predictor) = 98.13%, P-value (0.001)

Modelled representation of Renal Parameters

This section discusses the presentation of renal volume in terms of renal length, renal with and renal thickness. It also shows both the graphical relationship and the model equations of these parameters.

Renal Volume Presentation

Figure 45 represents the relationship between the RV and the product of renal length, renal with and renal thickness, R_e (R_L*R_W*R_T). It is a linear modeling approach for establishing a relationship between a dependent variable RV and an independent variables R_e. It shows a linear relationship between RV and R_e. This is also shown in Appendix K-1

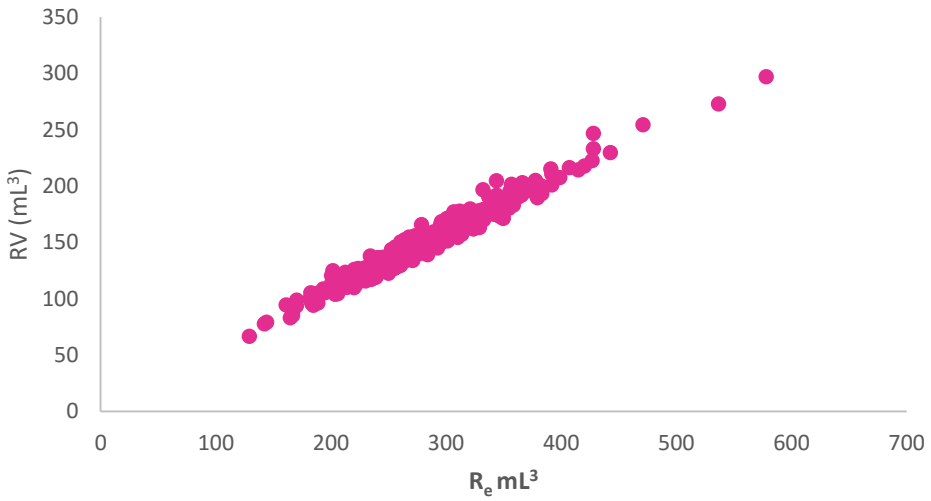

Figure 45: A plot of RV against Re variations

Male Model

$RV = 0.53 R_E + 1.19$ (4.7)

SD = 4.20, R-Sq (predictor) = 97.1%, P-value (0.005)

Female Model

$RV = 0.52 R_E + 1.81$ (4.8)

SD = 4.27, R-Sq (predictor) = 96.74%, P-value (0.001)

Modelled representation of Renal Volume-Related Body Parameters

This section present the graphical relationship between renal volume and its related body parameters. It also shows the model equations for both male and female renal volume related body parameters.

Renal Volume-Related BMI Presentation

Figure 46 represents the relationship between RV and BMI. It is a linear procedure for modeling the relationship between dependent variable RV and independent variables BMI. The graph depicts a linear relationship between RV and BMI, as presented in Appendix K-2.

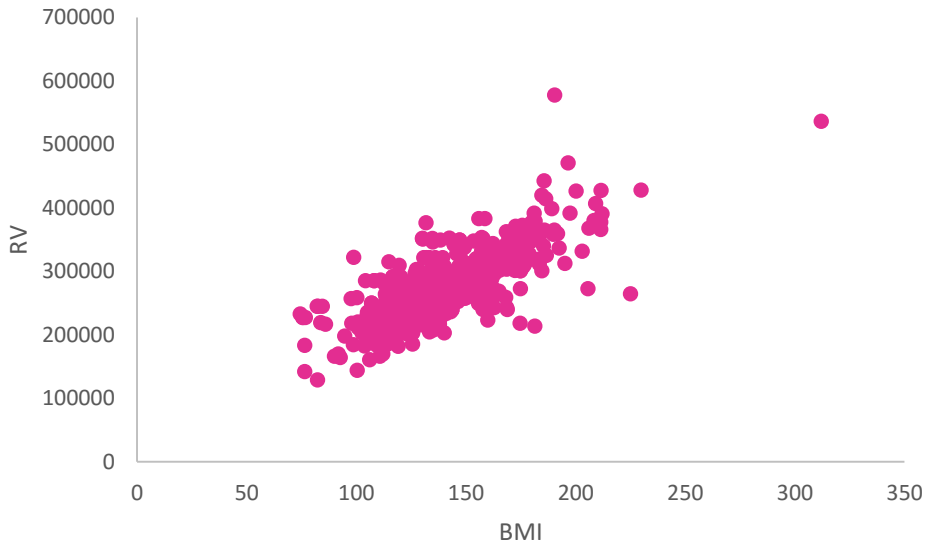

Figure 46: A plot of RV against BMI variations

Male Model

RV = 0.53 BMI + 135.97 (4.9)

SD = 24.80, R-Sq (predictor) = 97.79%, P-value (0.005)

Female Model

RV = 0.95 BMI + 120.58 (4.10)

SD = 23.39, R-Sq (predictor) = 96.83%, P-value (0.009)

Renal Volume-Related BSA Presentation

Figure 47 represents the relationship between RV and BSA. It is a modeling approach for building a relationship between a dependent variable RV and an independent variables BSA. The graph depicts a linear relationship between RV and BSA as shown in Appendix K-3.

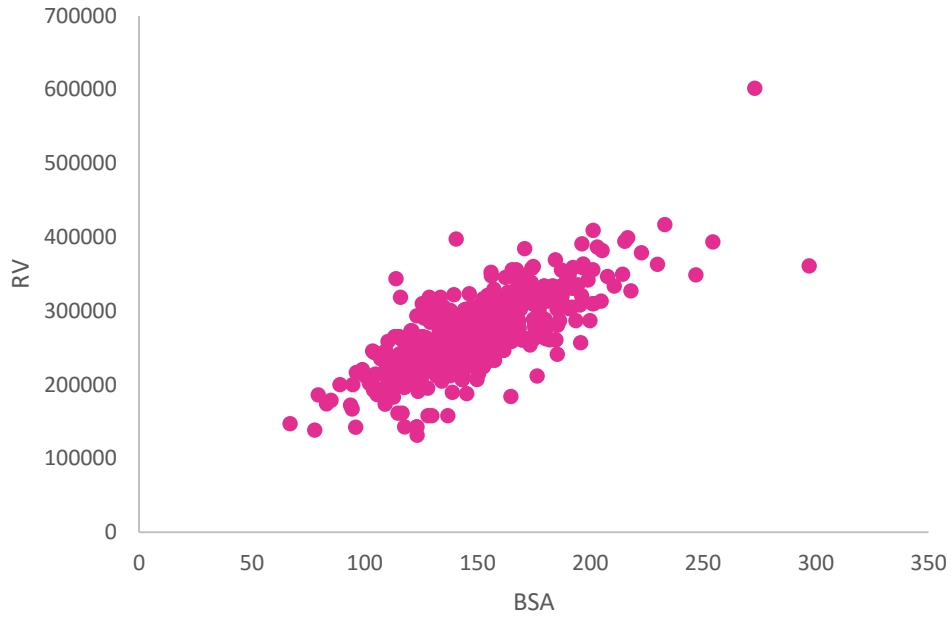

Figure: 47: A plot of RV against BSA variations

Male Model

RV = 0.399BSA + 148.65 (4.11)

SD = 24.9469, R-Sq (predictor) = 98.66%, P-value (0.000)

Female Model

RV = 0.999 BSA + 139.427 (4.12)

SD = 23.2760, R-SQ (Predictor) = 98.64%, P-value (0.000)

Renal Volume-Related BSI Presentation

Figure 48 represents the relationship between RV and BSI. The linear approach was applied for modeling the relationship between dependent variable RV and independent variables BSI. The graph depicts a linear relationship between RV and BSI as shown in Appendix K-4

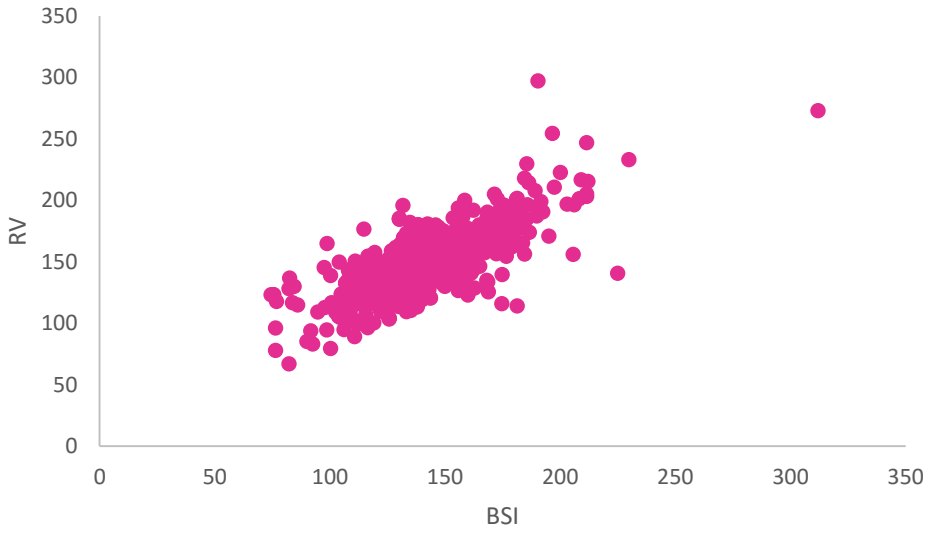

Figure 48: A plot of RV against BSI variations

Male Model

RV = 156.74 - 0.19BSI (4.13)

SD = 24.9363, R-Sq (predictor) = 98.95%, P-value (0.000)

Female Model

RV = 0.20BSI + 133.51 (4.14)

SD = 23.26, R-Sq (predictor) = 99.93%, P-value (0.000)

Modelled representation of Dose Parameters

Figure 49 shows variation of dose parameters (E, RD) based on the input parameters of CTDI and DLP, which were determined by mAs and the kVp. The RD increases with increasing E, however a number of the sample population had little variation in RD with increasing E as show in figure 49, in addition to Appendix L.

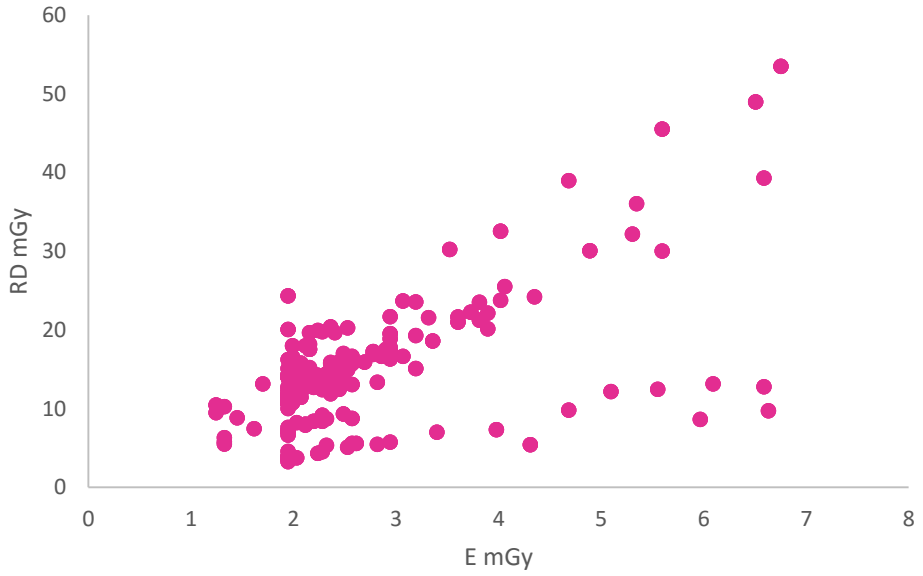

Figure 49: A plot of E against RD variations

Male Model

RD = 0.29 + 0.024 E (4.15)

SD = 0.12, R-Sq (predictor) = 97.27%, P-value (0.005)

Female Model

RD = 0.022 E + 0.39 (4.16)

SD = 0.28, R-Sq (predictor) = 85.05%, P-value (0.000)

Modelled representation of Exposure Parameters and Image Quality

The exposure parameters in relation to dose and image quality (SNR) were modelled with Minitab Statistical modelling tool and presented as follows:

CTDIvol = 0.21mAs -3.05 (4.17)

SD = 2.03, R-Sq (predictor) = 89.25%, P-value (0.005)

DLP = 27.60mAs -240.06 (4.18)

SD = 0.18, R-Sq (predictor) = 95.00%, P-value (0.005)

$SNR_{RD} = 6.83 + 0.1441RD$ (4.19)

SD = 2.00, R-Sq (predictor) = 97.05%, P-value (0.000)

$SNR_E = 7.10 + 0.0075E$ (4.20)

SD = 1.25, R-Sq (predictor) = 87.05%, P-value (0.000)

Experimental Models

The experimental models described the model equations designed from experimental data based on the standard volumetric ellipsoid equation as defined in Equation 2.20.

Renal Ellipsoid Model

The renal ellipsoid model were modelled based on age and sex variations and presented as follows.

Male Ellipsoid Models

20-40 years $RV = 0.5287 * RL * RT * RW$ (4.21)

41-60 years $RV = 0.5300 * RL * RT * RW$ (4.22)

61-80 years $RV = 0.5295 * RL * RT * RW$ (4.23)

Average Male Renal Ellipsoid Model:

$RV = 0.5290 * RL * RT * RW$ (4.24)

Females Ellipsoid Models

$$\text{20-40 years RV} = 0.5288 * \text{RL} * \text{RT} * \text{RW} \quad (4.25)$$

$$\text{41-60 years RV} = 0.5290 * \text{RL} * \text{RT} * \text{RW} \quad (4.26)$$

$$\text{61-80 years RV} = 0.5295 * \text{RL} * \text{RT} * \text{RW} \quad (4.27)$$

Average Female Renal Ellipsoid Model:

$$\text{RV} = 0.5292 * \text{RL} * \text{RT} * \text{RW} \quad (4.28)$$

General Renal Ellipsoid Model

$$\text{RV} = 0.53 * \text{RL} * \text{RT} * \text{RW} \quad (4.29)$$

Visual Indicators and GUI Models

The visual indicators in Figure 50 shows the variations of male renal volume model for various age groups. While Figure 51 shows the variation of female visual indicators for various age groups. The ages were group as 20-40, 41-60, 61-80 and 20-80 years and represented as A, B, C and D respectively.

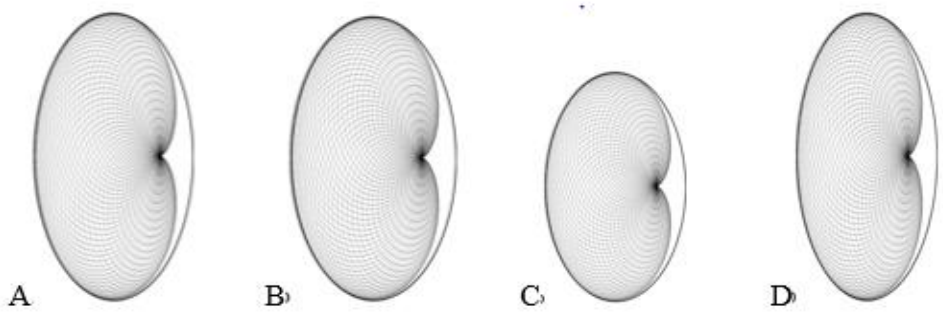

Figure 50: Male model visual indicators of renal shape variation

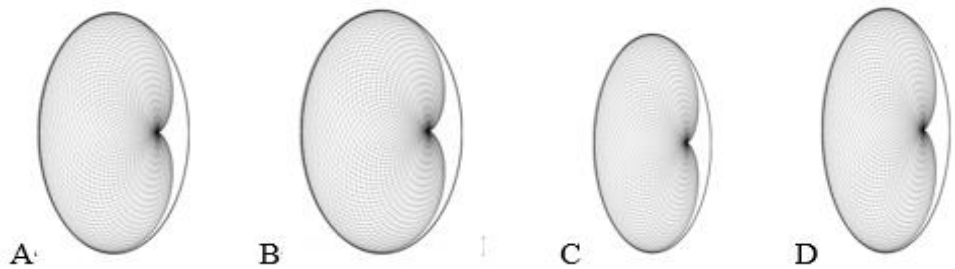

Figure 51: Female model visual indicators of renal shape variation

These visual indicators represent the mathematically modeled equation shown in Equations 4.21 to 4.24 for male, and modeled Equations 4.25 to 4.28 for female. Whilst the general equation is represented in Equation 4.29.

The written VB codes are shown in Appendix A, whilst the GUI are shown in Figure 52 and Figure 53.

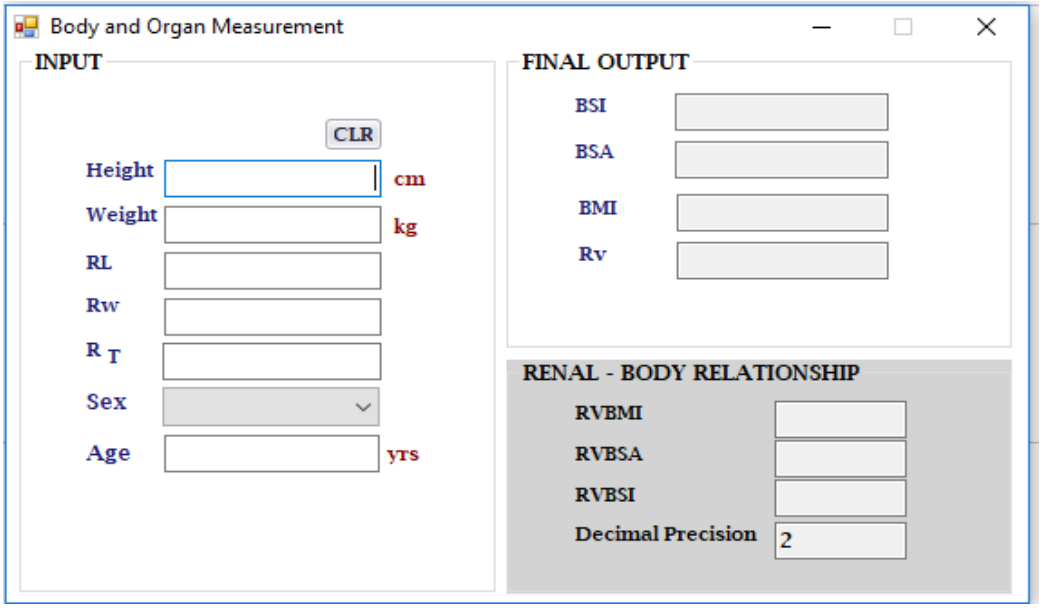

Figure 52: The design of GUI for body and renal measurements.

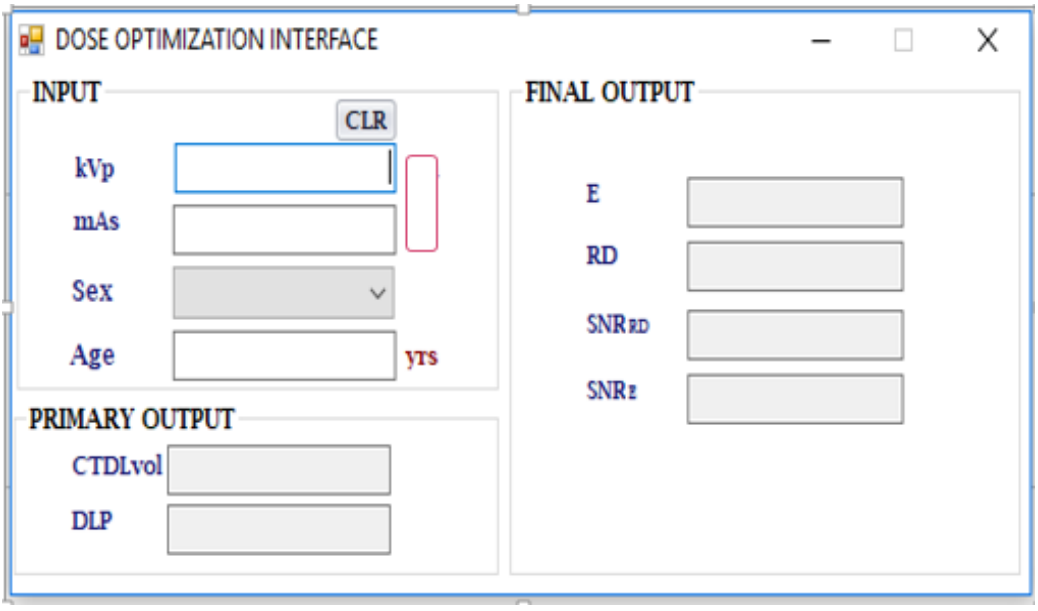

Figure 53: The design of GUI for dose optimization.

Description and Trend Analyses of Results

This section described and analysed all the measured parameters based on stated demographic statistics. Including renal, body and dose parameters.

Demographic Statistics

This section deals with the exploratory and inferential statistical analysis of the data obtained from the total sample population. The analysis focuses on the elaborate description of the data with regard to certain demographic factors. These include age and gender variation of renal and body parameters in relation to exposure and dose parameters based on the various standard acquisition protocols. The measured parameters were based along the population distribution of the sample population of Ghana, as presented by Ghana Statistical Service (Ghana Statistical Service, 2010)

Approximately, one thousand (1000) abdominal CT images were collected from ten selected CT centers, of which 660 images met the selection criteria. The selected images comprises; 344 females and 316 males, made up 52.12% female and 47.88% males. This reflected the gender population of Ghana based on Ghana Statistical Service 2010 report (Ghana Statistical Service. 2010). The report puts the total demographic gender population of Ghana as; 51.24% females and 48.76% males. Furthermore, the total sample population was categorized into three age groups comprising: 21-40, 41-60 and 61-80 years, of which the study population statistics was 175, 258 and 227, people which form: 26.5%, 39.1% and 34.4% respectively. These demographic statistics also reflected the age and the gender population distribution of Ghana (Ghana Statistical Service, 2010).

The various classified statistics are summarized in Table 13.

Table 13- *Sex and Age Distribution of Data*

Age (Years)	Gender	Sample size	No. of Kidneys	Percentage (%)
20-40	Male	108	216	61.71
	Female	67	134	38.29
	TOTAL	175	350	100
41-60	Male	119	238	46.12
	Female	139	276	53.88
	TOTAL	258	516	100
61-80	Male	89	178	39.21
	Female	138	276	60.79
	TOTAL	227	454	100
20-80	Male	316	632	47.88
	Female	344	688	52.12
	TOTAL	660	1320	100

This represents the age and gender distribution for all measured parameters. From the table, approximately 62% of the 175 patients between the ages 20-40 years were males, whiles that of the female population were approximately 38%. In addition, the percentage of males and females in both age groups 41-60 years (46% males and 54% females) and 61-80 years (39% males and 61% females) across the sample reflected the population distribution of Ghana.

Analysis of Body Parameters

Table 7 represents the average, upper limit and minimum age and gender variation of five body parameters. The five important body indices measured, including direct measurements of height and weight, in addition to BMI BSA and BSI, by applying Equation 3.7, 3.9 and 3.11 respectively.

The summarized measured Height, Weight, BMI, BSA and BSI values are shown in Table 14 and the details are presented in the Appendix B.

Table 14- *Summary of Measured Body Parameters*

SEX	Measure	AGE yrs	WEIGHT kg	HEIGHT cm	BMI kg/cm^2	BSA cm^2	BSI kg/m^2
Male							
	Mean	45	80.83	178.64	25.19	2.02	39.8
	Max	80	110	195	33.99	2.4	47.7
	Min	20	52.1	156	18.64	1.5	26.2
Female	Mean						
	Max	46	61.87	167.11	21.91	1.69	36.6
	Min	80	81.9	189	26.08	2.14	52.8
		20	43.7	146	18.19	1.39	30.5

The measured average male weight and height were 80.83 kg and 178.62 cm respectively. In addition, the average male BMI, BSA and BSI were 25.19±1.4 kg/m^2, 2.02±0.09 m^2 and 39.81 kg/m^2 respectively. The female measurements were 61.87 kg, 167.11 cm, 21.91±0.15 kg/m^2, 1.69±0.12 m^2 and 36.58 kg/m^2 for weight, height, BMI, BSA and BSI respectively.

These values are compared with international measured values by ICRP, Asian, American and the EC measurements as shown in Table 15. Generally, patient comments that satisfied the selection criteria showed that the majority of the patients reported for CT scan due to abdominal mass and pains for both genders.

Table 15- Comparison of *Study and International Body Parameters*

Parameter	Asian (1998)	Study Values	ICRP RM (1975)	ICRP RM (1995)	ICRP (2015)
Male					
Age years	35 (20-50)	45(20-80)	20-30	35(20-50)	42(20-80)
Race	Caucasoid	African	Caucasoid	Caucasoid	Caucasoid
Sex M/F	Male	Male	Male	Male	Male
Weight (kg)	60	81	70	73	76
Height (cm)	170	179	170	176	179
BMI (kg/m^2)	22	25	24	24	24
BSA (m^2)	1.78	2.02	1.80	1.90	1.95
BSI (kg/m^2)	33.71	39.81	38.25	38.42	38.95
Female					
Age	35(20-50)	46(20-80)	20-30	35(20-50)	42(20-50)
Race	Caucasoid	African	Caucasoid	Caucasoid	Caucasoid
Sex	Female	Female	Female	Female	Female
Body weight (kg)	51	62	60	60	63
Body height (cm)	160	167	161	163	165
BMI (kg/m^2)	22	22	22	23	23
BSA (m^2)	1.55	1.69	1.66	1.66	1.67
BSI (kg/m^2)	32.90	36.58	37.5	35.50	35.2

Source: ICRP

Analysis of Renal Parameters

As established on the selection criteria only images with two clear kidneys boundaries were included for measurement and subsequent analysis, with a description as left and right kidneys to the spinal column. In whole, six renal parameters (three (3) directly measured and three (3) calculated) were studied. The three (3) measured parameters include: renal length, lateral diameter and A-P diameter. Whereas, the 3 calculated parameters include: renal volume, renal shape index and renal volumetric ellipsoid coefficient. The male renal dimensions on the right of the spine were: the renal length 103.4± 1.6 mm, lateral diameter 60.8±1.0 mm and the A-P diameter 44.1±1.0 mm. To the left

the renal dimensions were: 105.1±1.5 mm, 60.4±1.1 mm and 45.0±0.6 mm in renal length, lateral diameter and A-P diameter respectively. Furthermore, the female renal dimensions on the right of the spine were: 101.4± 1.4 mm, 59.2±0.9 mm and 43.1±1.0 mm in renal length, lateral diameter and A-P diameter respectively. On the left, the female renal length was 103.0±1.3 mm, lateral diameters 59.2±1.0 mm, and the A-P diameter was 44.8±0.4 mm.

Renal length, lateral diameter and A-P diameter were used to estimate the renal volume, in order to predict renal size. The detailed measured renal dimensions are summarized in Table 8. The general reduction in renal dimensions was significant, which predicted the reduction of the total renal size, in terms of both age and gender variation. Indeed, the renal reductions were significant between ages 41-60 and 61-80 year groups, but were insignificant and less pronounced between 20-40 and 41-60 year groups. Details of the percentage reductions and summarized values are tabulated in Table 16.

Table 16- *Summary of Measured Renal Dimensions*

SEX	Age Yrs.	Sample	A-P_R mm	A-P_L mm	TRN_R mm	TRN_L mm	LNG_R mm	LNG_L mm
MALE	Mean							
	53	108	45.39	45.32	62.25	61.71	104.94	107.86
	33	119	44.59	45.60	61.80	61.14	105.21	106.90
	70	89	42.03	43.64	57.74	57.85	98.95	99.57
	49	316	44.12	44.95	60.79	60.39	103.35	105.13
			1.80%	-0.6	0.72%	0.90%	-0.30%	0.90%
			5.70%	4.40%	6.60%	5.40%	6.00%	6.90%
FEMALE								
	34	67	43.46	45.22	60.17	59.19	105.41	107.63
	53	138	44.02	45.25	60.11	60.47	103.86	105.25
	70	138	41.99	44.18	57.81	57.50	96.98	98.33
	55	344	43.09	44.82	59.20	59.02	101.43	102.98
			-1.30%	-0.10%	0.10%	-2.20%	1.50%	2.20%
			4.60%	2.40%	3.80%	4.90%	6.60%	6.60%

Three other important renal parameters were calculated, these include: renal volume (RV), renal shape index (RSI) and renal volumetric ellipsoid coefficient (VeC). The highlight of the summarized statistics is as follows; the mean male renal volume on the right of the spine was 146.7±8.3 cm^3 and on the left was 151.8±2.1 cm^3. The mean female right renal volume was 142.0±7.3 cm^3 and 148.3±5.3 cm^3 on the left. Renal volume together with renal dimensions (renal length, lateral and A-P diameters) were used to estimate VeC. The average VeC was approximately the same for both gender and age variations with the value of 0.53±0.01 for right and left, male and female and with all age variations. The relationship between the renal dimensions (renal length divided by the sum of lateral and A-P diameters) were used to estimate RSI. The average RSI was approximately 1.00±.01 for both genders and age variation.

Furthermore, the RSI and VeC distributions show insignificant variation as shown in Table 17.

Table 17- *Summary of Estimated Renal Parameters*

Age	Age Yrs.	Sample	RV_R mL^3	RV_L mL^3	VeC_R	VeC_L	RSI_R	RSI_L
Male	Mean		±26.96	±25.72	±0.008	±0.009	±0.02	±0.01
	33	107	155.5	159.5	0.529	0.5289	1.02	1.02
	53	122	152.6	158.0	0.528	0.5303	1.00	1.01
	70	59	128.3	133.9	0.529	0.5301	0.99	1.01
	49	288	146.7	151.8	0.528	0.5297	1.00	1.01
			1.89%	0.97%				
.			15.64 %	15.20 %				
Female	Mean		±27.08	±27.78	±0.020	±0.019	±0.01	±0.02
	34	68	147.38	153.55	0.526	0.532	1.02	1.03
	53	135	145.97	153.83	0.528	0.532	1.02	1.02
	70	122	124.54	132.26	0.529	0.530	0.97	0.98
	55	325	142.04	148.29	0.528	0.530	1.00	1.01
			0.96%	0.18%				
			14.7%	14.2%				

The VeC is an important renal parameter that represents the constant of proportionality for a renal ellipsoid equation that is unique for estimating Ghanaian renal volume. This has been made available to be utilized by clinicians in the configuration of GUI for clinical application. The statistical detailed age and gender representation of these renal parameters is shown in Table 9.

Renal volume is an important determining factor during renal development. It is the best renal parameters that is applied to estimate renal size. In view of this the data were sorted in order to trace a human organ development pattern based on age and gender in relation to changing renal size (renal length, breadth, thickness and volume) that takes place during human development. Furthermore, the hypotheses of various renal dimensions were examined to establish the relationship between various age groups (20-40, 41-60 and 61-80 years) and gender (male and female) variations. The period between 20 to 80 years is considered significant as it conforms to the natural renal developmental pattern, from a point of complete organ maturity at 20 years to a point of significant decline at 80 years. The left renal size was slightly bigger than the right renal size in both sexes. The relationship between mean renal lengths was significant when correlated with renal size in terms of age and gender. Renal volumes also showed a similar but much better relationship with renal size based on age and gender. The various significant relationships are shown in both the summarized data and graphical representations.

The study shows that male renal size starts an earlier decline before the age of 60 years than that of females, but at a slower rate. Female renal size on the other hand, starts to decline after the age of 60 years, but at a faster rate as

shown in Table 8 and 9. In addition, the overall age and gender renal size reduces significantly by age 80 years as shown by the modeled visual indicators. There is however very little variation between age group 20-40 and 41-60 years, but significant between age group 41-60 and 61-80 years. Furthermore, both genders in the visual indicators and graphical representation show similar variation. Generally, the study demonstrates that the male renal parameters are larger than the female renal parameters. The overall renal size reductions were extremely significant with left and females kidneys. The reductions for renal volume were 1.89% between the age ranges of 20-60 years and 15.64% between the age ranges of 41-80 years for the right kidney. Similar observations were seen with the left kidneys. However, the reductions were more pronounced in the female kidneys as shown in the summarized Table 8 and Table 9.

The hypotheses relating left and the right renal length and renal volume were tested and described as the relative renal length and renal volume parameters at various age groups and gender variation. These parameters were estimated by dividing either the left or right renal lengths or renal volumes by the total renal length or renal volume and found no significant variation between the left and right kidneys for the various age groups and gender. The relative renal length and volume are important parameters for purposes of renal development in terms of uniform, equal development of the left and right kidneys. The male mean estimated values were 0.4959 and 0.5041 for right renal length and renal volume respectively, however, in females the average relative length and volume for left kidney were 0.4919 and 0.5081 respectively. Furthermore, details of the estimated relative renal length and volume are shown in Appendix C. A strong symmetry was found between left and right kidneys

with the expected normal distribution of the relative renal length and renal volumes on both sides and nearly evenly distributed in kidney size.

The normal range of male relative renal length and renal volume lies between 0.58-0.42 and 0.62-0.39 respectively, while the normal range of the relative renal length and renal volume lies between 0.56-0.44 and 0.62-0.39 for female respectively. Nonetheless, both age and gender, together with volume and length variation lies within an approximate mean value of 0.50±0.12 for both left and right kidneys, as shown in Appendix H and indicated in summary Table 18.

Table 18- *Summary of Relative Renal Length and Renal Volume*

Sex	AGE Years	Total RL mm	R-RRL	L-RRL	TOTAL RV cm^3	R-RRV	L-RRV
Male							
	52	208.48	0.50	0.50	298.93	0.49	0.51
	80	251.1	0.61	0.55	584.93	0.62	0.62
	20	172.5	0.45	0.39	154.24	0.38	0.39
Female							
	56	204.41	0.50	0.50	282.23	0.49	0.51
	80	259.1	0.56	0.56	487.50	0.61	0.63
	20	157	0.44	0.44	149.14	0.38	0.39

These parameters have a major advantage over existing parameters to evaluate renal development in a simple and convenient means for clinical application. Indeed, the introduction of these parameters makes the analysis of the reference chart easier and more wide-eyed. For example, a relative renal volume and length less than 44% of the total renal volume and length or bigger than 56% renal volume, or greater than 20% for a remainder of either renal length or renal volume, should prompt the suspicion of a one-sided infection and therefore call for further investigation (Scholbach & Weitzel, 2012). In all,

98% of the measured relative renal length and renal volume parameters were within 56%-44% variations hence did not indicate any infection of the left or right kidney. Approximately 2% of the variations were outside the appropriate range of values. Even though this is generally insignificant, it is clinically significant and must further be investigated.

Relationship between RV and Body Parameters

The relationship between renal volume (RV) and three body indices (BMI, BSA and BSI) are important indicators in renal development in relation to total tissue growth and development. These three body parameters were hypothetically tested with renal volume for clinical application. Subsequently, the hypothesis that, BSA, BSI, BMI and renal volume grow proportionally in various age groups and gender variations were tested. This is because the ever changing renal volumes require continuous referral to normal renal volume charts in order to classify normal renal volume development, from clinical pathological renal volume in relation to standard body parameters. Admittedly, it is quite difficult and a challenge of inconvenience when a standard reference renal volume is not available for renal assessment. As a result, in clinical practice, assessment of renal development is often disregarded and kidneys are evaluated by their appearance and texture information only. Therefore, the hypothesis that BMI, BSI, BSA and renal volume grow proportionally were tested to make available standard reference values of theses parameters for clinical application. These were done by dividing the renal volume by its BMI BSA and BSI to get the renal volume related-BMI, BSA and BSI (RV-BMI, RV-BSA and RV-BSI) and no significant variation (less than 5%) was found

between left and right kidneys and a normal distribution for all kidneys regardless of the patient's age and gender (Table 11).

The mean male renal volume related-BMI BSA and BSI were 5.95 $mL^3/kg/m^2$, 72.97 mL^3/m^2, 3.75 $mL^3/kg/m^2$ for right and 6.12 $mL^3/kg/m^2$, 75.12 mL^3/m^2 and 3.87 $cm^3/kg/m^2$ for left kidneys respectively. In addition the mean female BMI, BSA and BSI-related renal volume was 6.29 $mL^3/kg/m^2$, 81.77 mL^3/m^2, 3.77 $mL^3/kg/m^2$ for right and 6.64 $mL^3/kg/m^2$, 86.40 mL^3/m^2 and 3.99 $mL^3/kg/m^2$ for left kidneys respectively. The RV-BMI, RV-BSA and RV-BSI have a common normal range for all age groups with various variations shown in Table 19.

Table 19- *Summary of BMI, BSI, BSA and Renal Volume*

SEX	AGE year	RV_R-BMI $mL^3/kg/m^2$	RV_L-BMI $mL^3/kg/m^2$	RV_R-BSA mL^3/m^2	RV_L-BSA mL^3/m^2	RV_RBS1 $mL^3/kg/m^2$	RV_L-BSI $mL^3/kg/m^2$
MALE	45	5.95	6.12	72.97	75.12	3.75	3.87
	80	12.36	10.81	144.4	126.4	7.56	6.61
	20	2.98	2.68	35.53	36.21	1.88	1.81
	4	2.27	1.93	2.58	2.19	2.27	1.93
FEMALE							
	46	6.29	6.64	81.77	86.40	3.774	3.99
	80	10.96	13.63	150.2	189.2	6.63	8.36
	20	3.59	2.95	40.09	38.0	2.18	1.80
	4	2.93	3.11	2.72	2.88	2.41	2.55

The RV-BMI, RV-BSA and RV-BSI elicit the correct evaluation of a patient's renal volume regardless of age and gender. The study revealed a pathological age and gender influences on theses parameters by the simple observation and in clinical practice; it enables convenient comparison to be made with standard reference values for diagnostic decision. Additionally, these parameters were found to correlate positively with both male (modeled equation

4.1, 4.3 and 4.5) and female (modeled equation 4.2, 4.4 and 4.6) for BMI, BSA and BSI related renal volume respectively. Therefore, deviations of these parameters from the standard reference values within a specific age group and gender variations may indicate pathological conditions and require further investigations.

Analysis of Effective and Renal Dose Parameters

Two reference dose parameters are commonly used for CT dose profile estimates in order to promote the use of the good CT imaging protocols and techniques. These include; CTDI and DLP, which are used for CT dosimetry. In addition, these parameters provide control on the selection of exposure settings, such as exposure (mAs) and the applied voltage. Accordingly, DLP also provides control of the volume of irradiated area and the overall total exposure for an examination.

The estimated pre-set parameters during the abdominal CT scan were the; tube current, kilovolts peak (kVp), exposure (mAs) and scan time, this parameter enables the prediction of exposure parameters, CTDI and DLP. In all the examinations, the average protocol setting in terms of exposure and kilovolts peak were 48.19 mAs and 120 kVp respectively. These parameters play an important role in the determination of the level of exposure (mAs) on renal and other tissues during the CT examinations. The effects of these parameters in abdominal scan depends on the slice thickness, scan time and scan scope, in addition to kilovolts peak (kVp) and exposure (mAs). The summarized data shows an average renal surface area of 29.5199 cm^2 and 30.6662 cm^2 on the right and left kidney respectively, with mean effective milliamp second (eff mAs) of 59.27 mAs and tube current of 94.22A. The minimum recorded

effective milliamp second (eff mAs) in all the abdominal examinations was 49.2mAs and the maximum recorded value was 154.98mAs. Furthermore, the minimum and the maximum tube current in all the examinations were 50A and 253A respectively. These parameters were used to estimate the effect of exposure on abdominal and kidney tissues, in terms of the level of exposure based on recommended ICRP publication 103 (ICRP Publication 103, 2007).

Admittedly, CTDI and DLP were the immediate measurable parameters that were recorded after exposures which gives a clue of doses to patients (E and RD) with the MDCT examinations (low-dose radiation exposure) using known kVp and mAs. The results of these parameters are linked to low-dose radiation exposures and tissue damage leading to stochastic effects of possible induced cancer, based on the LNT model supported by a number of publications including, the BIER VII committee (BEIR VII report, 2006; Feinendegen, 2005; Sanders, 2010; Mullenders *et al*. 2009). Generally, these parameters are used to estimate renal and effective doses in clinical CT examination. This enables a comparison between these parameters and the recommended reference dose levels of these parameters and those by ICRP. The detailed measured CTDI, DLP, RD and E in relation to age and gender variation are summarized in Table 12.

The analysis of the abdominal image data at the various CT centers in the study show that the mean male and female $CTDI_{VOL}$ values were 6.17 mGy and 6.48 mGy respectively. Furthermore, the mean recorded values of $CTDI_{VOL}$ were well within the proposed ICRP recommendation when the protocol was completed in a single scan. On the other hand, in the case of multiscan the total $CTDI_{Vol}$ was higher than the ICRP recommendations. Over 30% of the patients imaged exceeded the average $CTDI_{VOL}$ values for male

and female, in addition to ICRP publication 103 as presented by the black line in Figure 54. Furthermore, the female mean DLP was 950.97 mGy cm with minimum and maximum values recorded as 213.60 mGy-cm and 2568.30 mGy cm respectively. The corresponding male mean DLP was 921.53 mGy-cm with minimum and maximum value as 234.40 mGy-cm and 3496.4 mGy cm.

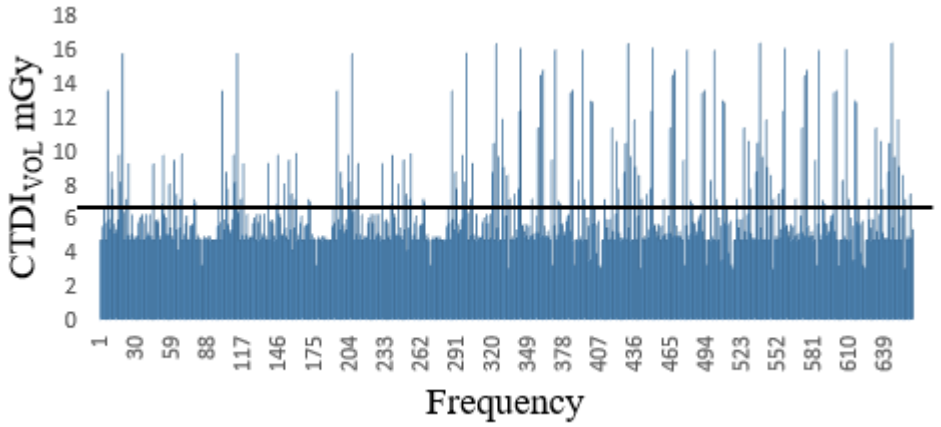

Figure 54: Recommended abdominal $CTDI_{VOL}$ level

The mean DLP values for both genders were higher than the recommended value of 780 mGy-cm by ICRP publication 103 as indicated with the black line in Figure 55.

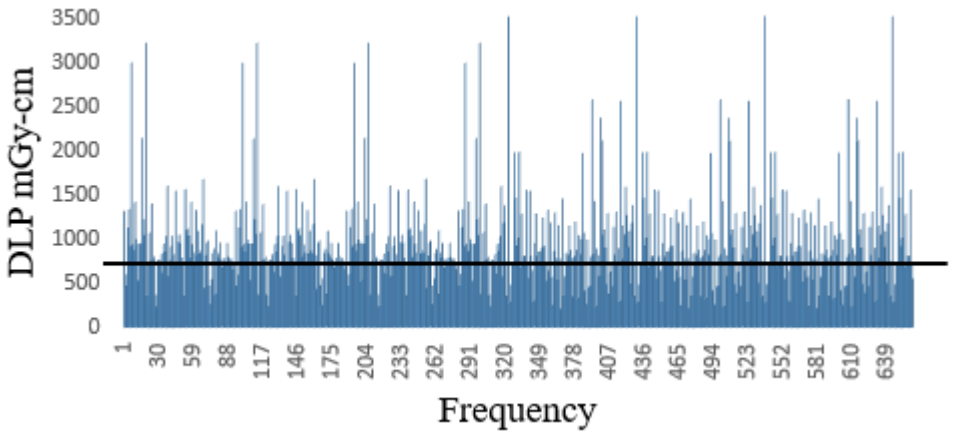

Figure 55: Recommended abdominal DLP level.

Additionally, approximately 37% of the total DLP values were higher than the recommended dose by ICRP as shown in Table 12.

To assess the health risks of low doses of ionizing radiation, the ICRP uses the concept of effective dose. The effective doses were calculated from the DLP of each completed examination using the conversion factors given by the ICRP publication 103 as shown in Table 2. The effective dose estimates were based on gender and age variation as shown in Table 20.

Table 20- *Summary of E, RD and related Dose Parameters*

Statistics	AGE Years	$CTDI_{VOL}$ mGy	$CTDI_{W}$ mGy	DLP mGy-cm	E MSv	RD MSv
Male Mean	48	6.17	5.0162	921.53	13.83	3.12
Maximum	80	16.3	13.252	3496.4	52.45	8
Minimum	20	3.2	2.6016	234.4	3.52	2.09
Female						
Mean	44	6.48	5.2682	950.97	14.35	3.39
Maximum	75	16.0	13.008	2568.3	38.53	8.31
Minimum	20	3.0	2.439	213.6	3.2	1.53

Several interesting observations were made on the basis of the data provided in Table 12. The calculated effective doses shows a variation from a minimum of 3.2 mSv to a maximum of 38.53 mSv with a mean value of 14.35 mSv for female. The corresponding male mean effective dose was 13.83 mSv and the distribution was in the range of 3.52 mSv to 52.45 mSv for minimum and maximum values respectively. The measured male mean renal dose was 3.12mSv to 8.00 mSv and 2.09 mSv being maximum and minimum recorded values respectively. The corresponding measured female mean renal dose was 3.39 mSv with 8.31 mSv and 1.53 mSv being maximum and minimum renal dose values respectively. The overall average values of 3.26 mSv and 14.09 mSv for renal and the effective dose values exceeded the accepted values of the ICRP recommendations of 3.00 mSv and 14.0 mSv respectively. However,

approximately 32.5% of the individual dose estimates were higher than the recommended effective dose and renal dose as indicated with the black line in Figure 56 and Figure 57 respectively.

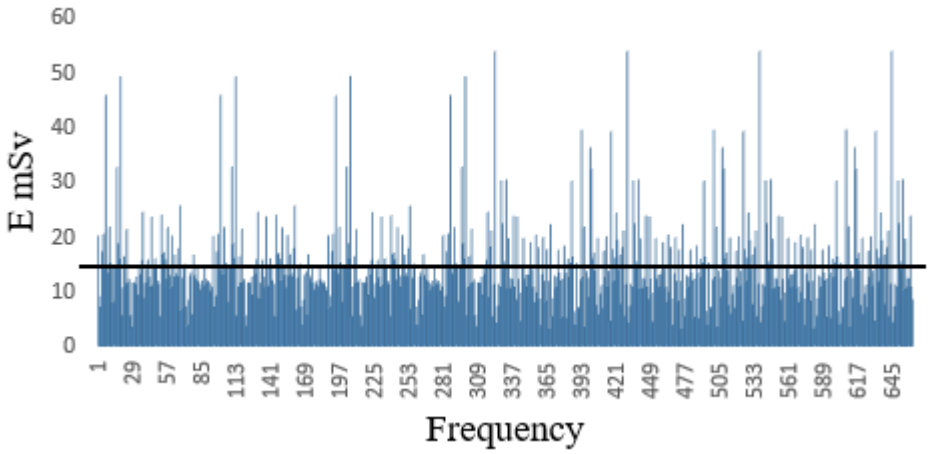

Figure 56: Recommended abdominal effective dose level

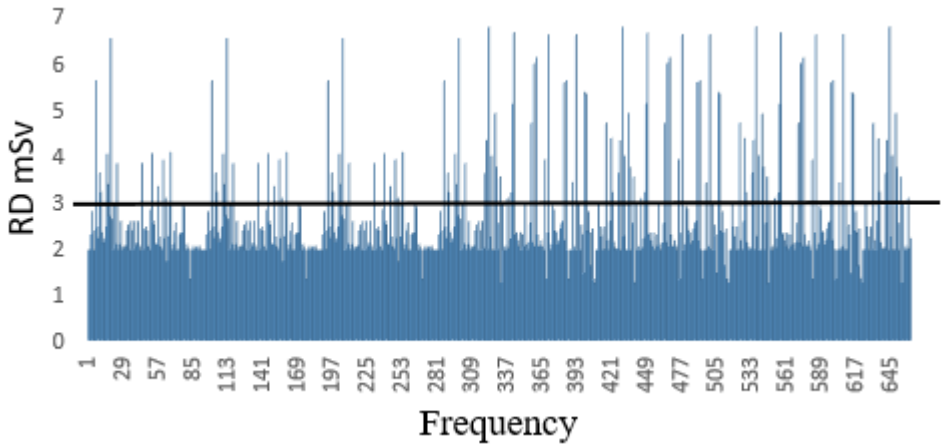

Figure 57: Recommended renal dose level

Table 21 shows the measured parameters in eight countries compared with measured study parameters in Ghana, in terms of weighted CTDI, DLP and effective dose. Comparatively, the average effective dose in this study is higher than all the countries reviewed except in Tanzania and Ireland. This has been attributed to the scan length used as compared to all the reviewed countries. This

protocol needs revision to avoid unnecessary tissue exposure, which extend beyond the anatomical abdominal area

Table 21- *Comparison of Dose Parameters*

Dose	Greece	Italy	Wales	Poland	Tanz.	Ireland	UK	Study
$CTDI_w$	19.1	24.3	27	25.7	17	19.1	9.5	5.15
DLP	633	517	745	550	982	433	446	936
E	9.49	7.8	9.4	8.1	15	15	7.0	14.1

Analysis of Dose Optimisation and Image Quality

To establish a tradeoff between image quality and corresponding dose for the patients' dose optimization procedure, a simple numerical method was used to calculate the SNR of CT image. That is, the ratio of the Signal (process average) over the Noise (standard deviation). The dose optimization process was caused by plotting a graph of SNR as against effective or renal dose (figure 58). Three different abdominal tissues (lungs, kidney and spinal column) in the abdominal image were analyzed to show the relationship between SNR and dose parameters. Detailed summaries of these parameters are presented in Table 22. Comparatively, the signal to noise ratio (SNR) against the dose parameters on the various tissues shows that the spine, which is a hard tissue received higher signals followed by the soft kidney tissues and then the air filled sponge lung tissues. Conversely, the spine has a smaller numerical value, followed by the kidney and then the lungs. This implied that as the signal increases due to an increase in tissue density, there is a corresponding reduction in the level of noise, resulting in an increased in the SNR (image quality), as shown in Figure 58

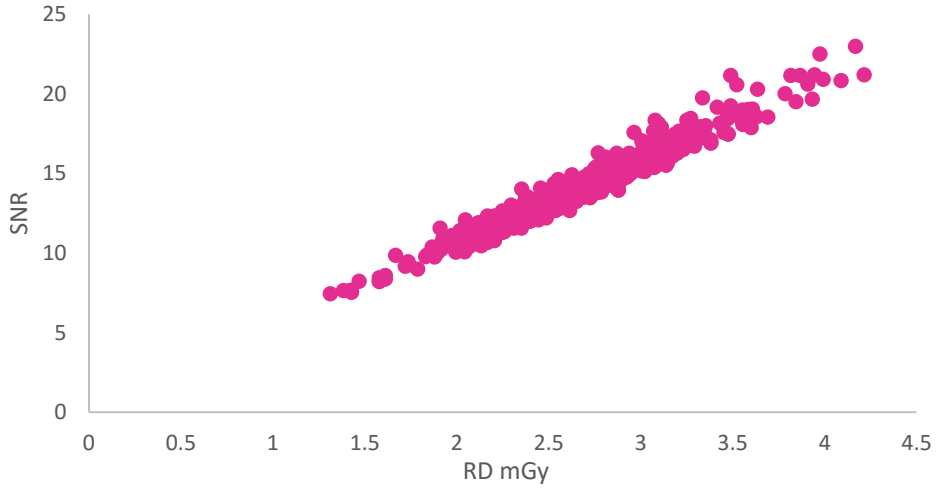

Figure 58: Plot of SNR against RD.

Table 22- *Summary of Estimated SNR*

Statistics	Signal	Noise	SNR
LUNGS			
Mean	82.47	11.83	8.186
Max	207.18	70.09	13.41
Min	38.28	6.99	1.149
KIDNEY			
Mean	125.16	20.10	7.21
Max	502.98	152.73	12.77
Min	9.14	7.02	1.00
SPINE			
Mean	421.67	129.66	4.39
Max	2189.82	896.13	10.21
Min	34.69	7.99	0.25

For dose optimization it is necessary to test run the system to obtain the expected output and at the same time check for image quality for patient specific scanning protocol using the mAs. This enables the organ and effective dose to be estimated together with the signal to noise ratio to ensure that the quality of the image will be good enough for clinical decision in order not to compromise the optimization procedure. The results of the model relationship are shown in

Equations (4.17) to (4.20) for pre-image settings to be determined for dose optimization before the start of imaging.

Converting Modelled Equations to CAD and GUI

The modeling process involved two techniques: Minitab statistical application software and mathematical ellipsoid analysis technique. The first modelling technique involved twenty (20) equations including six (6) equations for body parameters (Equation (4.1) to (4.6)) representing the relationship between height, weight and BSA in terms of BMI and BSI for male and female. In addition, it also include two (2) modeled equation representing the model relationship between RV and R_e (longitudinal, transverse and A-P diameter) for male and female (Equation (4.7) and (4.8)). Furthermore, six (6) equations showing the relationship between renal volume and body indices (Equations (4.9) to (4.14)) for male and female. These sets of data were used to design the GUI shown in Figure 52. The relationship between the dose parameters including effective and renal dose (Equations (4.15) and (4.20)) for male and female. These were used to design a comprehensive predictive GUI to represent the relationship between input dose parameters (kVp, mAs) and output dose parameters (CTDI, DLP, E and RD) as shown in Figure 53. In addition to the gender variation, the ellipsoid equations were also modeled based on three age groups (20-40, 41-60 and 61-80 years) forming three equations each for both male and female. These equations were compared with the international accepted standard ellipsoid equation with approximately 2% variation of the renal ellipsoid coefficient.

The GUI reduces the equation to user friendly interface for clinical application together with visual indicator as shown in Figure 50 and 51 for

males and females respectively. In addition, it simplified the dosimetric process and procedure by setting up standard protocol for dose measurements.

Discussion of Results

Comparatively, the measured body parameters shows that males had larger body dimensions (body weight, height, BMI, BSA and BSI) than females. Similarly, all the measured renal dimensions were within the range of accepted values, as published by ICRP and certified regulatory institutions and individuals (Garland, 2014; Scholbach & Weitzel, 2012; Osafo, 2012; Ozbek *et al*., 2012; Wong *et al*., 2009; ICRP Publication 102, 2007; Lee *et al*., 1999; Ferrer, McKenna, Bauer & Miller, 1997; Ninan, *et al*., 1990; Troell, Berg, Johansson, Wikstad, 1984). In terms of magnitude, the longitudinal diameter was established to be the longest (Figure 31), followed by the transverse diameter, whilst the A-P diameter was found to be the shortest. Indeed, a positive correlation has between established these parameters. Indeed, there is a positive correlation between these parameters. Consequently, an increase in one parameter resulted in a corresponding increase in the other. However, transverse diameter (renal width) deviated from the larger attributes of the left kidney compared to the right kidney. Conversely, in the case of the transverse diameter the right kidney was determined to be wider than the left kidney. Nevertheless, the left kidney was found to be denser and longer than the right kidney. However, this did not bear upon the overall attribute of renal mass, where the left kidney was found to be slightly bigger than the right kidney as evidenced in both the graphical relationship in Figure 32, Appendix F and the reference value chart (Table 9).

The study revealed that renal size (length, width and thickness) diminishes with advancing age; this has been attributed to a parenchymal reduction in the elderly as shown in Figures 50 and 51. Undoubtedly, it is of interest to note that, renal volume increases significantly with age from 20 to 60 years, but its decline significantly at age 61-80 years as shown in summary Table 9. Consequently, the evaluation shows a positive correlation between measured and calculated renal volume, in terms of gender and age variations. Furthermore, the estimated renal volume correlated well with age. This is a significant factor because age is recognized to be one of the risk factors of renal transplant survival and other renal performance. Hence, it will play an important role during renal grafting and other clinical decisions.

Comparatively, the model equations can best be used to accurately predict renal volume than the Trial-and-error method which is currently in vogue. Additionally, there is a strong positive correlation (at least 95% confidence level shown in Appendices J to L) between the renal volume and all the estimated renal parameters. This indicates that the anatomical description based on 3D CT models could provide evaluation of the anatomical assessments of kidneys for potential live kidney donors. The renal volume data in the shape of 3D volumetric analysis of CT data as shown could be a hopeful alternative to nuclear renography in potential kidney donors in terms of anatomical description. The findings also conclude that the consequences could be applied to study renal development in Ghana.

The outcomes of the evaluation of the relationships between measured body and renal parameters show a substantial correlation between body index and renal volume. These findings suggest that physical characteristics are significant

determinants of renal volume and hence the kidney size. This confirms other studies, which indicate that, BSI is a more dependable index of renal volume than all other renal dimensions. Nonetheless, both BMI and BSA are equally fairly good index of renal volume. Indeed, this study agreed with the recommendations that clinical and radiological considerations are necessary for the exact determination of kidney volume. The modeled equations (Equations (4.7) to (4.14)), shows a linear relationship between estimated body parameters (BMI, BSI and BSA) and renal volume during clinical assessment of patients' images. That is, there is a linear growth of the body parameters in relation to the growth of the internal organs.

Furthermore, in literature, the metabolic requirements are correlated with the body parameters (BMI, BSA, BSI), which owns a direct relationship with renal volume as expressed by the graphical relationship between these parameters (modeled equations of body parameters). In addition, the functional performance of the kidney must meet the metabolic requirements of the whole body. However, this is based on a number of factors, including the kidney size based on renal volume and other renal parameter. Secondly, a graphical relationship between renal volume and the body parameters shows a good and positive correlation which described the effect of body parameters in renal volume. It is of interest to note that all the three body parameters are directly proportional RV as described by the three modeled equations.

Renal volume gives a clue to the size of the kidneys, which is one of the most important investigable and reliable factors in examining the urinary system. Furthermore, fair knowledge of the renal volume plays an important role in clinical decision making of the urinary system by radiologist [12], for

instance, in diabetic patients, kidney size reduction is the foremost sign of diabetic kidney disease. Furthermore, in pyelonephritis (the most common cause of kidney failure in children), one of the signs of renal failure is increased kidney size [13]. Therefore, knowing the reference values of renal volume has special importance in analyzing renal morphology. In addition, renal volume related body indices are used during patients followed-up according to individual age groups, which, as with body indices, describes the individual prognosis of the renal volume development. Indeed, growth delay and other tissue deformation, which are often encountered due to chronic renal disease, can be unmasked easily.

Furthermore, the study agreed with a German researcher (Scholbach & Weitzel, 2012), whose publication on the study of body parameters related renal volume, has been referred extensively, especially in areas of Body Surface Area related Renal Volume, Body Surface Index related Renal Volume and Body Mass Index related Renal Volume. The study of these parameters has a major advantages over existing evaluation of renal volume without regard to body parameters. Firstly, it makes the many separate normal charts unnecessary and combines them in an easy to remember two number range: 2.02–146.7 (mL^3/m^2) -irrespective of age, sex, or body size. Secondly, renal volume related body indices that are greater than or less than the standard reference values should prompt the suspicion for further investigation. Thirdly, a physical structure-related renal volume overwhelms the artificial virtual breaks in the follow-up of an individual kidney development, which emanates from changing from one to the next normal value chart, during later stages in life.

Fourthly, in cases where followed ups are required to assess individual prognosis of kidney volume development after treatment or transplant, problems associated with kidney recovery, which are often encountered early in chronic renal disease, can be unmasked easily. All these promises a genuine advantage in studying renal disease by precocious detection of creeping renal volume changes. Therefore, body related-renal volumes examinations are necessary in renal development using CT imaging.

Unfortunately, ionizing radiation exposure is used as the source of CT imaging during renal studies due to these four points' advantages. Therefore, there is the need to assess various quantities that relate dose risk parameters together with the image quality for radiation dose optimization. The most important radiation exposure quantities that relate radiation dose to an organs from any given CT study depend on tube current scanning time in milliamp-seconds (mAs) and the tube voltage in kilovolt peaks (kVp). These quantities determine the relative image noise level by either increasing or reducing the mAs and kVp. However, reduction in relative noise in CT images will automatically give rise to an increase in radiation dose and vice visa. Hence, there will always be a need for a tradeoff between minimal image noise and low doses of radiation to patients in medical imaging (Sardinha, Silva, Minderico & Teixeira PJ., 2006)

To address this, there need to look at the effects of the two exposure parameters (CTDI and DLP) on the abdomen to assess the deposition of dose to the renal and abdominal tissue (renal dose and effective dose) based on the extrapolation by the LNT model which may contribute to cancer. Furthermore, optimization refers to the procedure of keeping the exposure of patients to the

minimum necessary to accomplish the required diagnostic objective. Patient dosimetry and DRLs are recognized as significant tools for optimization of patient radiation protection. Unfortunately, the values of these DRLs are not available for comparison in Ghana. Nevertheless, this study agreed with international regulatory organizations such as IAEA, AAPM ICRP and the EC, whose standards of practice, including that of the basic safety standard (BSS) by IAEA, whose requirements and recommendations are implemented based on the principle of optimization of radiation protection of patients in medical facilities using ionizing radiation. Recommendations from these international regulatory bodies are essential practical principles that assist clinicians in clinical practice. Hence, the values of this study were compared with those from these international organizations for purposes of optimization and not exact dose values to various tissues.

Generally, out of the 613 images, between 63-82% of all the parameters were within the accepted range of the recommendations while 18-37% failed to meet these recommendations as shown in the graphical relationship in Figure 54, 55, 56 and 57 for weighted CTDI, DLP, effective dose and renal dose respectively. Optimization in CT is necessary because CT examinations are associated with far higher radiation doses than other conventional radiography. In particular, the radiation doses from some CT scanners fall in the range shown by direct epidemiological evidence to be associated with increased cancer risk (Feinendegen, 2005). It should as well be mentioned that the evidence from this study indicates that the radiation doses from CT are highly varied between institutions. The effects of the measured and calculated exposures and dose parameters showed a broad range of values, even though, the average values

were mostly more depressed than the recommended average critical values by, approximately 63% to 82%. This may be misleading, since some of the individual renal dose and effective dose parameters exceeded the critical values, as much as 400%. The approximately 18% to 37% of the calculated values, were above the recommended values which may lead to prognostic health consequences.

The ability to detect an aberrant object (lesion) in a radiograph is related to the proportion of the differential intensity to the ambient noise level. This ratio is called the absolute image signal to noise ratio. This ratio was measured on abdominal CT images, the resolutions of which established a minimum SNR value of 0.8 with a corresponding minimum effective dose of 3.36 mSv. In addition, a maximum SNR of 12.77 was estimated with a corresponding maximum patient effective dose of 52.45 mSv.

In X-ray technology as in CT imaging, large numbers of photons, particles (increase mAs) and energy fluence (increase kVp) are absorbed to produce clearer images to enable clinical interpretation. However, introducing larger photons will increase the SNR of the image (improve image quality), where the signals are stronger with less noise in the image. In addition, the large photons will increase the amount of photon interaction with the body tissues hence increase possible dose deposits. Therefore the use of high kV and mAs will increase the number of photons and radiation dose to patients, hence increasing the SNR. Conversely, it was observed that measured SNR improved with increase slice thickness and by decreasing the kV and mAs, this would reduce the patient dose.

The renal organ dose was calculated by using a converting factor by ICRP publication 103 and a weighted CTDI (CTDIw). The conversion factor and the weighted CTDI depend on mAs and kVp as input parameters. The value of which are chosen based on age and gender variations, since higher values increases signal strength and the dose to patients. It is significant to recognize that by reducing the mAs implied an increase in image noise. However, as the radiation absorbed in the tissue (the dose) is reduced, the visual noise in the image is increased. An optimized imaging protocol is one in which the mAs is adjusted to attain an image noise level that is acceptable for clinical interpretation. Increasing the pitch factor technically reduces the radiation organ dose, but practically other factors must be considered. While increasing the pitch does reduce the dose if all other factors are the same, it also affects image quality. First, the pitch can place a limit on the maximum detail or spatial resolution that can be obtained in the axial slice thickness direction. Second, increasing pitch will increase image noise. However, most CT systems have a function that automatically increases the mAs and dose to maintain a specific noise level as other factors, including slice thickness, matrix size, field of view, and pitch are changed. An advantage of increasing pitch is to reduce scanning time, not to reduce dose. The appropriate action is to select pitch factor values that provide a balance between the image quality and scan time requirements to optimized patient exposure.

This comes with experience and the role of existing national or international guidelines and appropriate references, generally based on BSS by IAEA. The IAEA also offers regional and international training courses, particularly, in the field of optimization and image quality to various

professional including medical Physicist, Radiologist and Radiographers. The goal is to provide requisite skills and knowledge to various professionals to achieve the desired ultimate objective of obtaining high quality images through best practice of imaging procedure. For instance, the physicist duty is to establish quality control practices, provide measuring methodologies and support optimization process for patients, clinicians and general public safety. Whilst the radiologist duty is to undertake the imaging procedure, analysed and interpret images and write report based the requesting physicians note in order to answer all the clinical questions.

Finally, display information interface has been designed to assess patients' general and specific information. These basic patient information is accessed using the text-based or visual indicators approach. Which was developed to form part of the RIS GUI to give a comprehensive platform for all the members of the imaging team. In addition, a more specific GUI written with specific object-oriented programming language was designed to assess specific information about individual patients, in terms of organ and body measurements in addition to dose optimization protocol. This interface is displayed on a VB application platform and incorporated on the DICOM reader for use by the radiologist and radiographers during the decision making process.

In conclusion, Ghanaian reference body and renal parameters have been established and developed into a database chart for clinical application in Ghana as summarized in Table 23 and 24 respectively.

Table 23- *Ghanaian Reference Body Parameters*

Parameter	Male	Female
WEIGHT (kg)	80.83	61.87
HEIGHT (cm)	178.64	167.11
BMI (kg/cm^2)	25.19	21.91
BSA (cm^2)	2.02	1.69
BSI (kg/cm^2)	39.81	36.58

.

Table 24- *Ghanaian Reference Renal Parameters*

PARAMETER	M/R	M/L	MEAN	F/R	F/L	MEAN
RV mL^3	146.74	151.76	149.25	142.04	148.29	145.17
RM mg	288.09	295.75	291.92	235.76	255.05	245.41
V_eC	0.5283	0.5297	0.5290	0.5280	0.5304	0.5292
RSI	1.00	1.01	1.01	1.00	1.01	1.00
LNG mm	103.35	105.13	104.24	101.43	102.98	102.21
TRN mm	60.79	60.39	60.59	59.20	59.02	59.11
A-P mm	44.12	44.95	44.54	43.09	44.82	43.96
RSA (cm^2)	31.55	32.04	31.80	27.76	29.47	28.62

Furthermore, Table 25 shows a summarized Ghanaian reference body parameters as related to renal volume. These values enabled renal volume to be predicted with a known BMI, BSA or BSI. While Table 26 refers to established Ghanaian Reference Exposure and Dose Parameters for clinical applications.

Table 25- *Ghanaian Reference Body-Related Renal Parameters*

Parameter	Male	Female
RV_RBMI ($mL^3/kg/cm^2$)	5.94	6.29
RV_LBMI ($mL^3/kg/cm^2$)	6.12	6.64
RV_RBSA(mL^3/cm^2)	72.97	81.77
RV_LBSA (mL^3/cm^2)	75.12	86.40
RV_RBSI ($mL^3/kg/cm^2$)	3.75	3.77
RV_LBSI ($mL^3/kg/cm^2$)	3.87	3.99
Right-RRV	0.4919	0.5037
Left-RRV	0.5081	0.5136
Right-RRL	0.4959	0.4963
Left-RRL	0.5041	0.5037

Table 26- *Ghanaian Reference Exposure and Dose Parameters*

PARAMETERS	MALE	FEMALE	MEAN
$CTDI_{VOL}$ (mGy)	6.17	6.48	6.33
$CTDI_W$ (mGy)	5.02	5.27	5.15
DLP (mGy cm)	921.53	950.97	936.25
E (mSv)	13.83	14.35	14.09
RD (mSv)	3.12	3.39	3.26

Finally, the study, reviewed and compared measured parameters with international reference values and has been found to meet best practice all over the world as shown in Table 27, hence acceptable for adoption in Ghana for clinical application.

Table 27- *Comparison of Study and ICRP values*

Parameters	ICRP Recommendations	Average Study Values
MALE		
BMI	24	25.2
BSA	1.95	2.02
BSI	38.95	39.81
K*	0.52	0.5292
RV	120-170	149.1
RL	10-12	10.4
RW	5-6	6.1
RT	3-4	4.5
E	8-14	14.1
RD	1-3	3.12
FEMALE		
BMI	23	21.9
BSA	1.69	1.69
BSI	35.2	36.6
K*	0.52	0.5290
RV	120-170	145.2
RL	10-12	10.2
RW	5-6	5.9
RT	3-4	4.4
E	8-14	14.4
RD	1-3	3.4

Source: ICRP Publication 89

In addition, a GUI (Figures 52 and 53) and CAD (Figures 50 and 51) models were designed to adequately reflect a comfortable working process of all the mathematical model equations the displayed interface of the DICOM interface enabled the prediction of renal volume with known body indices. It also enables the accurate application of the renal ellipsoid equation. Furthermore, the

radiographers input display interface has been designed to capture dose parameters in relation to mAs and kVp and the expected CTDI and DLP values. These parameters were applied to estimate renal and effective dosage. The designed display interface enabled the prediction of renal dose with a known effective dose as shown in Equation 4.15 for male and 4.16 for females. This method is meant to be used to predict the expected radiation dose to patients and to optimize the radiation dose in relation to image quality before imaging. Hence, the outcome of the study is expected to give appropriate technical support to the imaging team not only for quality control, but for new measurement based assessment technologies and methods to improve on the analysis and dose optimization procedure.

Chapter Summary

In summary, this chapter discussed the various results of the measured parameters in tables and graphical representation. It provides a space platform to answer all the questions by presenting the data that are necessary to facilitate the implementation process in a tables and graphical representation. It also describes the relationship between the various measurable quantities that were used to calculate the derived quantities in order to draw reasonable conclusions. Furthermore, the analysis of the presented data using various practical and theoretical tools based on the study objectives is also captured in this chapter. It conclude with a comprehensive discussions on the presented results using tables and graphical representation. Finally the established reference values were presented in tables for easy understanding and use by clinicians.

CHAPTER FIVE

SUMMARY, CONCLUSIONS AND RECOMMENDATIONS

Introduction

The framework of this chapter is a comprehensive summary of the major findings in relation to the measured renal parameters, body indices, renal and effective dose optimization procedures during abdominal CT examination. This chapter also draws insightful conclusions on the development of mathematical and computed aided design models of the measured parameters for clinical application. It also stated various standard values of the kidney dimensions and dose optimization procedures which are now available to be used by clinicians during renal examination. It ends with the appropriate conclusions and relevant recommendations of the major findings to key stakeholders.

Summary

The study dealt with four broad areas: measurements of body parameters, measurement of renal dimensions/parameters and the relationship with the body parameters, the estimate of renal and effective dose and a tradeoff between dose and image quality. In view of this five body parameter were measured, including body height, weight, BMI, BSA and BSI based on age and gender variations. In addition, six renal parameters including: renal volume, renal length, lateral diameter, A-P diameter, renal volumetric ellipsoid coefficient and renal shape index were measured. Furthermore, the recorded $CTDI_W$ and DLP were used to estimate renal dose and effective dose respectively. Finally, SNR of all the acquired images in relation to the effective dose were determined to establish a tradeoff between dose received and the quality of images produced. These parameters were tabulated in four sets of tables in Appendices B, C, D and E

for body parameters, renal dimensions, renal parameters and dose parameters respectively. These four sets of data were summarized in chapter 4 to represent comprehensive information on the 660 image data.

The average measured reference body parameters of: 80.83 kg, 178.64 cm, 25.19 kg/cm^2, 2.02 cm^2 and 39.81 kg/cm^2 for male weight, height, BMI, BSA and BSI respectively, while the average female measured reference body parameters of: 61.87 kg, 167.11cm, 21.91 kg/cm^2, 1.69 cm^2 and 36.58 kg/cm^2 for weight, height, BMI, BSA and BSI respectively were determined.

Furthermore, three outstanding results of the measured renal parameters show the following interesting findings: the renal volumetric ellipsoid coefficient and the renal shape index was approximately 0.53±0.01 and 1.00±0.02 for both age and gender variations respectively. Generally, the mean RSI and the volumetric ellipsoid coefficient were not affected by either age or gender variation. The mean renal volumes were 149±23 cm^3 and 145±21 cm^3 for male and female respectively. These values vary from various other race-specific based studies on comparative study of methods of estimating the kidney length in kidney transplantation donors (Tsapaki, Kottou & Papadimitriou, .2001). This confirms the variations in the physical characteristics of the various populations. It confirms previous reports that states that renal dimensions differ according to geographical location (IAEA, 1989, IAEA-TECDOC-1005, 1998). The average male and female longitudinal diameters were 104±6 mm and 102±4 mm respectively, while the average transverse diameters were 61±2 mm and 59±2 mm for males and females respectively. In addition, the measured mean A-P diameters were approximately 45±4 mm and 44±3 mm for males and females respectively. Summarized values of this measured reference renal

parameters are presented in Table 24. Finally, the unified renal volume model was determined to be:

$RV = 0.53 * RL * RT * RW$, for clinical application in Ghana, this is comparable to standard international model presented as:

$RV = 0.52 * RL * RT * RW$

The outcomes of the evaluation show that females had smaller body indices (height, weight, body surface region, body surface index and body mass index), renal volume and other renal parameters as compared to their male counterparts. There were significant correlations between body indices and actual renal volume. These findings suggest that physical characteristics are significant determinants of renal volume and hence the kidney size. The study shows that, BMI, BSA and BSI are better indicators of renal volume than all other parameters as shown by the modeled relationship between renal volume, BSA BSI and BMI. The modeled equations in Chapter 4 are designed to predict renal volume using either BMI, BSA or BSI. Hence BMI BMA and BSI have been modeled and can be used to predict renal volume with a confidence level of 95% as shown in Appendix J to L. Even though at extreme values the confidence level of renal volume prediction by BMI reduces significantly, however, BSA and BSI continue to predict renal volume at all levels of body size.

Furthermore, all the measured renal dimensions in this study agreed with the reviewed international and other institutional measured values and could be adopted for implementation for clinical applications. The estimated ICRP measured BMI and BSA values were: 24 kg/m^2 and 1.91 m^2 for male and 23 kg/m^2 and 1.6 m^2 for female. While the measured values for this study were 25.19 kg/m^2 and 2.02 m^2 for male and 21.91 kg/m^2 and 1.69 m^2 for female. In

addition, BSI measured values were: 39.81 kg/m^2 and 36.58 kg/m^2 for male and female respectively.

The estimated male average dose parameters were: 6.17 mGy, 5.02 mGy, 950.97 mGy, 13.83 mSv and 3.12 mSv for $CTDI_{VOL}$, $CTDI_W$, DLP, E and RD respectively. Whereas female average dose estimates were 6.48 mGy, 5.27 mGy, 921.53 mGy, 14.35 mSv and 3.39 mSv for $CTDI_{VOL}$, $CTDI_W$, DLP, E and RD respectively the detailed of gender variations are shown in Table 26. Furthermore, the study revealed that patients with a high BMI receive a greater effective dose, as compared with patients with smaller BMI. This is because as the area and thickness of the tissues increases, the greater X-ray penetration is needed to create acceptable images, which increases radiation dose. Hence, the effective radiation dose of the study showed this trend, where patients who were examined with a high BMI received a much higher effective dose than those with smaller BMI. In addition, minimum values of mAs and kVp that provided image quality with enough information for clinical decision were 14 mAs and 80 keV. This gave enough information to maintain trade-off between patients' optimization procedures without loss of acceptable image quality during CT scan.

Conclusions

In conclusion, the results shows that the left kidneys are slightly larger than the right kidneys in all the parameters. The study confirmed that kidney development is gender dependent, with the male kidneys slightly larger than the female kidney. The study further concluded that kidney sizes diminishes with advancing age.

To address the challenges outlined in the problem statement a comprehensive Clinical Decision Support Application Software for both measurements of renal dimensions and dose Optimisation Procedure in CT has been developed for clinical application in Ghana.

Furthermore, the following conclusions were drawn based on the study objectives;

The standard reference body Weight, Height, BMI, BSA and BSI were determined and found to be appropriate for clinical application in Ghana.

The standard reference longitudinal diameter, transverse diameter and anterior-posterior diameter were found to be appropriate for clinical application in Ghana. An accepted unified local based standard reference renal volumetric ellipsoid coefficient was determined and led to the establishment of renal volume model for clinical application in Ghana.

The study enables the prediction of renal volume of an average Ghanaian adult with standard reference body parameters such as BMI, BSI and BSA using a GUI for clinical application.

An appropriate standard reference renal organ dose and effective dose values of an average adult Ghanaian undergoing abdominal CT examination for clinical application has been determined,

The study led to the establishment of patient's dose optimization protocols without loss of acceptable image quality during abdominal CT scan in Ghana.

Recommendations

Based on the study results, the following recommendations are addressed to stakeholders in order to help improved health care delivery in Ghana:

Recommendations for various facilities

Facilities are encouraged to acquire dose reduction technologies and techniques to help reduce radiation dose to patients compatible with what has been done during this research work.

Adequate and appropriate training be organised to ensure adequate protection of the patients.

Adequate and appropriate training schedules should be organized to ensure adequate protection of the patient.

Establish specific unified scanning protocols as established in this study. Data management units should be established and managed by qualified personnel for better Radiological Information System (RIS) in all the centers.

Recommendation to Radiographers

I recommend that the modeled equations should be used to aid in the selection of exposure parameters.

There is the need to work as a team with the physicist and the radiologist during scanning process in order to reduce radiation doses to patients.

Various dose optimization factors should be considered during pre-set imaging procedure. These include patient size, age and gender variations to avoid unnecessary dose to patients.

Recommendation to Radiologists

The radiologist should use the results obtained by this method in relation to the renal volumetric ellipsoid coefficient for clinical application in Ghana.

It is recommended that the established reference values be used as clinical guidelines values for the protection of patients.

Recommendation to Medical Physicists

It is recommended that Medical Physicists should adopt the method used in this study to develop other organ models to be used as standard reference values for clinical applications and research in Ghana.

The teamwork approach between the Radiologist, the Medical Physicists and Radiographers to reduce radiation dose to patients.

Medical physicist should carry out periodically (annually) estimate of the abdominal effective dose and organ doses in all the centers in Ghana using the method established in this work.

The results obtained can then be used to continuously monitor dose levels to advice clinicians appropriately in their clinical practice.

Recommendations to Regulatory Authority

The abdominal effective dose exceeded the recommendation of the EC and ICRP values. This is an indication that effective regulatory oversight is needed. The Nuclear Regulatory Authority should provide regulations and guidance documents that will assist registrants and licensees to meet regulatory requirements for the control of medical exposure.

Regular inspections should be conducted to ensure CT facilities are meeting regulatory requirements.

Recommendations for Future Works

In view of the observed cases of regional body dose variations and similar experiences observed elsewhere, further studies on dose optimization to patients

undergoing CT examinations in Ghana are needed. There are a number of observed parameters that need optimization.

The following recommendations are made:

Other body organs be modeled to determine the voxel phantom characteristics of a Ghanaian reference man for clinical application.

Finally, other studies be done with regard to organ model of infants and the neonates to justify the various age variations scanning protocols used in various CT centers in Ghana, in order to provide paediatric provide baseline data.

REFERENCES

Aabha D. (2016). *IAEA workshop to address challenges of unnecessary radiation exposure of patients*. Retrieved from https://www.iaea.org/newscenter/news/technical-meeting-to-justification-of-using-medical-procedures-using-ionizing-radiation

American Association of Physicists in Medicine (AAPM). (1993). *Specification and acceptance testing of computed tomography scanners*. New York: AAPM.

American Association of Physicists in Medicine (AAPM). (2008). *The measurement, reporting, and management of radiation dose in CT*. New York: AAPM.

Bakker, J. (1999). Renal volume measurement: Accuracy and repeatability of US compared with that of MR imaging. *Rad Num*., *211*(3), 623-628.

Berrington de Gonzalez, A. (2009). Projected cancer risks from computed tomographic scans performed in the United States in 2007. *Arch. Intern. Med*., *169*, 2071–2077.

Berrington Gonzalez, A., & Darby, S. (2004). Risk of cancer from diagnostic X-rays. *Lancet*, *363*(9406), 345-351

Boyd, E. (1935). *The growth of the surface area of the human body*. London: Oxford University Press.

Brandt, T. D., Neiman, H. L., Dragowski, M. J., Bulawa, W., & Claykamp, G. (1982). Ultrasound assessment of normal renal dimensions. *Journal of Ultrasound Medicine*, *7*(15), 49-52.

Breau, R. H., Clark, E., Bruner, B., Cervini, P., Atwell, T., Knoll, G., & Leibovich, B. C. (2013). A simple method to estimate renal volume from computed tomography. *Canadian Urol Assoc Journal*, *7*(5), 189–192.

Bryan, S., Weatherburn, G. C., Watkins, J. R., & Buxton, M. J. (1999). The benefits of hospital-wide picture archiving and communication systems, a survey of clinical users of radiology services. *Br J Radiol. 72*(857), 469–478.

Bushberg, J. T., Seibert, J. A., Leidholdt, E. M. Jr., & Boone, J. M. (2012). *The essential physics of medical imaging*. Philadelphia, PA: Lippincott Williams & Wilkins.

Bydder, G. M., Harry, D., Bassan, L., & Kreel, L. (1981). Computed tomography attenuation values in fatty liver. *Journal of Computed Tomography, 5*(1), 33-35

Chambers, J. M. (1983). *Graphical methods for data analysis*. Boston: Duxbury Press.

Charles, D. (2006). *Doctors expose BMI shortcomings*. London: Evening Standard.

Charles, J., & Gary, M. (1989). *Data analysis*. Harcourt: Brace Jovanovich.

Current, J. D. (1997). A linear equation for estimating the body surface area in infants and children. *Int J Anesth., 2*(2), 344-356.

Deak, P., Smal, Y., & Kalender, W. A. (2010). Multisection CT protocols: Sex- and age-specific conversion factors used to determine effective dose from dose length product. *INT J. Radiology, 257*, 158-166.

Digital Imaging and Communications in Medicine (DICOM). (2007). Supplement 127: *CT radiation dose reporting (Dose SR).* Rosslyn, VA: DICOM Standards Committee.

Du Bois, D., & Du Bois, E. F. (1916). A formula to estimate the approximate surface area if height and weight be known. *ArchInt Med*., *17*(6), 863–871.

Duncan, J. R., & Panahipour, S. (2014). *Tissue attenuation of X-rays.* Retrieved from http//www.ImageWisely.org

Egberongbe A. A, Adetiloye V. A, Adeyinka A. O, Afolabi O. T, Akintomide A. O, Ayoola O. O. (2013). Evaluation of renal volume by ultrasonography in patients with essential hypertension in Ile-Ife, South Western Nigeria. *Libyan Journal of Medicine, 5*, 55-61.

Einstein, A. J., Henzlova, M. J., & Rajagopalan, S. (2007). Estimating risk of cancer associated with radiation exposure from 64-slice computed tomography coronary angiography. *JAMA*, *298*, 317–323.

Einstein, A. J., Moser, K. W., Thompson, R. C., Cerqueira, M. D., & Henzlova, M. J. (2007). Radiation dose to patients from cardiac diagnostic imaging. *Circulation JAMA, 116,* 1290–1305.

Eknoyan, G. (2008). The average man and indices of obesity. *Journals of Medicine & Health, Nephrology Dialysis Transplantation*, *23*(1). 47-51.

Emamian, S. A., Nielsen, M. B., & Pedersen, J. F. (1995). Intraobserver and interobserver variations in sonographic measurements of kidney size in adult volunteers. A comparison of linear measurements and volumetric estimates. *Acta Radiol*. *36*(4), 399-401.

Emamian, S. A., Nielsen, M. B., Pedersen, J. F., & Ytte, L. (1993). Kidney dimensions at sonography: Correlation with age, sex, and habitus in 665 adult volunteers. *AJR, 160,* 83-86.

Faletra, F. F., D'Angeli, I., & Klersy, C. (2010). Estimates of lifetime

attributable risk of cancer after a single radiation exposure from 64-slice computed tomographic coronary angiography. *JAMA Heart, 96*, 927–932.

Feeman, T. G. (2010). *The mathematics of medical imaging: A beginner's guide*. Berlin: Springer Undergraduate Texts in Mathematics and Technology.

Feinendegen, L. E. (2005). Evidence for beneficial low level radiation effects and radiation Hormesis. *Br. J. Radiol*., *78*, 3–7.

Ferreira, F., & Duarte, J. A. (2014). Accuracy of body mass index, waist circumference and body surface index to characterize overweight and obesity in adolescents. *Arch exer Health and Dis*., *4*(3), 299-306.

Ferrer, F. A., McKenna, P. H., Bauer, M. B., & Miller, S. F. (1997). Accuracy of renal ultrasound measurements for predicting actual kidney size. *Journal of Urol., 157*(6), 78-81.

Frempong, G. A. (2013). *Perceived body weight and actual Body Mass Index (BMI) among urban poor communities in Accra, Ghan*a. Unpublished doctor of philosophy dissertation, University of Ghana, Legon.

Fujimoto, S., Watanabe, T., Sakamoto, A., Yukawa, K., & Morimoto, K. (1968). Studies on the physical surface area of Japanese. 18. Calculation Formulae in three stages over all ages. *Nihon Eiseigaku Zasshi*. *5*, 443–450.

Garland, J. S. (2014). *Elevated body mass index as a risk factor for chronic kidney disease: Current perspectives, diabetes Metab Syndr Obes*. Auckland: Dove Medical Press.

Gehan, E. A., & George, S. L. **(**1970). Estimation of human body surface area from height and weight. *Cancer Chemotherapy Rep 1, 54*(4), 225-235.

Geraghty, E. M., Boone, J. M., McGahan, J. P., & Jain, K. (2004). Normal organ volume assessment from abdominal CT. *EPUB Abdom Imaging*, *29*(4). 482-490.

Ghana Statistical Service. (2013). *2010 population and housing project, national analytical* report. Accra: GSS.

Glodny, B, (2009). Normal kidney size and its influencing factors a 64-slice MDCT study of 1,040 asymptomatic patients. *BMC Urol, 2*(5), 9-19

Haycock, G. B., Schwartz, G. J., & Wisotsky, D. H. (1978). Geometric method for measuring body surface area: A height-weight formula validated in infants, children and adults. *J Pediatric, 2*(93), 62–66.

Hendee, W. R. (1999). Physics and applications of medical imaging. *Medical College of Wisconsin, Milwaukee*, *71*(2), 444–450.

Huda, W., Ogden, K. M., & Khorasani, M. R. (2008). Converting dose-length product to effective dose at CT. *J. of Radiology*, *248*(3), 995-1003

Huesman, R. H. (1984). A new fast algorithm for the evaluation of regions of interest and statistical uncertainty in computed tomography. *Phys. Med. Biol. 29*. 543–552

Hutton, B. F., & Osiecki, A. (1998). Correction of partial volume effects in myocardial SPECT. *J. Nucl. Cardiol*ogy *5*(4), 402–413

ICRP. (2007). Managing patient dose in Multi-Detector Computed Tomography (MDCT). *ICRP Publication 102*, 37-41.

International Atomic Energy Agency. (1988). *Report of the project formulation meeting: Co-ordinated research project, compilation of anatomical, physiological and metabolic characteristics for a reference Asian Man*. Mito. Vienna: IAEA.

International Atomic Energy Agency. (1998). *Compilation of anatomical, physiological and metabolic characteristics for a reference Asian man Vol. 1: Data summary and conclusions and vol. 2 country reports, results of a coordinated research programmes 1988-1993.* Vienna: IAEA.

International Commission on Radiation Protection (ICRP). (2002). Basic anatomical and physiological data for use in radiological protection reference values. *ICRP Publication, 32*, 3-4.

International Commission on Radiation Protection. (1996). Radiological protection and safety in medicine. *ICRP Publication, 26*(2), 56-143

International Commission on Radiological Protection. (2007). The recommendations of the international commission on radiological protection. *ICRP*. *37*(2–4), 1–332

Janoff, D. M., Davol, P., Hazzard, J., Lemmers, M. J., Paduch, D. A., & Barry J. M. (2004). Computerized tomography with 3-dimensional reconstruction for the evaluation of renal size and arterial anatomy in the living kidney donor. *Journal of Urology, 171*(1), 27-30.

Jones, D. G., & Shrimpton, P. C. (1993). *Normalized organ doses for X-ray computed tomography calculated using Monte Carlo techniques*. Chilton: NRPB-SR250.

Kang, K. W. (2007). *A comparative study of methods of estimating kidney length in kidney transplantation donors*. Oxford: Oxford University Press.

Khan, F. M. (1984). *The physics of radiation therapy* (2nd ed.). Lippincott: Williams & Wilkins.

Krakauer, N. Y., & Krakauer, J. C. (2012). A new body shape index predicts mortality hazard independently of body mass Index. *PLoS ONE, 7*(7). 23.

Lee, B. H. (1999). Estimation of kidney size by ultrasonography in normal Korean Adults. *Korean J Nephrol., 18*, 46-51

Leitz, W., Axelsson, B., & Szendro, G. (1995). Computed tomography dose assessment a practical approach. *Radiat. Prot. Dosimetry, 57*, 377–380.

Lerner, L. B., Henriquez, H. F., & Harris, R. D. (1999). Interactive 3-dimensional computerized tomography reconstruction in evaluation of the living renal donor. *Journal of Urology, 161*(2), 403-407.

Link, F., Kuhagen, S., Boskamp, T., Rexilius, J., Dachwitz, S., & Peitgen, H. O. (2004). A flexible research and development platform for medical image processing and visualization. *RSNA Publications, 453*(6), 17-32.

Löfstedt, T., Ahnlund, O., Peolsson, M., & Trygg, J. (2012). Dynamic ultrasound imaging: A multivariate approach for the analysis and comparison of time-dependent musculoskeletal movements. *BMC Medical Imaging, 10*(1186), 1471-2342.

Lu, R. Z., & Nishikawa, R. (2012). *Contrast-to-Noise ratio is not an appropriate measure of CT image quality when comparing different iterative reconstruction algorithms.* 54th Annual Meeting, University of Chicago, Chicago, IL, Charlotte, NC.

Mattsson, S., & Söderberg, M. (2011). Radiation dose management in CT, SPECT/CT and PET/CT Techniques. *Rad Prot Dosim*, *147*(1), 13–21.

Mazonakis, M., Tzedakis, A., Damilakis, J., & Gourtsoyiannis, N. (2007). Thyroid dose from common head and neck CT examinations in children:

Is there an excess risk for thyroid cancer induction. *Eur Radiology. 17*(5), 1352-1357

McAfee, J. G., Cloutier, R. J., Edwards, C. L., & Snyder, W. S. (1969). *Problems in evaluating the radiation dose for radionuclides excreted by the kidneys in medical radionuclides: Radiation dose and effects symposium.* Oak Ridge: U.S. Atomic Energy Commission.

MeVis Medical Solutions. (2015). *Reference guide for the MeVisLab* GUI. Bremen: Author.

Monson, R. R. **(**2006). *Health risks from exposure to low levels of ionising radiation.* Washington DC: The National Academies Press.

Moorthy, H. K., & Venugopal, P. (2011). Measurement of renal dimensions in vivo: A critical appraisal. *Indian J Urol*., *27*(2), 169–175

Mosteller, R. D. (1987). Simplified calculation of body-surface area. N *English Journal of Medicine*, *317*(17), 1098.

Mullenders, L., Atkinson, M., Paretzke, H., Sabatier, L., & Bouffler, S. (2009). Assessing cancer risks of low-dose radiation. *Nat. Rev. Cancer*, *9*(8), 596–604.

Muto, N. S., Kamishima, T, Harris, A. A, Kato, F., Onodera, Y., Terae, S, Shirato, H. (2011). Renal cortical volume measured using automatic contouring software for computed tomography and its relationship with BMI, age and renal function, *Eur J Radiology, 78*(1), 151-156.

National Council on Radiation Protection and Measurements (NCRPM). (2009). *Ionizing radiation exposure of the population of the United States.* Maryland: National Council on Radiation Protection report no. 160.

National Research Council (NRC). (2006). *Commission on health risks from exposure to low levels of ionizing radiation*. Washington, D.C.: The National Academies Press.

Ninan, V. T. (1990). A comparative study of methods of estimating renal size in normal adults. *Oxford Journal of Medical Health, Nephr Dial Transpl*., *5*(10), 851-854.

Ojima, M., Ban, N., & Kai, M. (2008). DNA double-strand breaks induced by very low X-ray doses are largely due to bystander effects. *Radiat. Res. 170*, 365–371.

O'Neil, C., & Schutt, R. (2014). *Doing data science*. California: O'Reilly Media Inc.

Origgi, D., Vigorito, S., Villa, G., Bellomi, M., & Tosi, G. (2006). Survey of computed tomography techniques and absorbed dose in Italian hospitals: A comparison between two methods to estimate the dose-length product and the effective dose and to verify fulfillment of the diagnostic reference levels. *Eur. Radiol*., *16*(1), 227-237.

Osafo, C. (2012). Ghana kidney foundation, over 3000 Ghanaians are affected with kidney diseases annually. *Ghana News Agency*.

Ozasa, K, (2012). Studies of the mortality of atomic bomb survivors, report 14, 1950-2003: An overview of cancer and noncancer diseases. *Radiat. Res 177*, 229-243.

Ozbek, O. Solak Y, Guler I, Ozbiner H, Ozbek S, Turkmen K, Nayman A, Biyik Z, Samur C and Turk S. (2012). Predictors of kidney dimensions measured by Multi-Detector Computed Tomography (MDCT) in 930

middle-aged and elderly patients. *Renal Failure Informa Healthcare, 34*(1), 53-59

Perisinakis, K, Damilakis, J, Tzedakis A, Papadakis, A, Theocharopoulos, N, Gourtsoyannis, N. (2007). Determination of the weighted CT dose index in modern multi detector CT scanners. *Physics Medical Radiol. 52*, 6485-95.

Preston, D. L. (2003). Studies of mortality of atomic bomb survivors: Report 13 solid cancer and noncancer disease mortality, 1950–1997. *Radiant Res.; 160*, 381–407.

Rexilius, J., Spindler, W., Jomier, J., König, M., Hahn, H.K., Link, F., & Peitgen, H. O. (2005). A framework for algorithm evaluation and clinical application prototyping using ITK. *The Insight Journal, 6*(34). 65-96.

Rothkamm, K., & Lobrich, M. (2003). Evidence for a lack of DNA double-strand break repair in human cells exposed to very low x-ray doses. *Proc. Natl Acad. Sci., 100,* 5057–5062.

Saeed, Z., Mirza, W., Sayani, R., Sheikh, A., Yazdani, I., & Hussain, S. A. (2012). Sonographic measurement of renal dimensions in adults and its correlates. *International Journal of Collaborative Research Internal Medicine and Public Health. 4*(9), 1626-1641.

Sahni, D., Jit, I., & Sodhi, L. (2012). Weight and measurements of Kidneys in Northwest Indian Adults. *International Journal of Collaborative Research on Internal Medicine & Public Health, 4*(9), 726-732.

Sanders, C. (2010). *Radiation Hormesis and the linear-no-threshold assumption*. Pennsylvania: Springer

Sardinha, L. B., Silva, A.M., Minderico, C. S., & Teixeira, P. J. (2006). Effect of body surface area calculations on body fat estimates in non-obese and obese subjects. *Physioll Meas, 27*(11), 1197–1209.

Sargent, D. W. (1963). Weight-height relationship of young men and women. *Am J Clin Nutrition*, *13*, 318-325

Scholbach, T. H., & Weitzel, D. (2012). Body-surface-area related renal volume: A common normal range from birth to adulthood. *Scientifica*, *20*(12), 3-8.

Shin, H. S., Chung, B. H., Lee, S. E., Kim, W. J., Ha, H. I., & Yang, C. W. (2009). Measurement of kidney volume with multi-detector computed tomography scanning in young Korean. *Yonsei Medical Journal*, *50*(2), 262-265.

Shuter, B., & Aslani, A. (2000). Body surface area: Du bois and Du bois revisited. *Eur J Applied Physiology*, *82*(3), 250–254.

Smith-Bindman, R. (2009). Radiation dose associated with common computed tomography examinations and the associated lifetime attributable risk of cancer. *Arch. Intern. Med., 169*, 2078–2086.

Sullivan, L. (2010). *Hypothesis testing - Analysis of Variance (ANOVA).* Boston: Duxbury Press.

Troell, S., Berg, U., Johansson, B., & Wikstad, I. (1984). Ultrasonographic renal parenchymal volume related to kidney function and renal parenchymal area in children with recurrent urinary tract infections and asymptomatic bacteriuria. *Acta Radiol Diagn., 25*, 41-196.

Tsapaki, V., Kottou, S., & Papadimitriou, D. (2001). Application of European Commission reference dose levels in CT examinations in Crete, Greece. *British J Radiol*. *74*(885), 836-840.

Tzedakis A, Damilakis J, Perisinakis K, Stratakis J and Gourtsoyiannis N. (2005). The effect of z overscanning on patient effective dose from multidetector helical computed tomography examinations. *J. of Med Physics, 32*, 1621-1629

Velten, K. (2009*). Mathematical modeling and simulation: Introduction for scientists and engineers*. Weinheim: Wiley-Vch Verlag GmbH & Co.

Verbraecken, J., Van de Heyning, P., De Backer, W., & Van Gaal, L. (2006). Body surface area in normal-weight, overweight, and obese adults: A comparison study. *Metab Clin Exp*, *55*(4), 515–524.

Wald, H. (1937). The weight of normal adult human kidneys and its variability. *Arch Pathol Lab Medicine, 23*, 493-500.

WHO Expert Consultation. (2004). Appropriate body-mass index for Asian Populations and its implications for policy and intervention strategies *Lancet*, *363*(9403), 157-163.

Wong, I. Y., Copp, H. L., Clark, C. J, Wu, H. Y. (2009). Quantitative ultrasound renal parenchymal area correlates with renal volume and identifies reflux nephropathy. *Journal of Urology, 182*, 1683-1687.

Xu R., & Chen, Y. W. (2009). Generalized N-Dimensional Principal Component Analysis (GND-PCA) and its application on construction of statistical appearance models for medical volumes with fewer samples. *Neurocomputing, 72*(10), 2276–2287.

Young, R. W., & Kerr, G. D. (2005). *Reassessment of the atomic bomb*

radiation dosimetry for Hiroshima and Nagasaki—Dosimetry system (DS02). Hiroshima: Radiation Effects Research Foundation.

APPENDICES

APPENDIX A

VB CODES FOR GUI

Body and Organ Measurements

```
Public Class bodyandorganmeasurement
    Dim Rl, Rw, Rt, BSI, BSA, BMI, Rv, RvBMI, RvBSA, RvBSI, age, gen, ht,
wt, BMIf, BMIm

    Private    Sub    bodyandorganmeasurement_Load(ByVal    sender    As
System.Object, ByVal e As System.EventArgs) Handles MyBase.Load
        '
        '  cbosex.Text = "M"
    End Sub

    Public Sub computeBMI()
        gen = cbosex.Text


        If gen = "M" Then
            ht = Val(txtheight.Text) * 0.01
            wt = Val(txtweight.Text)
            BMI = (wt) / (ht ^ 2)
            txtbmi.Text = Format(BMI, "0.00")
        Else
            If gen = "F" Then
                BMIm = 25.19
                BMIf = BMIm * 0.8698

                txtbmi.Text = Format(BMIf, "0.00")
            End If
        End If

    End Sub

    Public Sub computeRv()
        age = Val(txtage.Text)
        gen = cbosex.Text
        Rl = Val(txtrl.Text)
        Rw = Val(txtRw.Text)
        Rt = Val(txtRT.Text)

        If gen = "M" Then 'Male RV calculation

'************************************************************
            If age >= 20 And age <= 40 Then
                Rv = 0.5287 * Rl * Rw * Rt
                txtrv.Text = Format(Rv, "0.00")
            Else
                If age >= 41 And age <= 60 Then

                    Rv = 0.53 * Rl * Rw * Rt
                    txtrv.Text = Format(Rv, "0.00")
                Else
                    If age >= 61 And age <= 80 Then
                        Rv = 0.5295 * Rl * Rw * Rt
                        txtrv.Text = Format(Rv, "0.00")
                    End If
```

```
                End If
            End If
            '*********************************************************
        Else

            If gen = "F" Then 'Female RV calculation

'*************************************************************
                If age >= 20 And age <= 40 Then
                    Rv = 0.5288 * Rl * Rw * Rt
                    txtrv.Text = Format(Rv, "0.00")
                Else
                    If age >= 41 And age <= 60 Then
                        Rv = 0.529 * Rl * Rw * Rt
                        txtrv.Text = Format(Rv, "0.00")
                    Else
                        If age >= 61 And age <= 80 Then
                            Rv = 0.5295 * Rl * Rw * Rt
                            txtrv.Text = Format(Rv, "0.00")
                        End If
                    End If
                End If

'*********************************************************
            End If
        End If


    End Sub

    Public Sub computeBSI()
        BMI = Val(txtbmi.Text)
        gen = cbosex.Text
        If gen = "M" Then

            BSI = (1.11 * BMI) + 11.86
            txtbsi.Text = Format(BSI, "0.00")
        Else
            If gen = "F" Then

                BSI = (0.58 * BMI) + 23.92
                txtbsi.Text = Format(BSI, "0.00")

            End If

        End If
    End Sub
    Public Sub computeBSA()


        gen = cbosex.Text


        If gen = "M" Then
            BMI = Val(txtbmi.Text)
            BSA = ((0.09 * BMI) - 0.26)
            txtbsa.Text = Format(BSA, "0.00")

        Else
            If gen = "F" Then
                BMIf = Val(txtbmi.Text)
                BSA = (0.3 * BMIf) - 4.78
```

```
            txtbsa.Text = Format(BSA, "0.00")
        End If

    End If
End Sub

Public Sub computeRVBSA()
    BSA = Val(txtbsa.Text)
    gen = cbosex.Text

    If gen = "M" Then

        RvBSA = 0.399 * BSA + 148.65
        txtrvbsa.Text = Format(RvBSA, "0.00")

    Else
        If gen = "F" Then

            RvBSA = 0.999 * BSA + 139.43
            txtrvbsa.Text = Format(RvBSA, "0.00")

        End If

    End If
End Sub

Public Sub computeRVBSI()
    BSI = Val(txtbsi.Text)
    gen = cbosex.Text
    If gen = "M" Then

        RvBSI = -0.19 * BSI + 156.74
        txtrvbsi.Text = Format(RvBSI, "0.00")

    Else
        If gen = "F" Then

            RvBSI = 0.2 * BSI + 133.51
            txtrvbsi.Text = Format(RvBSI, "0.00")
        Else

            '   MsgBox("Provide valid parameter")
        End If

    End If
End Sub

Public Sub computeRVBMI()
    BMI = Val(txtbmi.Text)
    gen = cbosex.Text
    If gen = "M" Then

        RvBMI = (0.53 * BMI) + 135.97
        txtrvbmi.Text = Format(RvBMI, "0.00")

    Else
        If gen = "F" Then

            RvBMI = (0.95 * BMI) + 120.58
            txtrvbmi.Text = Format(RvBMI, "0.00")

        End If
```

```
        End If
    End Sub

    Private Sub txtheight_KeyPress(ByVal sender As Object, ByVal e As
System.Windows.Forms.KeyPressEventArgs) Handles txtheight.KeyPress
   If e.KeyChar = "."c Or e.KeyChar = "-"c Then
            e.Handled = (CType(sender, TextBox).Text.IndexOf("."c) <> -1)
            e.Handled = (CType(sender, TextBox).Text.IndexOf("-"c) <> -1)
        ElseIf e.KeyChar <> ControlChars.Back Then
            e.Handled = ("0123456789".IndexOf(e.KeyChar) = -1)
            If txtheight.Text.IndexOf(".") <> -1 Then
                If txtheight.Text.Length >= txtheight.Text.IndexOf(".") +
3 Then  'replace 2 for greater numbers after decimal point
                    e.Handled = True
                End If
            End If
        End If


    End Sub

    Private Sub txtheight_TextChanged(ByVal sender As System.Object, ByVal
e As System.EventArgs) Handles txtheight.TextChanged
        computeBMI()
    End Sub

    Private Sub txtweight_KeyPress(ByVal sender As Object, ByVal e As
System.Windows.Forms.KeyPressEventArgs) Handles txtweight.KeyPress
        If e.KeyChar = "."c Or e.KeyChar = "-"c Then
            e.Handled = (CType(sender, TextBox).Text.IndexOf("."c) <> -1)
            e.Handled = (CType(sender, TextBox).Text.IndexOf("-"c) <> -1)
        ElseIf e.KeyChar <> ControlChars.Back Then
            e.Handled = ("0123456789".IndexOf(e.KeyChar) = -1)
            If txtweight.Text.IndexOf(".") <> -1 Then
                If txtweight.Text.Length >= txtweight.Text.IndexOf(".") +
3 Then  'replace 2 for greater numbers after decimal point
                    e.Handled = True
                End If
            End If
        End If
    End Sub

    Private Sub txtweight_TextChanged(ByVal sender As System.Object, ByVal
e As System.EventArgs) Handles txtweight.TextChanged
        computeBMI()
    End Sub

    Private Sub txtrl_KeyPress(ByVal sender As Object, ByVal e As
System.Windows.Forms.KeyPressEventArgs) Handles txtrl.KeyPress
        If e.KeyChar = "."c Or e.KeyChar = "-"c Then
            e.Handled = (CType(sender, TextBox).Text.IndexOf("."c) <> -1)
            e.Handled = (CType(sender, TextBox).Text.IndexOf("-"c) <> -1)
        ElseIf e.KeyChar <> ControlChars.Back Then
            e.Handled = ("0123456789".IndexOf(e.KeyChar) = -1)
            If txtrl.Text.IndexOf(".") <> -1 Then
                If txtrl.Text.Length >= txtrl.Text.IndexOf(".") + 3 Then
'replace 2 for greater numbers after decimal point
                    e.Handled = True
                End If
            End If
        End If
```

```
    End Sub

    Private Sub txtrl_TextChanged(ByVal sender As System.Object, ByVal e
As System.EventArgs) Handles txtrl.TextChanged
        If txtrl.Text = "" Then
        Else
            If txtRT.Text = "" Then
            Else
                If txtRw.Text = "" Then
                Else
                    If txtheight.Text = "" Then
                    Else

                        If txtweight.Text = "" Then
                        Else
                            If txtage.Text = "" Then
                            Else
                                computeBMI()
                                computeRv()
                                computeBSA()
                                computeBSI()
                                computeRVBMI()
                                computeRVBSA()
                                computeRVBSI()
                            End If
                        End If
                    End If
                End If
            End If
        End If

    End Sub

    Private Sub txtRw_KeyPress(ByVal sender As Object, ByVal e As
System.Windows.Forms.KeyPressEventArgs) Handles txtRw.KeyPress
        If e.KeyChar = "."c Or e.KeyChar = "-"c Then
            e.Handled = (CType(sender, TextBox).Text.IndexOf("."c) <> -1)
            e.Handled = (CType(sender, TextBox).Text.IndexOf("-"c) <> -1)
        ElseIf e.KeyChar <> ControlChars.Back Then
            e.Handled = ("0123456789".IndexOf(e.KeyChar) = -1)
            If txtRw.Text.IndexOf(".") <> -1 Then
                If txtRw.Text.Length >= txtRw.Text.IndexOf(".") + 3 Then
'replace 2 for greater numbers after decimal point
                    e.Handled = True
                End If
            End If
        End If
    End Sub

    Private Sub txtRw_TextChanged(ByVal sender As System.Object, ByVal e
As System.EventArgs) Handles txtRw.TextChanged
        If txtrl.Text = "" Then
        Else
            If txtRT.Text = "" Then
            Else
                If txtRw.Text = "" Then
                Else
                    If txtheight.Text = "" Then
                    Else

                        If txtweight.Text = "" Then
                        Else
```

```
                            If txtage.Text = "" Then
                            Else
                                computeBMI()
                                computeRv()
                                computeBSA()
                                computeBSI()
                                computeRVBMI()
                                computeRVBSA()
                                computeRVBSI()
                            End If
                        End If
                    End If
                End If
            End If

    End Sub

    Private Sub txtRT_KeyPress(ByVal sender As Object, ByVal e As
System.Windows.Forms.KeyPressEventArgs) Handles txtRT.KeyPress
        If e.KeyChar = "."c Or e.KeyChar = "-"c Then
            e.Handled = (CType(sender, TextBox).Text.IndexOf("."c) <> -1)
            e.Handled = (CType(sender, TextBox).Text.IndexOf("-"c) <> -1)
        ElseIf e.KeyChar <> ControlChars.Back Then
            e.Handled = ("0123456789".IndexOf(e.KeyChar) = -1)
            If txtRT.Text.IndexOf(".") <> -1 Then
                If txtRT.Text.Length >= txtRT.Text.IndexOf(".") + 3 Then
'replace 2 for greater numbers after decimal point
                    e.Handled = True
                End If
            End If
        End If
    End Sub

    Private Sub txtRT_TextChanged(ByVal sender As System.Object, ByVal e
As System.EventArgs) Handles txtRT.TextChanged
        If txtrl.Text = "" Then
        Else
            If txtRT.Text = "" Then
            Else
                If txtRw.Text = "" Then
                Else
                    If txtheight.Text = "" Then
                    Else

                        If txtweight.Text = "" Then
                        Else
                            If txtage.Text = "" Then
                            Else
                                computeBMI()
                                computeRv()
                                computeBSA()
                                computeBSI()
                                computeRVBMI()
                                computeRVBSA()
                                computeRVBSI()
                            End If
                        End If
                    End If
                End If
            End If
        End If
```

```
    End Sub

    Private Sub txtage_KeyPress(ByVal sender As Object, ByVal e As
System.Windows.Forms.KeyPressEventArgs) Handles txtage.KeyPress
        If e.KeyChar = "."c Or e.KeyChar = "-"c Then
            e.Handled = (CType(sender, TextBox).Text.IndexOf("."c) <> -1)
            e.Handled = (CType(sender, TextBox).Text.IndexOf("-"c) <> -1)
        ElseIf e.KeyChar <> ControlChars.Back Then
            e.Handled = ("0123456789".IndexOf(e.KeyChar) = -1)
            If txtage.Text.IndexOf(".") <> -1 Then
                If txtage.Text.Length >= txtage.Text.IndexOf(".") + 3 Then
'replace 2 for greater numbers after decimal point
                    e.Handled = True
                End If
            End If
        End If


        computeBMI()
        computeBSA()
        computeBSI()
        computeRv()

        computeRVBMI()
        computeRVBSA()
        computeRVBSI()

    End Sub

    Private Sub txtage_TextChanged(ByVal sender As System.Object, ByVal e
As System.EventArgs) Handles txtage.TextChanged



        computeBMI()
        computeBSA()
        computeBSI()
        computeRv()

        computeRVBMI()
        computeRVBSA()
        computeRVBSI()

    End Sub

    Private Sub cbosex_SelectedIndexChanged(ByVal sender As
System.Object, ByVal e As System.EventArgs) Handles
cbosex.SelectedIndexChanged



        computeBMI()
        computeRv()
        computeRVBMI()


        '                    If txtage.Text = "" Then
        '                   Else
        computeBSA()
        computeBSI()
        computeRVBSA()
```

```
        computeRVBSI()

        '  End If

    End Sub

    Private Sub txtbmi_TextChanged(ByVal sender As System.Object, ByVal e
As System.EventArgs)


        If txtrl.Text = "" Then
        Else
            If txtRT.Text = "" Then
            Else
                If txtRw.Text = "" Then
                Else
                    If txtheight.Text = "" Then
                    Else

                        If txtweight.Text = "" Then
                        Else
                            If txtage.Text = "" Then
                            Else
                                computeBMI()
                                computeRv()
                                computeBSA()
                                computeBSI()
                                computeRVBMI()
                                computeRVBSA()
                                computeRVBSI()
                            End If
                        End If
                    End If
                End If
            End If
        End If

    End Sub

    Private Sub txtrv_TextChanged(ByVal sender As System.Object, ByVal e
As System.EventArgs)


        If txtrl.Text = "" Then
        Else
            If txtRT.Text = "" Then
            Else
                If txtRw.Text = "" Then
                Else
                    If txtheight.Text = "" Then
                    Else

                        If txtweight.Text = "" Then
                        Else
                            If txtage.Text = "" Then
                            Else
                                computeBMI()
                                computeRv()
                                computeBSA()
                                computeBSI()
                                computeRVBMI()
                                computeRVBSA()
```

```
                                computeRVBSI()
                            End If
                        End If
                    End If
                End If
            End If
        End If

    End Sub

    Private Sub txtrvbmi_TextChanged(ByVal sender As System.Object, ByVal
e As System.EventArgs) Handles txtrvbmi.TextChanged
        '    computeRVBMI()
    End Sub

    Private Sub txtbsi_TextChanged(ByVal sender As System.Object, ByVal e
As System.EventArgs) Handles txtbsi.TextChanged
        computeRVBSI()
    End Sub

    Private Sub txtbsa_TextChanged(ByVal sender As System.Object, ByVal e
As System.EventArgs) Handles txtbsa.TextChanged
        computeRVBSA()
    End Sub

    Private Sub cborvbmiprecision_SelectedIndexChanged(ByVal sender As
System.Object, ByVal e As System.EventArgs)

    End Sub

    Public Sub changeprecisionbmi()
        '  If Val(cbobmiprecision.Text) = 2 Then
        'txtbmi.Text = Format(txtbmi.Text, "0.00")
        '    Else
        '   If Val(cbobmiprecision.Text) = 3 Then
        'txtbmi.Text = Format(txtbmi.Text, "0.000")
        '    End If
        '    End If
    End Sub

    Private Sub cbobmiprecision_SelectedIndexChanged(ByVal sender As
System.Object, ByVal e As System.EventArgs)

    End Sub

    Private Sub cbobmiprecision_TextChanged(ByVal sender As Object, ByVal
e As System.EventArgs)
        changeprecisionbmi()
    End Sub

    Private Sub cmdcl_Click(ByVal sender As System.Object, ByVal e As
System.EventArgs) Handles cmdcl.Click


        txtheight.Text = ""
        txtrl.Text = ""
        txtRT.Text = ""
        txtRw.Text = ""

        txtage.Text = ""
        txtrv.Text = ""
        txtweight.Text = ""
```

```
        txtbmi.Text = ""
        txtbsa.Text = ""
        txtbsi.Text = ""
        txtrvbmi.Text = ""
        txtrvbsa.Text = ""
        txtrvbsi.Text = ""
        txtbmi.Text = ""
        cbosex.Text = ""
    End Sub

    Private Sub cbosex_TextChanged(ByVal sender As Object, ByVal e As
System.EventArgs) Handles cbosex.TextChanged

    End Sub
End Class
```

Dose Optimisation Interface

```
Public Class DOSEOPTIMIZATIONINTERFACE
    Dim CTDIvol, mAs, age, DLP, gen, RD, E, SNRRD, SNRE
    Private Sub DOSEOPTIMIZATIONINTERFACE_Load(ByVal sender As
System.Object, ByVal e As System.EventArgs) Handles MyBase.Load

    End Sub
    Public Sub computeCTDIvol()

        mAs = Val(txtmAs.Text)

        CTDIvol = (0.21 * mAs) - 3.05
        txtCTDLvol.Text = Format(CTDIvol, "0.00")

    End Sub
    Public Sub computeDLP()

        mAs = Val(txtmAs.Text)

        DLP = (27.6 * mAs) - 240.06
        txtdlp.Text = Format(DLP, "0.00")

    End Sub
    Public Sub computeE()

        age = Val(txtage.Text)

        DLP = Val(txtdlp.Text)

        If age < 10 Then
            E = 0.0253 * DLP
        Else
            If age > 10 Then
                E = 0.0153 * DLP
            End If
        End If

        txtE.Text = Format(E, "0.00")

    End Sub

    Public Sub computeRD()

        gen = cbosex.Text
        E = Val(txtE.Text)
```

```
        If gen = "M" Then 'Male RV calculation

'*************************************************************
            RD = (0.0243 * E) + 0.29
            txtRD.Text = Format(RD, "0.00")
            '*************************************************************
        Else

            If gen = "F" Then 'Female RV calculation

'*************************************************************
                RD = (0.0224 * E) + 0.39
                txtRD.Text = Format(RD, "0.00")

'*************************************************************
            End If
        End If
    End Sub

    Public Sub computeSRNRD()

        gen = cbosex.Text
        RD = Val(txtRD.Text)



'*************************************************************
        SNRRD = (0.144 * RD) + 6.83
        txtsnrrd.Text = Format(SNRRD, "0.00")


    End Sub
    Public Sub computeSRNE()

        gen = cbosex.Text
        E = Val(txtE.Text)



'*************************************************************
        SNRE = (0.0075 * E) + 7.1
        txtsnre.Text = Format(SNRE, "0.00")

    End Sub

    Private Sub txtkVp_KeyPress(ByVal sender As Object, ByVal e As
System.Windows.Forms.KeyPressEventArgs) Handles txtkVp.KeyPress
        If e.KeyChar = "."c Or e.KeyChar = "-"c Then
            e.Handled = (CType(sender, TextBox).Text.IndexOf("."c) <> -1)
            e.Handled = (CType(sender, TextBox).Text.IndexOf("-"c) <> -1)
        ElseIf e.KeyChar <> ControlChars.Back Then
            e.Handled = ("0123456789".IndexOf(e.KeyChar) = -1)
            If txtkVp.Text.IndexOf(".") <> -1 Then
                If txtkVp.Text.Length >= txtkVp.Text.IndexOf(".") + 3 Then
'replace 2 for greater numbers after decimal point
                    e.Handled = True
                End If
            End If
        End If
    End Sub
```

```
    Private Sub txtkVp_TextChanged(ByVal sender As System.Object, ByVal e
As System.EventArgs) Handles txtkVp.TextChanged
        computeCTDIvol()
    End Sub

    Private Sub txtmAs_KeyPress(ByVal sender As Object, ByVal e As
System.Windows.Forms.KeyPressEventArgs) Handles txtmAs.KeyPress
        If e.KeyChar = "."c Or e.KeyChar = "-"c Then
            e.Handled = (CType(sender, TextBox).Text.IndexOf("."c) <> -1)
            e.Handled = (CType(sender, TextBox).Text.IndexOf("-"c) <> -1)
        ElseIf e.KeyChar <> ControlChars.Back Then
            e.Handled = ("0123456789".IndexOf(e.KeyChar) = -1)
            If txtmAs.Text.IndexOf(".") <> -1 Then
                If txtmAs.Text.Length >= txtmAs.Text.IndexOf(".") + 3 Then
'replace 2 for greater numbers after decimal point
                    e.Handled = True
                End If
            End If
        End If
    End Sub

    Private Sub txtmAs_TextChanged(ByVal sender As System.Object, ByVal e
As System.EventArgs) Handles txtmAs.TextChanged
        computeCTDIvol()
    End Sub

    Private    Sub    cbosex_SelectedIndexChanged(ByVal    sender    As
System.Object,     ByVal     e     As     System.EventArgs)     Handles
cbosex.SelectedIndexChanged

        If txtage.Text = "" Then
        Else
            If txtkVp.Text = "" Then
            Else
                If txtmAs.Text = "" Then
                Else


                                computeCTDIvol()
                                computeDLP()
                                computeE()
                                computeRD()
                            End If
                        End If
                    End If
    End Sub

    Private Sub txtage_TextChanged(ByVal sender As System.Object, ByVal e
As System.EventArgs) Handles txtage.TextChanged
        computeCTDIvol()
        computeDLP()
        computeE()
        computeRD()
    End Sub

    Private  Sub  txtCTDLvol_TextChanged(ByVal  sender  As  System.Object,
ByVal e As System.EventArgs) Handles txtCTDLvol.TextChanged
        computeCTDIvol()
        computeDLP()
        computeE()
        computeRD()
    End Sub
```

```
    Private Sub txtdlp_TextChanged(ByVal sender As System.Object, ByVal e
As System.EventArgs) Handles txtdlp.TextChanged
        computeCTDIvol()
        computeDLP()
        computeE()
        computeRD()
    End Sub

    Private Sub txtE_TextChanged(ByVal sender As System.Object, ByVal e
As System.EventArgs) Handles txtE.TextChanged
        computeCTDIvol()
        computeDLP()
        computeE()
        computeRD()
    End Sub

    Private Sub txtRD_TextChanged(ByVal sender As System.Object, ByVal e
As System.EventArgs) Handles txtRD.TextChanged
        computeSRNRD()
        computeSRNE()
    End Sub

    Private Sub cmdcl_Click(ByVal sender As System.Object, ByVal e As
System.EventArgs) Handles cmdcl.Click

        txtage.Text = ""

        txtCTDLvol.Text = ""
        txtdlp.Text = ""
        txtE.Text = ""
        txtRD.Text = ""
        txtsnre.Text = ""
        txtsnrrd.Text = ""
    End Sub
End Class
```

APPENDIX B

PRIMARY RAW DATA FORM A:

Measurements of Weight, Height, BMI, BSA and BSI

Patient ID	Age years	Sex M/F	W Kg	H cm	PATIENT COMMENTS	BMI kg/m^3	BSA m^2	BSI kg/m^2
KB-6	44	M	60.1	168	BLADDER CA	21.26	1.68	35.77
KB-7	63	M	76.9	174	GL IVEC	25.4	1.92	40.05
KB-10	38	M	68.3	187	BLADDER CA	19.53	1.92	35.57
KB-26	40	M	71.9	182	PANCREAS	21.71	1.92	37.45
KB-28	58	M	93.8	189	TUMOR	26.26	2.21	42.44
KB-31	80	M	110	192	HUGE MASS	29.83	2.4	45.83
KB-34	37	M	105.6	187	ABD PAINS	30.2	2.31	45.71
KB-35	28	M	100.5	189	ABD MALIGN	28.14	2.28	44.08
KB-36	78	M	71.2	183	MALIGNANCY	21.26	1.92	37.08
KB-37	32	M	69.2	177	MASS	22.09	2.15	32.19
KB-38	40	M	73.7	175	LT. SCROTUM	24.07	1.89	39
KB-40	74	M	89.5	185	UROLITHIASES	26.15	2.24	39.95
KB-42	22	M	56.5	167	CA	20.26	2.08	27.16
KB-46	20	M	100.1	186	ASCITES	28.93	2.25	44.49
KB-47	37	M	72.8	175	PANCREAS	23.77	2.15	33.86
KB-54	25	M	77.5	181	HYDRONE	26.66	2.21	35.07
KB-55	66	M	92.8	187	PANCREAS	26.3	2.26	41.06
KB-56	44	M	79	182	CA PROSTATE	23.85	2.21	35.75
KB-57	33	M	55.8	173	A. PANCREAS	18.64	2.13	26.2
KB-58	37	M	110	192	CA	29.83	2.4	45.83
KB-61	76	M	80.2	177	ABD PAIN	25.6	1.97	40.71
KB-63	47	M	73	182	MALIGNANCY	22.04	1.94	37.63
KB-65	78	M	89.2	178	M CA	28.15	2.11	42.28
KB-66	34	M	81.8	180	MASS	25.25	2.09	39.14
KB-71	69	M	92.6	185	P CA	27.06	2.13	43.47
KB-73	70	M	89.1	195	METASTASIS	23.43	2.22	40.14
KB-78	35	M	72.5	169	M CA	25.38	1.83	39.62
KB-79	52	M	105.6	191	HEPATOMEGALY	28.5	2.35	44.94
KB-83	62	M	98.6	178	ENDOMETRIA	31.12	2.16	45.65
KB-87	32	M	93.7	174	CA IVU	30.95	2.08	45.05
KB-88	36	M	89.2	188	MASS	25.24	2.16	41.3
KB-89	54	M	88.8	186	METS	25.67	2.14	41.5
KB-90	80	M	95.6	180	MALIGNANCY	29.51	2.15	44.47
KB-91	74	M	59.9	166	MASS	21.74	1.67	35.87
KB-92	37	M	89	187	TUMOR	25.45	2.15	41.4
KB-94	50	M	102.1	185	DUODENUM	29.83	2.26	45.18
KB-96	35	M	75.8	167	MASS	27.18	1.85	40.97
KB-97	46	M	76.5	176	JAUNDICE	24.7	1.93	39.64
KB-99	26	M	78	176	GASTRIC CA	25.18	1.94	40.21
KB-100	28	M	58	164	MALIGNANCY	21.56	1.63	35.58
KB-101	74	M	60.1	178	ASCITES	18.97	1.75	34.34
KB-102	28	M	80.2	172	CA STOMACH	27.11	1.93	41.55
KB-104	69	M	69.5	170	CT IVU	24.05	1.8	38.61
KB-105	56	M	88	189	JAUNDICE	24.64	2.15	40.93
KB-106	26	M	70.9	169	STONE	24.82	1.81	39.17
KB-41	75	F	71.9	176	CA CERVIX	23.21	1.88	38.25
KB-43	33	F	67.9	173	OBST. JAU	22.68	1.81	37.51
KB-44	40	F	65.8	167	TRAUMA	22.5	1.72	38.26
KB-45	59	F	59.7	165	MASS	21.75	1.65	36.18

KB-48	66	F	59.2	163	CA CERVIX	22.28	1.56	37.95
KB-49	70	F	60.1	166	ABD PAINS	21.81	1.67	35.99
KB-50	51	F	56.5	158	TRAUMA	22.63	1.57	35.99
KB-51	60	F	65.8	165	CA STOMACH	24.17	1.73	38.04
KB-52	65	F	58.8	169	LIVER MASS	20.59	1.67	35.21
KB-53	50	F	55.8	165	MASS	20.5	1.61	34.66
KB-59	45	F	61.9	178	WILMS'S TUM	19.54	1.78	34.78
KB-60	70	F	56.9	168	HEPATOMA	20.16	1.65	34.49
KB-62	78	F	55.5	163	PANCREAS	20.89	1.59	34.91
KB-64	25	F	68.3	168	ABD PAINS	24.2	1.78	38.37
KB-67	80	F	65.5	170	CA PANCREAS	22.66	1.76	37.22
KB-68	72	F	55.8	167	OVARIAN CA	20.01	1.62	34.44
KB-69	58	F	65.4	178	CA RECTUM	20.64	1.82	35.93
KB-70	48	F	55.8	158	MALIGN.	22.35	1.56	35.77
KB-72	40	F	79	182	L. MASS	23.85	2	39.5
KB-74	39	F	48.6	159	OVARIAN TU	19.22	1.47	33.06
KB-75	52	F	63.7	164	KOCK'S	23.68	1.69	37.69
KB-76	55	F	63.2	167	CA STOMACH	22.66	1.71	36.9
KB-77	60	F	61.2	169	MASS	21.42	1.7	36
KB-80	65	F	52.3	156	PELVIC M	21.49	1.5	34.87
KB-81	53	F	50.6	155	ILIAC MASS	23.68	1.62	31.24
KB-82	49	F	61.5	168	OVAR CA	21.79	1.7	36.18
KB-84	34	F	73.8	164	GASTRIC M	24.77	1.8	41
KB-85	45	F	59.1	160	CT IVU	23.09	1.61	36.76
KB-86	75	F	56.5	161	RECTA CA M	21.8	1.59	35.54
KB-93	80	F	50.8	157	MALIGNANCY	20.61	1.49	34.09
KB-95	53	F	55.8	165	HEPATECEL	20.5	1.61	34.66
KB-98	80	F	70.5	189	GASTRIC CA	19.48	1.61	43.79
KB-103	75	F	59	160	OVARIAN CA	20.23	1.52	38.82
KB-107	58	F	81.9	176	BL. TUMOR	22.64	1.55	52.84
KB-109	44	F	53	159	OBST. IO	20.96	1.53	34.64
KB-111	72	F	55.8	161	MALIGN.	21.53	1.58	35.32
KB-112	36	F	70.5	189	LYMPHOMA	19.5	1.61	43.79
KB-113	72	F	60.1	164	MASS	22.35	1.65	36.42
KB-119	47	F	65.9	177	JAUNDICE	21.04	1.82	36.21
KB-121	80	F	56.9	159	ABD MASS	22.51	1.58	36.01
KB-123	40	F	57.8	161	CA STOMACH	22.3	1.6	36.13
KB-124	77	F	65.1	172	LYMPHOMA	22.01	1.62	40.19
KB-125	73	F	55.5	165	PANCREAS	20.39	1.61	34.47
KB-126	37	F	60.1	162	CA OVARY	22.9	1.64	36.65
KB-132	53	F	56.9	164	JAUNDICE	21.15	1.62	35.12
KB-133	46	F	57.8	167	DISTENSION	20.73	1.65	35.03
KB-135	58	F	65.1	172	UROLITHIA	22.01	1.77	36.78
TT-81	40	F	71.9	176	CA CERVIX	23.21	1.88	38.25
TT-82	43	F	67.9	173	OBST. JAU	22.68	1.81	37.51
TT-83	80	F	65.8	167	TRAUMA	22.5	1.72	38.26
TT-84	53	F	59.7	165	MASS	21.75	1.65	36.18
TT-90	76	F	59.2	163	CA CERVIX	22.28	1.56	37.95
TT-91	20	F	60.1	166	ABD PAINS	21.81	1.67	35.99
TT-95	54	F	56.5	158	TRAUMA	22.63	1.57	35.99
TT-98	65	F	65.8	165	CA STOMACH	24.17	1.73	38.04
TT-100	48	F	58.8	169	LIVER MASS	20.59	1.67	35.21

APPENDIX C

SECONDARY PROCESS DATA FORM B:

Measurements of renal dimensions

Patient ID	A-P_R mm	A-P_L mm	LT_R mm	LT_L mm	LNG_R mm	LNG_L mm	RRRL	LRRL
KB-6	44.1	47	71.3	76.8	104.5	91.9	0.532077	0.467923
KB-7	43.1	44.2	55.1	53.9	96.8	96.7	0.500258	0.499742
KB-10	47.9	46.3	62.6	61.2	103.1	116.2	0.470132	0.529868
KB-26	48.5	44.8	53.2	58.9	105.4	97.8	0.518701	0.481299
KB-28	41.9	42.7	55.7	54.7	105.4	95.8	0.523857	0.476143
KB-31	42.9	43.2	62.3	50.6	96.9	109.7	0.469022	0.530978
KB-34	62.9	61.7	67.2	73	85.9	98.3	0.466341	0.533659
KB-35	46.3	42.6	60.4	63.5	124.8	124.6	0.500401	0.499599
KB-36	45	47.4	58.5	58.8	96.1	97.2	0.497155	0.502845
KB-37	43.3	46.5	65.8	66.9	116.1	117.5	0.497003	0.502997
KB-38	47.3	53.4	62.7	54.8	97.6	100.4	0.492929	0.507071
KB-40	50.8	54.5	66.3	56.3	106.9	106.8	0.500234	0.499766
KB-42	41.7	41	57	59.3	101.1	109.1	0.480971	0.519029
KB-46	41.8	40.1	57.6	55.5	91.6	106.4	0.462626	0.537374
KB-47	45.1	61.2	63.1	57.9	108.8	100.7	0.519332	0.480668
KB-54	58.9	54.6	61.2	63.8	87.7	88.5	0.49773	0.50227
KB-55	50.4	45.3	58.6	55.6	119.3	108.3	0.524165	0.475835
KB-56	45.5	48	53.2	52.5	95.1	109	0.465948	0.534052
KB-57	50.7	46.1	64.5	67.7	87	89.3	0.493477	0.506523
KB-58	52.2	54.3	64.6	66.1	118.4	113.4	0.510785	0.489215
KB-61	36.7	26.7	57.3	61.7	95	97.8	0.492739	0.507261
KB-63	37.6	38.5	51.5	47.8	109.9	105	0.511401	0.488599
KB-65	53.7	47.1	49.3	51.7	88.9	83.6	0.515362	0.484638
KB-66	47.8	51.6	59.4	59.5	105.9	102.2	0.50889	0.49111
KB-71	45.6	51.3	64.9	61.7	110.3	101.7	0.520283	0.479717
KB-73	36.8	38.3	53.8	51.7	117	101.5	0.535469	0.464531
KB-78	46.2	55.1	64.4	59.9	101.6	103.6	0.495127	0.504873
KB-79	42.7	48.7	58.8	51.2	93.2	100.8	0.480412	0.519588
KB-83	45.8	47.2	57.2	49	84.2	92	0.477866	0.522134
KB-87	51.3	53.3	68.8	65.2	115.9	109.5	0.514197	0.485803
KB-88	63.9	62.7	75.5	67.7	124.7	126.4	0.496615	0.503385
KB-89	43.3	49.4	64.7	64.9	102.3	119.5	0.461226	0.538774
KB-90	43.2	44.8	62.4	56.3	96.5	96.5	0.5	0.5
KB-91	49.5	50.1	54.9	50.2	95.2	103.2	0.479839	0.520161
KB-92	41.3	39.1	51.5	52.4	87.7	89.1	0.496041	0.503959
KB-94	45.5	46.3	60.8	54.6	99.5	98.3	0.503033	0.496967
KB-96	51.3	45.8	58.9	56.8	107.6	119.8	0.473175	0.526825
KB-97	48.4	47.5	61.7	53.1	106.7	86.7	0.551706	0.448294
KB-99	59.3	55.5	63.2	60.4	98.5	101.5	0.4925	0.5075
KB-100	41.1	44.5	57	51.3	89.4	95.3	0.484028	0.515972
KB-101	42.3	59.1	50.1	47.9	100.4	97.2	0.508097	0.491903

KB-102	42.8	43.2	57	48.1	92.2	102	0.474768	0.525232
KB-104	45.3	41.4	57.2	51.2	102.3	119.2	0.461851	0.538149
KB-105	54.1	59.5	58.3	62.6	89	93.5	0.487671	0.512329
KB-106	42.3	49.2	58.5	59.9	100.4	102.2	0.495558	0.504442
KB-108	31.9	31.9	50.1	50.8	86.6	87.7	0.496845	0.503155
KB-110	58.3	50.4	60.8	58	102.6	113.6	0.474561	0.525439
KB-114	54.2	55.5	57.2	58.2	110.2	111.4	0.497292	0.502708
KB-115	52.4	55.3	68.2	61.5	109.4	108.3	0.502526	0.497474
KB-116	53.2	45.5	69	56.4	108.3	103.2	0.512057	0.487943
KB-117	46.2	50.2	66.9	62.2	108.5	120.8	0.473179	0.526821
KB-118	44.6	47	62.3	60.6	116.2	106.7	0.52131	0.47869
KB-120	46.7	52.9	64.9	62	114.4	121.6	0.484746	0.515254
KB-122	52.9	52.8	60.1	58.5	124.1	126.6	0.495014	0.504986
KB-127	44.2	48.9	60	58	104.2	111.3	0.483527	0.516473
KB-128	41.4	43.2	50.4	53.3	107.8	106.4	0.503268	0.496732
KB-129	43.8	45.9	52	51.6	86	96	0.472527	0.527473
KB-130	57.2	57.4	65.1	65.1	93.9	111	0.458272	0.541728
KB-131	39.8	39.9	56.8	48.8	94.8	96.6	0.495298	0.504702
KB-134	47.5	49.5	56.1	49.9	114.3	107.1	0.51626	0.48374
KB-137	50.4	57.7	64.5	72	118.3	75.3	0.611054	0.388946
KB-139	49.3	50.9	59.8	62.7	102.9	113.6	0.475289	0.524711
KB-140	58.2	53.8	63.8	62.8	102.8	111.8	0.479031	0.520969
KB-141	55.6	51.9	60.3	60.3	96.4	85.9	0.528799	0.471201
KB-142	43.4	43.1	54.2	54.8	93.7	102.9	0.476602	0.523398
KB-144	46.3	51.9	56.3	54.5	90.2	96.6	0.482869	0.517131
KB-146	48.3	56.9	65.6	64.7	112.8	88.4	0.560636	0.439364
KB-148	50.7	59.4	60.6	63.9	106.5	110.7	0.490331	0.509669
KB-151	50.6	55.9	59.3	57.4	101.6	107.2	0.48659	0.51341
KB-152	48.9	55.3	68.7	71.8	112.7	107.5	0.511807	0.488193
KB-156	42.3	45.2	58.5	59.9	109.4	102.2	0.517013	0.482987
KB-158	38.9	39.9	56.1	57.8	92.6	92.7	0.49973	0.50027
KB-160	42.3	42.4	64.8	64	112.6	113.6	0.49779	0.50221
KB-164	44.2	45.5	57.2	58.2	110.2	111.4	0.497292	0.502708
KB-165	43.2	44.5	66	64.4	108.3	116.2	0.482405	0.517595
KB-166	44.2	44.8	64.9	65.2	108.5	110.8	0.494756	0.505244
KB-167	44.6	44.8	62.3	63.6	116.2	116.7	0.498927	0.501073
KB-169	41.7	42.9	64.9	62.8	114.4	121.6	0.484746	0.515254
TT-83	42.8	52.5	60.3	51.5	94.4	75.3	0.498789	0.511111
TT-84	41	46.5	64	57	102.9	105.2	0.499001	0.505679
TT-90	45.9	45.4	56.7	64.8	97.5	99.5	0.509871	0.499789
TT-91	48.5	42.9	60.1	66	106.3	106.4	0.501253	0.489999
TT-95	43.6	42.9	59.9	60.9	96.8	97.9	0.511621	0.500008
TT-98	39.1	48.1	57.9	57.1	102.1	106.2	0.510097	0.499677
TT-100	49.7	47.2	55.4	58.4	106.7	108	0.49999	0.511187

APPENDIX D

SECONDARY PROCESS DATA FORM C:

Estimated renal parameters

Patient ID	RV_R mL^3	RV_L mL^3	VeC_R	VeC_L	RSI_R	RSI_L	RSA_R cm^2	RSA_L cm2
KB-6	172.5715	173.1457	0.5252	0.52196	0.94	0.79	34.6898	34.4984
KB-7	124.7568	126.746	0.5427	0.55017	1.02	1.01	25.0868	25.488
KB-10	165.0549	170.4907	0.5339	0.5178	0.96	1.05	32.925	34.01
KB-26	149.8978	142.6851	0.5512	0.5529	1	0.93	30.1634	28.7162
KB-28	137.8774	126.9676	0.5605	0.56743	0.99	1	27.745	25.545
KB-31	135.0719	135.8585	0.5216	0.56656	0.96	1.05	27.071	26.917
KB-34	185.5385	229.7445	0.511	0.5189	0.79	0.77	37.254	46.137
KB-35	192.4278	190.6723	0.5514	0.5657	1.06	1.05	38.2578	37.9092
KB-36	143.5452	146.4692	0.5674	0.54066	0.95	0.98	28.8952	29.4804
KB-37	173.8408	192.0979	0.5255	0.52554	1.05	1.01	34.9641	39.7606
KB-38	149.2132	149.9597	0.5155	0.51041	0.97	0.95	30.0294	30.1433
KB-40	178.7364	174.7787	0.4964	0.53335	0.98	1.01	35.6346	34.8462
KB-42	132.9245	147.3756	0.5532	0.5556	1.01	1.01	26.5106	29.3938
KB-46	107.8458	134.7715	0.489	0.5691	0.98	1.03	21.441	26.796
KB-47	181.3159	201.5724	0.5856	0.5649	1	0.9	36.136	40.168
KB-54	168.8137	170.4216	0.534	0.5528	0.79	0.89	33.969	34.2973
KB-55	205.664	155.9607	0.5837	0.57176	1.05	1.05	41.1312	31.1904
KB-56	119.2938	152.9171	0.5182	0.5567	1	1.04	23.933	30.68
KB-57	142.371	165.9451	0.50042	0.59542	0.89	0.89	27.2118	32.3796
KB-58	209.052	216.5746	0.5236	0.5321	1	0.97	32.7327	35.0805
KB-61	106.1053	94.72902	0.53112	0.58796	1.25	1.27	9.0664	10.178
KB-63	108.5333	108.77	0.51	0.5629	1.06	1.02	21.8688	21.9136
KB-65	140.1279	119.171	0.59539	0.5854	0.9	0.9	28.176	23.968
KB-66	170.6111	167.656	0.56741	0.53432	1	0.9	34.038	33.4463
KB-71	175.4672	174.0942	0.53754	0.54083	1	0.95	35.005	17.365
KB-73	123.7242	114.4789	0.53412	0.5696	1.23	1.01	24.5994	22.7598
KB-78	168.1328	185.1897	0.5562	0.5416	0.94	0.95	33.4278	36.9474
KB-79	121.6581	137.8844	0.5199	0.5486	0.95	1.05	24.1878	27.4134
KB-83	115.1889	116.9638	0.5222	0.5497	0.87	1	23.0469	23.4039
KB-87	208.3353	201.3384	0.5093	0.5291	1	0.96	43.9641	42.4878
KB-88	311.9944	272.9386	0.5186	0.5087	0.95	1	62.077	54.303
KB-89	155.7928	193.5926	0.5436	0.5053	1	1.1	30.9876	38.4993
KB-90	136.3618	128.7566	0.5242	0.529	0.97	1	27.111	25.599
KB-91	137.8928	143.8686	0.533	0.5543	0.94	1.01	27.4134	28.602
KB-92	103.7313	105.4418	0.5561	0.5776	1	1	20.4384	20.7792
KB-94	143.051	134.6872	0.5197	0.542	0.95	1	28.576	26.9028
KB-96	183.3682	177.9536	0.564	0.571	1	1.05	36.57	35.4941
KB-97	174.6763	115.9218	0.5482	0.5301	0.98	0.96	30.372	23.34
KB-99	185.3524	184.5167	0.5021	0.5423	0.88	0.98	37.2008	37.0328
KB-100	114.1853	123.6369	0.5452	0.5683	0.98	1	22.701	24.5826
KB-101	114.1728	143.6623	0.5366	0.5221	1.1	0.98	22.7741	28.6571
KB-102	118.9661	120.3864	0.5289	0.568	0.97	1.01	23.688	23.968
KB-104	146.3218	141.7708	0.552	0.5611	1	1.25	29.0892	28.1862
KB-105	153.4634	185.5526	0.5467	0.5328	0.88	0.87	30.6952	37.1429
KB-106	137.4148	157.0112	0.5531	0.5213	1	0.95	27.3168	31.2186
KB-108	76.38475	77.85312	0.5519	0.5478	1.01	1.06	15.1872	15.477
KB-110	202.9698	196.8544	0.5581	0.5928	0.98	1.01	40.7212	39.494
KB-114	191.6637	198.9517	0.561	0.5529	1	1	39.2245	40.7141
KB-115	206.0362	196.2793	0.527	0.5329	0.96	0.97	41.0524	39.1094
KB-116	224.9722	140.5463	0.5659	0.5307	0.95	1	44.7944	27.9832
KB-117	179.9151	194.5173	0.5365	0.5157	1	1.01	36.1893	39.1134
KB-118	166.1171	170.1553	0.5145	0.5599	1.05	0.98	33.42	34.235
KB-120	189.1396	207.7074	0.5455	0.5208	1	1.01	37.6826	41.383

KB-122	211.9917	215.3469	0.5373	0.5507	1.07	1.01	42.2072	42.8792
KB-127	154.4732	175.4173	0.559	0.5557	1	1.05	31.08	35.295
KB-128	126.5013	134.5253	0.5624	0.5491	1.01	1.01	24.932	27.002
KB-129	105.8501	117.6186	0.5404	0.5173	0.96	1	21.0462	23.3814
KB-130	186.3324	214.3988	0.5329	0.5169	0.87	0.99	37.1697	42.7614
KB-131	109.1688	104.8236	0.5094	0.5573	1.07	1.01	22.0027	21.1243
KB-134	157.1333	147.3501	0.5159	0.557	1.06	1.05	31.35	29.395
KB-137	195.0922	170.9283	0.5073	0.5464	1	0.69	39.1404	34.294
KB-139	168.3971	190.3369	0.5551	0.525	0.98	1	33.462	37.8235
KB-140	211.4689	205.2218	0.554	0.5433	0.87	0.97	49.4004	40.7988
KB-141	165.0897	146.4317	0.5108	0.5447	0.88	0.8	32.9289	29.2068
KB-142	120.3872	136.4412	0.5462	0.5614	1	1.01	24.2622	27.5292
KB-144	119.9835	150.0076	0.5103	0.549	0.97	0.99	24.233	30.2995
KB-146	186.5652	174.0119	0.522	0.5347	1	0.79	37.22	34.72
KB-148	184.5807	217.9892	0.5641	0.5188	1	0.95	42.0087	43.6152
KB-151	162.3069	191.9343	0.5324	0.558	0.97	1	32.6388	32.6388
KB-152	200.1321	222.6788	0.5286	0.5217	1	0.9	40.2584	44.7909
KB-156	139.9601	141.7834	0.517	0.5124	0.95	0.97	27.8292	28.1862
KB-158	107.8299	110.549	0.5336	0.5171	1.03	1.03	31.9872	32.277
KB-160	160.8946	162.3632	0.5213	0.5267	0.95	0.91	25.9672	29.7584
KB-164	138.5816	149.4462	0.4974	0.5066	0.99	0.96	32.3703	32.5869
KB-165	157.1715	177.9917	0.509	0.5345	0.99	0.97	33.624	35.0832
KB-166	169.035	170.0741	0.5431	0.5255	1	0.99	32.9324	33.8894
KB-167	167.0212	170.2124	0.5173	0.5119	1.09	1.07	33.5944	34.16
KB-169	161.7372	168.8476	0.5224	0.5154	0.92	0.91	33.42	34.235
KB-219	121.6605	135.7044	0.5099	0.5059	1.07	1.15	28.8952	29.4804
KB-220	138.3503	180.1025	0.5267	0.5154	0.9	0.89	34.9641	39.7606
KB-222	106.1876	119.4305	0.4938	0.5295	1.11	1.11	30.0294	30.1433
KB-225	155.535	152.5756	0.5401	0.5382	1.06	1.08	35.6346	34.8462
KB-228	168.4936	172.2714	0.5167	0.5335	0.94	1.09	26.5106	29.3938
KB-229	144.2926	148.5589	0.514	0.5428	0.89	1.02	21.441	26.796
KB-230	151.6148	165.5055	0.5138	0.5446	0.99	1.04	36.136	40.168
KB-232	173.5589	168.4432	0.5187	0.5208	1.09	1.07	33.969	34.2973
KB-234	116.3427	118.1618	0.5091	0.5314	0.94	0.99	41.1312	31.1904
KB-239	141.3747	140.4228	0.5116	0.5207	1.04	1.05	23.933	30.68
KB-240	136.6132	145.7986	0.5068	0.5011	1.04	1.1	27.2118	32.3796
KB-241	134.9847	143.4031	0.5026	0.5082	1	1.05	32.7327	35.0805
KB-242	145.9377	179.9928	0.5058	0.5255	1.13	1.06	9.0664	10.178
KB-243	130.7018	164.4603	0.5013	0.5108	0.88	0.87	21.8688	21.9136
KB-246	104.1024	149.7345	0.5034	0.5245	0.97	1	28.176	23.968
KB-247	153.9452	146.5045	0.5227	0.5029	1.1	1.02	34.038	33.4463
KB-248	165.7451	161.7871	0.5243	0.5261	1.15	1.09	35.005	17.365
KB-250	137.9155	113.3126	0.5203	0.5221	0.93	1.14	24.5994	22.7598
KB-251	128.053	143.0749	0.4999	0.5306	0.96	0.95	33.4278	36.9474
KB-253	100.646	116.7367	0.5043	0.5292	1.02	0.9	24.1878	27.4134
KB-255	160.7373	161.2212	0.5081	0.5316	1	0.97	23.0469	23.4039
KA-1	151.2882	150.0219	0.5245	0.5302	1.03	1.08	43.9641	42.4878
KA-2	181.5191	189.7087	0.5259	0.5325	1.09	1.13	62.077	54.303
KA-3	172.5628	163.4841	0.5304	0.4969	0.98	1.08	30.9876	38.4993
KA-4	114.753	176.4518	0.5417	0.5595	1	1.03	27.111	25.599
KA-5	131.7502	136.5055	0.5201	0.5332	0..93	1.11	27.4134	28.602
KA-7	123.4507	149.5419	0.5235	0.5392	0.95	1.22	20.4384	20.7792
KA-8	139.265	173.2702	0.5433	0.5387	0.97	1.02	28.576	26.9028
KA-10	175.8464	162.451	0.5093	0.5255	1.03	1.11	36.57	35.4941
KA-11	185.7027	196.4368	0.5179	0.5376	1,14	1.15	30.372	23.34

APPENDIX E

SECONDARY PROCESS DATA FORM D

Determination of CTDI, DLP, SNR, E and RD

Patient ID	$CTDI_V$ mGy	DLP mGy-cm	SNR1	SNR2	SNR3	E mSv	$CTDI_W$ mGy	RD mSv
KB-6	4.7	1311.5	9.527273	9.041828	4.693352	20.06595	3.8211	1.947699
KB-7	4.7	468.8	3.58427	3.790169	2.548848	7.17264	3.8211	1.947699
KB-10	5.5	597.6	7.62394	3.859535	4.522313	9.14328	4.4715	2.279222
KB-26	6.7	1128	6.296296	6.73003	5.773821	17.2584	5.4471	2.776507
KB-28	5.7	1331.1	8.0709	7.375546	5.525239	20.36583	4.6341	2.362103
KB-31	4.7	911.4	9.315789	7.190947	4.253671	13.94442	3.8211	1.947699
KB-34	13.5	2975.6	9.848866	7.374534	2.971443	45.52668	10.976	5.594454
KB-35	5.9	935.4	4.905366	1.002193	3.638898	14.31162	4.7967	2.444984
KB-36	5.3	859.2	5.319321	6.98109	3.934609	13.14576	4.3089	2.196341
KB-37	8.7	1413.9	10.58281	7.935919	2.433696	21.63267	7.0731	3.605315
KB-38	7.7	987	10.61444	7.009751	2.793424	15.1011	6.2601	3.190911
KB-40	5.6	942.6	7.383732	8.869666	6.025152	14.42178	4.5528	2.320662
KB-42	5.1	524.8	8.19052	6.358374	4.847047	8.02944	4.1463	2.11346
KB-46	5.3	942.6	12.07609	10.01709	8.57299	14.42178	4.3089	2.196341
KB-47	5.9	935.4	5.050095	4.21519	2.703816	14.31162	4.7967	2.444984
KB-54	9.7	2127.2	7.421365	7.747962	5.786687	32.54616	7.8861	4.019719
KB-55	8.1	1215.9	5.112412	5.961563	9.738104	18.60327	6.5853	3.356672
KB-56	6.5	1038.6	9.527273	9.041828	4.693352	15.89058	5.2845	2.693626
KB-57	15.7	3200	3.58427	3.790169	2.548848	48.96	12.764	6.506143
KB-58	6.3	364.8	7.62394	3.859535	4.522313	5.58144	5.1219	2.610745
KB-61	4.7	703.2	6.296296	6.73003	5.773821	10.75896	3.8211	1.947699
KB-63	7.1	1065.6	8.0709	7.375546	5.525239	16.30368	5.7723	2.942268
KB-65	5	747	9.315789	7.190947	4.253671	11.4291	4.065	2.07202
KB-66	9.2	1389	9.848866	7.374534	2.971443	21.2517	7.4796	3.812517
KB-71	4.7	759	4.905366	1.002193	3.638898	11.6127	3.8211	1.947699
KB-73	5	792.6	5.319321	6.98109	3.934609	12.12678	4.065	2.07202
KB-78	6.2	364.8	10.58281	7.935919	2.433696	5.58144	5.0406	2.569305
KB-79	4.7	234.4	10.61444	7.009751	2.793424	3.58632	3.8211	1.947699
KB-83	4.9	757.2	7.383732	8.869666	6.025152	11.58516	3.9837	2.03058
KB-87	4.8	754.8	8.19052	6.358374	4.847047	11.54844	3.9024	1.989139
KB-88	4.9	744	12.07609	10.01709	8.57299	11.3832	3.9837	2.03058
KB-89	5.7	824.9	5.050095	4.21519	2.703816	12.62097	4.6341	2.362103
KB-90	6	609.9	7.421365	7.747962	5.786687	9.33147	4.878	2.486424
KB-91	4.7	937.6	5.112412	5.961563	9.738104	14.34528	3.8211	1.947699
KB-92	6.2	852.9	9.527273	9.041828	4.693352	13.04937	5.0406	2.569305
KB-94	5.7	1026.3	3.58427	3.790169	2.548848	15.70239	4.6341	2.362103
KB-96	4.7	1590.9	7.62394	3.859535	4.522313	24.34077	3.8211	1.947699
KB-97	6.2	572.6	6.296296	6.73003	5.773821	8.76078	5.0406	2.569305
KB-99	4.9	745.2	8.0709	7.375546	5.525239	11.40156	3.9837	2.03058
KB-100	5.1	915.3	9.315789	7.190947	4.253671	14.00409	4.1463	2.11346
KB-101	6.2	1026	9.848866	7.374534	2.971443	15.6978	5.0406	2.569305
KB-102	4.9	820.2	4.905366	1.002193	3.638898	12.54906	3.9837	2.03058
KB-104	4.7	703.2	5.319321	6.98109	3.934609	10.75896	3.8211	1.947699
KB-105	9.2	1537.2	10.58281	7.935919	2.433696	23.51916	7.4796	3.812517
KB-106	4.7	717	10.61444	7.009751	2.793424	10.9701	3.8211	1.947699
KB-108	5.8	956.1	7.383732	8.869666	6.025152	14.62833	4.7154	2.403543
KB-110	5.9	1042.5	8.19052	6.358374	4.847047	15.95025	4.7967	2.444984
KB-114	5.7	947.1	12.07609	10.01709	8.57299	14.49063	4.6341	2.362103
KB-115	4.9	779.1	5.050095	4.21519	2.703816	11.92023	3.9837	2.03058
KB-116	4.7	739.5	7.421365	7.747962	5.786687	11.31435	3.8211	1.947699
KB-117	6.8	356.4	5.112412	5.961563	9.738104	5.45292	5.5284	2.817947
KB-118	9.7	1553.7	9.527273	9.041828	4.693352	23.77161	7.8861	4.019719

KB-120	6.2	1088.7	3.58427	3.790169	2.548848	16.65711	5.0406	2.569305
KB-122	6	1111.8	7.62394	3.859535	4.522313	17.01054	4.878	2.486424
KB-127	5	1031.2	6.296296	6.73003	5.773821	15.77736	4.065	2.07202
KB-128	5	788.1	8.0709	7.375546	5.525239	12.05793	4.065	2.07202
KB-129	8	1410.6	9.315789	7.190947	4.253671	21.58218	6.504	3.315232
KB-130	5.4	931.4	9.848866	7.374534	2.971443	14.25042	4.3902	2.237782
KB-131	4.9	837.6	4.905366	1.002193	3.638898	12.81528	3.9837	2.03058
KB-134	4.7	703.2	5.319321	6.98109	3.934609	10.75896	3.8211	1.947699
KB-137	9.4	1316.1	10.58281	7.935919	2.433696	20.13633	7.6422	3.895397
KB-139	5.3	828.9	10.61444	7.009751	2.793424	12.68217	4.3089	2.196341
KB-140	7.4	1086.9	7.383732	8.869666	6.025152	16.62957	6.0162	3.066589
KB-141	4.1	860.4	8.19052	6.358374	4.847047	13.16412	3.3333	1.699056
KB-142	5.4	832.5	12.07609	10.01709	8.57299	12.73725	4.3902	2.237782
KB-144	7.1	1163.4	5.050095	4.21519	2.703816	17.80002	5.7723	2.942268
KB-146	9.8	1668	7.421365	7.747962	5.786687	25.5204	7.9674	4.061159
KB-148	4.7	434	5.112412	5.961563	9.738104	6.6402	3.8211	1.947699
KB-151	5	812.4	9.527273	9.041828	4.693352	12.42972	4.065	2.07202
KB-152	5.7	954.5	3.58427	3.790169	2.548848	14.60385	4.6341	2.362103
KB-156	6.1	976.2	7.62394	3.859535	4.522313	14.93586	4.9593	2.527864
KB-158	4.7	468.8	6.296296	6.73003	5.773821	7.17264	3.8211	1.947699
KB-160	4.7	255.2	8.0709	7.375546	5.525239	3.90456	3.8211	1.947699
KB-164	5.5	549.4	9.315789	7.190947	4.253671	8.40582	4.4715	2.279222
KB-165	5.6	838.2	9.848866	7.374534	2.971443	12.82446	4.5528	2.320662
KB-166	5.6	883	4.905366	1.002193	3.638898	13.5099	4.5528	2.320662
KB-167	7.1	376.5	5.319321	6.98109	3.934609	5.76045	5.7723	2.942268
KB-169	6.9	1088.4	10.58281	7.935919	2.433696	16.65252	5.6097	2.859388
KB-171	4.7	836.1	10.61444	7.009751	2.793424	12.79233	3.8211	1.947699
KB-176	5	792.6	7.383732	8.869666	6.025152	12.12678	4.065	2.07202
KB-177	4.8	950	8.19052	6.358374	4.847047	14.535	3.9024	1.989139
KB-178	4.7	765.9	12.07609	10.01709	8.57299	11.71827	3.8211	1.947699
KB-179	3.2	669.6	5.050095	4.21519	2.703816	10.24488	2.6016	1.326093
KB-180	4.7	744.9	7.421365	7.747962	5.786687	11.39697	3.8211	1.947699
KB-183	4.9	780.3	5.112412	5.961563	9.738104	11.93859	3.9837	2.03058
KB-186	4.7	714.3	9.527273	9.041828	4.693352	10.92879	3.8211	1.947699
KB-188	4.8	950.4	3.58427	3.790169	2.548848	14.54112	3.9024	1.989139
KB-189	4.9	792.3	7.62394	3.859535	4.522313	12.12219	3.9837	2.03058
KB-190	4.7	744.9	6.296296	6.73003	5.773821	11.39697	3.8211	1.947699
KB-191	4.9	775.8	8.0709	7.375546	5.525239	11.86974	3.9837	2.03058
KB-193	4.7	744.9	9.315789	7.190947	4.253671	11.39697	3.8211	1.947699
KB-195	4.7	654	9.848866	7.374534	2.971443	10.0062	3.8211	1.947699
KB-197	4.7	703.2	4.905366	1.002193	3.638898	10.75896	3.8211	1.947699
KB-200	4.7	1311.5	5.319321	6.98109	3.934609	20.06595	3.8211	1.947699
KB-201	4.7	468.8	10.58281	7.935919	2.433696	7.17264	3.8211	1.947699
KB-206	5.5	597.6	10.61444	7.009751	2.793424	9.14328	4.4715	2.279222
KB-207	6.7	1128	7.383732	8.869666	6.025152	17.2584	5.4471	2.776507
KB-211	5.7	1331.1	8.19052	6.358374	4.847047	20.36583	4.6341	2.362103
KB-213	4.7	911.4	12.07609	10.01709	8.57299	13.94442	3.8211	1.947699
KB-217	13.5	2975.6	5.050095	4.21519	2.703816	45.52668	10.976	5.594454
KB-218	5.9	935.4	7.421365	7.747962	5.786687	14.31162	4.7967	2.444984
KB-219	5.3	859.2	5.112412	5.961563	9.738104	13.14576	4.3089	2.196341
KB-220	8.7	1413.9	9.527273	9.041828	4.693352	21.63267	7.0731	3.605315
KB-222	7.7	987	3.58427	3.790169	2.548848	15.1011	6.2601	3.190911
KB-225	5.6	942.6	7.62394	3.859535	4.522313	14.42178	4.5528	2.320662
KB-228	5.1	524.8	6.296296	6.73003	5.773821	8.02944	4.1463	2.11346
KB-229	5.3	942.6	8.0709	7.375546	5.525239	14.42178	4.3089	2.196341
KB-230	5.9	935.4	9.315789	7.190947	4.253671	14.31162	4.7967	2.444984

APPENDIX F

ANALYSIS OF BODY PARAMETERS

Appendix F-1: Analysis of mean male and female weight

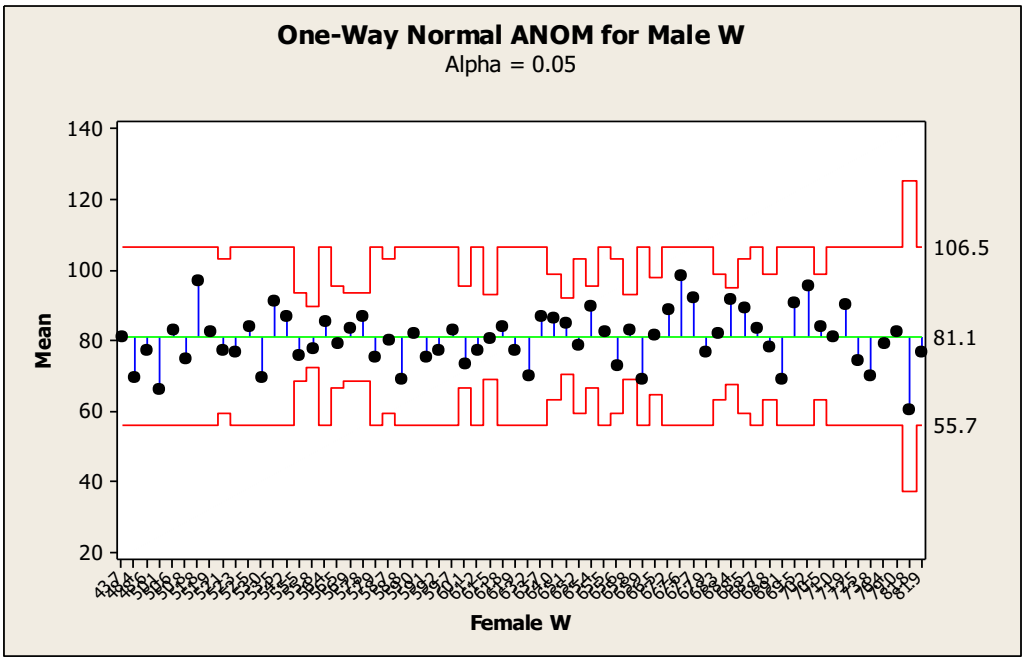

Appendix F-2: Analysis of mean with male and female height

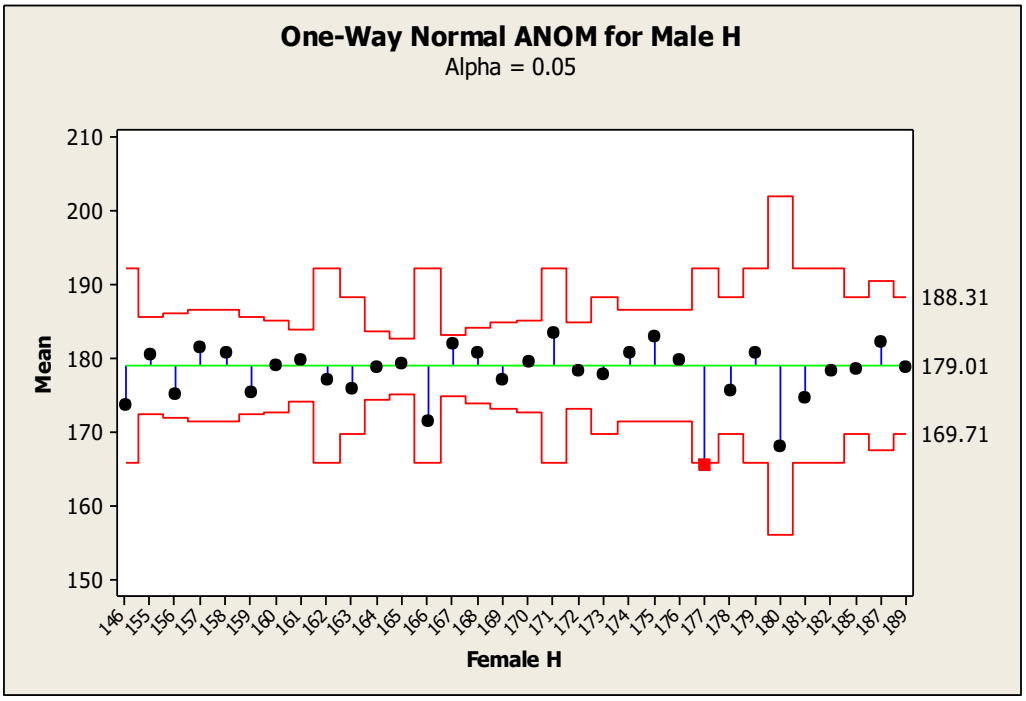

Appendix F-3: Analysis of mean male and female BSI

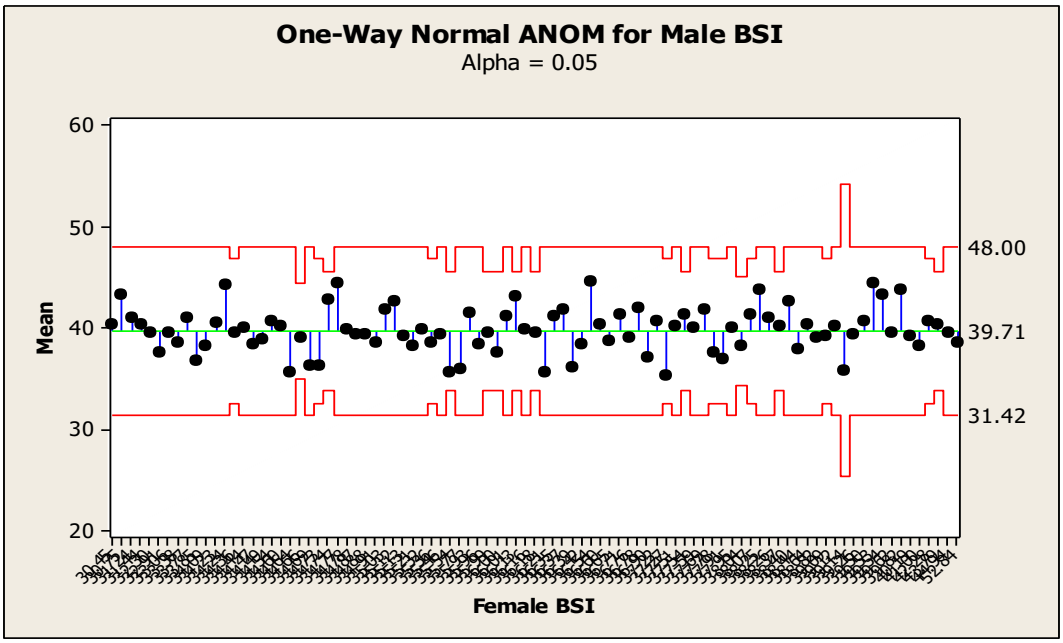

Appendix F-4: Analysis of mean male and female BMI

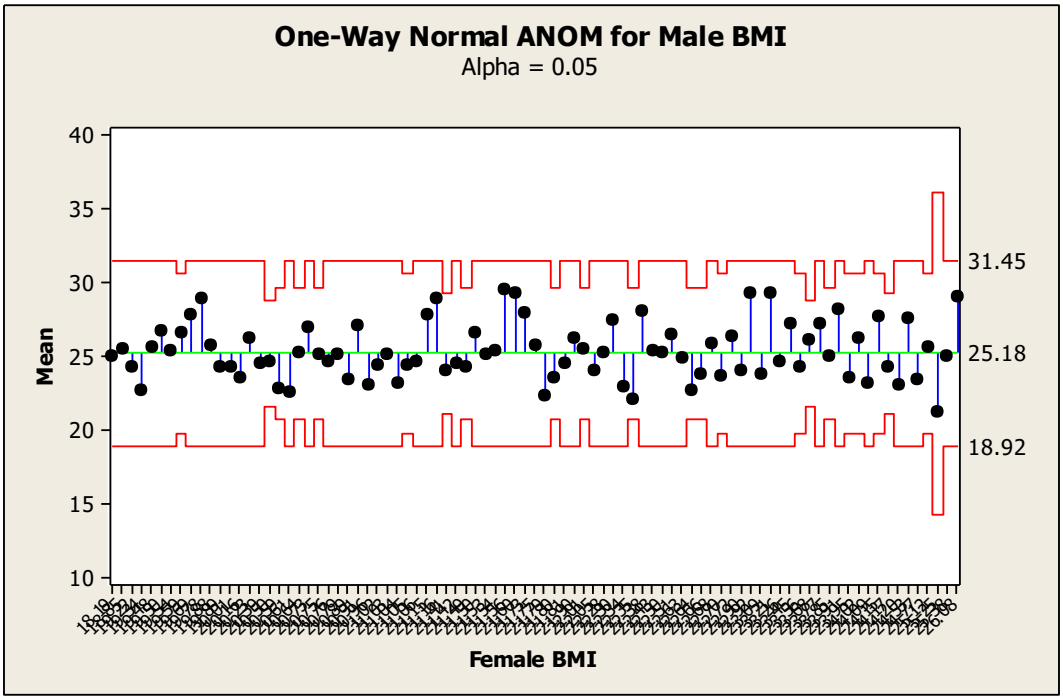

Appendix F-5: Analysis of mean male and female BSA

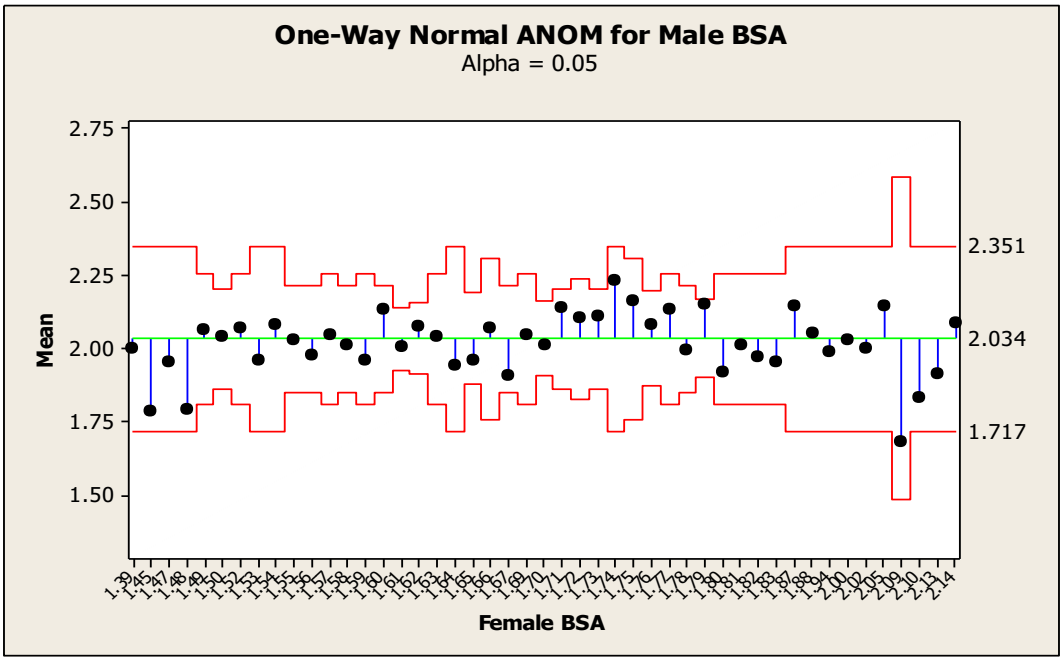

APPENDIX G

ANALYSIS OF RENAL PARAMETERS

Appendix G-1: Test of Variance of male and female renal length

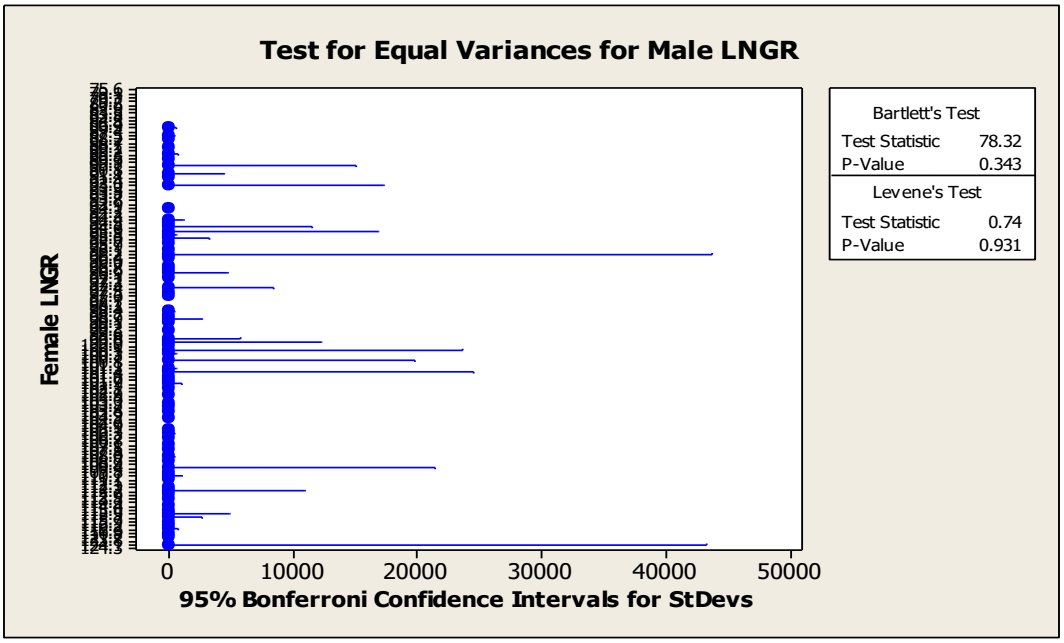

Appendix G-2: Test of Variance male and female renal volume

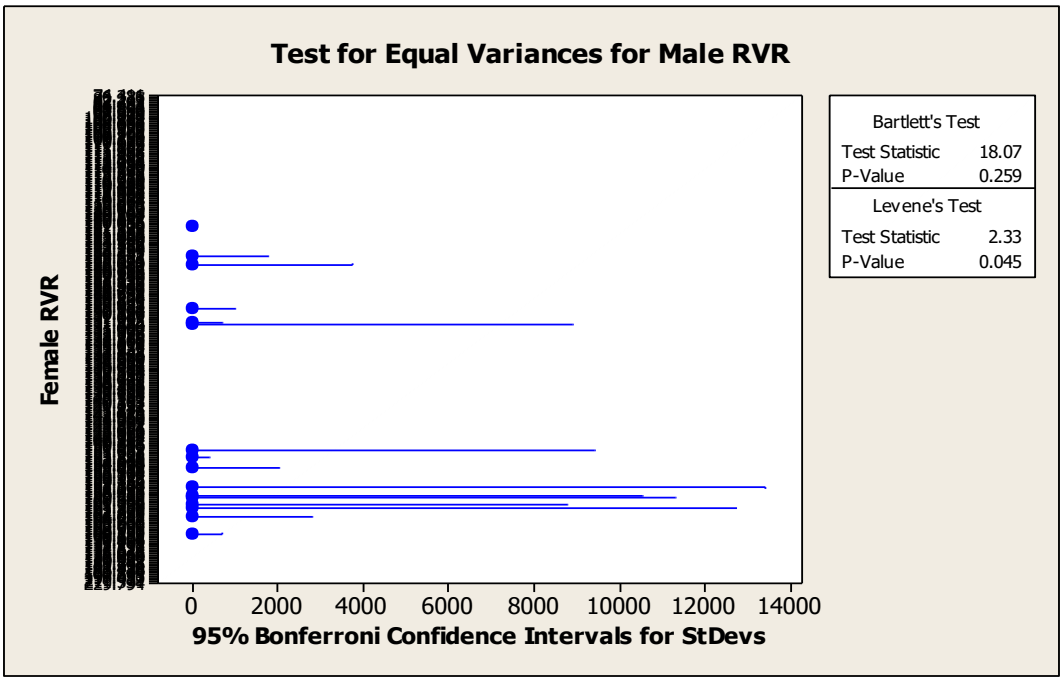

APPENDIX H

ANALYSIS OF RELATIVE RENAL PARAMETERS

Appendix H-1: Normal distribution relative male renal length

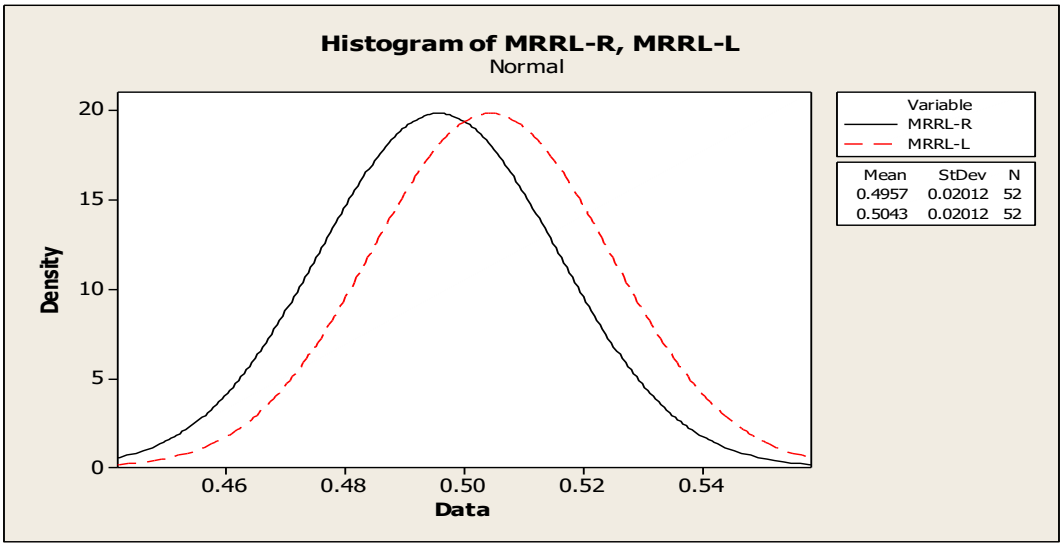

MRRLR-male right relative renal length, MRRLL-male left relative renal length

Appendix H-2: Normal distribution of relative female renal length

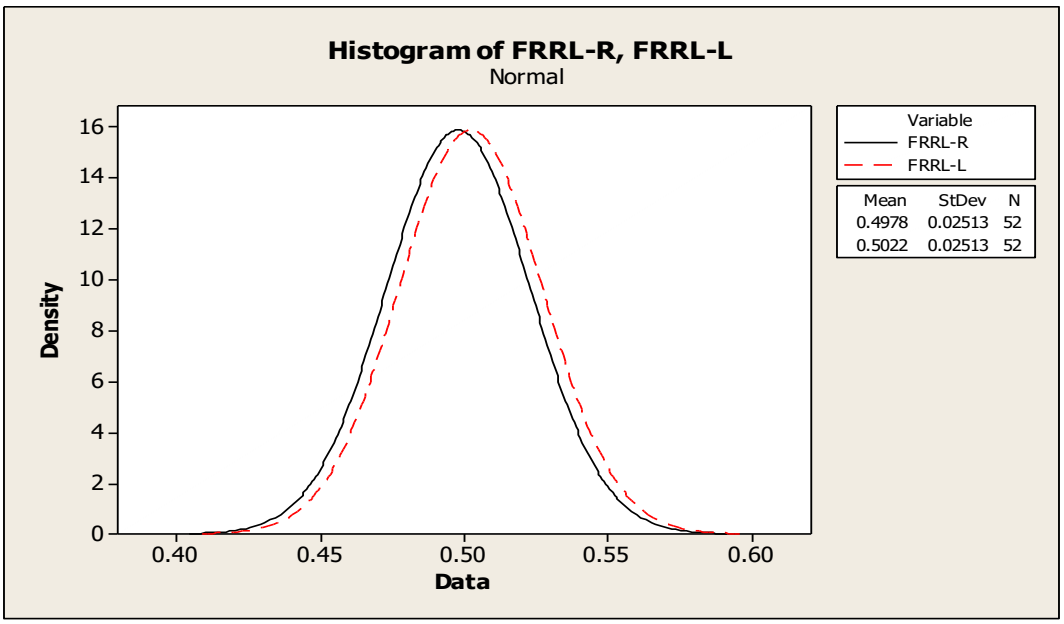

FRRLR-female right relative renal length, FRRLL-female left relative renal length

Appendix H-3: Normal distribution of relative male renal volume

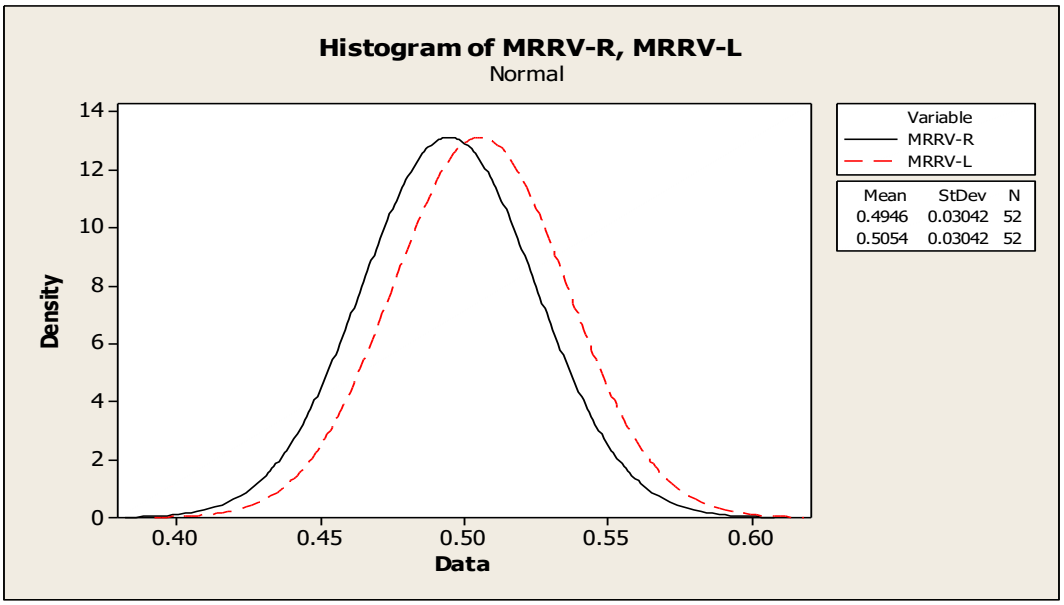

MRRVR-male right relative renal volume, MRRVL-male left relative renal volume

Appendix H-4: Normal distribution of relative female renal volume

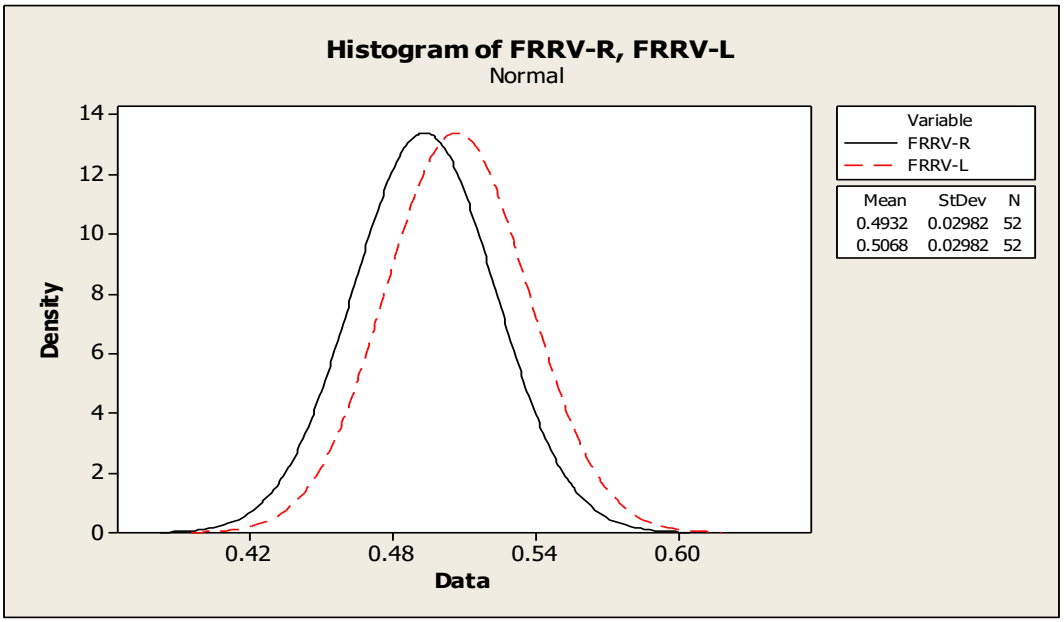

FRRLR-female right relative renal volume, FRRLL-female left relative renal volume

APPENDIX I

ANALYSIS OF DOSE PARAMETERS

APPENDIX I-1: Analysis of mean female and male E

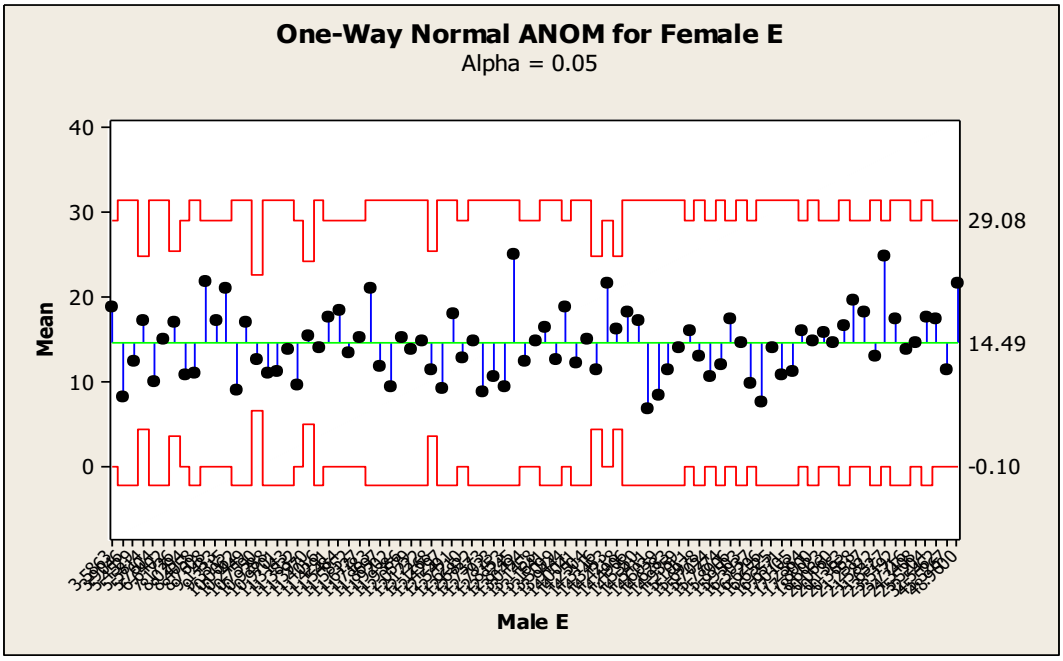

Appendix I-2: Analysis of mean female and male RD

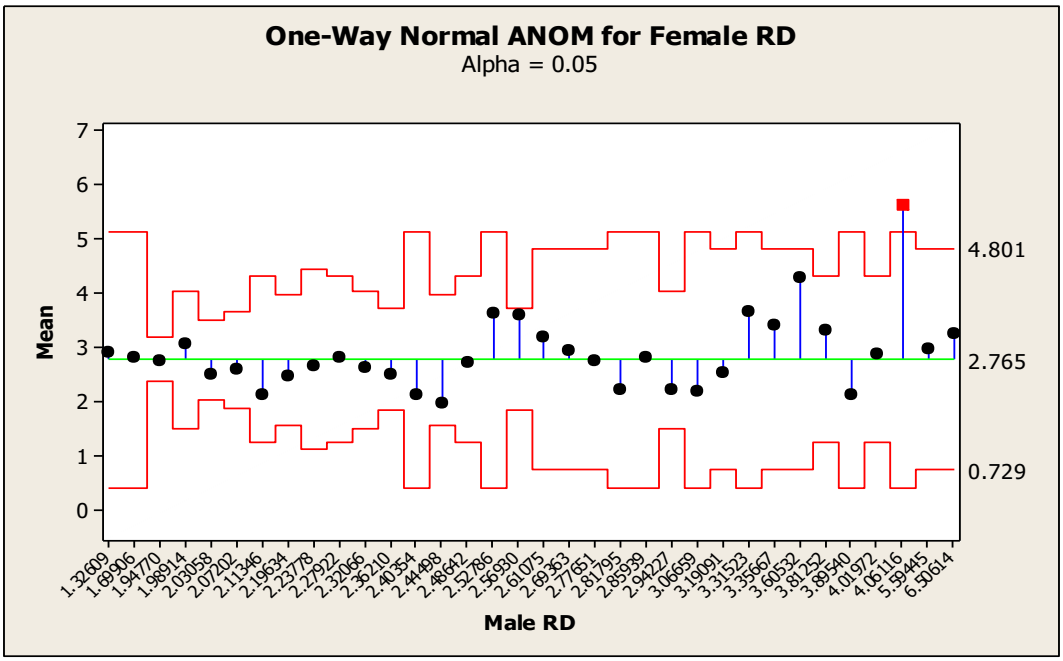

Appendix I-3: Analysis of mean male E and RD.

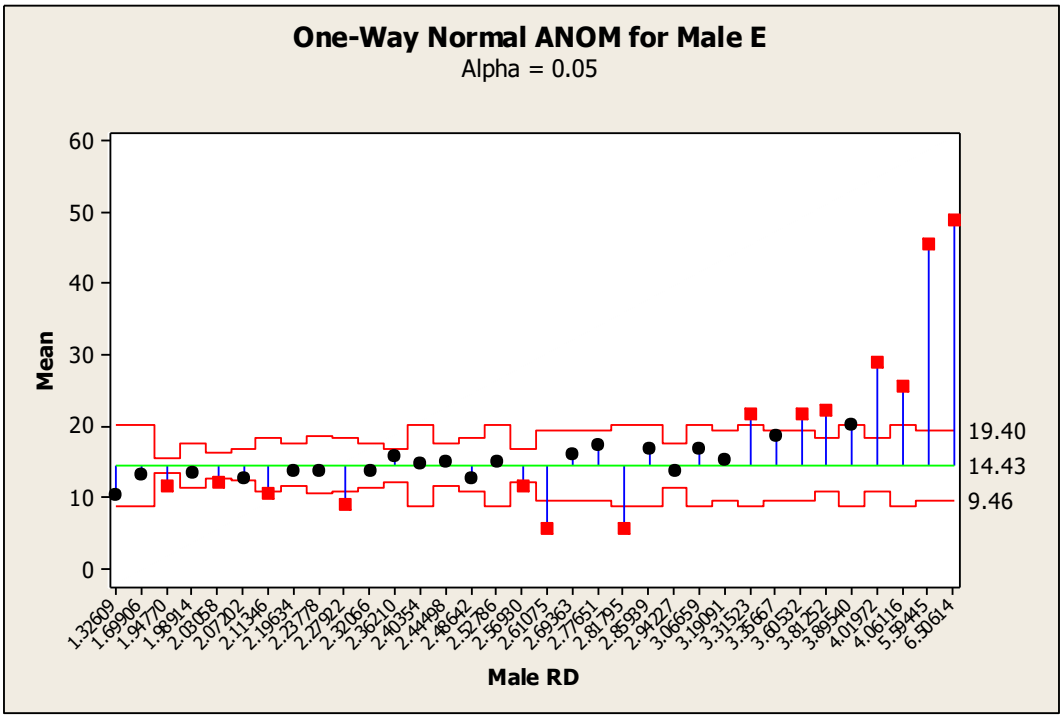

Appendix I-4: Analysis of mean female E and RD.

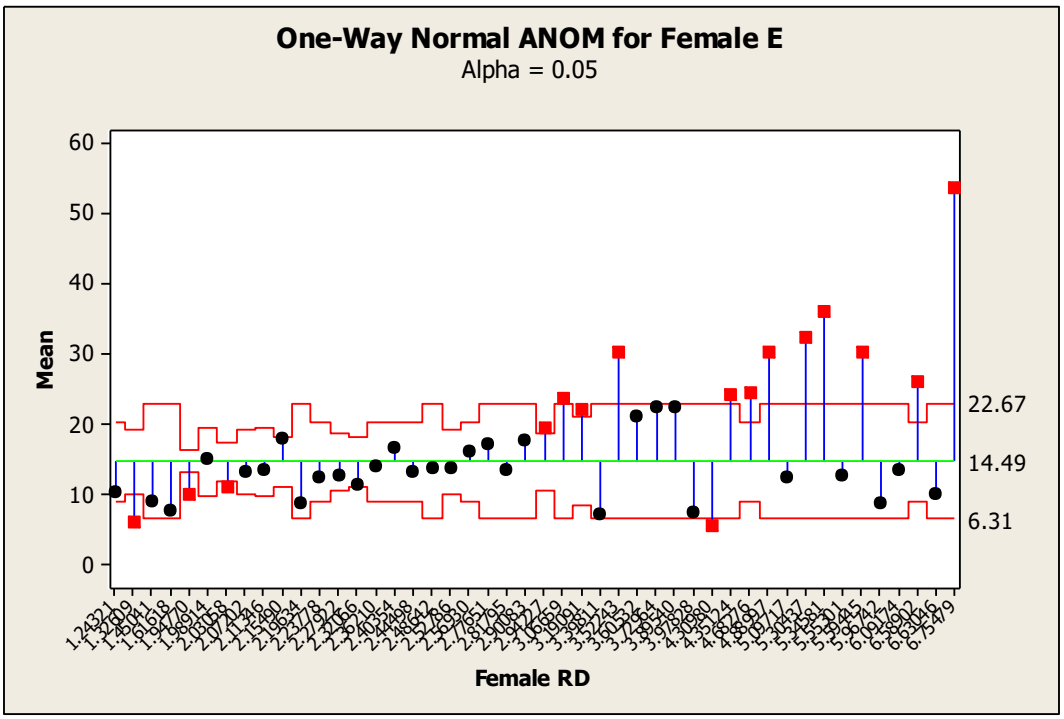

APPENDIX J

MODELING BODY PARAMETERS

Appendix J-1: Linear Height and Weight

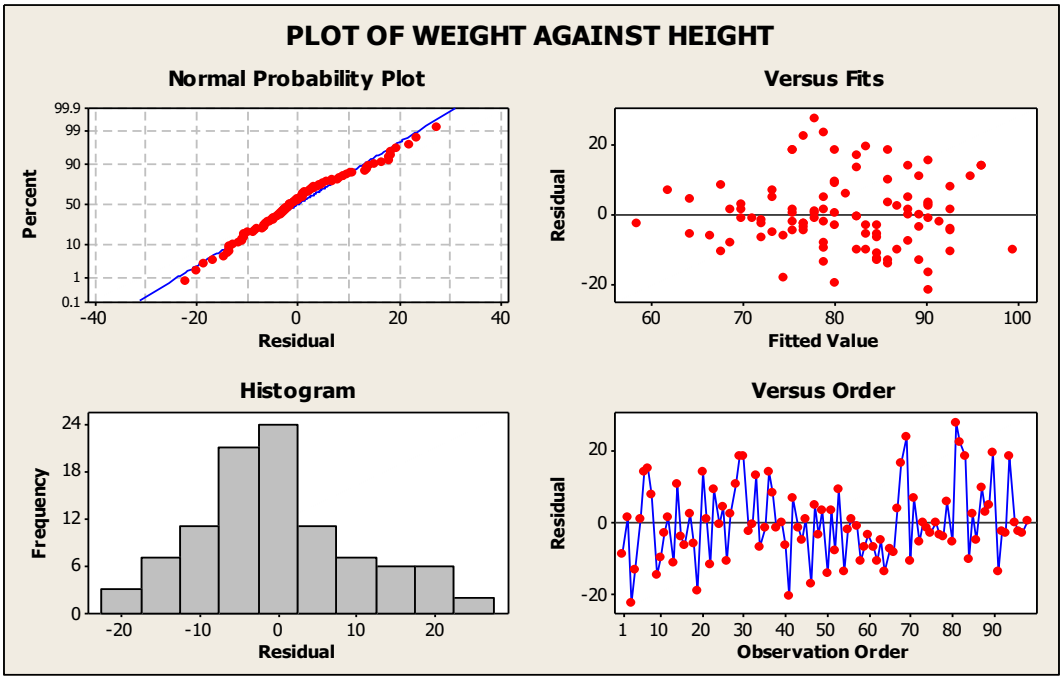

MALE

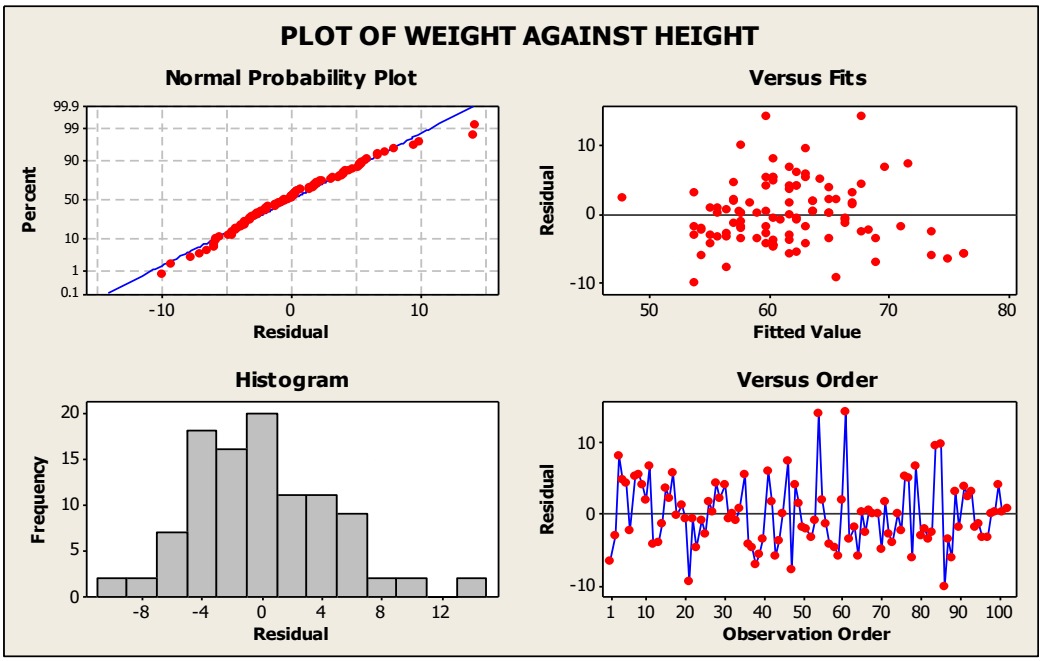

FEMALE

Appendix J-2: BSI in relation BMI variations

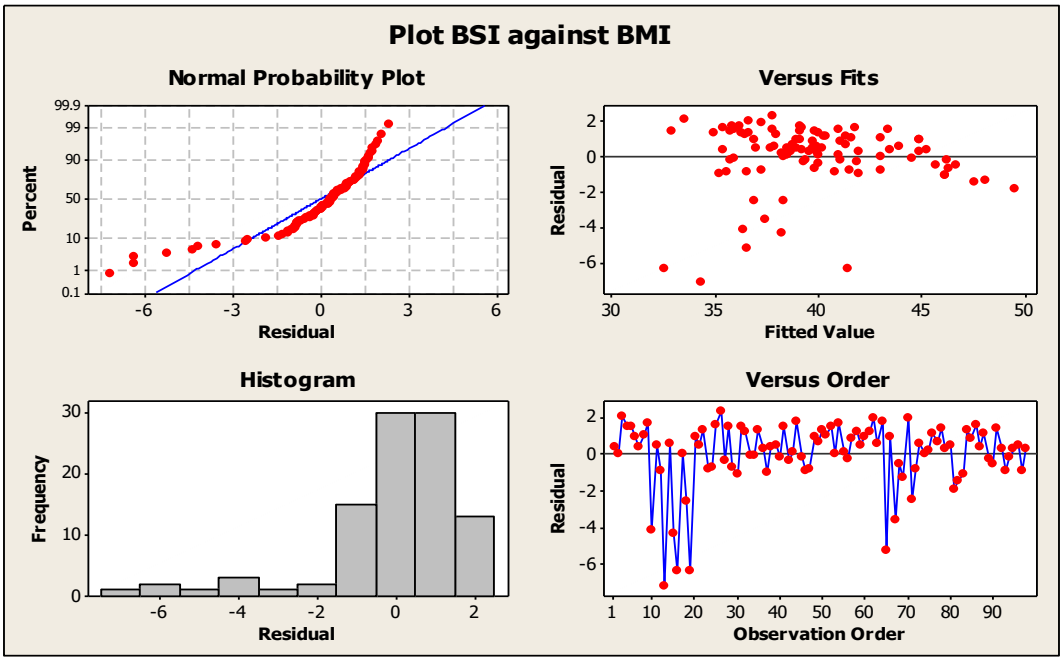

MALE

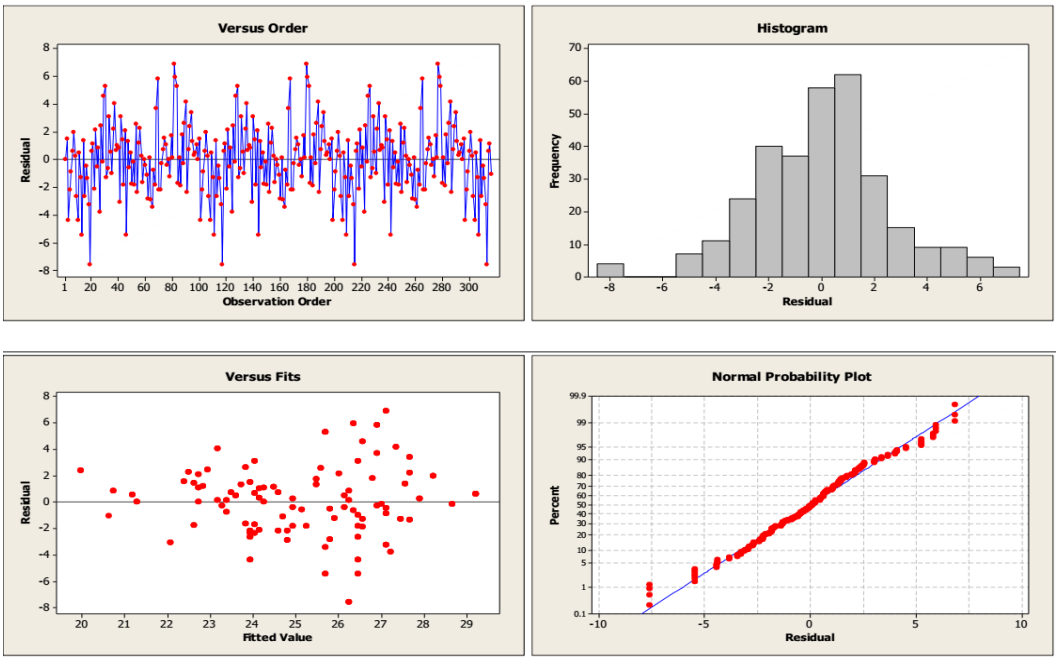

FEMALE

Appendix J-3: BSA related BMI

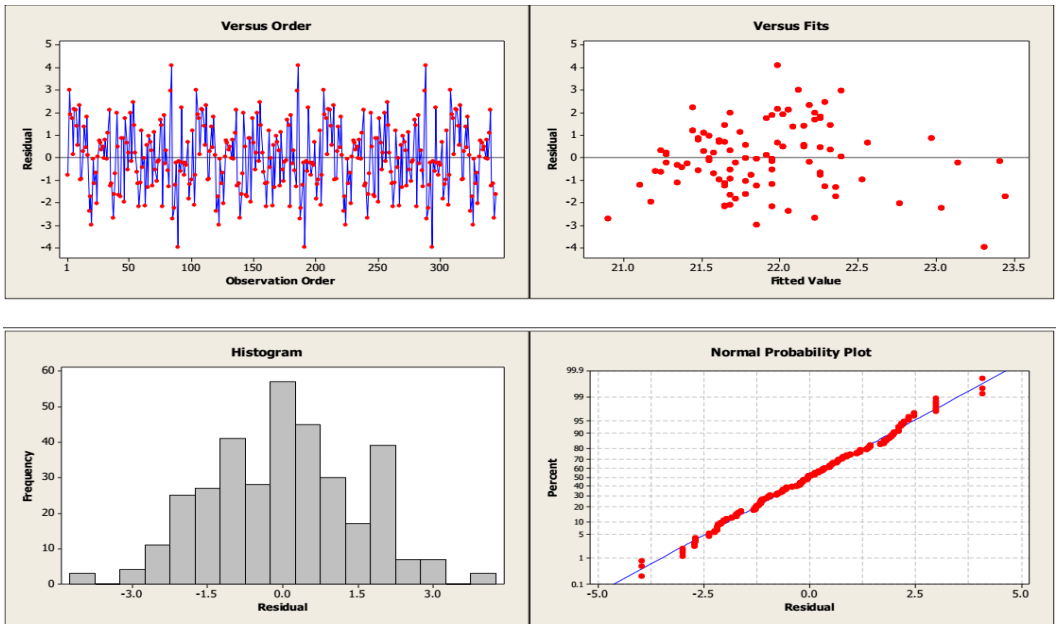

MALE

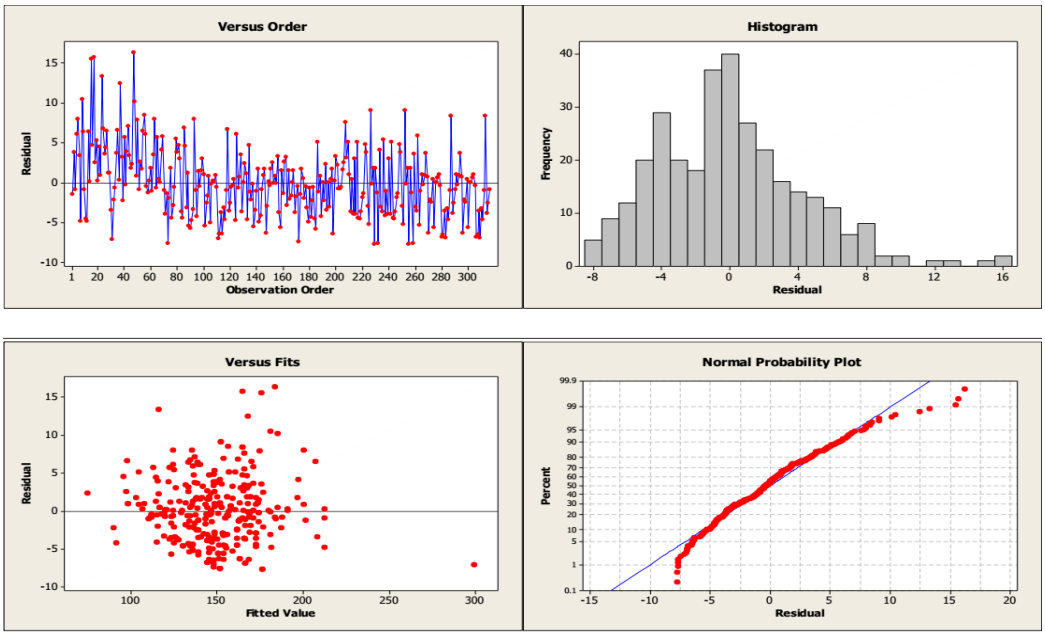

FEMALE

APPENDIX K

MODELING RENAL VOLUME-RELATED BODY PARAMETERS

Appendix K-1: Renal volume in relation to Re variations

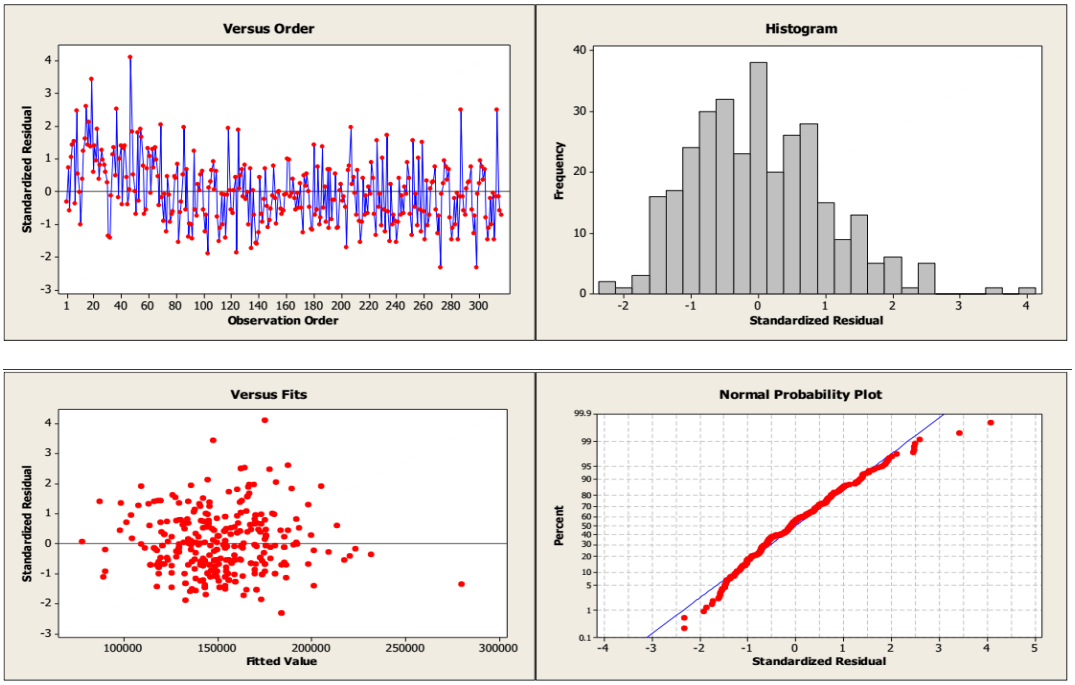

MALE

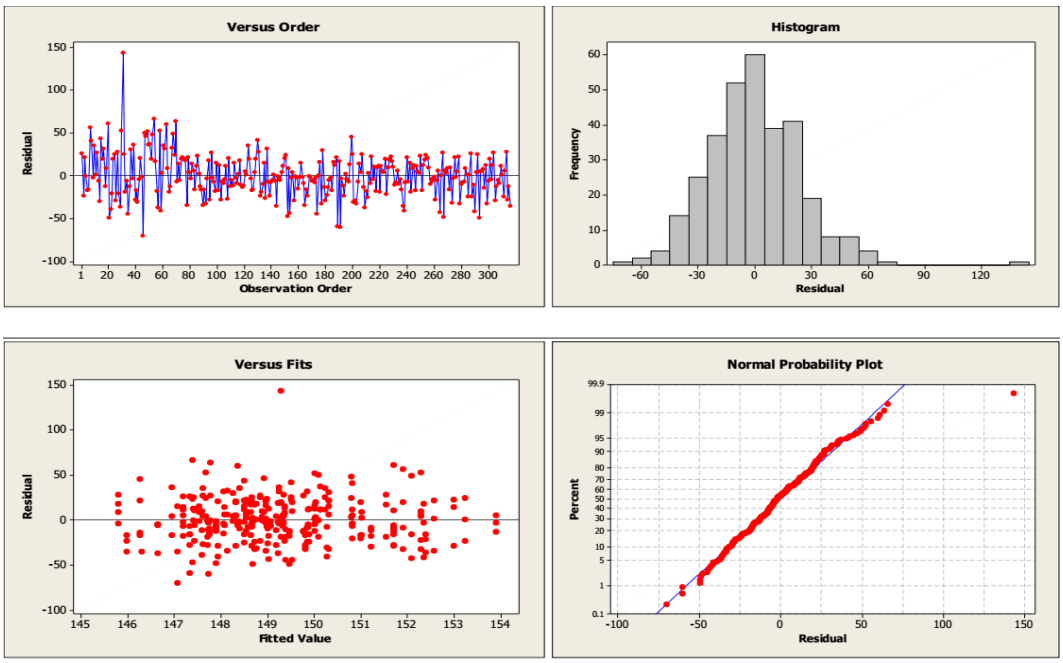

FEMALE

Appendix K-2: Renal volume in relation to BMI variations

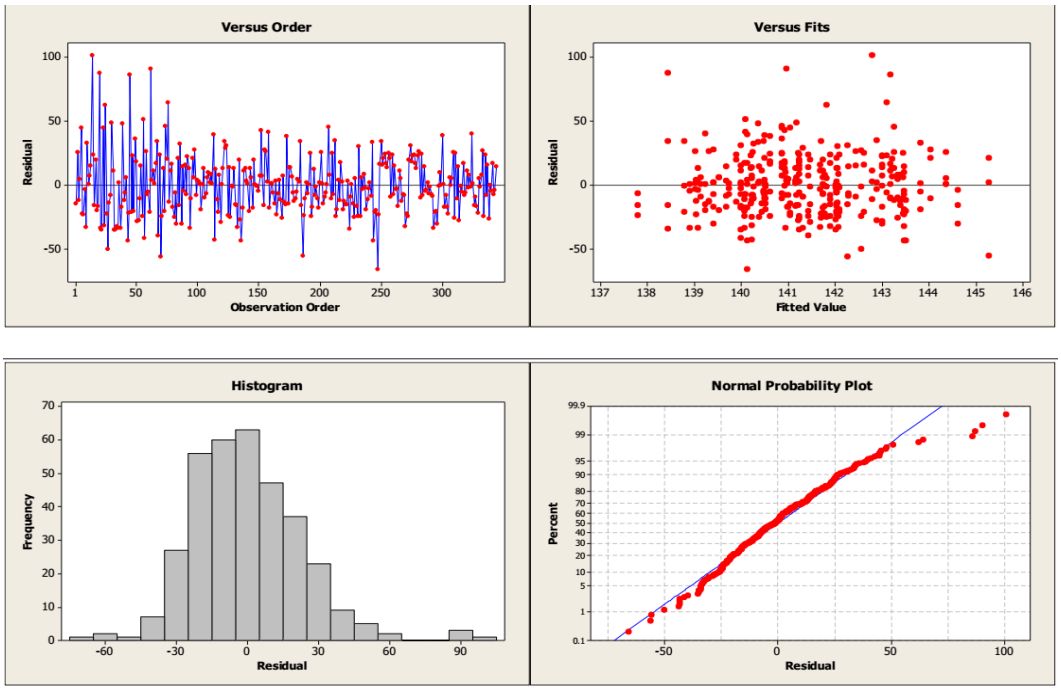

MALE

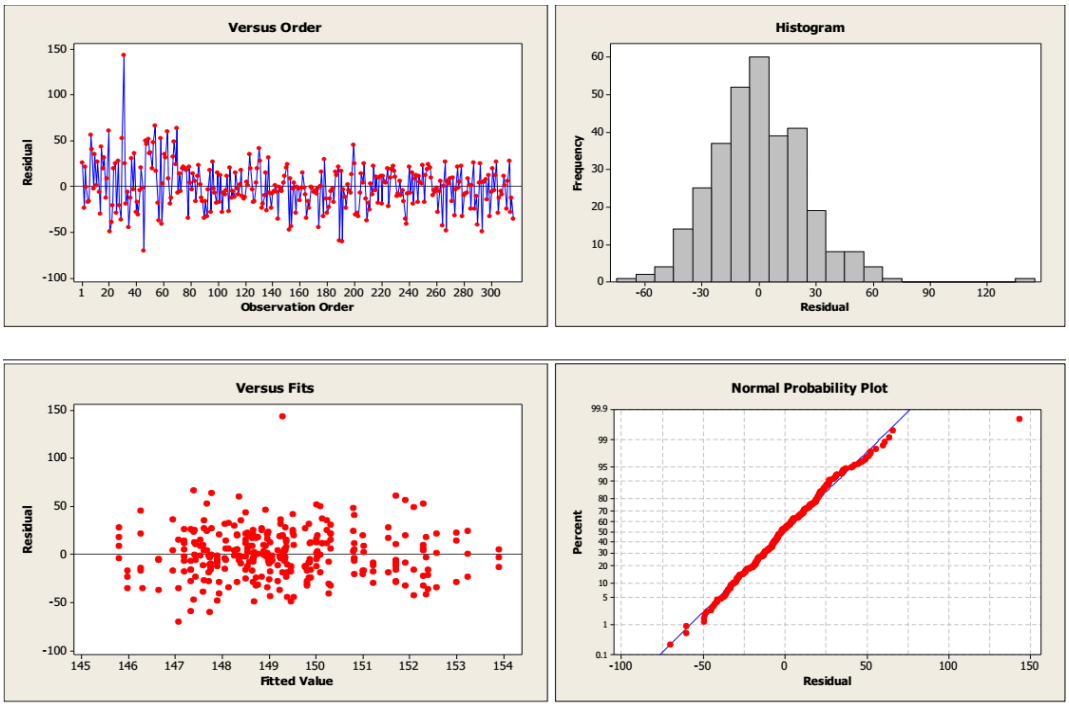

FEMALE

Appendix K-3: Renal volume in relation to BSA variations

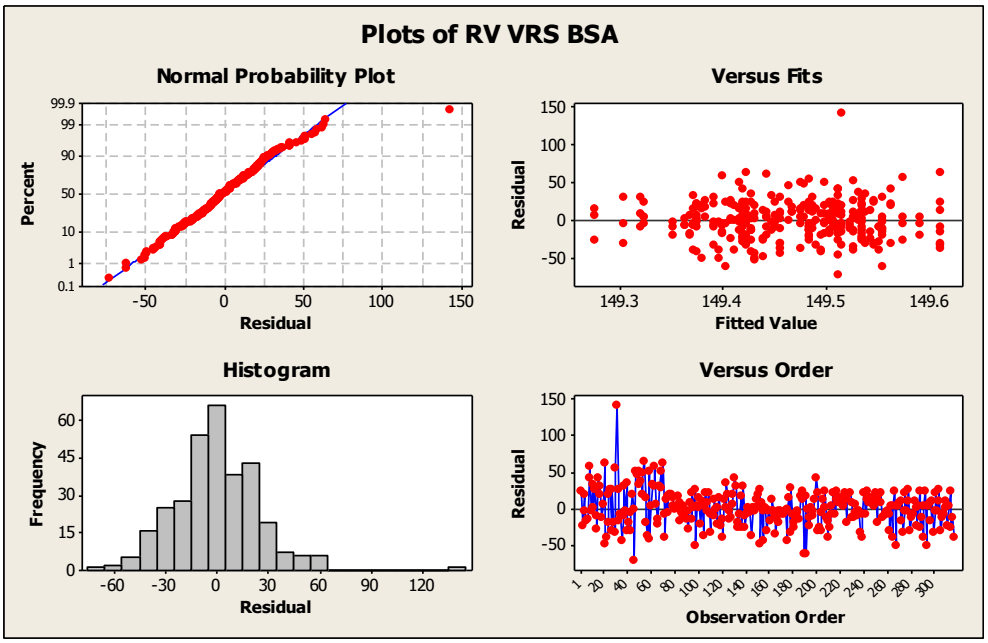

MALE

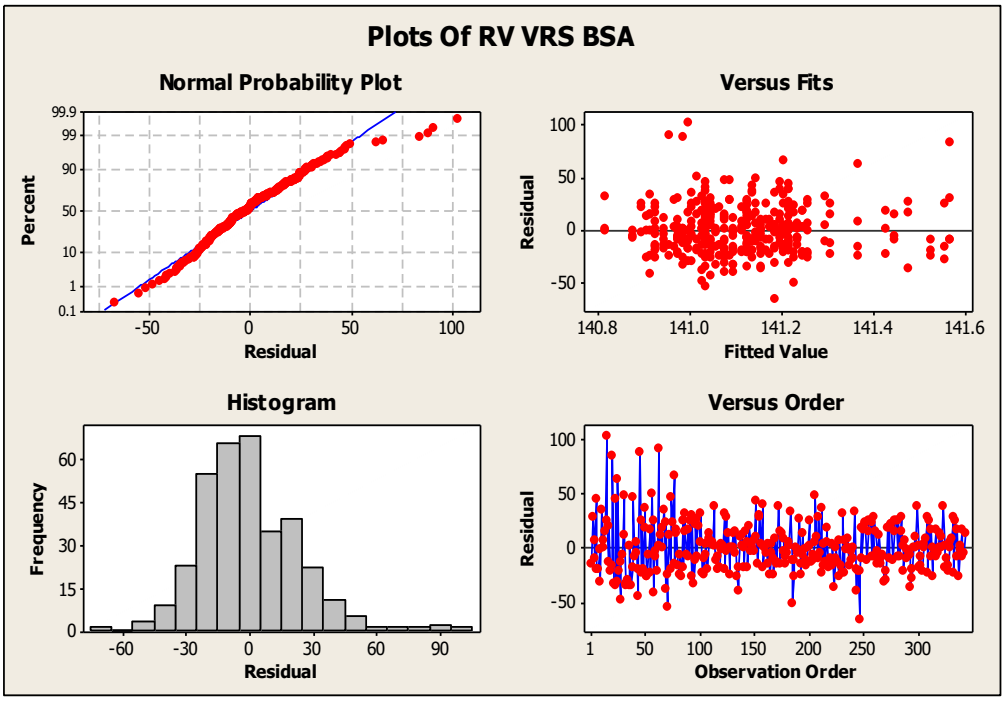

FEMALE

Appendix K-4: Renal volume in relation to BSI variations

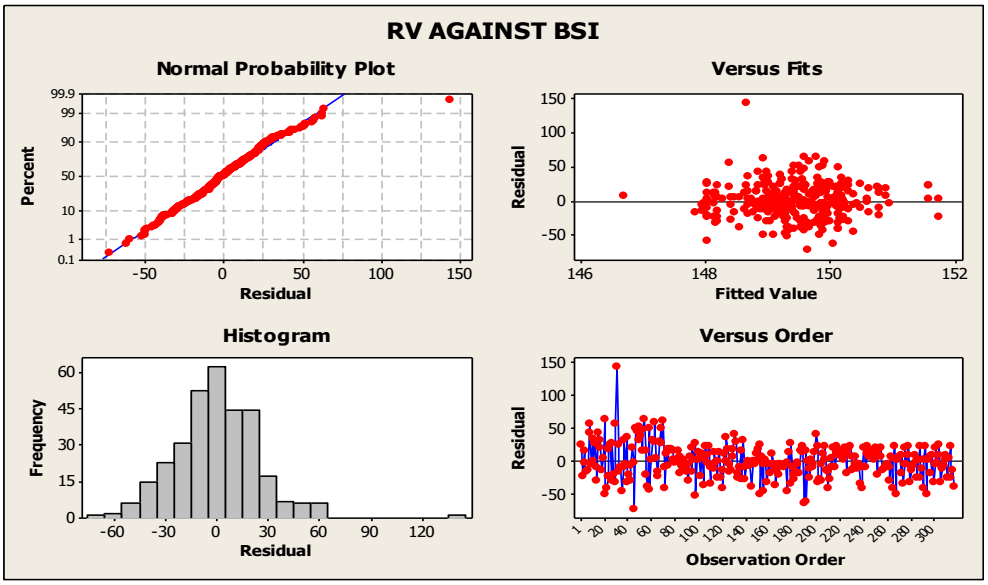

MALE

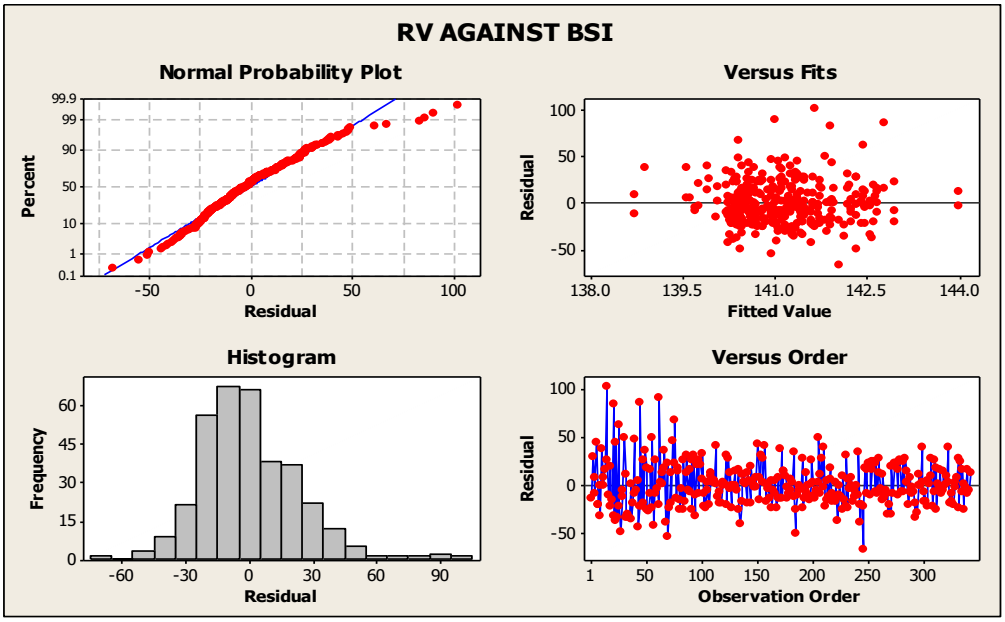

FEMALE

APPENDIX L

MODELING DOSE PARAMETERS

Renal dose in relation to effective dose variations

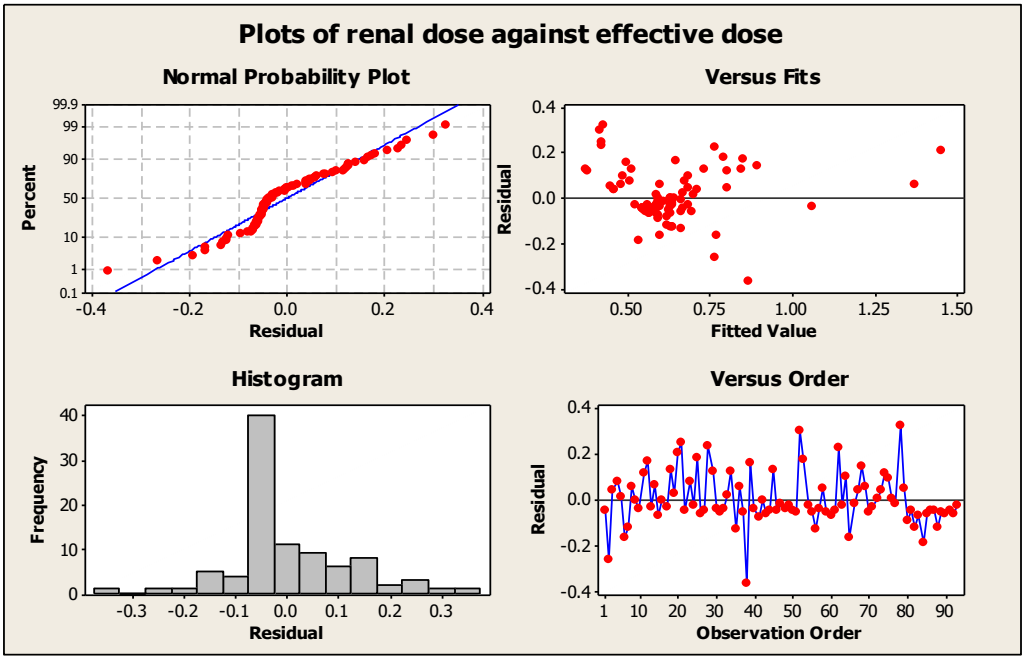

MALE

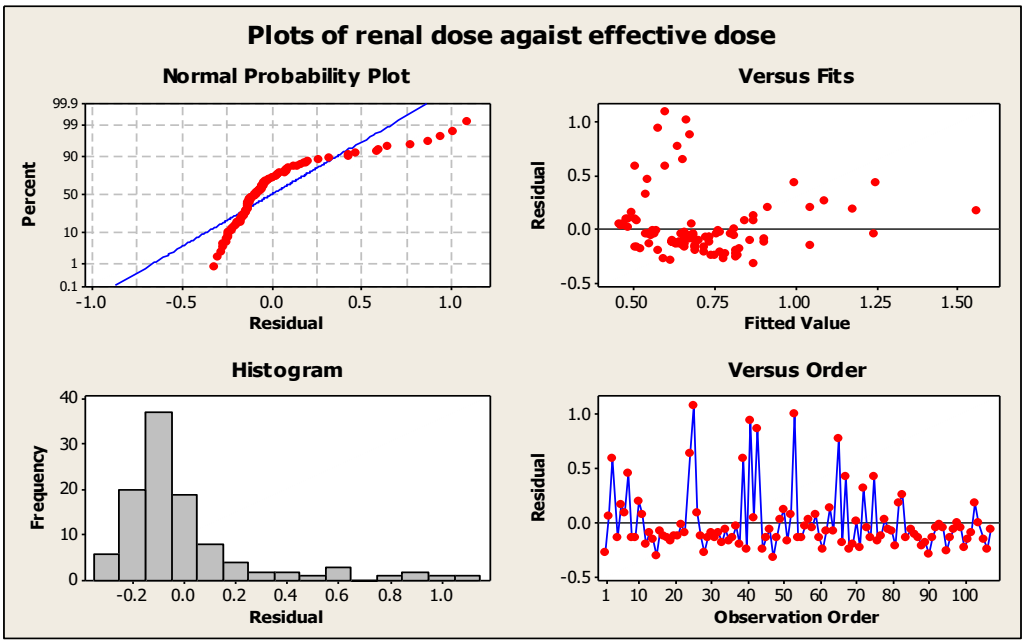

FEMALE

APPENDIX M

ETHICAL CLEARANCE

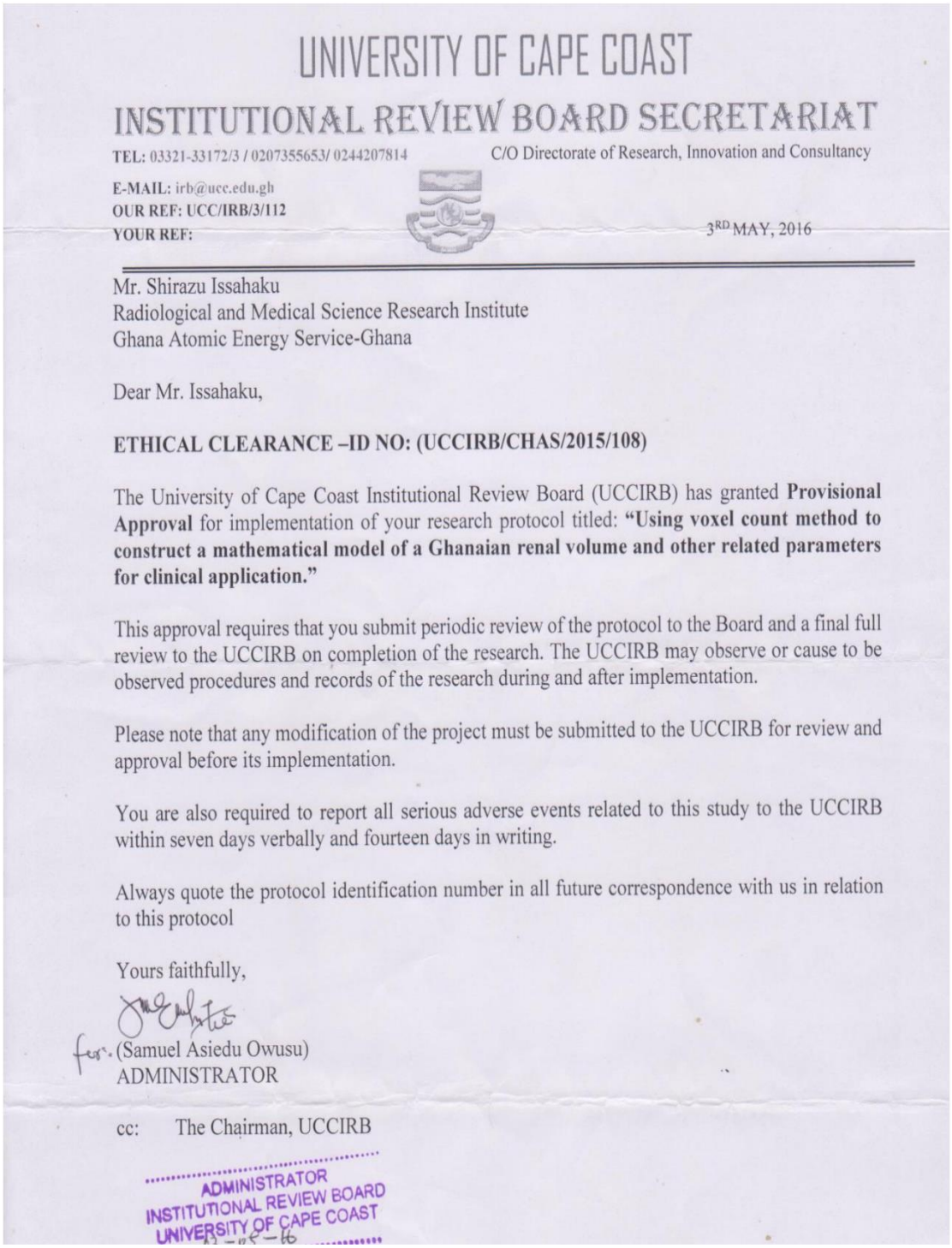

UNIVERSITY OF CAPE COAST

INSTITUTIONAL REVIEW BOARD SECRETARIAT

TEL: 03321-33172/3 / 0207355653/ 0244207814 C/O Directorate of Research, Innovation and Consultancy

E-MAIL: irb@ucc.edu.gh
OUR REF: UCC/IRB/3/112
YOUR REF:

3RD MAY, 2016

Mr. Shirazu Issahaku
Radiological and Medical Science Research Institute
Ghana Atomic Energy Service-Ghana

Dear Mr. Issahaku,

ETHICAL CLEARANCE –ID NO: (UCCIRB/CHAS/2015/108)

The University of Cape Coast Institutional Review Board (UCCIRB) has granted **Provisional Approval** for implementation of your research protocol titled: **"Using voxel count method to construct a mathematical model of a Ghanaian renal volume and other related parameters for clinical application."**

This approval requires that you submit periodic review of the protocol to the Board and a final full review to the UCCIRB on completion of the research. The UCCIRB may observe or cause to be observed procedures and records of the research during and after implementation.

Please note that any modification of the project must be submitted to the UCCIRB for review and approval before its implementation.

You are also required to report all serious adverse events related to this study to the UCCIRB within seven days verbally and fourteen days in writing.

Always quote the protocol identification number in all future correspondence with us in relation to this protocol

Yours faithfully,

for (Samuel Asiedu Owusu)
ADMINISTRATOR

cc: The Chairman, UCCIRB

ADMINISTRATOR
INSTITUTIONAL REVIEW BOARD
UNIVERSITY OF CAPE COAST

APPENDIX N

RESEARCH PUBLICATIONS

Issahaku Shirazu, Y. B. Mensah, Cyril Schandorf, S. Y. Mensah, "Measurement of Renal Dimensions to Determine Standard Reference Renal Volume Model for Clinical Application in Ghana", International Journal of Scientific Research in Science and Technology(IJSRST), Print ISSN : 2395-6011, Online ISSN : 2395-602X, Volume 3, Issue 1, pp.212-224 , January-February-2017.

Issahaku Shirazu, Yaw B. Mensah, Cyril Schandorf, S. Y. Mensah. Determination of standard reference body indices for clinical application in Ghana. "International Journal of Scientific & Technology Research (IJSTR)" Print IJSTR Volume 6 - Issue 2, February 2017.

Issahaku Shirazu, Yaw B. Mensah, Cyril Schandorf, S. Y. Mensah. Estimate of renal and effective dose during abdominal CT scan for dose optimization procedures in Ghana. International Journal of Scientific & Technology Research (IJSTR)" Print IJSTR Volume 6 - Issue 2, February 2017

Issahaku Shirazu, Y. B. Mensah, Cyril Schandorf, S. Y. Mensah, " Determination of the Relationship between Renal Volume Model and Related Body Indices for Clinical Application in Ghana", International Journal of Scientific Research in Science, Engineering and Technology(IJSRSET), Volume 3 Issue 1, Pp.313-320, January-February 2017.

Issahaku Shirazu, Y. B. Mensa, Cyril Schandorf, S. Y. Mensah , " A Comprehensive Clinical Decision Support Application Software for dose

Optimisation Procedure in CT", International Journal of Scientific Research in Science, Engineering and Technology(IJSRSET), Volume 3 Issue 1, pp.466-470, January-February 2017.

Issahaku Shirazu, Y. B Mensah, Cyril Schandorf, S. Y. Mensah, "Comparison of Measured Values of CTDI and DPL with Standard Reference values of Different CT Scanners for dose Management", International Journal of Scientific Research in Science and Technology (IJSRST), Volume 3, Issue 1, pp.185-190, January-February-2017.

Issahaku Shirazu, Y. B. Mensah, Cyril Schandorf, S. Y. Mensah, "Using Age and Weight Specific CT Protocol to Estimate Reference Effective Dose to Patients Undergoing CT Examination", International Journal of Scientific Research in Science and Technology(IJSRST), Volume 3, Issue 1, pp.191-196 , January-February-2017.

Issahaku Shirazu, Y. B. Mensah, Cyril Schandorf, S. Y. Mensah, "Optimization of Dose Parameters to Patients Undergoing CT Scan Using Four Different CT Scanners with International Guidelines", International Journal of Scientific Research in Science and Technology(IJSRST), Volume 3, Issue 1, Pp.197-203 , January-February-2017.

Issahaku Shirazu, Y. B. Mensah, Cyril Schandorf, S. Y. Mensah, " A Comprehensive Clinical Decision Support Application Software for Measurements of Body and Renal Dimensions In Ghana", International Journal

of Scientific Research in Science, Engineering and Technology(IJSRSET), Volume 3 Issue 1, pp.356-359 , January-February 2017.

Issahaku Shirazu, Cyril Schandorf, Y. B Mensah, S. Y. Mensah, Theophilus Sackey, Ernest Kojo Eduful, Mark Pokoo-Aikins, " The Effect of Linear Energy Transfer, Particle and Energy Fluence on Renal Surface Area during Abdominal CT Scan", International Journal of Scientific Research in Science, Engineering and Technology(IJSRSET), Print ISSN : 2395-1990, Online ISSN : 2394-4099, Volume 3 Issue 3, pp.671-677, May-June 2017.